GEORGIA INSTITUTE OF TECHNOLOGY
OFFICE OF CONTRACT ADMINISTRATION
SPONSORED PROJECT INITIATION

Date: 12/6/79

Project Title: Proposal for Modification of ORNL Subcontract No. 3986, Involving Analytic Reactor Physics and Design Investigations

Project No: E-26-B01 (20

Project Director: Dr. J.M. Kallfelz

Sponsor: Union Carbide Corporation, Nuclear Division, Oak Ridge, TN 37830

Agreement Period: From 10/1/79 Until 9/30/80

Type Agreement: Project Authorization No. X01 under Basic Agreement No. 7802 (under DOE Prime No. W-7405-eng-26)

Amount: $98,938

Reports Required: Monthly Progress Reports; Final Report

Sponsor Contact Person (s):

Technical Matters	Contractual Matters (thru OCA)
C.R. Weisbin Engineering Physics Division Oak Ridge National Laboratory Building 6025, X-10 Oak Ridge, TN 37830 Telecopier No. 615/574-6069 Verification No. 615/574-6068	Mr. W.R. Osborn Contract Administrator Purchasing Division Union Carbide Corporation Nuclear Division P.O. Box M Oak Ridge, TN 37830 615/483-8611, ext. 34705

NOTE: CONTINUATION OF E-26-610, E-26-633, and E-26-645

Defense Priority Rating: N/A

Assigned to: Nuclear Engineering (School/~~Laboratory~~)

COPIES TO:

- Project Director
- Division Chief (EES)
- School/Laboratory Director
- Dean/Director–EES
- Accounting Office
- Procurement Office
- Security Coordinator (OCA)
- Reports Coordinator (OCA)
- Library, Technical Reports Section
- EES Information Office
- EES Reports & Procedures
- Project File (OCA)
- Project Code (GTRI)
- Other OCA Research Property Coordinator

GEORGIA INSTITUTE OF TECHNOLOGY OFFICE OF CONTRACT ADMINISTRATION

SPONSORED PROJECT TERMINATION SHEET

Date 6/6/83

Project Title: Analytic Reactor Physics & Design Investigations

Project No: E-26-B01

Project Director: J. M. Kallfelz

Sponsor: Union Carbide Corp., (under DOE Prime)

Effective Termination Date: 9/30/80

Clearance of Accounting Charges: 9/30/80

Grant/Contract Closeout Actions Remaining:

None required - project continued under E-26-B02.
(No final report required under E-26-B01)

- ☐ Final Invoice and Closing Documents
- ☐ Final Fiscal Report
- ☐ Final Report of Inventions
- ☐ Govt. Property Inventory & Related Certificate
- ☐ Classified Material Certificate
- ☐ Other _____

Assigned to: Nuclear Engr. (School/~~Laboratory~~)

COPIES TO:

Administrative Coordinator	Research Security Services	EES Public Relations (2)
Research Property Management	Reports Coordinator (OCA)	Computer Input
Accounting	Legal Services (OCA)	Project File
Procurement/EES Supply Services	Library	Other Kallfelz

FORM OCA 10:781

GEORGIA INSTITUTE OF TECHNOLOGY

SCHOOL OF NUCLEAR ENGINEERING E-26-601

Atlanta, Georgia 30332 (404) 894-3720

October 15, 1979

MEMORANDUM

TO: C.R. Weisbin, J.H. Marable and M.L. Williams (ORNL)

FROM: J.M. Kallfelz and P. Levin

SUBJECT: Progress Report on Work for ORNL Subcontract 3986, Period 11 September - 12 October, 1979

1. Summary

1.1 Accomplishments for Report Period

- EPRI-CELL calculations for six mixed-oxide criticals (1,2) and BAPL-1 through -3 (3) have been repeated and analyzed. These calculations were repeated to incorporate various corrections in the code, the cross section set, and the models used. Our results now generally agree well with the calculated results for integral parameters published in Reference 2.

- A study was made of the economic aspects of sensitivity and uncertainty analysis for reactor design, and the results have been summarized in Reference 4.

- References (5 - 7) were obtained and studied to initiate investigations of isotopics of PWRs utilizing EPRI-CELL. Based on the material available, we have decided to begin with the Yankee Rowe reactor.

- EPRI-CMP activity was devoted mainly to literature studies related to both development of the interface between NJOY and CPM, and preparation for the power reactor isotopic calculations. Some effort was devoted to overcoming minor operational problems for the ORNL version.

1.2 Plans for work through October 30

- EPRI-CELL calculations to analyze the isotopics of the Yankee Rowe reactor (5, 6) will be initiated.

- A more thorough physics analysis of the EPRI-CELL calculations which we have just completed will be accomplished.

- If the EPRI-CELL ENDF/B-V tape is operational in time at ORNL, we will begin benchmark calculations utilizing this data.

- The influence of correlation between integral parameters on the variance of costs will be further studied, particularly the considerations involving the k-reset mechanism discussed in an earlier report (8).

2. EPRI-CELL Calculations

2.1 Changes from Previous Calculations

Various changes in the cross sections set, the code, and the models used were made since the previously calculated results were reported (9, 10). The following changes have been incorporated in the results reported herein.

2.1.1 Cross-section Set

Some minor errors were contained in the old ENDF/B tape, and in September a corrected version was obtained from Los Alamos. The results reported herein all use this corrected version (11).

2.1.2 Coding changes in EPRI-CELL

The results reported herein were all calculated with the EPRI-CELL version which included corrections made through 10 October 1979. The principal changes made since our previous report (9) are:

(a) The coding for the disadvantage factor, DISAD, has been corrected. For U-L212, the code now calculates a value identical to the hand-calculated results of Mark Williams (0.56).

(b) Subsequently, the coding was changed to give correct results for DISAD and the GAM cell cross sections when the "heavy scattering ring" boundary condition is used (see (b) of the following section).

2.1.3 Model Changes

For all the lattices for which results are reported herein, the following changes in the calculational model were made:

(a) The mesh was made finer, as suggested in our previous report, with 9, 4 and 9 mesh points in the pin, clad, and moderator, respectively, rather than the previous mesh of 3, 2 and 3 points. For the lowest pitched lattice, U-L266, k_{eff} changed by 0.14% and the various reaction rate ratios changed by up to 1%. For some of the other lattices the fine mesh case stopped too far from the convergence criterion to draw conclusions about the observed differences. However, for the cited case of U-L266 iterations continued to within a factor of 3 from the convergence criterion, so the impact of the failure to reach complete convergence should be negligible.

In this context, it should be noted that in the "engineering input" of EPRI-CELL, 4 and 8 mesh points in the fuel are recommended for UO_2 and MO_2 pins, respectively. (14)

(b) The heavy scattering ring (HSR), boundary condition was used instead of the isotopic boundary condition, since the "EPRI-CELL Criticals Benchmarking" section of the ARMP documentation (14) states that for lattices which are "more watery" than those having "practical" pitches, the HSR option must be used.

One advantage of using the HSR was that for the fine mesh mentioned in (a) all calculations converged in less than the 50 iteration limit presently in the code. It was observed that when using the isotopic boundary condition, whereas all cases converged for the coarse mesh, the fine mesh has

an influence which is not yet understood. For the later the convergence criterion "PT CONV" was as much as a factor of 30 greater than the convergence criterion, after 50 iterations. However, the indicated maximum value of "PT CONV" was always at or near the cell boundary, in one of the lowest energy groups.

The EPRI-CELL description states that, for the HSR option, the "heavy scatterer" should have a density of 1.0 atoms/barn-cm, and the ring thickness should be 0.2 cm (15). We observed that for the cases considered, convergence was obtained with one mesh point in this ring, but not with two points.

Based on comparison with previous results, the combined influence of the HSR boundary condition and the degree of non-convergence discussed above have a very small influence on the integral results. Only for the largest borated lattice was there a significant change (0.4%) in k_{eff}.

(c) The resonance overlap correction, "appropriate for mixed oxide fuel only" (16), was not applied, because of an apparent inconsistency in this method (17).

For the three borated MO_2 lattices, the following change was also made:

(d) The B^{10} concentration was corrected by increasing our previous values by about 5%. Our calculated B_{nat} atom concentration was correct, and agrees with the values given by Ullo (18). However, to determine the B^{10} concentration we used the B^{10} isotopic abundance (by atom) of 18.8% given

in many older references (19 - 21). On checking this number further we were somewhat startled to find that the published value has changed appreciably over the years. For the 1972 chart of the nuclides (22), a value of 19.8% is given while the 1977 version (23) gives 20.0%. Furthermore, the reference booklet for the 1977 version states that "natural variation in boron from 19.8% B^{10} to 20.1% have been measured" (24).

After noting this discrepancy, we found that one of the references (25) gives the isotopic analysis of the boron used in the experiment as 19.8 ± 0.1 atom percent, which was unfortunately previously overlooked. Thus the 19.8% value has been used to obtain corrected B^{10} densities. This change reduced the k_{eff} values from -0.3% for the low pitched lattice (U-L250) to -0.9% for the other two lattices.

In this conjunction, it should be noted that there are some discrepancies in the ppm of B_{nat} reported for these experiments in the various references (1, 2, 18). We used the ppm values given in Reference 2, which we used to obtain our models and calculated integral parameter values with which to compare our results. The ppm values given in References 1 and 2 are identical, but those in Reference 3 are different by up to about 1% for U-L250. This lattice has the lowest B^{10} concentration of the borated assemblies. Presumably because of this and its harder spectrum, the 5% change in boron discussed in the previous paragraph had a much smaller effect on the k_{eff} of this lattice than on that of the other two. For the other two lattices the percent discrepancy in the B^{10} concentration stated in the various references is luckily much smaller. We estimate that this discrepancy would cause an uncertainty in k_{eff} of less than 0.1% for all the assemblies.

While on the topic of such discrepancies, we note that for U-L282 the number of critical rods is given as 160 and 161 in References 2 and 18, respectively.

For the three BAPL lattices, the following minor changes were made. As stated in our previous report (10) the minor errors which these changes correct were previously incorporated in our models, to be consistent with BAPL-1 results of MacFarlane (26) for purposes of comparison.

(e) The oxygen density in the moderator was changed from .0338 to .03338.

(f) The clad atom density was reduced to 0.04899 atoms/barn-cm to account for its homogenization with the void. (MacFarlane apparently simply replaced the 0.02 cm void with clad).

A further effect which has been investigated, but for which further EPRI-CELL analysis is necessary, is the following:

(g) As pointed out in the ARMP benchmarking chapter, corrections for the grain heterogeneities should be applied for the MO_2 cases (27). The effective spherical diameter of the fuel for the MO_2 lattices is 25 μm (28). For all the MO_2 lattices, runs were performed with the grain heterogeneity included, and comparison with previous runs indicated a change in the expected direction on the thermal cross sections, but a negligible influence on k_{eff} and the reaction rate ratios.

However, Table 1 shows the estimated impact of the effect on k_{eff} from References 2 and 18, which based their determinations thereof from information in References 29 and 30, respectively. As can be seen, for the larger lattice spacings the effect on k_{eff} is not negligible. We will investigate further the fact that EPRI-CELL apparently does not calculate this effect properly. Possible it is simply because of an error in the input description (e.g. wrong units for the grain size) in the EPRI-CELL documentation (12).

Our values reported in Table 2 should presumably be reduced for this effect. It appears probable, but not certain, from Reference 2 that the corrections shown in Table 1 have been applied to their k_{eff} and k_{∞} values, reported in Table 2.

2.2 EPRI-CELL Results

The EPRI-CELL results (EC) for the MO_2 lattices are presented in Table 2, compared to calculated results (NP) from NP-691 (2). The NP results for k_{eff} were calculated with HAMMER, including the resonance correction factor discussed in NP-691. The NP results for the other parameters, from Table XII of Reference 2, are very probably for the same calculational method, based on discussions with the two co-authors of NP-691, R. Sher of Stanford and S. Fiarman of BNL. However, neither author was positive about this point, and they are checking further.

As can be seen, the comparison between the results from the two sources is reasonably good. k_{eff} values differ by a maximum of 0.7% (for the low pitch lattices). The reaction rate ratios are defined as follows:

ρ_{28} = epi-thermal to thermal U-238 capture rate

δ_{25} = epi-thermal to thermal U-235 fission rate

δ_{28} = U-238 fission rate to U-235 fission rate

CR = U-238 capture rate to U-235 fission rate

The ρ_{28} and CR values show excellent agreement within about 1% except for U-L250, for which the discrepancy is slightly higher. δ_{25} and δ_{28} values are generally about 5% higher for the EC results than for the NP values.

With reference to the discussion of point (g) in paragraph 2.1.3, if in fact the grain heterogeneity corrections indicated in Table 1 should be applied to the EC k_{eff} values, then the maximum deviation for the medium and high pitch lattices would be slightly reduced.

Table 3 presents the results for the BAPL lattice models from (3), compared to the experimental values from the same reference. The δ_{25} values exhibit excellent agreement between calculation and experiment. However, the calculated ρ_{28} and δ_{28} values are up to about 10% higher and lower, respectively, than the experimental values.

One question which should be considered is the accuracy of the B^2 approximation. The B^2 values for the MO_2 lattices are examined thoroughly in (2), but a comparison with calculations which do not use this approximation can perhaps shed some light on the accuracy thereof. Several characteristics can be noted from Table 4. First, with the exception of U-L266 the agreement between the two calculations is within less than 0.4%. The trend to larger k_{eff} values with increasing pitch, mentioned in Reference 31, is more evident for these results than for those reported in Table 2. The k_{eff} deviation above 1.0 for U-L282 is not nearly as great for these results as for the cell calculations reported in Table 2.

In this context, it should be noted that the CPM pin cell calculations which we previously reported (9), performed with the original ENDF/B-3 library (12), yielded k_{eff} values which agreed to within 0.3% of our EC values for the non-borated cases in Table 2. This is further evidence that the B^2 approximation should be investigated.

Of course the data processing techniques and codes used have some influence on the results, and it should be noted that the ANISN results from NP-691 (2) used cross sections from HAMMER, the same code used for the NP cell calculations of k_{eff} in Table 2.

3. EPRI-CPM

Most of the CPM related activity was aimed at creating an interface between NJOY and CPM. This included reviewing the literature relevant to these codes. The study of that literature and program listings has been discontinued since the entire interfacing task was reassigned to LASL.

Preparation has been made for isotopic calculations of power reactor assemblies starting with Yankee Rowe Core V (6). We shall start with a pin cell calculation, concurrently with EPRI-CELL, but it is our plan to upgrade the calculations to an assembly cell.

Some time was spent tracing divide check errors encountered by ORNL when using their CPM version for calculating assemblies (unlike Berkeley's version). The work was done in cooperation with R.Q. Wright. The subroutine EXTEND fails in a statement where a division by a formal parameter is done, whenever the actual parameter is the numerical constant 1 (not a variable having that value). This indicates that the constant 1 is possibly destroyed somewhere. Since the standard fixup corrects it somehow, no further action has been taken by P. Levin.

REFERENCES

1. R.I. Smith and G.J. Konzek, "Clean Critical Experiment Benchmarks for Plutonium Recycle in LWRs," EPRI NP-196, Electric Power Research Institute, April 1976.

2. R. Sher and S. Fiarman, "Analysis of Some Uranium Oxide and Mixed-Oxide Lattice Measurements," EPRI NP-691, Electric Power Research Institute, February 1978.

3. H. Alter et.al., "Cross Section Evaluation Working Group Benchmark Specification," BNL-19302 (ENDF-202), Brookhaven National Laboratory, Revised September, 1978. Pages T(18-20)-1-3.

4. J.M. Kallfelz, "Cost Effectiveness of Sensitivity and Uncertainty Analysis for Reactor Design," Memorandum to C.R. Weisbin dated October 7, 1979.

5. R.J. Nodvik et.al., "Supplementary Report on Evaluation of Mass Spectrometric and Radiochemical Analyses of Yankee Core I Spent Fuel, Including Isotopes of the Elements Thorium Through Curium," WCAP-6086 (September 1969).

6. J.B. Melehan, "Yankee Core Evaluation Program, Final Report," WCAP-3017-6094 (January 1971).

7. R.J. Nodvik, "Saxton Core II Fuel Performance Evaluation Part II, Evaluation of Mass Spectrometric and Radiochemical Analysis of Irradiated Saxton Plutonium Fuel," WCAP-3385-56 Part II (July 1970).

8. J.M. Kallfelz, D. Rinaldis, M. Segev and P. Levin, "Progress Report on Work for ORNL Subcontract 3986, Period June 1-30, 1979," Memorandum to C.R. Weisbin, J.H. Marable and M.L. Williams dated July 8, 1979.

9. J.M. Kallfelz and P. Levin, "Progress Report on Work for ORNL Subcontract 3986, Period August 1 - September 10, 1979," Memorandum to C.R. Weisbin and M.L. Williams, dated September 14, 1979.

10. J.M. Kallfelz, P. Levin and M. Segev, "Progress Report on Work for ORNL Subcontract 3986, Period July 1-31, 1979," Memorandum to C.R. Weisbin and M.L. Williams dated August 1, 1979.

11. ENDF/B-IV - Based transport corrected EPRI-CELL libraries existing at ORNL were used: GAM library (FT03) - Tape #X05013, file 2.
    DSN = RQW. EPCELL.ENDFB4.GAMTAP.MOD1
    THERMOS library (FT04) - Tape #X20252, file 1.
    DSN = RQW.EPCELL.ENDFB4.LIBRAR

12. "Advanced Recycle Methodology Program System Documentation," EPRI Report, CCM-3 Electric Power Research Institute, September 1977.

13. See page 5-64, Chapter 5, Part II, of Reference 12.

14. See page 2-2, Chapter 2, Part I, of Reference 12.

15. See page 5-46, Chapter 5, Part II, of Reference 12.

16. See page 5-50, Chapter 5, Part II, of Reference 12.

17. M.L. Williams, "August Progress Report for ORNL Fuel Cycle Contract," letter to O. Ozer (EPRI) dated September 11, 1979.

18. J.J. Ullo, "Analyses of UO_2 - PuO_2 Fueled Rod Lattices with ENDF/B-IV," WAPD-R(D)-496, Westinghouse (undated, probably from about 1978).

19. H. Etherington, Editor, Nuclear Engineering Handbook, McGraw Hill, New York, 1958 (page 2-15).

20. General Electric Chart of the Nuclides, Fifth Edition, KAPL, April 1956.

21. Nuklidkarte, Kernreaktor Bau-und Betriebs-GmbH, Karlsruhe, October 1958.

22. Chart of the Nuclides, KAPL, Eleventh Edition, April 1972.

23. Chart of the Nuclides, KAPL, Twelfth Edition, 1977.

24. Nuclides and Isotopes, Twelfth Edition, General Electric, KAPL, Schenectady, New York, 1977. (Explanation booklet for Reference 23).

25. See page 8, Vol I of Reference 1.

26. R.E. MacFarlane (LASL), memo to O. Ozer (EPRI) "Thermal Transport and Removal Cross Sections in EPRI-CELL," April 18, 1979.

27. See page 2-4, Chapter 2, Part I of Reference 12.

28. See page 28, Reference 2.

29. H. Windsor and R. Goldstein, "Analysis of Lattices Containing Mixed-Oxide Fuel in Particulate Form," Trans. Am. Nucl. Soc. 15, 107 (1972).

30. R.C. Liikala et.al., "Lattices of Plutonium-Enriched Rods in Light Water - Part II: Theoretical Analysis of Plutonium - Fueled Systems," Nucl. Tech 15, 272, August 1972.

31. See page 2-11, Chapter 2, Part I, of Reference 12.

Table 1 Estimated Granulation Reactivity Effect

Lattice	Δk (NP)[a]	Δk (Ullo)[b]
U-L266	0.0	-.0008
U-L250	0.0	-.0008
U-L189	-.0018	-.0024
U-L212	-.0018	-.0024
U-L282	-.0025	-.0030
U-L232	-.0025	-.0030

(a) Table XI of Reference 2

(b) Table 7 of Reference 18

Table 2 Results for MO_2 Lattices from NP-691 and 196, for ENDF/B-4 Cross Sections[d]

Lattice	k_∞		k_{eff}		ρ_{25}		δ_{25}		δ_{28}		CR	
	EC[a]	NP	EC[a]	NP[b]	EC	NP	EC	NP	EC	NP	EC	NP
U-L266 (low pitch)	1.296	1.294	1.003	.997	5.09	5.11	.301	.288	.461	.441	3.24	3.28
U-L250 (low pitch, borated)	1.233	1.228	.994	.987	5.44	5.51	.323	.308	.482	.460	3.38	3.45
U-L189 (med. pitch)	1.386	1.384	.996	.996	2.24	2.23	.125	.120	.258	.242	1.95	1.95
U-L212 (med. pitch, borated)	1.164	1.151	1.009	1.005	2.72	2.71	.154	.148	.297	.281	2.20	2.20
U-L282 (high pitch)	1.373	1.367	1.017	1.018	1.55	1.54	.0860	.0825	.197	.185	1.59	1.58[c]
U-L232 (high pitch, borated)	1.143	1.128	1.009	1.004	1.89	1.86	.105	.101	.230	.216	1.77	1.76[c]

(a) EPRI-CELL results, for Pu-239 $\chi(E)$, B1, with MacFarlane's disadvantage factor, using heavy scattering ring boundary condition. Without grain heterogeneity correction (see section 2.1.3).

(b) Calculated results from NP-691. HAMMER was used for the k_{eff} calculations, and probably also for the other parameters.

(c) NP-691 values assumed to have only decimal point error, and hence multiplied by ten in this table.

(d) Latest ENDF/B-4, tape at ORNL as of 10 October was used for EC results. (11)

Table 3 Some Results for BAPL Critical Assemblies. Calculated Results are for the ORNL EPRI-CELL Version.[a] Experimental Values are from (3).

Parameter	Source	BAPL-1	BAPL-2	BAPL-3
k_{eff}	ENDF	.9893	.9914	.9937
δ_{25}	EXP	.085(±2.4%)	.068(±1.5%)	.052(±1.9%)
"	ENDF	.0843	.0686	.0525
ρ_{28}	EXP	1.39(±0.7%)	1.12(±0.9%)	.906(±1.1%)
"	ENDF	1.458	1.208	.944
δ_{28}	EXP	.078(±5.1%)	.070(±5.7%)	.057(±5.2%)
"	ENDF	.072	.062	.051

a) EPRI-CELL results, for U-235 $\chi(E)$, B1, with MacFarlane's disadvantage factor, using heavy scattering ring boundary condition. The latest ENDF/B-4 tape at ORNL as of 10 October was used (11).

Table 4 k_{eff} Results for the Mixed-oxide Lattices Using ENDF/B-4 Cross Sections, from ANISN (2) and Monte Carlo Calculations (18)

Lattice	NAISN	Monte Carlo[a]
U-L266	.983	.996
U-L250	.993	.997
U-L189	1.001	.998
U-L212	1.003	1.000
U-L282	1.006	1.003
U-L232	1.000	1.004

a) The Monte Carlo results have a 1σ statistical uncertainty of about .002.

GEORGIA INSTITUTE OF TECHNOLOGY

SCHOOL OF NUCLEAR ENGINEERING E-26-201

Atlanta, Georgia 30332 (404) 894-3720

November 7, 1979

MEMORANDUM

TO: C. R. Weisbin, J. H. Marable, and M. L. Williams (ORNL)

FROM: J. M. Kallfelz and P. Levin

SUBJECT: Progress Report for ORNL Subcontract 7802, Period October 13 - November 6, 1979

Summary

Accomplishments for Report Period

- EPRI-CELL calculations have been performed for the BAPL and mixed oxide lattices using the ENDF/B-5 library which recently arrived at ORNL. The results are analyzed and compared to those of previous calculations.

- Investigations concerning the inclusion of the k-reset mechanism in reactor cost performance studies have been continued. An approach suggested by J. H. Marable has been shown to be consistent with the basic equations and an expression we suggested in a previous report. Values for the fuel cycle cost standard deviation with and without explicit inclusion of the k-reset mechanism in the sensitivity coefficients are compared.

Plans for Work for Next Report Period

- For EPRI-CELL, investigation of the convergence behaviour using a heavy scatterer ring will be completed, reference results will be established, and the fine mesh effect will be evaluated. Also, the grain effect formulation in EPRI-CELL will be checked further.

- When the corrected ENDF/B-5 libraries arrive at ORNL the BAPL and mixed oxide criticals will be recalculated with EPRI-CELL.

- With the participation of Ron Cobb, a consultant for the project, we will initiate isotopic calculations for Yankee Rowe core V.

- We will discuss with General Electric the cost performance studies, to try to determine the impact of their reorganization on the level and responsibility division of our oft-proposed joint research. Investigations of the inclusion of k-reset mechanisms will be continued.

- CPM work has a lower priority than the above topics, but if time allows we will initiate CPM calculations of the Yankee Rowe core V for isotopics evaluation.

1. EPRI-CELL (P. Levin)

1.1 General

When the ENDF/B-5 based EPRI-CELL libraries arrived at ORNL, we reran the BAPL (1) and mixed oxides (2,3) critical lattices. These runs were done with the same version of EPRI-CELL as the ENDF/B-4 runs most recently reported. Yet it turned out that the ν values used in the libraries are incorrect. As far as $\bar{\nu}$ for the THERMOS is concerned, R. Q. Wright has manually installed a fixup to correct these numbers in the program. The epithermal range is kept unaltered for the time being and it should be kept in mind while evaluating the results. Yet since 90% of fissions are in the thermal range, the overall error is expected to be a small one. A corrected library tape is being prepared by R. E. MacFarlane and once it arrives in ORNL we shall try it.

As previously reported (4), we have applied the grain heterogeneity correction option of EPRI-CELL on the MO_2 lattices, but the calculated influence on k_{eff} is negligible. In order to verify that the program does expect the grain size to be entered in cm, we reran a case with the grain size entered in μm. The problem did not converge, with part of fluxes being negative. It is obvious that the underestimation of the grain effect is caused by the program rather than by input.

1.2 Results

The results for the three BAPL critical lattices are presented in Table 1. The Mixed Oxides calculations are presented in Table 2.

1.2.1 BAPL Critical Lattices

The ENDF/B-5 cross sections are more reactive than those of ENDF/B-4: k_∞ is 1.0% to 1.1% higher, and k_{eff} is 1.2% to 1.3% higher.

Table 1 Some Results for BAPL Critical Assemblies. Calculated Results are for the ORNL EPRI-CELL Version.[a] Experimental Values are from (1).

Parameter	Source	BAPL-1	BAPL-2	BAPL-3
k_∞	ENDF/B-4	1.1254	1.1317	1.1207
"	ENDF/B-5	1.1380	1.1436	1.1317
k_{eff}	ENDF/B-4	.9893	.9914	.9937
"	ENDF/B-5	1.0019	1.0035	1.0051
δ_{25}	EXP	.084 (±2.4%)	.068(±1.5%)	.052(±1.9%)
"	ENDF/B-4	.084	.069	.053
"	ENDF/B-5	.083	.068	.052
ρ_{28}	EXP	1.39(±0.7%)	1.12(±0.9%)	.906(±1.1%)
"	ENDF/B-4	1.46	1.21	.944
"	ENDF/B-5	1.42	1.17	.917
δ_{28}	EXP	.078(±5.1%)	.070(±5.7%)	.057(±5.2%)
"	ENDF/B-4	.072	.062	.051
"	ENDF/B-5	.075	.064	.053

a) EPRI-CELL results, for U-235 $\chi(E)$, B1, with MacFarlane's disadvantage factor, using heavy scattering ring boundary condition. The latest ENDF/B-4 tape at ORNL as of 10 October was used. The latest ENDF/B-5 tape at ORNL was used with R.Q. Wright's mannual correction of $\bar{\nu}$.

Table 2 Results for MO_2 Lattices from NP-691 (3) and for ENDF/B-4[d] and ENDF/B-5[e] Cross Sections

Lattice	Library	k_∞		k_{eff}		ρ_{28}		δ_{25}		δ_{28}		CR	
		EC[a]	NP	EC[a]	NP[b]	EC	NP	EC	NP	EC	NP	EC	NP
U-L266	ENDF/B-4	1.296	1.294	1.003	.997	5.09	5.11	.301	.288	.461	.441	3.24	3.28
	ENDF/B-5	1.308		1.012		4.94		.296		.481		3.18	
U-L250	ENDF/B-4	1.233	1.228	.994	.987	5.44	5.51	.323	.308	.482	.460	3.38	3.45
	ENDF/B-5	1.244		1.002		5.29		.318		.503		3.32	
U-L189	ENDF/B-4	1.386	1.384	.996	.996	2.24	2.23	.125	.120	.258	.242	1.95	1.95
	ENDF/B-5	1.396		1.004		2.16		.123		.266		1.92	
U-L212	ENDF/B-4	1.164	1.151	1.009	1.005	2.72	2.71	.154	.148	.297	.281	2.20	2.20
	ENDF/B-5	1.168		1.013		2.65		.153		.309		2.17	
U-L282	ENDF/B-4	1.373	1.367	1.017	1.018	1.55	1.54	.0860	.0825	.197	.185	1.59	1.58[c]
	ENDF/B-5	1.379		1.024		1.50		.0848		.203		1.56	
U-L232	ENDF/B-4	1.143	1.128	1.009	1.004	1.89	1.86	.105	.101	.230	.216	1.77	1.76[c]
	ENDF/B-5	1.143		1.010		1.85		.105		.239		1.75	

a) EPRI-CELL results, for Pu-239 $\chi(E)$, B1, with MacFarlane's disadvantage factor, using heavy scattering ring boundary condition. Without grain heterogeneity correction.

b) Calculated results from NP-691. HAMMER was used for the k_{eff} calculations, and probably also for the other parameters.

c) NP-691 values assumed to have only decimal point error, and hence multiplied by ten in this table.

d) Latest ENDF/B-4, tape at ORNL as of 10 October was used.

e) Latest NEDF/B-5 tape at ORNL was used, with R.Q. Wright's manual correction of $\bar{\nu}$.

ENDF/B-5 results, in general, are closer to the experimental (1) than those of ENDF/B-4. (Except for δ_{25} of BAPL-1: -1.2% v:s 0.0% with ENDF/B-4.)

The following are deviations from experimental results:

k_{eff}: 0.2% to 0.5%

ρ_{28}: 1.2% to 4.5%

δ_{25}: 0.0% to -1.2%

δ_{28}: -3.9% to -8.6%

There is no distinct mode of relating the above deviations to water-to-fuel ratios.

Odelli Ozer has recently cited (5) results of calculations for these critical lattices using a combination of Monte Carlo and transport theory. Our results are rather close to his with deviations of up to -0.09% in k_{eff}, -1.2% in δ_{25}, 0.4% in ρ_{28} and -1.6% in δ_{28}. Our results for k_{eff} are closer to unity than Ozers' for BAPL-1 and 3. Yet, Ozers' reaction rates ratios are closer to the experimental values.

1.2.2 Mixed Oxides Critical Lattices

The ENDF/B-5 cross sections yield higher k (both k_∞ and k_{eff}) but the deviation from ENDF/B-4 values decreases with the increase of water to fuel ratio and borating. In no case does the deviation between the versions exceed 0.9%.

In general, the ENDF/B-5 is worse k-wise in comparison with ENDF/B-4 since it deviates further from NP (3) results (0.9% to 1.3% in k_∞ and 0.6% to 1.5% in k_{eff}).

ρ_{28} and CR decrease as trade-off for reactivity gain:

ρ_{28}: -0.5% to -4.0%

CR: -0.6% to -3.8%

δ_{25} is somewhat lower than ENDF/B-4 but still above NP (2.5% to 4.0% v:s 4.0% to 4.9%).

δ_{28} results are higher than both ENDF/B-4 and NP (up to 10.7% v:s up to 6.6% at ENDF/B-4).

2. Inclusion of k-reset Mechanism in Evaluation of Integral Parameter Correlations and Reactor Cost Performance (J. Kallfelz)

The study reported in our ANS paper (6) used sensitivity coefficients which did not include a "k-reset" mechanism, although the correlation between the breeding ratio (BR) and the critical enrichment (ε_c) is included. In Appendix A of our June progress report, I discuss some considerations concerning the inclusion of the k-reset mechanism.

A topic which concerned me was the definition of a cost coefficient accounting for k-reset enrichment changes, $\left(\frac{\partial \$}{\partial BR}\Big|_r\right)$. The proper definition of this coefficient and the appropriate method of calculating it with COROPT were not clear to me. As mentioned in (7), it appeared to me that it might be necessary to use the cross sections as the basic parameters, rather than the integral parameters. For this approach the cost sensitivity associated with the k-reset mechanism seemed easier to define, since it could be associated with each σ_i.

In a subsequent discussion (8), Jim Marable suggested that perhaps the proper inclusion of the k-reset mechanism did not require the definition of such a coefficient. The expression suggested by Jim is:

$$VAR(\$) = \left(\frac{\partial \$}{\partial BR}\right)^2 SD_r^2(BR) + \left(\frac{\partial \$}{\partial E_c}\right)^2 SD^2(E_c) + 2\,\frac{\partial \$}{\partial BR}\,\frac{\partial \$}{\partial E_c}\,COV_r(E_c, BR) \qquad (1)$$

where, as in Ref. 7,

SD = the standard deviation

COV = Covariance

VAR = Variance

$ = Fuel Cycle Cost

and a subscript r indicates that the enrichment k-reset mechanism has been included in the definition.

Note that while the BR standard deviation and COV include the k-reset mechanism, the $\frac{\partial \$}{\partial BR}$ coefficient does not.

In this section it is shown that Eqn. (1), involving integral parameters, is at least consistent with the basic equations, involving cross sections, given in Appendix B of Ref. 7. The difference between the results for VAR($) with and without a k-reset mechanism will be numerically demonstrated, and the question as to which is "most appropriate" for cost sensitivity studies is unfortunately still not resolved.

In the following discussion, the expressions will generally be in terms of the multiplication constant k rather than ϵ_c, for simplicity. The conversion between the two parameters can be performed as in Ref. 6.

2.1 Derivation Using Basic Equations

As stated in Ref. 7, (Eqns. B-21 and B-22), the basic equations are

$$VAR(\$) = \sum_{i,j} \frac{\partial \$}{\partial \sigma_i} \frac{\partial \$}{\partial \sigma_j} COV(\sigma_i, \sigma_j) \qquad (2)$$

and

$$\frac{\partial \$}{\partial \sigma_i} = \sum_h \frac{\partial \$}{\partial I_h} \frac{\partial I_h}{\partial \sigma_i} \qquad (3)$$

Let us consider two variables, k and BR, and include the k-reset mechanism in the $\frac{\partial BR}{\partial \sigma_i}$ sensitivity coefficient. It may be argued

that this inclusion automatically leads to Eqn. (1). However, it appears to me easier to justify this expression in Eqn. (3), explicity involving the cross section sensitivity coefficients, than in Eqn. (1).

For this case:

$$\frac{\partial \$}{\partial \sigma_i} \simeq \frac{\partial \$}{\partial BR} \frac{\partial BR}{\partial \sigma_i}\Big|_r + \frac{\partial \$}{\partial k} \frac{\partial k}{\partial \sigma_i} \qquad (4)$$

where $\frac{\partial \$}{\partial k}$ can be defined in terms of ε_c.

Eqns. (4) and (2) yields

$$VAR(\$) = \left(\frac{\partial \$}{\partial BR}\right)^2 \underbrace{\sum_{i,j} \frac{\partial BR}{\partial \sigma_i}\Big|_r \frac{\partial BR}{\partial \sigma_j}\Big|_r COV(\sigma_i, \sigma_j)}_{SD_r^2(BR)}$$

$$+ \left(\frac{\partial \$}{\partial k}\right)^2 \underbrace{\sum_{i,j} \frac{\partial k}{\partial \sigma_i} \frac{\partial k}{\partial \sigma_j} COV(\sigma_i, \sigma_j)}_{SD^2(k)}$$

$$+ 2 \frac{\partial \$}{\partial BR} \frac{\partial \$}{\partial k} \underbrace{\sum_{i,j} \frac{\partial BR}{\partial \sigma_i}\Big|_r \frac{\partial k}{\partial \sigma_j} COV(\sigma_i, \sigma_j)}_{COV_r(BR,k)} \qquad (5)$$

Eqn. (5) is identical to Eqn. (1), except for the conversion from k to ε_c.

2.2 "k-reset" Mechanism in Cost Coefficients for Individual Cross Sections

In section B.2.3 of Ref. 7, I considered the use of the cross sections rather than integral parameters as the basic parameters, including the cost sensitivity associated with the k-reset mechanism for each σ_i. I assumed only one independent variable, BR, and defined the cost sensitivity in Eqn. (B-27) of Ref. 7:

$$\left.\frac{\partial \$}{\partial \sigma_i}\right|_r = \left.\frac{\partial BR}{\partial \sigma_i}\right|_r \frac{\partial \$}{\partial BR} - \left(\frac{\partial k/\partial \sigma_i}{\partial k/\partial \varepsilon}\right)\frac{\partial \$}{\partial \varepsilon} \qquad (6)$$

where the second term on the right hand side is the k-reset cost component.

It is trivial to show that this approach is actually identical to that in Sec. 2.1., if we define the $\frac{\partial \$}{\partial k}$ term in Eqn. (4) in terms of ε_c, as follows:

$$\frac{\partial \$}{\partial k} = \frac{\partial \$}{\partial \varepsilon_c} \Big/ \frac{\partial k}{\partial \varepsilon_c} \qquad (7)$$

$$\frac{\partial \$}{\partial \varepsilon} = \frac{\partial \$}{\partial \varepsilon_c} \qquad (8)$$

$$\frac{\partial k}{\partial \varepsilon_c} = -\frac{\partial k}{\partial \varepsilon} \qquad (9)$$

Thus

$$\frac{\partial \$}{\partial k} = -\frac{\partial \$}{\partial \varepsilon} \Big/ \frac{\partial k}{\partial \varepsilon} \qquad (10)$$

With Eqn. (10), Eqns. (4) and (6) are identical. Then Eqn. (6) in Eqn. (2) yields the same result as that given for Sec. 2.1 in Eqn. (5).

2.3. Numerical Example with k-reset

The covariance elements in Table 3 were supplied by Jim Marable (11). They are calculated for the studies reported in your Gatlinburg paper (10).

Table 3. Covariance Values for Study in Ref. 10

	k	BR	BR_r
k	3.951-4		
BR	-1.075-3	3.698-3	
BR_r	-2.883-4	1.559-3	9.856-4

The k and BR values in Table 3 are the same values as those which we used in our ANS paper (6). The values are relative, i.e. the k, BR term is:

$$[COV(k, BR)]/(k \cdot BR)$$

Converting from k to ε_c; using $\frac{k}{\varepsilon_c}\frac{d\varepsilon_c}{dk} = -1.82$, from Ref. 6,

$$\frac{SD^2(\varepsilon_c)}{\varepsilon_c^2} = \frac{SD^2(k)}{k^2}\left(\frac{k}{\varepsilon_c}\frac{d\varepsilon_c}{dk}\right)^2 = (3.951-4)(-1.82)^2$$

$$= 1.306-3 \qquad (11)$$

similarly

$$\frac{COV_r(\varepsilon_c, BR)}{\varepsilon_c \cdot BR} = \frac{COV_r(k, BR)}{k \cdot BR}\left(\frac{k}{\varepsilon_c}\frac{d\varepsilon_c}{dk}\right)$$

$$= (-2.883-4)(-1.82) = 5.247-4 \qquad (12)$$

For relative units, Eqn. (1) has the following form:

$$\frac{VAR(\$)}{\$^2} = \left(\frac{BR}{\$}\frac{\partial \$}{\partial BR}\right)^2 \frac{SD_r^2(BR)}{BR^2} + \left(\frac{\varepsilon_c}{\$}\frac{\partial \$}{\partial \varepsilon_c}\right)^2 \frac{SD^2(\varepsilon_c)}{\varepsilon_c^2}$$

$$+ 2\left(\frac{BR}{\$}\frac{\partial \$}{\partial BR}\right)\left(\frac{\varepsilon_c}{\$}\frac{\partial \$}{\partial \varepsilon_c}\right) COV_r(\varepsilon_c, BR) \qquad (13)$$

Using the cost coefficients from Ref. 6

$$\frac{BR}{\$}\frac{\partial \$}{\partial BR} = -1.14 \quad \text{and} \quad \frac{\varepsilon_c}{\$}\frac{\partial \$}{\partial \varepsilon_c} = 0.35$$

and the values from Eqns. (11) and (12) and Table 3, we calculate the following value with Eqn. (13)

$$\frac{VAR(\$)}{\$^2} = 10.25 - 4 \qquad (14)$$

and

$$\frac{SD(\$)}{\$} = 3.20 - 2 \qquad (15)$$

The latter value is much smaller than the $\frac{SD(\$)}{\$}$ value of 5.84-2 calculated in Ref. 6, using the covariance terms without k-reset.

Incidentally, it is of interest to note that using the values in Table 3,

$$COR_r(BR,k) = \frac{COV_r(BR,k)}{SD_r(BR)\,SD(k)} = -0.463 \qquad (16)$$

This is considerably higher than the value of -0.10 given in your later work (12), which includes methods uncertainties.

2.4 Integral Relations

In the course of examining the relation between the various expressions, the following relations were derived, which may be useful for future comparisons.

From Refs. 6 and 9,

$$\mathrm{cov}(I_k, I_l) = \sum_{i,j} \frac{\partial I_k}{\partial \sigma_i} \frac{\partial I_l}{\partial \sigma_j} \mathrm{cov}(\sigma_i, \sigma_j) \qquad (17)$$

Furthermore (10):

$$\left.\frac{\partial BR}{\partial \sigma_i}\right|_r = \frac{\partial BR}{\partial \sigma_i} - \frac{\partial k}{\partial \sigma_i} b \qquad (18)$$

where

$$b = \left[\frac{\partial BR}{\partial \varepsilon} \Big/ \frac{\partial k}{\partial \varepsilon}\right]$$

Eqn. (18) and $\frac{\partial k}{\partial \sigma_j}$ in Eqn. (17) yields:

$$\mathrm{cov}_r(BR, k) = \mathrm{cov}(BR, k) - b\, SD^2(k) \qquad (19)$$

Similarly, we can derive

$$SD_r^2(BR) = SD^2(BR) + b^2 SD^2(k) - 2b\,\mathrm{cov}(BR, k) \qquad (20)$$

References

1. H. Alter et al., "Cross Section Evaluation Working Group Benchmark Specification," BNL-19302 (ENDF-202), Brookhaven National Laboratory, Revised September, 1978, pages T(18-20)-1-3.

2. R. I. Smith and G. J. Konzek, "Clean Critical Experiment Benchmarks for Plutonium Recycle in LWRs," EPRI NP-196, Electric Power Research Institute, April 1976.

3. R. Sher and S. Fiarman, "Analysis of Some Uranium Oxide and Mixed-Oxide Lattice Measurements," EPRI NP-691, Electric Power Research Institute, February 1978.

4. J. M. Kallfelz and P. Levin, "Progress Report on Work for ORNL Subcontract 3986, Period September 11 - October 12, 1979," Memorandum to C. R. Weisbin and M. L. Williams, dated October 15, 1979.

5. O. Ozer, "Nuclear Data Needs for LWR Applications," Proc. International Conf. on Nuclear Cross Sections for Technology, Knoxville, October 1979, Table 5.

6. D. Rinaldis, J. M. Kallfelz, E. Kujawski, and J. H. Marable, "Evaluation of Integral Parameter Correlations and Reactor Performance Using Nuclear Data Covariances," to be published in Trans. ANS, San Francisco Meeting (Attachment A to Ref. 7).

7. J. M. Kallfelz, D. Rinaldis, M. Segev, and P. Levin, "Progress Report on Work for ORNL Subcontract 3986, Period June 1-30, 1979," memorandum to C. R. Weisbin, J. H. Marable, and M. R. Williams, dated July 8, 1979.

8. J. H. Marable, private communication, August 15, 1979,

9. C. R. Weisbin, J. M. Kallfelz, H. S. Bailey, and E. Kujawski, "Economic Impact of Uncertainties in Data Adopted for Core Design," Attachment 1 to letter from D. B. Trauger, ORNL, to R. G. Staker, DOE, dated September 25, 1978.

10. J. H. Marable and C. R. Weisbin, "Uncertainties in the Breeding Ratio of a Large LMFBR," Proc. ANS Reactor Physics Division Topical Meeting, Gatlinburg, Tennessee (April 1978).

11. J. H. Marable, private communication, July 13, 1979.

12. J. H. Marable, C. R. Weisbin, and G. de Saussure, "Uncertainty in the Breeding Ratio of a Large LMFBR: Theory and Results," submitted to Nucl. Sci. Engr. in October 1979.

SCHOOL OF NUCLEAR ENGINEERING E-26-801

Atlanta, Georgia 30332 (404) 894-3720

December 7, 1979

MEMORANDUM

TO: C. R. Weisbin. J. H. Marable, and M. L. Williams (ORNL)

FROM: J. M. Kallfelz and P. Levin

SUBJECT: Progress Report for ORNL Subcontract 7802, Period November 7 - December 6, 1979

Summary

Accomplishments for Report Period

- A presentation concerning our joint work with General Electric on cost implications of data uncertainties was prepared and given at the San Francisco ANS meeting.
- A meeting was held at GE-ARSD to discuss future plans for possible joint work on sensitivity analysis and reactor performance studies. Based on comments of the GE staff, recommendations and information concerning addition of several important integral parameters to the capability of the ORNL sensitivity codes are presented.
- The first test EPRI-CELL calculations of isotopics for the Yankee Rowe PWR Core V have been performed.
- Various EPRI-CELL methods and characteristics, including convergence, grain effect treatment, and mesh size influence, have been investigated. Results are presented for these investigations, as well as the initial testing of some improved routines developed by J. Barhen.
- Implementation of the new Israeli version of ANISN-B1 has been initiated.

Plans for Work for Next Report Period

- EPRI-CELL calculations of isotopics for the Yankee Rowe PWR will be performed and analyzed for the cases of ENDF/B-IV and ENDF/B-V data.
- Testing of Barhen's improvements to EPRI-CELL will be completed.
- Work on implementation of the new Israeli version of the ANISN-B1 will be continued.

jhr

Enclosure (Report)

1. Sensitivity Study Activities (J. Kallfelz)

1.1. ANS Presentation and Visit to GE

A presentation concerning our joint work with General Electric on cost implications of data uncertainties was prepared and given at the San Francisco ANS meeting. The abstract of this joint paper[1] was Attachment A of a previous progress report[2].

On November 13, J. M. Kallfelz, C. R. Weisbin, and D. G. Cacuci visited General Electric Advanced Reactor Systems Department (GE-ARSD) to discuss future plans for possible joint work on sensitivity analysis and reactor performance studies. Primary contact was with Charley Cowan, and we also met with Ed Kujawski and several individuals involved in the development of COROPT[3], Nelson Deane and Bob Protsik. This development is now the responsibility of a group headed by Ron Murata.

Charley feels that the economic component of these studies should be downgraded for the time being, and that we should concentrate on uncertainties of more basic integral performance parameters. Both he and others to whom we spoke emphasized the importance of the maximum linear power and hot channel factors, and recommended that these parameters be considered in our further studies.

Charley Cowan said that he would respond by letter in about a month to questions listed by Chuck Weisbin concerning GE's potential commitment to a joint program.

1.2. Comments on Maximum Linear Power and Hot Channel Factors

Based on the comments mentioned above, it appears that it would be useful to add the maximum linear power to the integral parameters that can be analyzed with the ORNL sensitivity codes. This parameter is the maximum

allowable power produced per linear unit of fuel or fertile pin, and depends strongly on the conductivity and melting point of the fuel and fertile material, as well as other factors such as the clad material and the pellet-clad gap. A typical value is 16 kw/ft (530 w/cm) specified for mixed-oxide fuel for level II of the Large Heterogeneous Reference Fuel Design Study (LHRFDS)[4]. A thorough analysis of this value for various materials and pin designs was performed in conjunction with the Proliferation Resistant Preconceptual Core Design Study (PRPCDS)[5].

This parameter is directly related to an integral ratio which can easily be incorporated into the ORNL sensitivity code capabilities, namely the ratio of the peak and average power densities. The power densities for a homogeneous reactor model are calculated by many codes (including VENTURE[13]) in w/cm^3. Thus, given the pitch and design of the fuel assemblies, the linear power can be derived from the power density. If one assumes that all energy is released in the pellet, which should be adequate for initial sensitivity studies of homogeneous LMFBRs, then the linear power is simply the power density divided by the fuel volume fraction. For more precise values coupled neutron-gamma transport calculations are necessary.

Generally the peak linear power occurs either at the core center or at the inner radius of a core enrichment zone. COROPT[4] considers a two-zone reactor and contains the constraint that the peak power at the core reactor and the inner edge of the second core zone are equal. Since this is obviously not the case for all designs, and the sensitivity to cross section changes would be somewhat different at the two points, the sensitivity code should consider the ratio (point power density)/(average power density) at both these locations for a simple two zone homogeneous reactor.

For the general case, VENTURE[13] has the capability of determining the location and value of the maximum power density.

Hot channel factors are arrived at by complicated analysis involving many factors. Table 1 from the LHRFDS[4] guidelines gives an example of such factors for the CRBR. Note that determination of these factors is obviously an area which would benefit from development of systematic sensitivity analysis methods which would include nuclear, thermo-hydraulic and material data and calculational methods. Apparently the "nuclear data" factors in this table could be determined with the ORNL codes by an uncertainty analysis of the previously-discussed maximum linear power. Note also the first footnote in Table 1, concerning the uncertainties due to physics methods.

For a general discussion of allowances for power peaking and hot channels, see pages 127-141 of reference 6.

Table 1 (Table V of Ref. 4)

CRBRP FUEL ASSEMBLIES ROD TEMPERATURES HOT CHANNEL/SPOT FACTORS

		Coolant	Film	Cladding	Gap	Fuel	Heat Flux
DIRECT(+)							
Power Level Measurement and Control System Dead Band		1.03					1.03
Inlet Flow Maldistribution		1.05					
Subassembly Flow Maldistribution			1.035				
Calculational Uncertainties		1.08					
Cladding Circumferential Temperature Variation			1.0(◊) 1.7(*)	1.0(◊)			
STATISTICAL (3σ)(o)							
Inlet Temperature Variation		1.02(φ) 1.0(+)					
Reactor ΔT Variation		1.04(φ) 1.0(+)					
Nuclear Data		1.06					1.065
Fissile Fuel Maldistribution		1.01					1.035
Wire Wrap Orientation		1.01					
Subchannel Flow Area		1.028	1.0				
Film Heat Transfer Coefficient			1.12				
Pellet-Cladding Eccentricity			1.15	1.15			
Cladding Thickness & Conductivity				1.12			
Gap Conductance					1.48(1)		
Fuel Conductivity						1.10	
Coolant Properties		1.01					
TOTAL	2σ	1.232(φ) 1.221(+)	1.168 1.986(*)	1.128			1.081
	3σ	1.264(φ) 1.248(+)	1.234 2.101(*)	1.192	1.48	1.10	1.106

(+) Uncertainties due to physics analysis calculational methods and control rod effects (4% on coolant enthalpy rise and 5% on heat flux) are applied directly on nuclear radial peaking factors.

(*) For cladding midwall temperature calculations. Applies to nominal temperature drop between cladding midwall and bulk coolant.

(◊) For fuel temperature calculations.

(o) In addition, the assembly inlet temperature will be increased by 16°F. to account for primary loop temperature control uncertainties.

(1) Applies to BOL conditions.

(φ) Applies to Plant Expected Operating Conditions.

(+) Applies to Plant T&H Design Conditions.

Table 1 (Continued)

CRBRP FUEL ASSEMBLIES PLENUM PRESSURE HOT CHANNEL FACTORS

		Plenum Temperature	Burnup
DIRECT(+)			
Power Level Measurement		1.02	1.02
Inlet Flow Maldistribution		1.05	
Subassembly Flow Maldistribution Calculational Uncertainties		1.08	
STATISTICAL (3σ)(o)			
Inlet Temperature Variation		1.02(ϕ) 1.0(†)	
Reactor . T Variation		1.04(ϕ) 1.0(†)	
Nuclear Data		1.06	1.06
Fissile Fuel Maldistribution		1.01	1.01
Wire Wrap Orientation		1.01	
Coolant Properties		1.01	
TOTAL	2σ	1.216(ϕ) 1.205(†)	1.061
	3σ	1.246(ϕ) 1.229(†)	1.082

(+) Uncertainties due to physics analysis calculational methods and control rod effects (4% for both plenum temperature and burnup) are applied directly on nuclear radial peaking factors.
(ϕ) Applies to Plant Expected Operating Conditions.
(†) Applies to Plant T&H Design Conditions.
(o) In addition, the assembly inlet temperature will be increased by 16°F to account for primary loop temperature control uncertainties.

2. EPRI-CELL Power Reactor Isotopics (J. Kallfelz)

Isotopic calculations for Yankee Rowe Core V[7] have been initiated with EPRI-CELL. The results are for zircaloy-clad fuel elements, those referred to as "Yankee Zircaloy results" in Part I, Chapter 3, the EPRI-CELL isotopics benchmarking section of the ARMP documentation[8].

The input for this case was obtained from Odelli Ozer and is that used by NAI for the results reported in the above-mentioned ARMP benchmarking chapter. As a test we first calculated this case on the Berkeley computer using the NAI cross sections and, as shown in Figure 1, our results are identical with those of the ARMP documentation, as they should be.

Runs for this case have been attempted for ENDF/B-IV on the ORNL-360, but have not yet run due to the absence of zirconium from the ENDF/B-IV tape. The input will be changed and rerun when R. Q. Wright has resolved a reported problem with an EPRI-CELL case involving burn-up which he attempted.

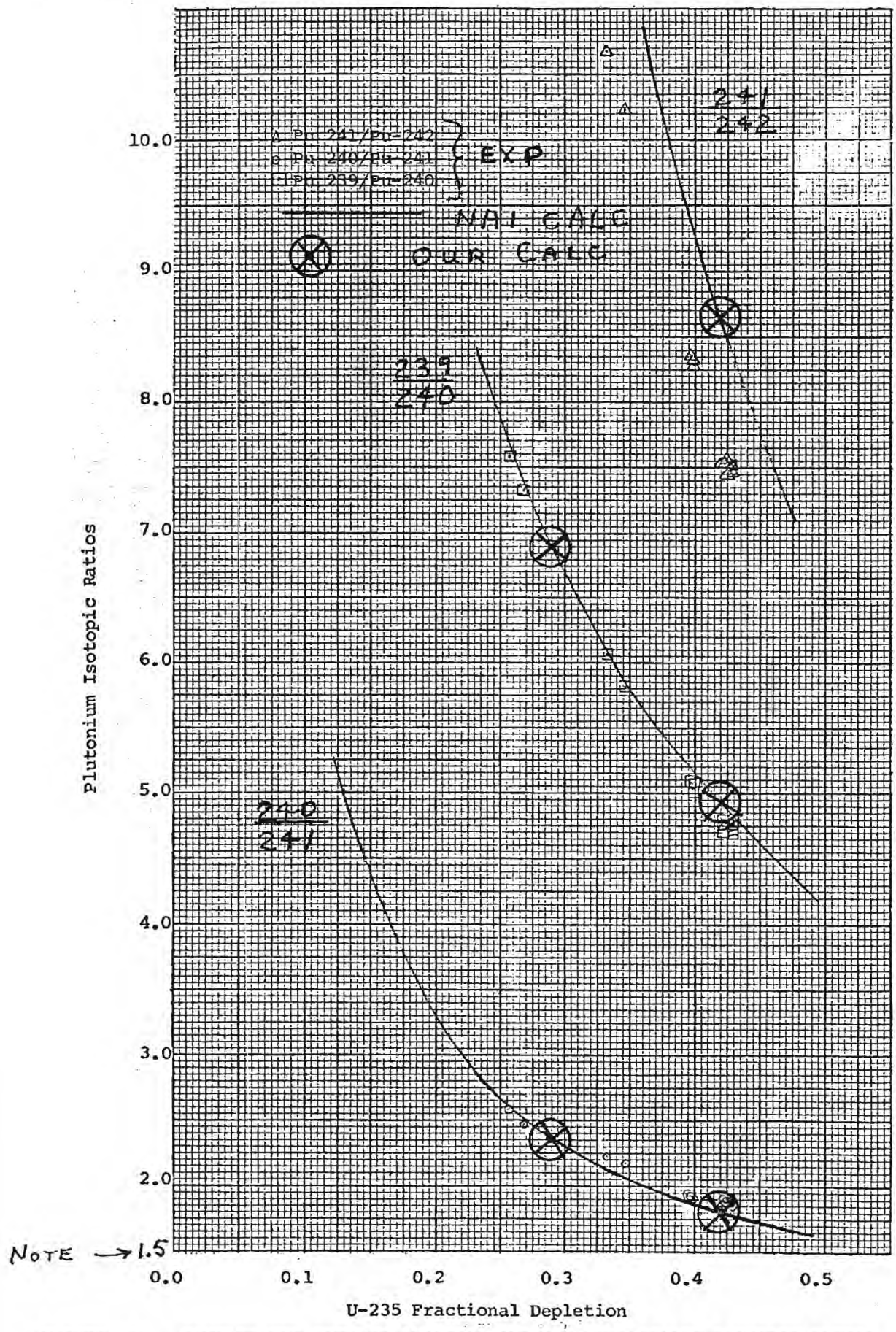

FIGURE 1 COMPARISONS BETWEEN ANALYSIS AND YANKEE ZIRCALOY ISOTOPIC RATIOS
(From Fig. 3-1, Part 1, Chapter 3 of Ref. 8)

3. EPRI-CELL Methods Investigations (P. Levin)

3.1. General

The short period reported was mainly dedicated to the completion of standing unresolved effects. Namely: convergence, grain heterogeneity mesh refinement and small changes in temperature.

All the work referred to in this section used the ENDF/B-5 based libraries as cited in our previous report[9]. We still await the new ENDF/B-5 version to arrive in ORNL.

This seems to conclude the present set of critical lattices tests and, as mentioned in section 2, we plan to proceed with the power reactor isotopics now.

3.2. Convergence

As we had not been able to converge our fine mesh runs with the "isotropic" boundary option, we had to use the heavy scatterer on the periphery of the cell to get the same effect. The guidelines[10] for such a technique call for two mesh points in the heavy scattering ring (HSR). Yet, we could not get a convergence with more than one mesh point. It turned out that one should avoid the use of the "isotropic" boundary option (i.e. OPTION (8) = 1) when using the heavy scattering ring.

The tables of our previous report[9] were altered in the last moment to incorporate the corrected results. Yet, several points should be mentioned:

a. The "isotropic" boundary option prevented convergence but still yielded results within less than 1% deviation from the correct HSR runs (less than .5% for k_{eff}) both for BAPL and MO_2 lattices.

b. The wrong HSR runs (single point in HSR) deviate from the correct runs within .3% (.2% for k).

An improved version of several EPRI-CELL routines was received from J. Barhen in ORNL. These routines should eliminate the need for HSR to obtain isotropic boundary conditions and convergence as well. Some results for the BAPL-3 lattice without and with these improvements are compared in Table 2.

The coarse mesh will be discussed later, but for the fine 9-4-9 arrangement there is an agreement within less than 0.2% deviation from the HSR case. Yet, the "unconverged" standard case does not seem worse than that (except for the execution time).

A similar test is being done with several MO_2 lattices, and the results will be reported separately.

3.2. Grain Effect

As already reported[11] our calculations of the grain reactivity effect in MO_2 lattices resulted in values 10 times smaller than the predicted[12]. This effect has been checked with the original NAI version at Berkeley and the results are of the same order of magnitude as ORNL/ENDF calculations. Apparently there is a mistake in the program.

3.3 Mesh Size

In contradiction to our early EPRI-CELL calculations, our most updated results are based on a rather fine mesh (9-4-9), as discussed in a previous report[11]. The effect of changing the mesh size was tested for the "loosest" lattices: BAPL-3 and MO_2 lattice U-L282. The results are presented in tables 3 and 4 respectively, for calculations without the Barhen improvements but using the correct HSR options.

Observations:

(i) Within a range of tripling the mesh-size the changes are quite small, often insignificant considering the convergence criterion

Table 2. Calculation of BAPL-3 Lattice Using the Standard[a] and the Improved[b] Versions of EPRI-CELL

Version	Standard		Improved	
Arrangement	9-4-9-2 (HSR)[c]	9-4-9	9-4-9	3-2-3
# of Interactions	19	51[d]	8	7
Execution time (sec)/Model	38.02/91	29.20/3A	15.33/3A	9.23/91
k_∞	1.1317	1.1298	1.1300	1.1307
k_{eff}	1.0051	1.0035	1.0037	1.0043
ρ_{28}	.916930	.918438	.918332	.917821
δ_{25}	.0519294	.0519803	.0519671	.0519326
δ_{28}	.0527374	.0528302	.0528194	.0527853
CR	.660350	.660879	.660781	.660543

(a) DSN = E.RQW00000.ORNL.ECELL.MODULE

(b) Corrections according to J. Barhen

(c) Heavy Scattering Ring Zone added to obtain isotropic boundary conditions

(d) Did not converge. Max Flux Deviation: 5.5-3 while the required convergence: 3.4-4. ("Isotropic" boundary option used for this case only.)

Table 3. Results for BAPL-3 Lattice with Various Mesh Sizes

Arrangement[a]	k_∞	k_{eff}	ρ_{28}	δ_{25}	δ_{28}	CR
9-4-9[b]	1.1317	1.0051	.916930	.0519294	.0527374	.660350
7-2-7	1.1319	1.0053	.916719	.0519321	.0527252	.660298
5-2-5	1.1311	1.0046	.917362	.0519323	.0527645	.660489
4-2-4	1.1305	1.0041	.917859	.0519547	.0527940	.660660
3-2-3	1.1308	1.0043	.917600	.0519621	.0527793	.660607

[a] There is an additional Heavy Scattering Ring Zone which is the same for all the cases and contains 2 mesh points.

[b] The Reference Case.

Table 4. Results for MO_2 Lattice U-L282 with Various Mesh Sizes

Arrangement[a]	k_∞	k_{eff}	ρ_{28}	δ_{25}	δ_{28}	CR
9-4-9[b]	1.3792	1.0240	1.50233	.0847635	.203082	1.56161
8-2-8	1.3792	1.0240	1.50201	.0847290	.203045	1.56142
7-2-7	1.3790	1.0239	1.50168	.0846899	.203006	1.56122
6-2-6	1.3789	1.0237	1.50132	.0846560	.202963	1.56101
5-2-5	1.3786	1.0236	1.50052	.0845783	.202865	1.56053
4-2-4	1.3793	1.0241	1.49891	.0844888	.202661	1.55965
3-2-3	1.3796	1.0242	1.49621	.0842732	.202325	1.55808

[a] There is an additional Heavy Scattering Ring Zone which is the same for all cases and contains 2 mesh points.

[b] The Reference Case.

(1.0-4) and the number of IBM 360 significant figures.

(ii) The effects on k are within 0.1% for BAPL-3 and 0.04% for U-L282.

(iii) The BAPL reaction rates are slightly effected (within 0.1%), yet the MO_2 reaction rates are changed by up to 0.6%.

(iv) The BAPL k generally decreases with the increase of mesh-size. The trend for the MO_2 lattice is insignificant in contrast to previous reported results for the tightest MO_2 lattice[11], which were, however less reliable due to convergence problems.

(v) There is a clear trend for the various reaction rate ratios to decrease for the MO_2 lattice while increasing mesh size. The general trend of the BAPL-3 lattice is just the opposite.

3.4 Small Changes in Temperature

The actual temperatures for the MO_2 critical experiments were nearly 295°K. Our calculations were done with 300°K. Although one does not expect these 5°K to appreciably change the results, we did check it. The effect on k was of 0.02% and the most sensitive ratio ρ_{28} was changed by -0.1%.

4. Other Accomplishments (P. Levin)

I visited ORNL on November 27-28, 1979 and started implementing the new Israeli version of ANISN-B1 into the one currently in operation at ORNL. This work is being continued at Georgia Tech.

References

1. D. Rinaldis, J. M. Kallfelz, E. Kujawski, and J. H. Marable, "Evaluation of Integral Parameter Correlations and Reactor Performance Using Nuclear Data Covariances," Trans. ANS 33, 859 (1979).

2. J. M. Kallfelz, D. Rinaldis, M. Segev, and P. Levin, "Progress Report on Work for ORNL Subcontract 3986, Period June 1-30, 1979," Memorandum to C. R. Weisbin, J. H. Marable, and M. L. Williams dated July 8, 1979.

3. G. V. Neill and D. P. Johnson, "COROPT: A Computer Program for Finding Optimum LMFBR Mixed-Oxide Fuel Cores," GEFR-00006, UC-78, General Electric Fast Breeder Reactor Department, Sunnyvale, California (January 1977).

4. "Ground Rules Large Heterogeneous Reference Fuel Design Study," Revision II, Combustion Engineering, Inc., Windsor, Connecticut, November 24, 1976.

5. J. C. Chandler et al., "The Proliferation Resistant Preconceptual Core Design Study," TC-1082, Hanford Engineering Development Laboratory, March 1978.

6. A. Sesonske, Nuclear Power Plant Design Analysis, TID-26241, Technical Information Center, USAEC (1973).

7. J. B. Melehan, "Yankee Core Evaluation Program, Final Report," WACP-3017-6094 (January 1971).

8. "Advanced Recycle Methodology Program System Documentation," EPRI Report, CCM-3 Electric Power Research Institute (September 1977).

9. J. M. Kallfelz and P. Levin, "Progress Report on Work for ORNL Subcontract 7802, Period October 13 - November 6, 1979," Memorandum to C. R. Weisbin, J. H. Marable, and M. L. Williams, dated November 7, 1979.

10. J. Barhen, private communications.

11. J. M. Kallfelz and P. Levin, "Progress Report on Work for ORNL Subcontract 3986, Period September 11 - October 12, 1979," Memorandum to C. R. Weisbin, J. H. Marable, and M. L. Williams, dated October 15, 1979.

12. J. J. Ullo, "Analysis of UO_2 - PuO_2 Fueled Rod Lattices with ENDF/B-IV," WAPD-R(D)-496.

13. D. R. Vondy, T. B. Fowler, and G. W. Cunningham, "VENTURE: A Code Block for Solving Multigroup Neutronics Problems Applying the Finite-Difference Diffusion-Theory Approximation to Neutron Transport, Version II," ORNL-5062/R1, Oak Ridge National Laboratory (November 1977).

SCHOOL OF NUCLEAR ENGINEERING E-26-801

Atlanta, Georgia 30332 (404) 894-3720

GEORGIA INSTITUTE OF TECHNOLOGY

January 9, 1980

MEMORANDUM

TO: C. R. Weisbin, J. H. Marable, and M. L. Williams (ORNL)

FROM: P. Levin and J. Kallfelz

Subject: Progress Report for ORNL Subcontract 7802, Period December 7, 1979 - January 8, 1980

Accomplishments

- For the Zr-clad Yankee Rowe Core V elements, a BOL EPRI-CELL calculation has been performed with ENDF/B-IV data, and the results are close to those for the NAI data.

- Attempts to calculate a burn-up problem for the above case with the ORNL version of EPRI-CELL failed for both the NAI and ENDF/B-IV data, due to lack of convergence in THERMOS. Many runs with varying input options and iteration schemes were performed in our attempt to isolate the source of this problem which has not yet been resolved.

Plans for Work for the Next Report Period

- Investigations of the source of the above problem of THERMOS convergence will be continued.

- Calculations of isotopics for other power reactors included in the EPRI-CELL benchmarking will be performed.

- A response to the letter from C. Cowan concerning our proposed joint program with GE will be prepared in cooperation with Jim Marable.

1. EPRI-CELL

As already reported[1], we have been initiating the isotopic calculations with EPRI-CELL. The first case to be run is for the Zr-clad elements in the Yankee Rowe Core V[2]. It was a part of the EPRI-CELL isotopic benchmark[3], and the deck for reproducing NAI's reported results was obtained from Odelli Ozer. The reproduction run with NAI cross sections was done in Berkeley by J. Kallfelz and the reported results[1] are identical with those of ARMP documentation.

Since then we have been trying to run the same reproduction and a ENDF/B-IV version at ORNL. So far we have not been able to proceed beyond the first time step of the depletion calculation. The initial step converges rapidly without any difficulty. The k_{eff} and k_{∞} values at BOL are identical to those of the Berkeley run for the NAI cross sections while for the ENDF/B-IV data these values are about 1% lower than the NAI results. The burn-up calculation by CINDER yields densities very close to Berkeley's (Table 1). Yet the following THERMOS calculation does not converge.

Most of the reported period was dedicated to various trials to converge the runs. Nearly twenty different attempts, using different boundary conditions and/or iteration schemes have been run. Except for very short depletion steps (1 MWD/T) we have not been able to converge the thermal calculations.

Investigations are continuing of the source of this problem, which will hopefully be resolved soon. Attention is being focused on the influence of elements not present for the BOL case, particularly the fission products, since a BOL case with isotopic concentrations similar to those at the end of the first time step did not converge.

Table 1. Fuel Homogenized Number Densities Yankee Zr Case After 100 Hours Depletion Step.

Site :	Berkeley	ORNL	ORNL
Library :	NAI	NAI	ENDF/B-IV
Xe-135	7.747-9	7.746-9	7.833-9
Sm-149	3.067-8	3.066-8	3.063-7
U-235	6.550-4	6.550-4	6.551-4
U-236	3.141-6	3.141-6	3.118-6
U-238	2.182-2	2.182-2	2.182-2
Pu-239	2.444-6	2.443-6	2.477-6
Pu-240	1.022-8	1.022-8	1.020-8
Pu-241	1.020-10	9.960-11	1.015-10
Pu-242	1.298-13	1.266-13	1.181-13
FP EPITH	7.336-5	7.390-5	7.521-5
FP THERM	5.506-4	5.503-4	5.480-4

References

1. J. M. Kallfelz and P. Levin, "Progress Report on Work for ORNL Subcontract 7802, Period November 7 - December 6, 1979," Memorandum to C. R. Weisbin, J. H. Marable, and M. L. Williams, dated December 7, 1979.

2. J. B. Melehan, "Yankee Core Evaluation Program, Final Report," WACP-3017-6094 (January 1971).

3. "Advanced Recycle Methodology Program System Documentation," EPRI Report, CCM-3 Electric Power Research Institute (September 1977), Part I, Chapter 3.

SCHOOL OF NUCLEAR ENGINEERING E-26-801

Atlanta, Georgia 30332 (404) 894-3720

February 12, 1980

MEMORANDUM

TO: C. R. Weisbin. J. H. Marable, and M. L. Williams (ORNL)

FROM: J. M. Kallfelz and P. Levin

SUBJECT: Progress Report for ORNL Subcontract 7802, Period January 9 - February 11, 1980

Accomplishments

- A response to C. Cowan concerning our proposed joint program has been prepared in cooperation with Jim Marable (Refs. 3 and 4).
- The effect of the 1 eV resonance of Pu-240 on isotopic calculations in EPRI-CELL has been studied, as reported in Ref. 24.
- A study has been made of the feasibility of performing sensitivity analysis of the maximum linear power, utilizing VENTURE. The pertinent equations and approximations are discussed in this report. Based on discussions with Dave Vondy, it appears that development of a VENTURE capability to calculate functions for this analysis would be quite appropriate.
- Work on the initiation of EPRI-CELL isotopic calculations at ORNL for PWRs was continued. Various problems with regard to the code, nuclear data, and reactor modeling are discussed in this report.

Plans for Work for the Next Report Period

- The effort to develop a capability for sensitivity analysis of the maximum linear power will be continued.
- Work on EPRI-CELL isotopic calculations at ORNL will be continued. The goal is to complete runs for the Yankee Row reactor cases for Zr and SS clad assemblies by March, and to provide a report detailing the preparation of the code input using the basic references (e.g. Ref. 27).
- For ANISN-B1, steps will be taken to execute correctly the test problem. Further, additional programming will be performed to provide various desired edits, when the specifications of these edits are received from Mark Williams.

jhr

cc: D. Vondy, ORNL (w/o Appendix)
C. Cowan, GE-ARSD (w/o Appendix)

1. Sensitivity Analysis Capabilities for Further Integral Performance Parameters (J. Kallfelz)

This topic has been discussed in conjunction with our proposed joint program with GE[1-4], and much analysis has already been performed for the breeding ratio and critical enrichment[5-7]. It has been agreed that the further parameters most appropriate to initially consider are the maximum linear power and the hot channel factor (HCF), and our previous report[8] discusses these parameters.

As pointed out in our previous report[8] and Cowan's letter[2], the HCF is a complicated function of many components, derived from operational, thermal-hydraulic, and materials characteristics as well as nuclear data. On the other hand, the principal contribution to the calculated maximum linear power is from nuclear data and methods. The other major statistical contribution to the uncertainty of this parameter is maldistribution of fissile fuel. Thus, the maximum linear power is simpler to analyze with nuclear codes than is the HCF, and for this reason we shall initially concentrate on the former parameter.

The determination of the allowable maximum linear power is a complicated process, and in Ref. 8 we give some typical values and refer to a thorough analysis of this value for various fuel materials and pin designs performed in conjunction with the PRPCDS study[9]. We have also discussed this parameter in previous reports[10-11] for our studies of heterogeneous LMFBR cores with alternative fuel cycles.

The determination of the absolute value of the calculated maximum linear power is at any rate not an objective of this work. Rather, we desire to determine the uncertainty of the value, which for the approximations discussed below, will be more significant than the absolute value. Actually, we propose to investigate the uncertainty of the ratio of the peak power to the average power.

The generalized perturbation theory formalism of Gandini deals only with ratios of functionals of the real and adjoint fluxes. While Jim Marable has informed me that a theory has been developed at ORNL which can treat any response function, the treatment of a ratio for this case will probably be easier and should present no serious handicap, as discussed below.

1.1 Basic Equations

In this section we will summarize some of the basic equations of generalized perturbation theory and discuss their relation to the ratio of interest. This section should prove useful in further discussions with Dave Vondy and others about calculation of the related generalized adjoint functions, $\psi_j^*(\vec{r})$, with VENTURE[16].

If the linear power is assumed proportional to the power density, as will be discussed in sec. 1.3, then the peak-to-average linear power ratio can be expressed in terms of the power density peak-to-average ratio, calculated by CITATION[15] and VENTURE[16].

Let us consider a general expression for a reaction rate ratio[13]

$$R = \frac{\int_{Vol_1} \sum_j \Sigma_{1j}(\vec{r})\phi_j(\vec{r})\,d\vec{r}}{\int_{Vol_2} \sum_j \Sigma_{2j}(\vec{r})\phi_j(\vec{r})\,d\vec{r}} = \frac{a_1}{a_2} \qquad (1)$$

The relative change in this ratio due to changes in nuclear data has two components, the "direct" and "indirect" effects. The former component arises because of changes in the components of Σ_1 and Σ_2, and can be calculated by a trivial expression involving the unperturbed flux[17,18]. The following discussion will be concerned solely with the calculation of the indirect effect, which is calculated in the generalized perturbation theory formalism of Gandini[12] with the following multigroup expression[12,13].

$$\left.\frac{\delta R}{R}\right|_{indirect} \simeq \int \vec{\psi}^*[\delta B]\vec{\phi}\,d\vec{r} \qquad (2)$$

$\vec{\psi}^*(\vec{r})$ is the generalized adjoint function with group components $\psi_j^*(\vec{r})$ which give the importance of neutrons to R. $[B]$ is the Boltzman operator used to solve for $\vec{\phi}$, and $[\delta B]$ gives the changes in $[B]$ for the nuclear data changes of interest. The article of Cecchini and

Salvatores[13] is an excellent reference for the explicit form of the terms of Eqn. (2) in multi-group diffusion theory.

$\vec{\psi}^{*}(\vec{r})$ is a solution to the adjoint Boltzmann equation with a fixed source given for ratio R by:

$$S_j^*(\vec{r}) = \frac{\Sigma_{1j}(\vec{r})}{a_1} - \frac{\Sigma_{2j}(\vec{r})}{a_2} \qquad [3]$$

where Σ_1 and Σ_2 are zero outside Vol_1, and Vol_2, respectively.

Note that R as given in Eqn. (1) is quite general, and is the form for many ratios of interest, e.g. the breeding ratio, microscopic isotopic reaction rate ratios, and power density ratios. For the later case, which we are considering, both Σ_1 and Σ_2 have the same <u>form</u>[18]:

$$\Sigma_{ij}(\vec{r}) = \sum_k P^k \Sigma_{f,j}^k(\vec{r}) \qquad (4)$$

where P^k is the total recoverable energy release for one fission in the k-th isotope (assumed constant with fissioning energy, as in CITATION). As noted after Eqn. (3) Σ_{1j} and Σ_{2j} differ in their space range.

Since we are interested in the power density peak-to-average ratio, we can consider Vol_1 as a unit volume at the point of maximum power density, $\vec{r}_m$, and define the numerator of Eqn. (1) as a point value,

$$a_1 = \sum_j \Sigma_{1j}(\vec{r}_m)\,\phi_j(\vec{r}_m) \qquad [5]$$

The denominator can be defined as an average value,

$$a_2 = \int_{Vol_2} \sum_j \Sigma_{2j}(\vec{r})\,\phi_j(\vec{r})\,d\vec{r} \Big/ Vol_2 \qquad [6]$$

where Vol_2 is some appropriately defined volume, e.g. the core for a homogeneous reactor. (As noted in Sec. 1.3, the "core" may not be appropriate for a heterogeneous reactor if it is defined to include the interior fertile regions.)

In summary, the source needed to calculate the appropriate $\psi_j^*(\vec{r})$ in VENTURE is:

$$S_j^*(\vec{r}) = \frac{\Sigma_{1j}(\vec{r})}{a_1} - \frac{\Sigma_{2j}(\vec{r})}{a_2} \qquad (7)$$

with the $\Sigma_{ij}(\vec{r})$ defined in Eqn. (4).

$$\Sigma_{1j}(\vec{r}) = 0, \quad \vec{r} \neq \vec{r}_m$$

$$\Sigma_{2j}(\vec{r}) = 0, \quad \vec{r} \text{ outside } Vol_2$$

and a_1, a_2 defined in Eqns. (5) and (6).

1.2 Calculations with VENTURE

After discussions with Dave Vondy, I am optimistic about the prospects of using VENTURE for calculations of the desired ψ^* functions.

In principle, a general input capability to prepare S* for any ratio of the form given by Eqn. (1) is not difficult to develop. The basic reason that this capability has not been developed internal to VENTURE is that VENTURE does not have direct access to microscopic σ values. However, at the beginning of the "code chain" when the macroscopic cross section set is determined, certain macroscopic reaction cross sections are prepared and used in VENTURE, including those for the breeding ratio and the power density.

Thus, it appears that the cross sections in Eqn. (7) are available in VENTURE (which also determines $\vec{r}_m$) and that it would be simple to determine the desired S* and ψ^* in the same manner that this is presently accomplished for the breeding ratio, as follows.

After calculating ϕ and ϕ^*, VENTURE solves for the breeding ratio S*, and then "reaccesses" itself to calculate ψ^*. VENTURE writes out on files integrals such as

$$\int_{\text{region}} \vec{\psi}^*(\vec{r})\,\vec{\phi}(\vec{r})\,d\vec{r} \qquad [8]$$

which can then be used in Eqn. (2) to determine $\frac{\delta R}{R}$ for a given $\delta\sigma$.

1.3 Comments on Problems and Approximations for Linear Power Calculations

The approximations proposed for the first linear power rate calculations are reasonable, but some of them may need to be investigated further later. Also, there are certain problems in calculating this parameter that are not found in other reaction rate parameters such as the breeding ratio. Following is a potpourri of comments on such topics.

(a) Determination of relative rather than absolute value

As discussed in the previous sections, we propose to investigate the peak-to-average power ratio. It appears that the uncertainty in the calculated absolute value of the average power density can be considered zero, since this is actually a normalization term which depends on the required MWth. The impact of uncertainties in nuclear data which influence this term and hence the ratio R in Eqn. (1) are contained in the sensitivity expressions for R.

It appears to me that the proper place to treat the uncertainty in the average power density in the operating reactor is in the "direct" term of Table 1, Ref. 8, related to power level measurement.

(b) Recoverable energy released per fission

There are uncertainties in this parameter for the various nuclides, and it should also be a function of the fissioning neutron energy. In the sensitivity studies for LWRs by the RPI group[19], such uncertainties were shown to be significant for LWR operation. Furthermore, care must be exercised in the definition of this parameter, e.g. I believe ENDF/B-V has the recoverable energy tabulated, (i.e., sans neutrino energy) whereas an earlier ENDF/B version tabulated the total fission energy.

(c) Location of energy deposit

A conservative assumption is that all the recoverable fission energy is deposited at the point of fission, i.e. in the fuel pellet. More than 85% of the fission energy is in fission fragments and β particles, for which this assumption is essentially exact. Furthermore, much of the neutron and γ energy is also deposited in the fuel.

For more precise determinations, coupled n-γ transport calculations are necessary (see Appendix III, Ref. 20). In this context the use of the kerma technique[21] commonly used to analyze energy deposit in fusion reactor blankets[22] should prove useful.

(d) Capture γ energy deposit

For an LMFBR, this energy can typically amount to 6-7% of the fission energy. The precise determination of its site of deposition involves the problems discussed in (c). A first approximation is to correct the total recoverable fission energy for this added contribution.

(e) Heterogeneous cores

As discussed in Refs. 2-4, it is proposed to begin our investigations with a heterogeneous core model. This design has some further problems which are either nonexistent or less significant in a homogeneous core, as follows.

(e.1) Change of peak power location

The shape of heterogeneous core power distributions are much more complex than those of a homogeneous core[20,23]. In particular, the location of the peak power may change with burnup and with cross section changes.

(e.2) Transport effects

Due to the fertile elements in the interior of the heterogeneous core, coupled n-γ transport effects discussed in (c) and (d) are more significant for determining energy deposit distributions in a heterogeneous core than in a homogeneous model[20].

(e.3) Definition of volume for average power distribution

For a homogeneous core the Vol_2 in Eqn. (6) is often the core volume. For a heterogeneous core, the "core" is often defined to include the internal fertile elements. If this definition is used to determine the "core" average power density, the peak-to-average value can be considerably higher than those to which we are accustomed.

However, ultimate interest is in the absolute value of the peak linear power, and for proper power normalization to the reactor MWth, a_2 in Eqn. (6) should reflect the total recoverable energy in the entire reactor. Thus, the determination of the appropriate Vol_2 becomes primarily a matter of keeping the definitions straight, with appropriate corrections if a_2 does not include the total energy.

2. EPRI-CELL (P. Levin)

The report period was mainly devoted to get the isotopic calculations started at ORNL. That included:

a) Convergence: By isolating the lumped fission products (ZAS IDs 999998 and 999999) it was proven that the group rebalance scheme of ORNL THERMOS cannot cope with them since they are pure absorbers. These cross sections result from lumping of hundreds of fission products in CINDER into two fictitious materials that preserve merely the absorption reaction rates (in CINDER 4 groups structure). By switching off the rebalance mechanism for time step 2 and the subsequent ones the ORNL version does calculate the depletion and converges. This is a temporary solution, since any restart run that contains the above materials is not going to converge at the first time step of that run.

b) Pu-240 1 eV Resonance: This subject was reported separately[24]. As long as the NAI cross section libraries are used, the ORNL EPRI-CELL yields lower production of Pu-241 and Pu-242 due to the unbroadening of the 1 eV resonance for Pu-240 capture.

c) EPRI-CELL Libraries: Scanning the NAI GAM library (with R. Q. Wright) several inconsistencies have been found. One would be less concerned with these had the other libraries been adequate. According to Odelli Ozer[25] for both ENDF/B-IV and ENDF/B-V libraries not only the range of F-factor is incomplete (as is already known in ORNL), but the scheme of interpolating for the F-factor is suspected. R. E. MacFarlane is working on the necessary improvement. Yet for the time being, the ENDF libraries are not to be used for depletion runs.

d) Yankee-Zr Cell Calculations: All our tests of EPRI-CELL depletion options have been done using the input data we obtained from Odelli Ozer. This is the same deck used by the NAI to generate their results as cited in ARMP documentation[26].

Appendix I summarizes a modeling of the same CELL calculations, starting from the basic available data[27]. This model will be tested against both NAI's input and the experimental results. Certain assumptions will be tested (especially referring to the sensitivity of the depletion calculation to several temperatures). This will form a basis to model the other reactors in the future.

References

1. C. R. Weisbin, J. M. Kallfelz, H. S. Bailey, and E. Kujawski, "Economic Impact of Uncertainties in Data Adopted for Core Design," Attachment 1 to letter of same subject from D. B. Trauger (ORNL) to R. G. Staker (DOE), dated September 25, 1978.

2. C. L. Cowan (GE-ARSD), "Impact of Data and Methods Uncertainties on Fast Reactor Design Parameters," letter to C. R. Weisbin, ORNL, and J. M. Kallfelz, Ga. Tech, dated December 11, 1979.

3. J. M. Kallfelz, "Draft Response to Charley Cowan's Letter of December 11, 1979," memo to C. R. Weisbin and J. H. Marable, ORNL, dated January 17, 1980.

4. J. M. Kallfelz, J. H. Marable, and C. R. Weisbin, letter to C. L. Cowan (GE-ARSD), dated January 25, 1980.

5. J. H. Marable and C. R. Weisbin, "Uncertainties in the Breeding Ratio of a Large LMFBR," Proc. ANS Physics Division Topical Meeting, Gatlinburg, Tennessee (April 1978).

6. J. H. Marable, C. R. Weisbin, and G. de Saussure, "Uncertainty in the Breeding Ratio of a Large LMFBR: Theory and Results," to be published in NS&E, (1980).

7. D. Rinaldis, J. M. Kallfelz, E. Kujawski, and J. H. Marable, "Evaluation of Integral Parameter Correlations and Reactor Performance Using Nuclear Data Covariances," Trans. Am. Nucl. Soc. 33, 859 (1979).

8. J. M. Kallfelz and P. Levin, "Progress Report on Work for ORNL Subcontract 7802, Period November 7 - December 6, 1979," Memorandum to C. R. Weisbin, J. H. Marable, and M. L. Williams, dated December 7, 1979.

9. J. C. Chandler et al., "The Proliferation Resistant Preconceptual Core Design Study," TC-1082, Hanford Engineering Development Laboratory, March 1978.

10. J. M. Kallfelz, A. Livrieri, and D. M. Rowland, "Investigations of Heterogeneous LMFBR Cores with Alternative Fuel Cycles," Progress Report for ORNL Subcontract 3986, GITNE-78/1, Ga. Inst. of Tech., March 1978. (See sec. 3 and page III-11).

11. J. Kallfelz, "ORNL Project Report," Attachment to agenda for meeting with T. Burns at Georgia Tech, March 8, 1977 (see Table IV).

12. A. Gandini, J. Nuclear Energy 21, 755 (1967).

13. G. P. Cecchini and M. Salvatores, Nuclear Science Engineering 46, 304 (1971).

14. I. Dal Bono, V. Leproni, and M. Salvatores, "The CIAP-ID Code," CNEN RT/FI (68)9, Comitato Nazionale per l'Energia Nucleare, Rome (1968).

15. T. B. Fowler, D. R. Vondy, and G. W. Cunningham, "Nuclear Reactor Analysis Code: CITATION," ORNL-TM-2496, Rev. 2, Oak Ridge National Laboratory (1971).

16. D. R. Vondy, T. B. Fowler, and G. W. Cunningham, "VENTURE: A Code Block for Solving Multigroup Neutronics Problems Applying the Finite-Difference Diffusion-Theory Approximation to Neutron Transport, Version II," ORNL-5062/R1, Oak Ridge National Laboratory (November 1977).

17. I. Dal Bono, V. Leproni, and M. Salvatores, "The GLOBERT-1D Code," CNEN RT/FI (68)10, Comitato Nazionale per l'Energia Nucleare, Rome (1968).

18. J. M. Kallfelz, G. B. Bruna, G. Palmiotti, and M. Salvatores, "Burnup Calculations with Time-Dependent Generalized Perturbation Theory," Nucl. Sci. Eng., 62, 304 (1977).

19. D. R. Harris, M. Becker, A. Parvez, and J. M. Ryskamp, Nucl. Tech. 46, 82 (1979).

20. W. P. Bathold and C. P. Tzanos, "Performance Potential of Reference Fuel in 1200 MWe LMFBRs," FRA-TM-104, Argonne National Lab, November 15, 1977.

21. M. A. Abdou and C. W. Maynard, Nucl. Sci. Engr. 56, 360 (1975).

22. M. L. Williams, R. T. Santoro, and T. A. Gabriel, Nucl. Tech. 29, 384 (1976).

23. G. B. Bruna, G. P. Cecchini, J. M. Kallfelz, G. Palmiotti, and M. Salvatores, "Studies of the Heterogeneous LMFBR Core Concept and Its Sensitivity to Design and Cross Sections Variations," NIRA Report T-NA-E-344047-F, Nucleare Italiana Reattori Avanzati, Genoa, Italy (1977).

24. P. Levin, "The Effect of the 1 eV Resonance of Pu-240 on Isotopic Calculations in EPRI-CELL," Memorandum to M. L. Williams, dated January 22, 1980.

25. Odelli Ozer, Telecom, dated February 6, 1980.

26. "Advanced Recycle Methodology Program System Documentation," EPRI Report CCM-3, Electric Power Research Institute (September 1977), Part I, Chapter 3, Section 3.

27. J. B. Melehan, "Yankee Core Evaluation Program, Final Report," WCAP-3017-6094 (January 1971).

28. "Advanced Recycle Methodology Program System Documentation,"EPRI Report CCM-3, Electric Power Research Institute (September 1977), Part II, Chapter 5, Section 3.

Appendix I. Modeling of Yankee-Rowe Zircaloy-clad Fuel Elements for EPRI-CELL

1. Operation Conditions

1.1 Location: We refer to axial sample zone 3 (Fig 12-1 of Ref 27). The gamma activity there exhibits almost no gradient at that point.

1.2 Temperatures etc.: Since we cannot change temperatures during a run, one has to chose "average" temperatures to be used for the entire depletion calculation. Refering to Table C-3 of Ref 27, the BOL conditions are close to the average and, after the initial rise in power and temperatures, close to the "asymptotic" conditions.

We adapt: Specific power = 45.212 (kw/kg)

Fuel Average Temp.	TFUEL	= 1515.50°F
Clad —"—	TCLAD	= 578.95°F
Moderator —"—	TMOD	= 530.00°F
Resonance Effective Temp.	TRES	= 1377.60°F

.. Geometry

.1 Cold Dimensions

(Ref: Sec 2 of 27)

Pellet O.D. = .3145"
clad O.D. = .362"
clad Thickness = .021"
Fuel Rod Pitch = .465"

Cell Equivalent Radius:

$$\pi R_{eq}^2 = p^2$$

i.e. $$R_{eq} = \frac{p}{\sqrt{\pi}} = .6664 \text{ cm}$$

Cold Radii: Fuel : .3994 cm
Clad Inner: .4064 cm
Clad Outer: .4597 cm

.2 Dimensional Expansion

The functions used here are built in EPRI-CELL ENGINEERING input and are described in Appendix F of EPRI-CELL documentation [28].

2.1 The Fuel

$$PELOR = PELOR_{cold}\,(1+(TFUEL-68)*TBLF(TFUEL))$$

TBLF is a tabulated function of TFUEL(°F) yielding a value of 4.97-6 for TFUEL = 1515.5°F

$$\boxed{PELOR = 1.0072 * PELOR_{cold} = .4023\ cm}$$ ∴

2.2 The Clad (Zircaloy)

$$CLADIR = CLADIR_{cold} * (1+3.25E\text{-}6*(TCLAD-68))$$

$$CLADOR = CLADOR_{cold} * (1+3.25E\text{-}6*(TCLAD-68))$$

for TCLAD = 578.95°F:

$$\boxed{\begin{aligned} CLADIR &= 1.0018 * CLADIR_{cold} = .4071\ cm \\ CLADOR &= 1.0018 * CLADOR_{cold} = .4605\ cm \end{aligned}}$$ ∴

Densities

We use the convention that all the effects of both temperature and voids are accounted for in the PUREDN number densities.

3.1 The Fuel

According to Table D-1 of Ref 27 the weight fractions of the various isotops in the uranium are: (initial isotopic composition)

WF234 = 2.577-4

WF235 = 2.90495-2

WF236 = 1.339-4

WF238 = 9.705589-1

Manipulating that data:

$$WFALLU = \frac{2.577-4}{234.041} + \frac{2.90495-2}{235.044} + \frac{1.339-4}{236.044} + \frac{9.705589-1}{238.0508} = 4.202\text{4}-3$$

Atomic Fractions:

AF234 = 2.6202-4

AF235 = 2.9410-2

AF236 = 1.3499-4

AF238 = 9.7019-1

$$A_{UO_2} = AF234*234.041 + AF235*235.044 + AF236*236.044 + AF238*238.0503 + 31.99 = 269.95$$

The theoretical density at room temperature is 10.96 gr/cm³. According to p. 2-1 of (27) the actual cold density was only 94% of it

i e $\boxed{\rho_{UO_2\ cold} = 10.302\ gr/cm^3}$

The temperature effect is:

$$RHFUEL = \rho_{UO_2\,cold} * (1 - 3*(TFUEL-68) * TBLF(TFUEL))$$

TBLF is the tabulated function evaluated at section 2.2.1 to be 4.97-6

$$\boxed{RHFUEL = .9784 * \rho_{UO_2\,cold} = 10.080\ gr/cm^3}$$

No dishing information is given in the Ref. we assume it is zero.

Number densities for the fuel: (atom/barns-cm)

$$N_{16} = \frac{10.080 * .6023}{269.95} * 2 = 4.4980-2$$

$$N_{234} = AF234 * \frac{N_{16}}{2} = 5.8927-6$$

$$N_{235} = AF235 * \frac{N_{16}}{2} = 6.6143-4$$

$$N_{236} = AF236 * \frac{N_{16}}{2} = 3.0358-6$$

$$N_{238} = AF238 * \frac{N_{16}}{2} = 2.1819-2$$

2 The clad

The cladding material is Zircaloy-4 for which the room temperature number density is .04333 (atom/barn-cm).

The gap between the fuel and clad is too narrow to be represented in the zone allocation. Thus the clad is smeared over the entire volume of R_F to R_{CO} reducing the nuber density by a factor of: (in cold conditions)

$$\frac{R_{CO}^2 - R_{CI}^2}{R_{CO}^2 - R_F^2} = \frac{.4597^2 - .4064^2}{.4597^2 - .3994^2} = 8.9140\text{-}1$$

The temperature effect is given by:

$$1 - 3 * 3.25E\text{-}6 * (TCLAD - 68) = 9.9502\text{-}1$$

$$N_{22} = .04333 * .8914 * .99502 = 3.8432\text{-}2 \ (\text{atom/barn-cm})$$

.3 The Moderator

No information is given on the pressure in core V. The nominal pressure for cores I-IV was 2000 psi, so we assume that it was valid for core V two. Using that value and the TMOD = 530°F the built in function VCL yields water density:

.76819 (gr/cm³)

The standard EPRI-CELL number densities for 1 gr/cm³ are:

N_H = .066874
N_O = .033437 (atoms/barn-cm)

The actual number densities:

N_H = 5.1372-2
N_O = 2.5686-2 (atoms/barn-cm)

.4 Boron

Since Boron is used to compensate for the excess reactivity, its concentration decreases from a time step to another. That variation

can be input in the ENGINEER mode, where the variable PPMB is the actual concentration in ppm.

For the GENERAL mode no variation of Boron density is allowed. One must assume an "average" Boron content for the entire depletion.

This subject deserves further consideration. We shall report on it seperately.

4. Resonance Data

4.1 Thermal Resonances

As long as NAI library is used the Pu^{240} 1ev resonance is represented by resonance parameter. One has to provide the variable TEMP (1) which is the resonance effective temperature. Following Appendix F of EPRI-CELL documentation this is set to the same value as the other resonances. Namely:

$$\boxed{TEMP(1) = TRES = 1020.71°K}$$

(1377.6°F)

2 Epithermal Resonances

2.1 Nuclides

The four resonant nuclide used are:
U^{235}, U^{238}, Pu^{239} and Pu^{240}

2.2 Temperature

We use the resonance effective temp. of the Ref.

$$\boxed{TRES = 1020.71°K} \equiv RES(1,)$$

2.3 The Mean Chord Length

$$\boxed{\bar{\ell} = 2 * PELOR = 2 * .4023 = .8046 \text{ cm}}$$

(defined as RES(2,))

2.4 Dancoff Factor

The built in routine yields for a square pitch of 1.1811 cm (uniform)

$$\boxed{DF = .394437}$$

(defined as Res(3,))

2.5 Excess Potential σ^s

Defined for Nuclide J as: $\frac{1}{N_J} \sum_{I=J} N_I \lambda_I \sigma_I^p$
(Ref: pp. 5-54, 5-59 ARMP, PT II)

Using the N_I as calculated in sec 3.1 and the Table for $\lambda\sigma_p$ one gets for

$$RES(5, i) \equiv N_i$$

$$RES(4, i) \equiv \frac{1}{N_i} \sum_{j \neq i} N_j \lambda_j \sigma_{p_j}$$

Nuclide	RES(4,)	RES(5,)
U^{235}	298.605	6.6143-4
U^{238}	7.348	2.1819-2
Pu^{239}	1.9899+19	1.-20
Pu^{240}	1.9899+19	1.-20

These are BOL values. The code updates them for the subsequent time steps.

Miscellaneous Data

.1 POWER

This variable indicates the representative power power (watts/cm) for the entire cycle.
Using the specific power adapted in sec 1.2:

$$P = 45.212 \text{ Kw/kg}$$

The hot density of Uranium is:

$$\rho_u = RHFUEL - \frac{N_{16} * 15.995}{.6023} = 8.885 \left(gr/cm^3\right)$$

The amount of Uranium contained in 1 cm length of hot element is:

$$G_u = \rho_u * \pi (PELOR)^2 = 4.518 \text{ gr}$$

POWER = 204.25 (watts/cm)

4.2 Buckling

Since this is a modeling of a cell in an operating core where the keff is always kept the same, one should use the search option.

i.e. OPTION(7) = 1

The desired k is 1 since that was the practical keff, and we do not know of any biasing factor.

DSIRDK = 1.0

For initial guess we use equivalent cylindrical core with a reflector saving of 6 cm.

Cor Height $H_c = 91.68'' = 232.87$ cm (cold)

Hot core height $H = [1 + (TFUEL - 68) * TBLF(TFUEL)] * H_c$

$H = 234.54$ cm

Each fuel assembly is a 16x16 rods(*) array with cell area of p^2 each.

(*) we substitute fuel for the control rods for this calculations.

The 76 fuel assemblies can be cylindrized with an equivalent Radius

$$\pi R^2 = 76 * 16 * 16 * p^2$$

ie $R = 92.95$ cm

$$\boxed{B^2 = \left(\frac{\pi}{H+12}\right)^2 + \left(\frac{2.405}{R+6}\right)^2 = 7.531 - 4 \text{ cm}^{-2}}$$

3 Fission Spectrum

Since the main contributor to fissions is U^{235} (after 10,000 hrs it still provides almost 50% vis less than 40% by Pu^{239}) the U^{235} fission spectrum is used

ISPEC = 9 for NAI library
ISPEC = 5 for ENDF libraries

Geometry Input

This is a 3 zones problem: Fuel, clad and Moderator. We do not know of structural components to set an XTRA zone.

Nor is a heavy scattering ring required: NAI version of EPRI-CELL uses the "isotropic" boundary option (OPTION(8) = 1). The ORNL version generates its boundary conditions regardless of the OPTION.

.1 Mesh size

EPRI-CELL documentation reccomends on coarse mesh of 4 points in the fuel. We use the fine mesh of 8 points right now For clad and moderator we use the recomended values of 1 and 7 points respectively

.2 Region Assignment

For the sake of ORDER each mesh point in the fuel is a seperate region. Thus we have

$8 + 1 + 1 = 10$ regions

. Materials

Since we deal with several libraries, the materials rather than their ID will be given here.

.1 Fuel

The following materials are entered with their calculated N (sec 3.1):

O^{16}, U^{235}, U^{236}, U^{238}

The following materials are entered with N = 1-20:
Xe^{135}, Sm^{149}, Pu^{239}, Pu^{240}, Pu^{241}, Pu^{242}, EFP, TFP.
(The last two are fictitious epithermal and thermal lumped fission products.)

TEMPID : 0 for EFP and TFP
for all the other, except for O^{16}, it depends on the installation:
At ORNL – use TFUEL
At Berkeley – use listed TEMPID closer to TFUEL

2 Clad

It is zirc-4 and the TEMPID is TCLAD
(same rules as for fuel.)

3 Moderator

The following materials are entered:
H, B^{10}, O^{16}
Densities for H and O were discussed in sec 3.3.
The boron problem is left open right now.

TEMPID is TMOD (same rules as for fuel.)

SCHOOL OF NUCLEAR ENGINEERING E-26-B01

Atlanta, Georgia 30332 (404) 894-3720

March 5, 1980

MEMORANDUM

TO: C. R. Weisbin, J. H. Marable, and M. L. Williams (ORNL)

FROM: J. M. Kallfelz and P. Levin

SUBJECT: Progress Report for ORNL Subcontract 7802, Period February 12 - March 4, 1980

Accomplishments

- A program for sensitivity analysis of a heterogeneous LMFBR to be performed jointly with GE has been developed. A model of a reactor typical to that being considered by GE for the CDS has been received, and decisions have been made concerning the codes and cross section sets to be utilized. The program includes development of capability to calculate Γ^* for the peak/total power ratio with VENTURE.

- Work has been initiated concerning modes of impact of cross section improvements on operating thermal reactor systems, Topic A of the recommended program plan elements in Reference 10. The latter has been distributed to two industrial consultants, R. Carlson and Ron Cobb, with the assignment that they review the issues raised therein and provide pertinent comments and analysis.

- Considerable progress was accomplished in the modeling of PWR reactors for EPRI/CELL isotopics calculations. Preparation of "ENGINEERING" and "GENERAL" inputs for the Yankee-Zr case using the basic references was completed, and runs were performed both at Berkeley and at ORNL. The input and results are compared for those cases and the input used by NAI for the original ARMP documentation.

  Parametric studies were performed of the influence of the differences in these inputs. These studies indicated that the calculated results for these inputs should not differ more than a few percent, which was in fact, the case.

  Calculations were also performed for the YANKEE stainless steel case, and compared to the NAI benchmark calculations. Errors in the ORNL code treatment of zero power shutdown periods were detected.

Plans for Work for the Next Month

- Sensitivity analysis of the GE heterogeneous LMFBR will be pursued, with the goal of performing the necessary calculations in time to submit a summary for the 1980 ANS RP Division Topical Meeting.

- Consultation with several individuals concerning the modes of impact of cross section improvements on operating thermal reactors will be continued.

- PWR isotopics calculations with EPRI-CELL will be continued. An effort will be made to model the Robinson-2 plant with the limited references we have available. If problems with the use of ENDF/B-IV and -V data are resolved at ORNL, runs for this data will be performed.

- A detailed report will be prepared describing the methods and sources used in the preparation of the input for the PWR isotopics calculations.

- For ANISN-B1, steps will be taken to execute correctly the test problem.

- If the above mentioned problems with the use of ENDF/B-IV and -V data are not resolved this month, work will be initiated on CSEWG thermal data testing. Information is necessary from ORNL on the cases and data to be tested.

1. Sensitivity Analysis of a Heterogeneous LMFBR (J. Kallfelz)

As discussed during my recent visit to ORNL, we have decided to accelerate the initiation of our proposed joint work[1-3] with General Electric by attempting to perform the necessary calculations in time to submit a summary for the ANS RP Division 1980 Topical Meeting. The goal of this work is to perform uncertainty analysis similar to that previously performed for a homogeneous LMFBR[4-5], but using a heterogeneous model characteristic of that being considered by GE for the CDS studies.

As discussed in our previous progress report[6], we plan to develop capabilities for sensitivity studies of a further integral parameter, the peak power density, and to include this parameter in our investigations.

A model for the studies has been received from Charley Cowan[7], and we have discussed various options for cross section sets and codes to use for these studies. Present plans are to use VENTURE[8] for the ϕ, ϕ^* and Γ^* calculations, probably with the 32 group cross section set used for the previous studies[4-5].

1.1 Peak Power Density Sensitivity Studies

As stated in our previous progress report[6], our discussion of sensitivity studies for the peak power density concentrated on the "indirect effect", caused by changes in $\phi(E, \vec{r})$. Following are comments on several more aspects of these sensitivities, extracted from my memo to D. Vondy[9].

a) Direct Effect

Eqn. (1) of Ref. 6 gives the expression for the ratio

$$R = \frac{\int_{Vol_1} \sum_j \Sigma_{1j}(\vec{r})\,\phi_j(\vec{r})\,d\vec{r}}{\int_{Vol_2} \sum_j \Sigma_{2j}(\vec{r})\,\phi_j(\vec{r})\,d\vec{r}} = \frac{a_1}{a_2} \qquad (1)$$

where a_1 and a_2 represent the peak and total power, respectively.

The "direct effect" of changes in the σ which appear in Σ_1 and Σ_2 of R does not include changes in ϕ, and can be calculated with a trivial expression:

$$\left.\frac{\delta R}{R}\right|_{direct} = \frac{R_d' - R}{R} \qquad (2)$$

where the value of R considering the "direct effect" of these σ changes is given by

$$R_d' = \frac{a_1 + \int_{Vol_1} \sum_j \delta\Sigma_{1j}\,\phi_j}{a_2 + \int_{Vol_2} \sum_j \delta\Sigma_{2j}\,\phi_j} \qquad (3)$$

For the breeding ratio, this effect can be much larger than the indirect effect, for fissile and fertile perturbations. For many cases the relative importance of the direct effect for the power density ratio will probably be much smaller. E.g., <u>if</u> the fissile and fertile concentrations were constant in the reactor, R_d' would equal R, since the percent change to the numerator and denominator of R would be equal.

This is in contrast to the breeding ratio, where the numerator and denominator involve different reactions in different isotopes. Thus, investigations of the Γ^* (indirect) component of the sensitivity coefficient should be particularly pertinent for the power density.

b) k-Reset Mechanism Effects

For the same reasons discussed in (a), the magnitude of the sensitivity coefficient component due to k-reset by enrichment should generally not be as great for the power density as for the case of the breeding ratio. However, due to the smaller importance of the power density direct effect discussed in (a), the power density sensitivity coefficients

without k-reset may often be small compared to those for the breeding ratio. Hence, the relative impact of the k-reset component is not clear.

In response to questions about the recoverable energy/fission, P^k in Eqn. (4) of Ref. 6, we used the following ENDF/B-III values in our studies of burn-up sensitivities[11].

Isotope	P^k [w-sec/fiss]$\cdot 10^{11}$
U-235	3.076
U-238	3.108
Pu-239	3.156
Pu-240	3.108
Pu-241	3.188

I do not have information on more recent values.

1.2 Modeling of the Reactor

The model sent by Charley Cowan[7], is a full-height R-Z model, with various burn-up zones given in figure 1 of Ref. 7. However, the atom densities are given as average values for a particular core region. Charley said he would send us a model with average compositions for the middle of the equilibrium cycle (MOEC). I have not been able to confirm this with Charley since receiving the model, but the model obviously has burn-up, since Pu isotopes are in the various blanket zones. (Fission products are not indicated, however.)

I recommend that we use a "half-height" reactor model without shield, to save computer time. Such a model should be adequate for our calculations. Initial control search calculations will be necessary to obtain criticality.

Charley suggested that we simply insert the control rods and search on the B^{10} concentration. To obtain a better value for the average axial

blanket composition, one can mix one-half of the "control-in" and "control-out" compositions for the blanket control regions, since the upper and lower blankets control zones have the former and latter compositions, respectively. It further appears appropriate to use the "control-out" composition for the secondary control regions in the core.

Assuming that at MOEC the primary control is inserted about to the core midplane, it seems appropriate to mix half of the "control-in" and "control-out" compositions in the core primary control regions, and then search on the B^{10} concentration. If the resulting B^{10} density is considerably different from the initial value, the calculations can be repeated with an appropriately adjusted mix of "control-in" and "control-out" compositions. I will consult further with Charley on this topic as our calculations proceed.

2. EPRI-CELL (P. Levin)

The reported period was devoted to the isotopics calculations and modeling. As already reported[1] we were using the NAI original input deck for running the Yankee-Zr calculations. Concurrently, we have been developing our model for the same cell. It became necessary to test the sensitivity of the isotopic ratios to variations in several uncertain parameters. In addition, the ENGINEERING input for both Zr and SS clad Yankee elements was prepared and run. All calculations reported herein are for the NAI cross section set.

Our modeling was reviewed by Roger Carlson[16]. He agreed with most of it, except for the use of the buckling search, which we did not regard as "standard practice", although it is recommended by NAI[17]. This particular subject will be reported separately.

2.1. Parametric Studies

In Appendix I we summarize the comparison between NAI original input and our model. There are differences in several temperatures, especially the resonance effective temperature; the average boron concentrations differ; we assume critical buckling, while NAI use constant buckling with varying k_{eff}.

The effect of the above differences on the isotopic ratios was tested in a series of runs with NAI input (which is referred to as "Odelli Ozer's Case" in the tables), changing one parameter at a time. Table 1 is the reference NAI run; Table 2 presents the same case with the resonance effective temperature increased; Table 3 presents a case with critical buckling and Table 4 presents a run without boron.

All of these cases were run in Berkeley. It was noted[12] that the ORNL version of EPRI-CELL overestimates the buildup of Pu-240, while

underestimating the buildup of Pu-241 and Pu-242. Yet, we checked the effect of variations in boron concentration in ORNL too. Table 5 is the ORNL equivalent of Table 1, and Table 6 is the ORNL equivalent of Table 4. Table 7 presents an ORNL case with 700 ppm boron.

Results: (For depletion of U^{235} to half)

(a) Resonance Temperature: Increasing the temperature from 998.5°K to 1020.7°K effects the ratios by 0.5% at most.

(b) Critical Buckling instead of constant: Pu^{239} production is increased by 0.8% and the ratio of 241/242 increased by 0.9%.

(c) The Boron Effect: The effect of removing 285 ppm boron is a decrease of Pu^{239}/U^{238} ratio by 1.8% and an increase of 240/241 ratio by 1.6%. The ORNL runs prove that these effects are linear within the 700 ppm range tested.

2.2 Our Model of Yankee-Zr

In Appendix II the ENGINEERING input of our model is presented. Both this case and the GENERAL input (Appendix I of Ref. 6) were run in ORNL. The results are given in Table 8 for the ENGINEERING and in Table 9 for the GENERAL input.

Referring to the GENERAL input case as an approximation for the ENGINEERING one, it is observed that:

a) The 239/240 ratio is overestimated by about 1.1%.

b) The 241/242 ratio is overestimated by about 1.2%.

c) There is underestimation by about 0.3% of the Pu^{239}/U^{238} ratio.

Since both cases should represent the same cell as for the NAI input data, we compare them with the NAI results at ORNL (Table 5). By a quadratic least square fit this case yields:

U^{235} Frac. Depl.	Pu^{239}/U^{238}	Pu^{239}/Pu^{240}	Pu^{240}/Pu^{241}	Pu^{241}/Pu^{242}
.4344	4.9559-3	4.4561	1.9912	8.1856
.4349	4.9595-3	4.4508	1.9899	8.1713

Comparing these values with the appropriate ones in Table 8 and 9:

a) Pu^{239}/U^{238}: Our ENGINEERING input yields a ratio 2.6% higher than NAI. The GENERAL input ratio is 2.1% higher than NAI.

b) Pu^{239}/Pu^{240}: ENGINEERING is lower than NAI by 0.9% while GENERAL is higher than NAI by 0.4%.

c) Pu^{240}/Pu^{241}: ENGINEERING is 1.6% lower than NAI. GENERAL is lower also by 1.7%.

d) Pu^{241}/Pu^{242}: ENGINEERING is lower than NAI by 1.7% while GENERAL is almost identical with NAI.

Note: Since the function discussed are changing rapidly and the differences are comparably small, there is no point in trying to plot the results.

2.3. Yankee-SS Calculations

The description of the Yankee stainless clad fuel elements is given in Ref. 18. Our modeling, which is quite similar to the Zr case, will be reported separately. The ENGINEERING input is presented in Appendix III.

We ran the same case both in ORNL and in Berkeley with essentially the same input (except for the different notation for U^{235} fission spectrum). Their results are given in Table 10 - for Berkeley, and Table 11 - for ORNL. The results are also plotted on the NAI benchmarking curves (14) in figures 2-1 - 2-3.

Results

After having run the problem on both computers we doubt the basis for comparing the results. Both runs start with "clean." UO_2 fuel and the same specifications for watts/cm. The densities, number densities and dimensions are identical. Yet:

a) A constant factor of .9914 is somehow applied to the ORNL densities in comparison with Berkeley's at the end of the edit.

b) There is a power density (kw/liter) and a specific power (kw/kg). It is not clear to us which results from which. Yet both these power indicators are different for ORNL and Berkeley (although for both an input longitude power of 117.33 w/cm was set).

Consequently, the accumulated fissions differ even for the first step (.53% higher for ORNL) where it should be still the same. Since we have no idea of the "correct" set of calculations, we present them as they are (they both may well differ from NAI curves in the same sense).

c) The runs intended to represent both Core I and II including the zero power 3096 hrs. period of loading-unloading. It turns out that the ORNL version treats that period incorrectly: The Xe-135 does not decay at all, nor does the Pu-241, nor does Am-141 grow. The FP Therm and FP Epitherm that represent a lump of fission products should decay to a certain extent but not vanish; the ORNL version set these materials to 1-20 following the zero power step.

This may indicate wrong treatment of the zero power step due to the program's response to zero flux, or it may even indicate incorrect treatment of decay, etc. which is seen when the flux is zero.

Observations

General trends can be observed, in spite of the above discussion:

a) Berkeley results are closer to the NAI curves than ORNL. The deviations between the first two cases are less than 5% in any of the ratios. The poor agreement for the ORNL case is to be expected, based on the aforementioned error in the buildup of the higher plutonium isotopes due to improper treatment of the Pu-240 1 eV resonance[12].

b) All Berkeley results and ORNL results for 239/240 and 241/242 are lower than NAI.

c) As expected, ORNL production of Pu-241 is too small, thus the ratio 240/241 is higher than both Berkeley and NAI.

Table 1. Isotopic Buildup for Yankee-Zr. Odelli Ozer's Case* (285 ppm B) at Berkeley - Reference

End of step #	U^{235} Frac. Depl.	Atomic Ratios			
		$\frac{Pu^{239}}{U^{238}}$	$\frac{Pu^{139}}{Pu^{240}}$	$\frac{Pu^{240}}{Pu^{241}}$	$\frac{Pu^{241}}{Pu^{242}}$
1	.0071	1.1202-4	2.3909+2	1.0018+2	7.8646+2
4	.0996	1.4905-3	1.7958+1	6.5105	5.1866+1
8	.2144	2.9305-3	9.0084	3.0536	2.1359+1
12	.3137	3.9681-3	6.4366	2.2119	1.3060+1
15	.4205	4.8845-3	4.9373	1.7783	8.6537
17	.4943	5.4145-3	4.2374	1.6081	6.7386

*In this and the following Tables, the original NAI input is referred to as "Odelli Ozer's", since he supplied this input.

TABLE 2. Isotopic Buildup for Yankee-Zr. Odelli Ozer's Case with Resonance T_{eff} of 1020.7°K - at Berkeley

End of Time Step #	U^{235} Fract. Depl.	Atomic Ratios Pu^{239}/U^{238}	Pu^{239}/Pu^{240}	Pu^{240}/Pu^{241}	Pu^{241}/Pu^{242}	k_∞ Step #	k_∞ %Dev[a]
						BOL	-.05
1	.0071	1.1221-4 (+.17%)[a]	2.3912+2 (+.01%)	1.0023+2 (.05%)	7.8652+2 (.01%)	2	-.06
2	.0347	5.4767-4 (.17%)	4.9216+1 (.04%)	1.9499+1 (.01%)	1.5687+2 (.01%)	3	-.07
4	.0996	1.4932-3 (.18%)	1.7960+1 (.01%)	6.5176 (.11%)	5.1875+1 (.02%)	5	-.05
6	.1592	2.2766-3 (.18%)	1.1724+1 (-.02%)	4.0564 (.18%)	3.0555 (.03%)	7	-.04
8	.2144 (-.02%)	2.9357-3 (.18%)	9.0029 (-.06%)	3.0615 (.26%)	2.1364+1 (.03%)	9	-.04
12	.3137 (-.03%)	3.9750-3 (.17%)	6.4279 (-.13%)	2.2204 (.39%)	1.3065+1 (.04%)	13	-.04
17	.4940 (-.04%)	5.4241-3 (.18%)	4.2259 (-.27%)	1.6168 (.54%)	6.7448 (.09%)	18	-.03

[a] Deviations Relative to Table 1. (Where T_{eff} = 998.5°K).

TABLE 3. Isotopic Buildup for Yankee-Zr. Odelli Ozer's Case with Critical Buckling Search - at Berkeley

End of step #	U^{235} Frac. Depl.	Atomic Ratios $\frac{Pu^{239}}{U^{238}}$	$\frac{Pu^{239}}{Pu^{240}}$	$\frac{Pu^{240}}{Pu^{241}}$	$\frac{Pu^{241}}{Pu^{242}}$
4	.0991 (-.48%)[a]	1.5154-3 (1.67%)	1.8078+1 (.67%)	6.5628 (.80%)	5.2308+1 (.85%)
8	.2134 (-.49%)	2.9762-3 (1.56%)	9.0585 (.56%)	3.0756 (.72%)	2.1570+1 (.99%)
12	.3122 (-.48%)	4.0226-3 (1.37%)	6.4620 (.39%)	2.2249 (.59%)	1.3193+1 (1.02%)
17	.4921 (-.44%)	5.4582-3 (.81%)	4.2381 (.02%)	1.6115 (.21%)	6.7982 (.88%)

[a] Deviations Relative to Table 1. (Where constant buckling is used).

TABLE 4. Isotopic Buildup for Yankee-Zr. Odelli Ozer's Case without Boron - at Berkeley

End of step #	U^{235} Frac. Depl.	Atomic Ratios				k_∞	
		$\frac{Pu^{239}}{U^{238}}$	$\frac{Pu^{239}}{Pu^{240}}$	$\frac{Pu^{240}}{Pu^{241}}$	$\frac{Pu^{241}}{Pu^{242}}$	Step #	% dev
						BOL	+2.64
1	.0071	1.1007-4 (-1.74%)[a]	2.3976+2 (.28%)	1.0209+2 (1.91%)	7.8498+2 (-.19%)		
4	.0998 (+.19%)	1.4663-3 (-1.62%)	1.7936+1 (-.12%)	6.6291 (1.82%)	5.1710+1 (-.30%)	5	+2.34
8	.2152 (+.36%)	2.8834-3 (-1.61%)	8.9554 (-.59%)	3.1057 (1.71%)	2.1254+1 (-.49%)	9	+2.17
12	.3151 (+.44%)	3.9026-3 (-1.65%)	6.3774 (-.92%)	2.2480 (1.63%)	1.2967+1 (-.72%)	13	+2.02
15	.4226 (+.49%)	4.7993-3 (-1.74%)	4.8764 (-1.23%)	1.8068 (+1.60%)	8.5676 (-.99%)	16	+1.88
17	.4969 (+.52%)	5.3151-3 (-1.84%)	4.1763 (-1.44%)	1.6342 (1.62%)	6.6560 (-1.23%)	18	+1.78

[a] Deviations Relative to Table 1.

TABLE 5. Isotopic Buildup for Yankee-Zr. Odelli Ozer's Case (285 ppm B) at ORNL

End of step #	U^{235} Frac. Depl.	Atomic Ratios			
		$\frac{Pu^{239}}{U^{238}}$	$\frac{Pu^{239}}{Pu^{240}}$	$\frac{Pu^{240}}{Pu^{241}}$	$\frac{Pu^{241}}{Pu^{242}}$
1	.0071	1.1200-4	2.3921+2	1.0270+2	7.8698+2
8	.2143	2.9267-3	8.7939	3.3025	2.1158+1
9	.2404 (-.05%)[a]	3.2157-3 (-.17%)	7.9041 (-2.91%)	3.0089 (+9.19%!)	1.8306+1 (-1.01%)
15	.4204 (-.02%)	4.8548-3 (-.61%)	4.6084 (-6.66%)	2.0314 (+14.23%!)	8.5959 (-.67%)

[a] Deviations Relative to Table 1.

TABLE 6. Isotopic Buildup for Yankee-Zr. Odelli Ozer's Case without Boron - at ORNL

End of step #	U^{235} Frac. Depl.	Atomic Rates $\frac{Pu^{239}}{U^{238}}$	$\frac{Pu^{239}}{Pu^{240}}$	$\frac{Pu^{240}}{Pu^{241}}$	$\frac{Pu^{241}}{Pu^{242}}$	k_∞ step #	k_∞ % dev[a]
						BOL	+2.65%
1	.0071	1.1004-4 (-1.75%)[a]	2.3987+2 (.28%)	1.0467+2 (1.92%)	7.8552+2 (-.19%)	2	+2.52%
8	.2150 (.33%)	2.8796-3 (-1.61%)	8.7461 (-.54%)	3.3564 (1.63%)	2.1054+1 (-.49%)	9	+2.17%
9	.2413 (.37%)	3.1637-3 (-1.62%)	7.8543 (-.63%)	3.0571 (1.60%)	1.8206+1 (-.55%)	10	+2.13%
15	.4225 (.49%)	4.7717-3 (-1.71%)	4.5594 (-1.06%)	2.0613 (1.47%)	8.5091 (-1.01%)	16	+1.87%

[a] Deviations Relative to Table 5.

TABLE 7. Isotopic Buildup for Yankee-Zr. Odelli Ozer's Case with 700 ppm B - at ORNL

End of step #	U^{235} Frac. Depl.	Atomic Ratios Pu^{239}/U^{238}	Pu^{239}/Pu^{240}	Pu^{240}/Pu^{241}	Pu^{241}/Pu^{242}	k_∞ Step #	k_∞ % dev[a]
						BOL	-3.6%
1	.0071 (-.59%)[a]	1.1481-4 (2.51%)	2.3830+2 (-.38%)	1.0003+2 (-2.6%)	7.8914+2 (.28%)	2	-3.43%
8	.2133 (-.49%)	2.9939-3 (2.30%)	8.8543 (.69%)	3.2321 (-2.13%)	2.1313+1 (.74%)	9	-2.92%
9	.2392 (-.52%)	3.2895-3 (2.30%)	7.9665 (.79%)	2.9461 (-2.09%)	1.8455+1 (.81%)	10	-2.87%
15	.4176 (-.68%)	4.9742 (2.46%)	4.6788 (1.53%)	1.9908 (-2.00%)	8.7210 (1.46%)	16	-2.53%

[a] Deviations Relative to Table 5.

TABLE 8. Isotopic Buildup for Yankee-Zr. My Case - ENGINEERING INPUT at ORNL

End of step #	U^{235} Frac. Depl.	Atomic Ratios			
		$\frac{Pu^{239}}{U^{238}}$	$\frac{Pu^{239}}{Pu^{240}}$	$\frac{Pu^{240}}{Pu^{241}}$	$\frac{Pu^{241}}{Pu^{242}}$
1	.0059	9.8698-5	2.8358+2	1.1698+2	9.5648+2
4	.0293	4.9263-4	5.7818+1	2.2297+1	1.8818+2
5	.0611	1.0022-3	2.8137+1	1.0491+1	8.7248+1
7	.1523	2.3023-3	1.1999+1	4.1949	3.1988+1
9	.2182	3.1129-3	8.6312	3.1016	2.0499+1
12	.2719	3.7018-3	7.0307	2.6384	1.5462+1
15	.3779	4.6777-3	5.1165	2.1092	9.9265
16	.4072	4.9037-3	4.7400	2.0219	8.9011
17	.4344	5.0839-3	4.4145	1.9601	8.0490
18	.4771	5.3747-3	4.0159	1.8497	7.0171

TABLE 9. Isotopic Buildup for Yankee-Zr. My Case - GENERAL Input at ORNL

End of step #	U^{235} Frac. Depl.	$\frac{Pu^{239}}{U^{238}}$	Atomic Ratios $\frac{Pu^{239}}{Pu^{240}}$	$\frac{Pu^{240}}{Pu^{241}}$	$\frac{Pu^{241}}{Pu^{242}}$
1	.0059 (-.32%)[a]	9.6384-5 (-2.34%)	2.8700+2 (1.21%)	1.2141+2 (3.79%)	9.5056+2 (-.62%)
4	.0292 (-.17%)	4.7731-4 (-3.11%)	5.8321+1 (.87%)	2.3230+1 (4.18%)	1.8877+2 (.31%)
5	.0611 (-.11%)	9.7128-4 (-3.09%)	2.8337+1 (.71%)	1.0890+1 (3..80%)	8.7630+1 (.44%)
7	.1523 (.01%)	2.2410-3 (-2.66%)	1.2039+1 (.33%)	4.3190 (2.96%)	3.2173+1 (.58%)
9	.2185 (.10%)	3.0443-3 (-2.20%)	8.6568 (.30%)	3.1612 (1.92%)	2.0670+1 (.83%)
12	.2723 (.13%)	3.6333-3 (-1.85%)	7.0564 (.37%)	2.6722 (1.28%)	1.5602+1 (+.91%)
15	.3785 (.15%)	4.6209-3 (-1.21%)	5.1425 (.51%)	2.1227 (.64%)	1.0009+1 (.83%)
16	.4078 (.14%)	4.8569-3 (-.95%)	4.7726 (.69%)	2.0293 (.37%)	8.9880 (.98%)
17	.4349 (.13%)	5.0633-3 (-.40%)	4.4696 (1.25%)	1.9567 (-.17%)	8.1663 (1.46%)
18	.4777 (+.12%)	5.3578-3 (-.32%)	4.0586 (1.06%)	1.8491 (.03%)	7.1042 (1.24%)

[a] Deviations Relative Table 8. (ENGINEERING Input).

TABLE 10. Isotopic Buildup for Yankee-SS at Berkeley

End of step #	Accumulated Fissions	$\frac{Pu^{239}}{U^{238}}$	Atomic Ratios $\frac{Pu^{239}}{Pu^{240}}$	$\frac{Pu^{240}}{Pu^{241}}$	$\frac{Pu^{241}}{Pu^{242}}$
7	5.45039-5	3.2635-3	10.328	2.7417	25.070
8	6.52712-5	3.7268-3	9.0699	2.3798	20.681
13	1.18725-4	5.4968-3	6.0255	1.6186	10.858
14[a]	1.18725-4	5.4967-3	6.0256	1.6493	10.656
19	1.51596-4	6.2737-3	5.1366	1.4518	8.3414

[a] Following a zero power period of 3096 hrs.

TABLE 11. Isotopic Buildup for Yankee-SS at ORNL

End of step #	Accumulated Fissions	Atomic Ratios			
		$\frac{Pu^{239}}{U^{238}}$	$\frac{Pu^{239}}{Pu^{240}}$	$\frac{Pu^{240}}{Pu^{241}}$	$\frac{Pu^{241}}{Pu^{242}}$
5	3.30482-5	2.1929-3	15.005	4.4494	42.231
7	5.47894-5	3.2756-3	10.065	2.9300	24.747
8	6.56125-5	3.7383-3	8.7770	2.5752	20.396
10	8.71764-5	4.5388-3	7.1020	2.1508	15.025
12	1.08643-4	5.2046-3	6.0474	1.9078	11.863
13	1.19342-4	5.4950-3	5.6506	1.8214	10.731
15	1.20554-4	5.5270-3	5.6076	1.8186	10.585
16	1.25374-4	5.6502-3	5.4512	1.7866	10.154
19	1.52389-4	6.2584-3	4.7497	1.6367	8.2853
21	1.70333	6.5971-3	4.3981	1.5638	7.3799

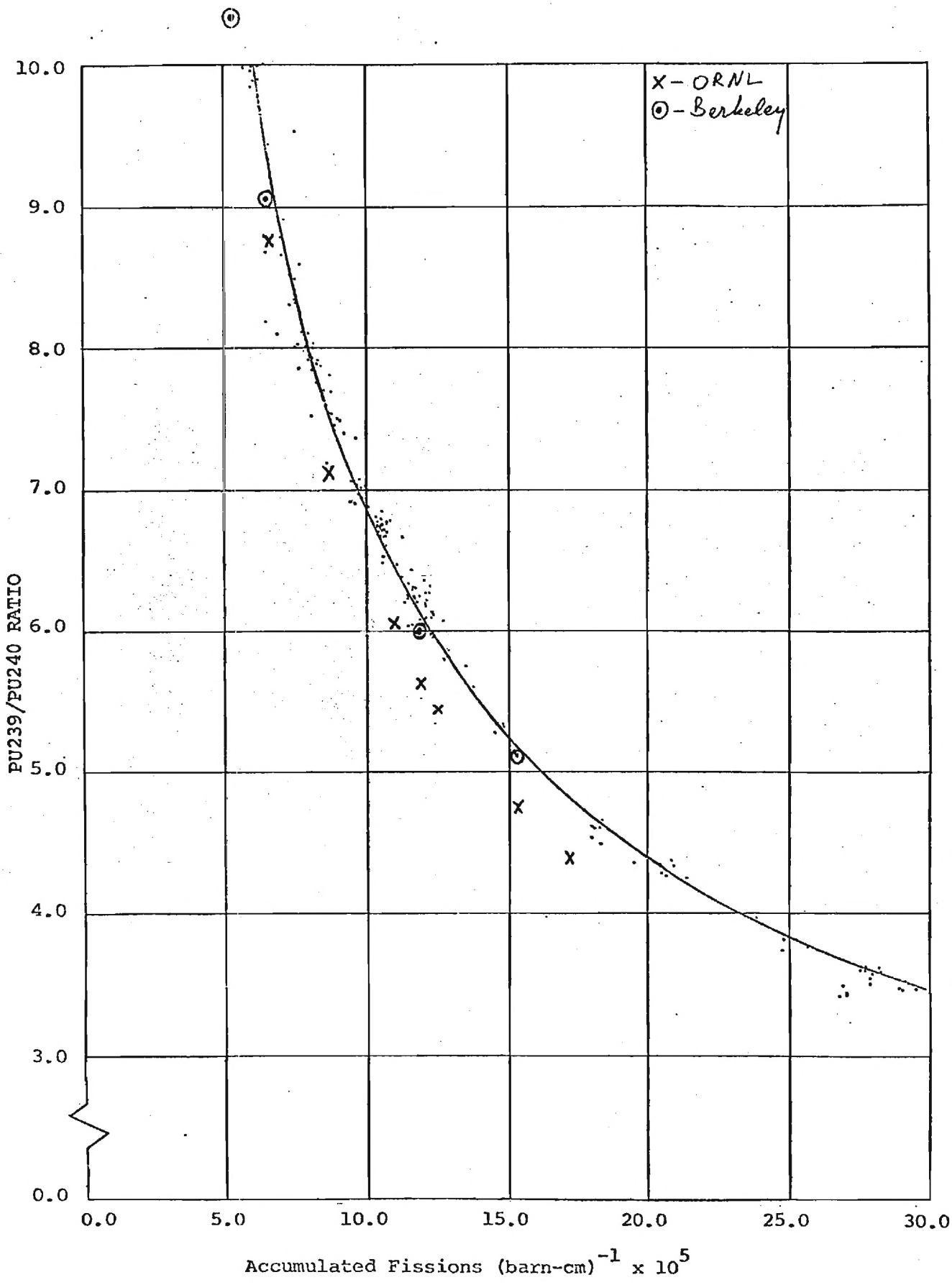

FIGURE 2-1. COMPARISON BETWEEN ANALYSIS AND YANKEE STAINLESS ISOTOPIC RATIOS (From: Ref. 14 p. 3-3.)

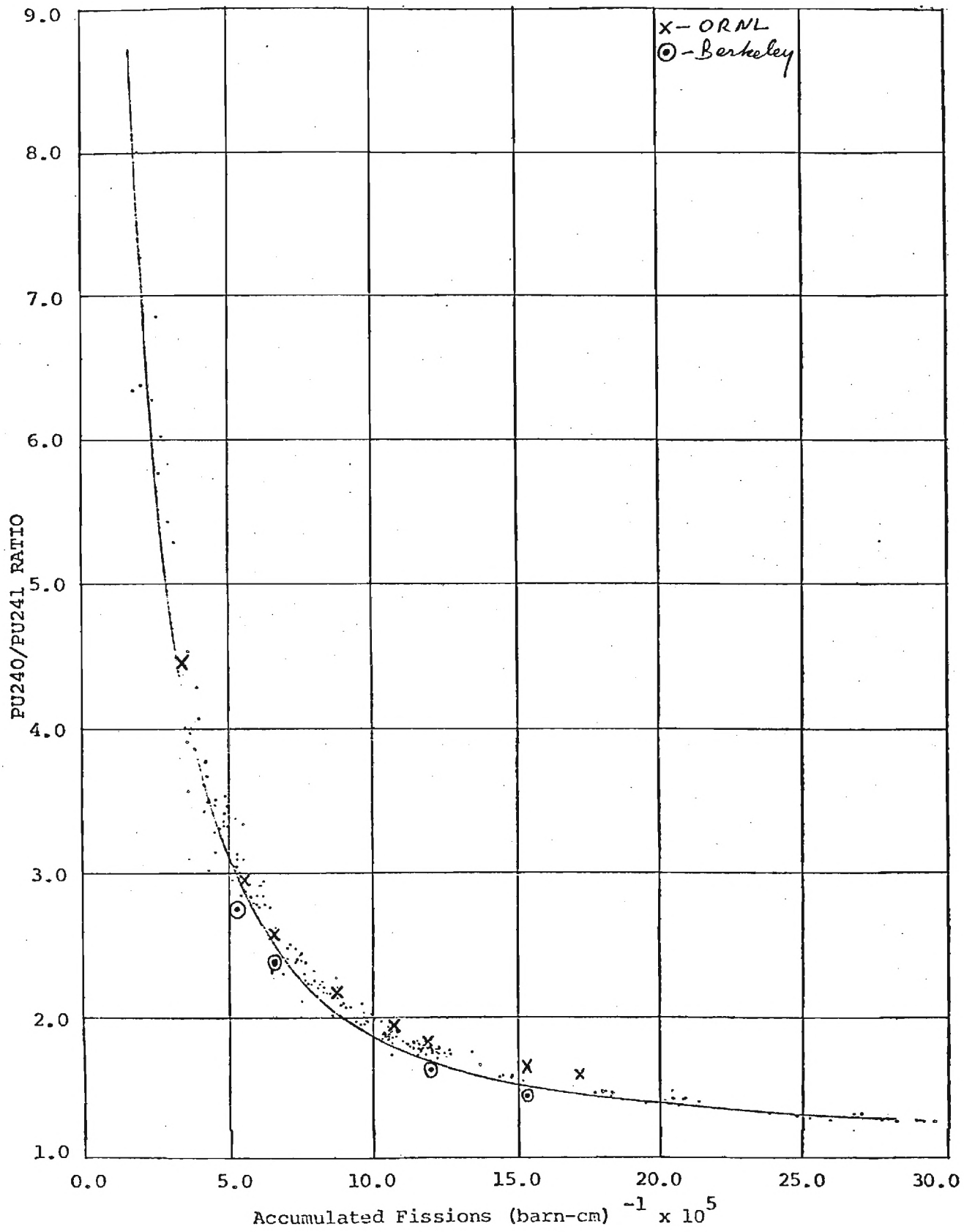

FIGURE 2-2. COMPARISON BETWEEN ANALYSIS AND YANKEE STAINLESS ISOTOPIC RATIOS (From: Ref. 14 p. 3-4)

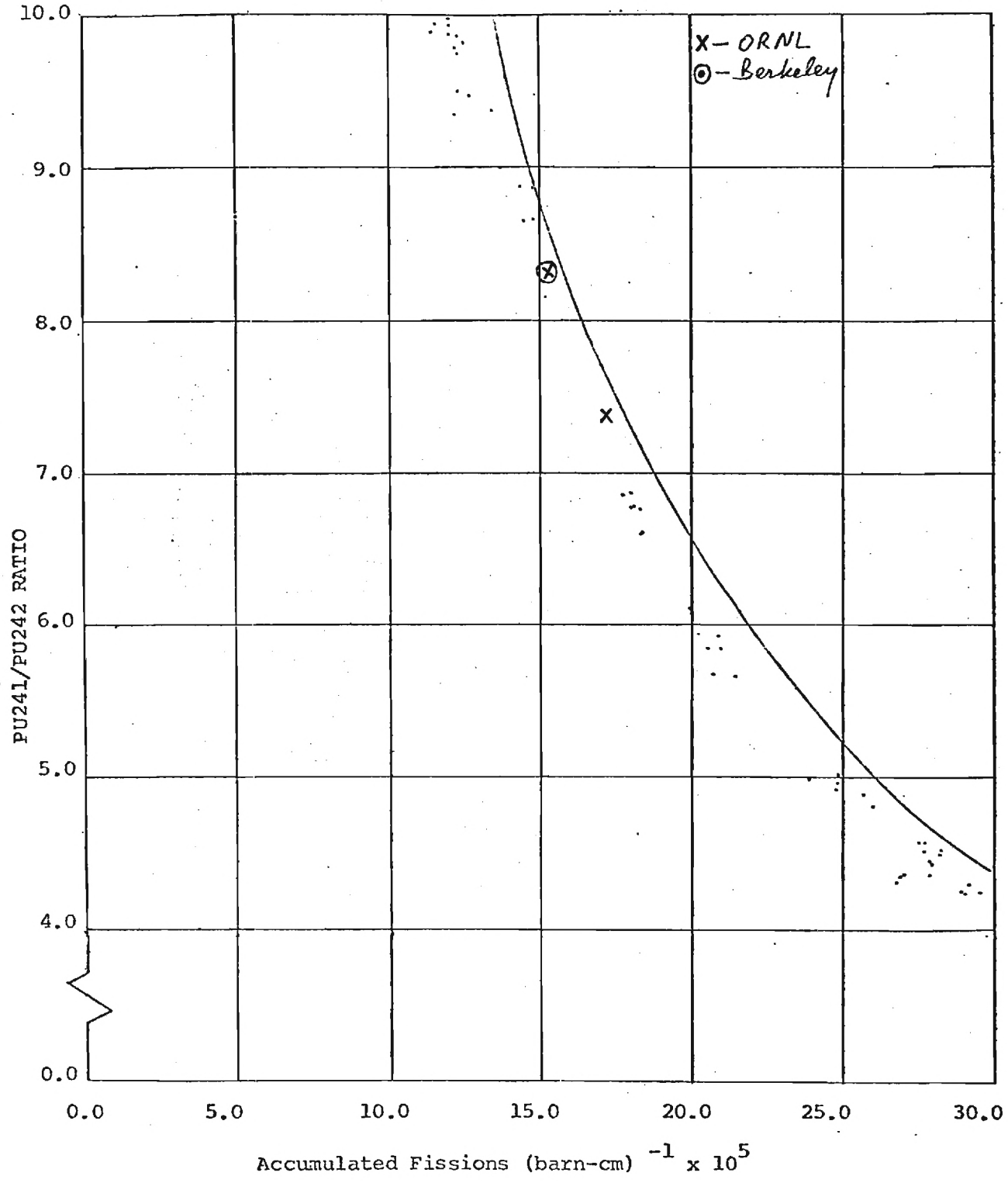

FIGURE 2-3. COMPARISON BETWEEN ANALYSIS AND YANKEE STAINLESS ISOTOPIC RATIOS
(From: Ref. 14 p. 3-5)

References

1. C. R. Weisbin, J. M. Kallfelz, H. S. Bailey, and E. Kujawski, "Economic Impact of Uncertainties in Data Adopted for Core Design," Attachment 1 to letter of same subject from D. B. Trauger (ORNL) to R. G. Staker (DOE), dated September 25, 1978.

2. C. L. Cowan (GE-ARSD), "Impact of Data and Methods Uncertainties on Fast Reactor Design Parameters," letter to C. R. Weisbin, ORNL, and J. M. Kallfelz, Ga. Tech, dated December 11, 1979.

3. J. M. Kallfelz, J. H. Marable, and C. R. Weisbin, letter to C. L. Cowan (GE-ARSD), dated January 25, 1980.

4. J. H. Marable and C. R. Weisbin, "Uncertainties in the Breeding Ratio of a Large LMFBR," Proc. ANS Physics Division Topical Meeting, Gatlinburg, Tennessee (April 1978).

5. J. H. Marable, C. R. Weisbin, and G. de Saussure, "Uncertainty in the Breeding Ratio of a Large LMFBR: Theory and Results," to be published in NS&E, (1980).

6. J. M. Kallfelz and P. Levin, "Progress Report on Work for ORNL Subcontract 7802, Period January 9 - February 11, 1980," Memorandum to C. R. Weisbin, J. H. Marable, and M. L. Williams, dated February 12, 1980.

7. C. L. Cowan (GE-ARSD), letter to J. M. Kallfelz and J. H. Marable, dated February 29, 1980.

8. D. R. Vondy, T. B. Fowler, and G. W. Cunningham, "VENTURE: A Code Block for Solving Multigroup Neutronics Problems Applying the Finite-Difference Diffusion-Theory Approximation to Neutron Transport, Version II," ORNL-5062/R1, Oak Ridge National Laboratory (November 1977).

9. J. M. Kallfelz, "VENTURE Γ^* Calculations, Peak/Ave Power Density," Memo to D. Vondy, ORNL, dated February 25, 1980.

10. J. M. Kallfelz, "Economic Impact of Uncertainties in Cross Sections for Thermal Reactors," Memo to C. R. Weisbin and M. L. Williams, dated January 14, 1980.

11. J. M. Kallfelz, G. B. Bruna, G. Palmiotti, and M. Salvatores, "Burnup Calculations with Time-Dependent Generalized Perturbation Theory," Nucl. Sci. Eng., 62, 304 (1977).

12. P. Levin, "The Effect of the 1 eV Resonance of Pu-240 on Isotopic Calculations in EPRI-CELL," Memorandum to M. L. Williams, dated January 22, 1980.

13. J. B. Melehan, "Yankee Core Evaluation Program, Final Report," WCAP-3017-6094 (January 1971).

14. "Advanced Recycle Methodology Program System Documentation," EPRI Report CCM-3, Electric Power Research Institute (September 1977), Part I, Chapter 3, Section 1.

15. "Advanced Recycle Methodology Program System Documentation," EPRI Report CCM-3, Electric Power Research Institute (September 1977), Part II, Chapter 5.

16. R. Carlson, Memorandum to J. M. Kallfelz and P. Levin, dated February 23, 1980.

17. "PWR Core Modeling Procedures for Advanced Recycle Methodology Program," EPRI Draft (August 1979).

18. R. J. Nodvik, "Supplementary Report on Evaluation of Mass Spectroscopic and Radiochemical Analyses of Yankee Core I Spent Fuel, Including Isotopes of Elements Thorium through Curium," WCAP-6086 (August 1969).

Appendix I

Comparison: Yankee-Zr Between Odelli Ozer's Input to Ours (GENERAL Input)

1. Geometry (Hot) (cm)	Ozer's	Ours
PELOR fuel outer radius:	.402133	.4023
CLADOR clad outer radius:	.460502	.4605
Cell equivalent radius:	.669369	.6664

2. Densities (Hot)

2.1 Fuel

	Ozer's	Ours
Number Densities:		
O^{16} :	4.49696-2	4.4980-2
U^{235} :	6.59704-4	6.6143-4
U^{236} :	2.27096-6	3.0358-6
U^{238} :	2.18228-2	2.1819-2
Enrichment (w/o):	2.898	2.905
RHFUEL UO_2 density (gr/cm^3):	10.0705	10.080

2.2 Clad (Odelli uses Zirconium instead of Zirc-4)

Number Densities:	3.96387-2	3.9778-2

2.3 Moderator (Hot)

Number Densities:		
O^{16}	2.57569-2	2.5686-2
H	5.15138-2	5.1372-2
Water density (gr/cm^3)	.7704	.76819

---

*This is the correct value. The reported value (6) was incorrectly calculated with cold dimensions.

2.4 Boron (Hot)

	Ozer's	Ours
Number Densities:	2.42065-6	3.38907-6
PPMB	285	400

3. Operation Conditions

	Ozer's	Ours
POWER (watts/cm):	189.95	204.25
TFUEL fuel avg. temp (^{o}F):	1538.32 (*)	1515.50
TCLAD clad avg. temp. (^{o}F):	530.32 (*)	578.95
TMOD Moderator avg. temp. (^{o}F):	527.60 (**)	530.00
TRES Resonance effective temp. (^{o}F):	1337.62	1377.60

4. Resonance Data

	Ozer's	Ours
4.1 Temperatures (^{o}K)		
Thermal Res. temp.:	1067.5	1020.7
Epithermal Res. temp.:	998.5	1020.7
4.2 Mean Chord length (cm):	.804266	.8046
4.3 Dancoff correction factor:	.382015	.39437

4.4 Excess Potential (barns) BOC values

Nuclide:		
U^{235}:	301.561	298.605
U^{238}:	9.11615	7.348

5. Buckling (cm^{-2})	7.008-4	7.531-4 (***)

---

*Temperatures used for TEMPID on cross section tape. Not necessarily the actual ones.

**Temperature required to maintain the water density assuming pressure of 2000 psi.

***Our B^2 is just a guess since we ran a search problem (for $k_{eff} = 1$).

Appendix II

Yankee-Zr/My Case
ENGINEERING Input

NOTE: The notations are described in section 3.2 of (15)

Arrays and Variables

WF234 = 2.577-4
WF235 = 2.90495-2
WF236 = 1.339-4

RHFUEL = .94 (94% of 10.96)

CLAD = 2 (Zirc-4)
GRID = 1 (Zirc-4 grid)
PRESS = 2000 (psia)

OPTION (7) = 1 (buckling search)
OPTION (22) = 1 (^{o}F)
OPTION (23) = 1 (psia)
OPTION (24) = 1 (time steps in hrs)

NTS = 20 (time steps)

POWR = 205.77 (= $\rho_u * \pi * PELOR^2 * p = 9.0815 * \pi * .3994^2 * 45.212$)

BUCKL = 7.531-4 (initial guess for search)

DSIRDK = 1 (desired k)
EPSILN = .01 (for search)

SPECT = 1 (U^{235} spectrum NAI library. -1 @ ORNL).

TFUEL = 1515.50 (^{o}F)
TCLAD = 578.95
TMOD = 530.00

PELOR = .3994 (cm)
CLADIR = .4064
CLADOR = .4597
PITCH = 1.1811

MESH = 1 (8 pts @ fuel)

(Refer to Table II-1 for the following data).

TIMSTP(1) = 96., 100., 188., 24., 376., 500., 708., 660., 2*390.,
TIMSTP(11) = 72., 444., 816., 744., 636., 744., 823., 2*1064.

RELPWR(1) = .796, 2*.978, 3*1.165. 1.105, 1.031, 2*1.079,
RELPWR(11) = 2*1.069, .987, .962, .994, .883, .775, 3*1.

PPMB(1) = 1012, 994, 969, 950, 2*859, 719, 598, 2*470, 9*400

TRES(1) = 1273.42, 2*1370.84, 3*1453.91, 1425.70, 1395.55, 2*1417.33,
TRES(11) = 2*1411.12, 1375.79, 1363.53, 1378.70, 1319.51, 1245.23, 2*1377.6

DRATIO(1) = 1.0146, 2*.9962, 3*.9924, .9937, .9924, 2*.9899,
DRATIO(11) = 2*.9924, .9950, .9962, .9950, 1.0086, 1.0374, 2*1.

DISAD = -1.0 for NAI @ ORNL

TABLE II-1. Time Dependent Variables

Time step #	Δt (hrs)	Accum. Time (hrs)	TMOD (°F)	Specific PWR (kw/kg)	PPMB	RELPWR	DRATIO	Original[a] time step #
1	96	96	518	35.970	1012	.796	1.0146	1
2	100	196	533	44.214	994	.978	.9962	2
3	188	384	533	44.212	969	.978	.9962	3
4	24	408	536	52.669	950	1.165	.9924	4
5	376	784	536	52.669	859	1.165	.9924	6
6	500	1284	536	52.669	859	1.165	.9924	6
7	708	1992	535	49.938	719	1.105	.9937	7
8	660	2652	536	46.630	598	1.031	.9924	8
9	390	3042	538	48.783	470	1.079	.9899	9
10	390	3432	538	48.783	470	1.079	.9899	9
11	72	3504	536	48.310	400[b]	1.069	.9924	10
12	444	3948	536	48.310	400[b]	1.069	.9924	12+13
13	816	4764	534	44.635	400[b]	.987	.9950	14
14	744	5508	533	43.479	400[b]	.962	.9962	15
15	636	6144	534	44.950	400[b]	.994	.9950	16+17
16	744	6888	523	39.909	400[b]	.883	1.0086	18+19
17	823	7711	498	35.025	400[b]	.775	1.0374	20+21
18	1064	8775	530	45.212	400[b]	1.	1.	22+23
19	1064	9839	530	45.212	400[b]	1.	1.	22+23

(a) Table C-3 of Ref. 13.

(b) Actual PPMB 400, but we use 400

Appendix III

Yankee-SS/My Case
ENGINEERING Input

Arrays and Variables

WF234 = 2.1-4
WF235 = 3.4-2
WF236 = 2.0-4

RHFUEL = .93 (93% of 10.96)

DISH = .0144 (1- .9856)

VFMOD (3) = .007 (SS fraction in moderator)

CLAD = 3 (SS-304)

PRESS = 2000. (psia)
OPTION (7) = 1 (buckling search)
OPTION (22) = 1 (^{o}F)
OPTION (23) = 1 (psia)
OPTION (24) = 1 (time steps in hrs)

POWR = 117.33 (w/cm = $\pi * R_F^2 * \rho_u * p = \pi * .37338^2 * 8.9736 * 29.854$)

BUCKL = 8.02-4 (See: "The fuel" below - for ρ_u)

SPECT = -1 (U^{235} fission spect. - @ ORNL!)

DSIRDK = 1. (desired k)
EPSILN = .01 (for search)

TFUEL = 1219. (^{o}F)
TCLAD = 549.
TMOD = 514.

PELOR = .3734 (cm)
CLDIR = .3785
CLDOR = .4318
PITCH = 1.0719

MESH = 1 (8 pts. @ fuel)

NTS = 27

TIMSTP (1) = 100., 400., 500., 10*983.6, 3096., 100., 400., 10*749.3

RELPWR (1) = 13*1., 1-7, 12*1.1097

TRES (1) = 14*1149., 12*1188.

DISAD = -1 (for NAI @ ORNL)

The Fuel

Initial isotopic weight fractions:

WF234 = 2.1-4
WF235 = 3.4-2
WF236 = 2.0-4
WF238 = 9.6559-1

$$\text{WFALLU} = \frac{2.1\text{-}4}{234.041} + \frac{3.4\text{-}2}{235.044} + \frac{2.0\text{-}4}{236.044} + \frac{9.6559\text{-}1}{238.0508} = 4.2026\text{-}3$$

Atomic fractions: AF234 = 2.1350-4
AF235 = 3.4420-2
AF236 = 2.0161-4
AF238 = 9.6517-1

AUO_2 = AF234*234.041 + AF235*235.044 + AF236*236.044 + AF238*238.0508 + 31.99 = 269.936

Cold RHFUEL = 10.18 gr/cm^3

$$N_{16_{cold}} = \frac{10.18*.6023}{269.936} *2 = 4.5429\text{-}2$$

$$\rho_o = \frac{N_{16}*15.995}{.6023} = 1.2064 \text{ gr/cm}^3$$

$$\rho_u = \text{RHFUEL} - \rho_o = 8.9736 \text{ gr/cm}^3$$

$$\rho_u = 10.18 \left(1 - \frac{31.99}{269.936}\right) = 8.9736 \text{ gr/cm}^3$$

SCHOOL OF NUCLEAR ENGINEERING

Atlanta, Georgia 30332 (404) 894-3720

E26-B01

April 2, 1980

MEMORANDUM

TO: C. R. Weisbin, J. H. Marable, and M. L. Williams (ORNL)

FROM: J. M. Kallfelz and P. Levin

SUBJECT: Progress Report for ORNL Subcontract 7802, Period March 5 - March 31, 1980

Accomplishments

- The initial phase of the joint Ga. Tech/ORNL/GE work on the sensitivity analysis of a CDS-type heterogeneous LMFBR has been completed. A summary describing the present status of this task has been submitted for presentation at the September ANS Reactor Physics Division Topical Meeting.

- EPRI-CELL isotopic calculations have been performed for the H. B. Robinson 2 reactor, and the results are reported.

- Detailed summaries have been prepared describing the techniques and data sources employed to model the three LWRs for which EPRI-CELL isotopics calculations have been performed. These summaries, attached to this report, will serve as a valuable guide for future power reactor calculations.

- Execution of the ANISN-B1 test case has been attempted, but thus far this case has not run successfully.

- For CSEWG data testing, work has been initiated with XSDRN to collapse 91 group cross sections for the TRX-1 and TRX-2 criticals.

Plans for Work for Next Month

- Work will continue on the analysis of the CDS-type heterogeneous LMFBR. Based on the results presented in attachment 4, J. Kallfelz and J. Marable have prepared a list of further topics to investigate, and these will be pursued jointly with ORNL and GE.

- The ANISN-B1 test case will be further investigated, with the goal of successful execution thereof.

- Calculations for CSEWG thermal data testing with TRX-1 and TRX-2 will be performed.

1. Design and Sensitivity Analysis of an LMFBR Heterogeneous Core (J. M. Kallfelz)

In our previous progress reports,[1-3] we have proposed a joint analysis with General Electric of a CDS-type LMFBR heterogeneous core. We have discussed[1-3] the theoretical aspects of including a new parameter, the peak/total power ratio (PPD), in the VENTURE generalized adjoint (Γ *) calculational capability, as well as other aspects of determining the uncertainty in the peak linear power. Considerable progress has been made on this task this month.

We have run simple benchmark cases for Γ * for the above ratio,[4] and they have been used in the successful implementation of the new capability into VENTURE. We have assisted in the analysis of VENTURE runs for this new capability performed at ORNL, using a reactor model supplied by GE which is characteristic of those being considered for the CDS study.

Jointly with many ORNL staff members, a sensitivity analysis of several performance parameters has been performed for the above model, with particular emphasis on studies related to the peak linear power. Besides the sensitivity studies of k, the breeding ratio, and PPD, neutron-gamma transport effects and energy deposit were studied.

The lead responsibility for this task had been assigned to this author, who spent considerable time during this report period at ORNL, coordinating this effort. The present status of this work is given in Attachment 4, a summary[5] submitted for presentation at the September ANS Reactor Physics Division Topical Meeting.

2. EPRI-CELL (P. Levin)

The EPRI-CELL effort has been concluded, for the time being. The reported period was devoted accordingly: For terminating the isotopics calculations, and documentation.

2.1 H. B. Robinson Unit #2 Isotopic Calculations

The Robinson-2 isotopic calculations were part of EPRI-CELL isotopics benchmarking reported by NAI.[8] The information about this core is limited regarding both its operation and measurements. Our modeling is described in attachment 3. We refer to a pin cell of 2.56% U^{235} enriched Zirc-4 cladded UO_2 fuel element. The fuel was irradiated 487 days in Cycle I, cooled for 64 days, irradiated for an additional 312 days in Cycle II, and cooled for 669 days prior to measurements. The calculations were performed on the Berkeley computer with the NAI cross section library.

2.1.1 Results

There were merely 3 samples in the entire experiment, of which only 2 results are cited by NAI (24,750 and 30,920 MWD/T). The NAI actually benchmarked EPRI-CELL against CPM.

Our results are listed in Table 1 and plotted (for Pu^{239}/Pu^{240} ratio) in Fig. 2-1.

a. Pu^{239}/Pu^{240} Ratio: Our EPRI-CELL results are higher than CPM by 5.2% (at 16100 MWD/T) to 11.6% (at 27600 MWD/T). On the other hand, CPM results are lower than the measured Pu^{239}/Pu^{240} ratios by 5.1% (at 24570 MWD/T) to 4.7% (at 30920 MWD/T).

b. Pu^{240}/Pu^{241} Ratio: Our results are lower than CPM by 15% (at 16100 MWD/T) to 19% (at 27600 MWD/T). Yet, CPM ratios are 6.6 - 6.7% higher than the measured ones.

2.1.2 Discussion: Effect of Cooling Period on Isotopic Ratios

EPRI-CELL calculates isotopic concentrations for each depletion step. These densities are valid for that very particular time. Several isotopes decay naturally, so that their concentrations keep on changing even though the flux is zero.

For its accounting CINDER calculates the Pu production:

$$U^{238} \xrightarrow{n,\gamma;2\beta^-} Pu^{239} \xrightarrow{n,\gamma} Pu^{240} \xrightarrow{n,\gamma} Pu^{241} \xrightarrow{n,\gamma} Pu^{242}$$

No time delay is assumed (i.e. the Np^{239} half life is ignored in this chain). Nor does any material contribute to this chain by decay. Thus, at zero power no Pu isotope is produced. Yet, each of the four decays according to $N(t) = N_o e^{-\lambda t}$ with its decay constant .

Isotope	Pu^{239}	Pu^{240}	Pu^{241}	Pu^{242}
λ (sec^{-1})	9.017-13	3.25-12	1.689-9	5.795-14

For comparison of calculated results with measured values, one has to account for the decay - especially that of Pu^{241}.

For H. B. Robinson Unit 2, a cooling period of 669 days preceded the measurements. During that period the various isotopes decayed:

Isotope	239	240	241	242
$\frac{N}{N_o}$	.99995	.99981	.90699	practically 1.0000

The decay is almost negligible for 239, 240, and 242. Yet, there is a reduction of 9.3% in Pu^{241}. This effects both 240/241 and 241/242 isotopic ratios.

Plutonium Isotopic Weight Ratios at 24,570

Measurement[a]	239/240	240/241	241/242
	2.55 ± .07 (2.75%)[c]	1.83 ± .07 (3.83%)	3.03 ± .27 (8.91%)
EPRI-CELL[b]:			
w/o decay	2.700 (+5.89%)[d]	1.617 (-11.6%)	3.594 (+18.6%)
corrected		1.738 (-2.56%)	3.260 (+7.58%)

[a] Table 5-1, p. 3-20 of Ref. 8

[b] Linear interpolation from results of 24,087 and 24,935 MWD/T

[c] Relative error in measurements

[d] Deviation from measured values

2.2 Modeling the CELL Calculations

As we conclude the EPRI-CELL effort, we summarized the modeling of the three isotopics calculations. The main purpose of that summary is to present the assumptions and methods by which one arrives at our input, starting from the available information. This is by no means a universal "transfer function", and there are specific assumptions for each case. Thus, the summary is composed of three separate modeling guides (attachments 1-3).

Our experience has been limited to NAI cross-section libraries. The summaries provide for ENDF libraries as well.

The ENGINEERING input is far more versatile than the GENERAL input. We have adapted it as a standard input for our calculation, thus getting rid of many problems of "averaging" (see our discussion of Yankee-Zr GENERAL input (7)).

Finally, the summaries do not replace EPRI-CELL documentation.[9] It is assumed that the reader is familiar with this documentation and its terminology.

References

1. J. M. Kallfelz and P. Levin, "Progress Report for ORNL Subcontract 7802, Period February 12 - March 4, 1980," Memorandum to C. R. Weisbin, J. H. Marable, and M. L. Williams, dated March 5, 1980.

2. J. M. Kallfelz and P. Levin, "Progress Report for ORNL Subcontract 7802, Period January 9 - February 11, 1980," Memorandum to C. R. Weisbin, J. H. Marable, and M. L. Williams, dated February 12, 1980.

3. J. M. Kallfelz and P. Levin, "Progress Report for ORNL Subcontract 7802, Period November 7 - December 6, 1980," Memorandum to C. R. Weisbin, J. H. Marable, and M. L. Williams, dated December 7, 1979.

4. J. M. Kallfelz, "Test Cases for Γ^*, Peak/Total Power," Memorandum to D. Vondy, dated March 12, 1980.

5. J. M. Kallfelz, C. L. Cowan, J. H. Marable, M. L. Williams, C. R. Weisbin, J. D. Drischler, and T. B. Fowler, "Design and Sensitivity Analysis of a CDS-Type LMFBR Heterogeneous Core," Summary submitted for presentation at the ANS Topical Meeting, Advances in Reactor Physics and Shielding, to be held September 14-17, 1980, in Sun Valley, Idaho.

6. "Advanced Recycle Methodology Program System Documentation," EPRI Report CCM-3, Electric Power Research Institute (September 1977).

7. P. Levin, "Modeling of Yankee Rowe Zircaloy-clad Fuel Elements for EPRI-CELL," Appendix I of a Memorandum to C. R. Weisbin, J. H. Marable, and M. L. Williams (ORNL) from J. M. Kallfelz and P. Levin, dated February 12, 1980.

8. Part I of Ref. 6, Chapter 3, Section 5.

9. Part II of Ref. 6, Chapter 5.

Table 1. EPRI-CELL Results for H. B. Robinson-2

Burnup (MWD/T)	Weight Ratios			
	$\frac{Pu^{239}}{U^{238}}$	$\frac{Pu^{239}}{Pu^{240}}$	$\frac{Pu^{240}}{Pu^{241}}$	$\frac{Pu^{241}}{Pu^{242}}$
3683	1.9262-3	11.480	4.6783	30.877
16099	4.6780-3	3.6761	1.8093	5.9467
18337	4.8830-3	3.3377	1.7319	5.1060
18337[(a)]	4.8830-3	3.3377	1.7481	5.0585
20987	5.0595-3	3.0166	1.6842	4.3201
24087	5.2119-3	2.7368	1.6250	3.6776
24935	5.2438-3	2.6727	1.6116	3.5307
27611	5.3231-3	2.4972	1.5756	3.1293
27611[(b)]	5.3228-3	2.4975	1.7368	2.8383

(a) Following 64 days of zero power.

(b) Following a cooling down period of 669 days.

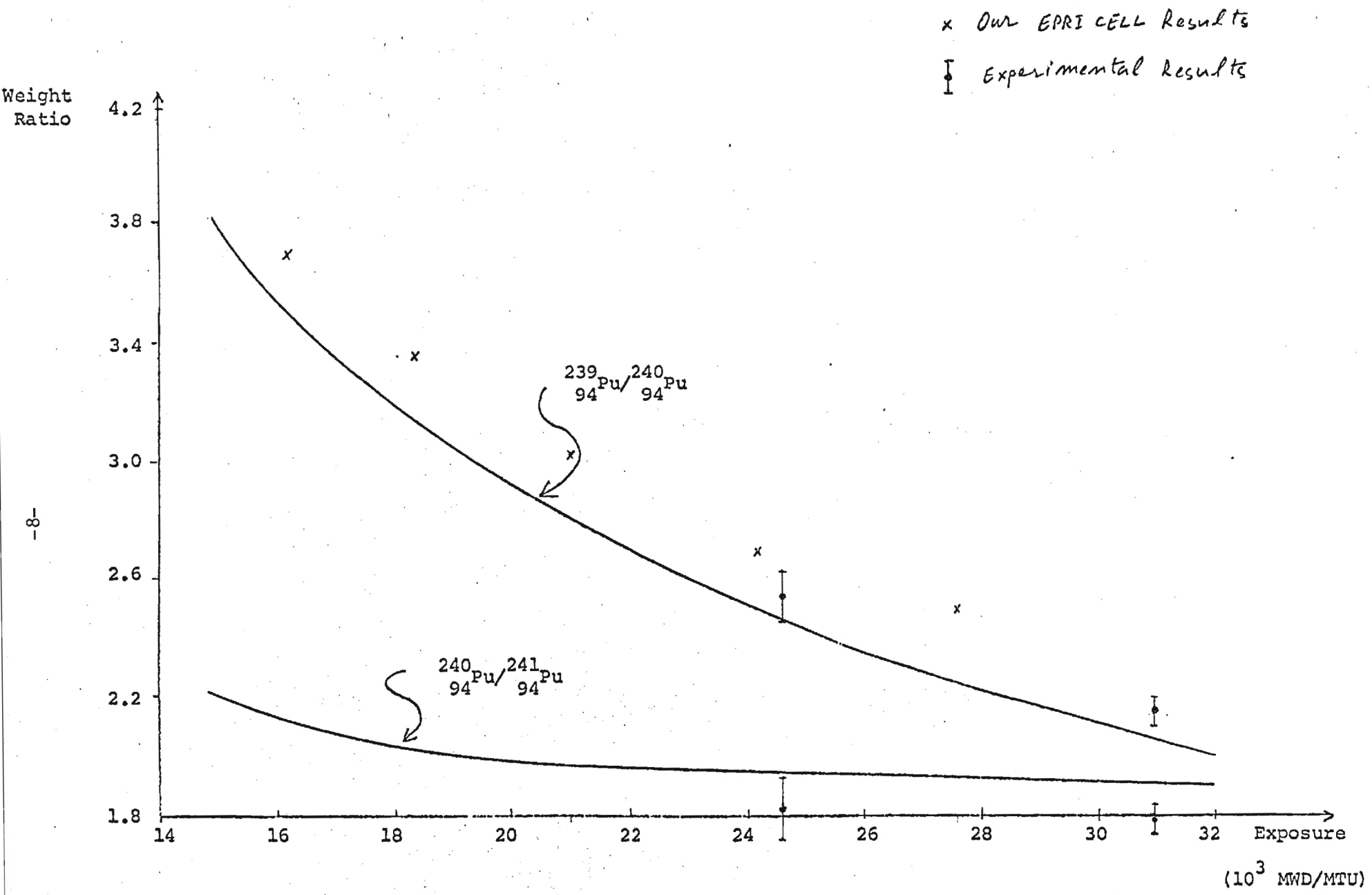

Figure 2-1. Weight Ratio of Plutonium Isotopes Predicted by CPM
(From Ref. 8, p. 3-21)

Modeling of Yankee Rowe SS-clad Fuel Elements for EPRI-CELL (P. Levin)

1. Introduction

This modeling refers to fuel elements of Yankee Rowe Core I, including also those recycled in Core II and those recycled in Core IV. The complete description of the experimental program is given in Ref. 1. Supplementary information is found in Refs. 2 and 3.

It is assumed that the reader is familiar with the EPRI-CELL document[8] and its terminology. ARMP Modeling Procedures[5] are referred to as guidelines in several items.

2. Operation Conditions

A pin cell calculation refers essentially to a certain site in core and the associating operation conditions. A-priori such a calculation cannot represent the entire core. There were many sampling sites in the experimental program, and the calculation represents a subset of all the sites that underwent similar conditions such as fluxes and temperatures. As can be seen from Fig. 2-1 of Ref. 1, the assemblies E5, F5 and E6 are expected to behave quite similarly, and calculation for one is valid for the others. E5 was unloaded at the end of Core I; F5 was unloaded at the end of Core II; E6 was stored during core III outside the core, and was reloaded for Core IV. (Ref. Fig. 2-2 of (1)).

Within the assembly we refer to the innermost sampled rods (subassembly c in Fig. 3-1 of (1)). According to a discussion in chapter 4 of (2) those rods are in an asymptotic region away from control rods or gaps.

Along the rod, samples were taken from six axial zones (Fig. 3.3.2 of (6)). From experimental scanning of the rods, Zone 3 (Figs. 6.7-6.12 of (2)) seems to have the smallest gradient and we shall refer to it in the following modeling.

Time Dependence

We do not know the variation of the temperatures within the cycle. We use cycle averaged temperatures, etc., as given in Table 10-1 of (1). The length of cycles and "cooling" periods are taken from Table 10.2 of (1).

State Variable	Core I	Core II	Core IV
Specific Power (kw/kg)	29.8540	33.1280	24.291
Moderator Temp. (^{o}F)	514	514	513
Clad Temp. (^{o}F)	549	553	542
Fuel Avg. Temp. (^{o}F)	1219	1268	1119
Resonance Eff. Temp. (^{o}F)	1149	1188	1066
System Pressure (psia)	2000	2000	2000
Cycle Length (hrs)	10836	7993	8089

Zero power periods of 3096 hours between Core I and II and of 8880 hours between Core II and IV.

No boron presented in Core I and II. In Core IV boron varied from 845 ppm at BOC to 0 at 5000 hours.

Assumptions

We follow procedure C2 (p. 7-3) of (5) by assuming critical buckling throughout the operation. The ARMP document (7) assumes "infinite lattice" which cannot be justified from the flux shapes discussed above. A consultant of ours claims that one should use the actual overall buckling, rather than the critical one. From a study that we made for Yankee Core V[9] it seems as if the isotopic ratios are quite insensitive to variation of the buckling. (Less than 1% change in either isotopic content or ratios.)

3. Preparation of the ENGINEERING Input

3.1 Geometry (Cold Dimensions)

(Table 2-1 of (1))

Pellet O.D. = .294"

Clad O.D. = .340"

Clad thickness = .021"

Fuel rod pitch = .422"*

Input items

PELOR = .3734 cm (pellet outer radius)

CLADIR = .3785 cm (clad inner radius)

CLADOR = .4318 cm (clad outer radius)

PITCH = 1.0719 cm

We do not use XTRA region in this modeling, since the sampled rods are not next to control rods or instrumentation.

3.2 Materials

3.2.1 Fuel

UO_2 cold density : 10.18 gr/cm^3** (i.e. 93% of theoretical 10.96 gr/cm^3). The volume reduction by dishing, etc. is a factor of .9856**.

The isotopic content of the uranium (nominal enrichment of 3.4%) is given in p. 10-16 of (1).

Input Items

RHFUEL = .93

DISH = .0144 (1-.9856)

WF234 = 2.1-4
WF235 = 3.4-2
WF236 = 2.0-4
} weight fractions

---

*In the asymptotic region discussed above.

**Ref. 2, p. 4

3.2.2 Clad and Grid

The clad is stainless steel, and the only reference to its type is on p. 4 of (2), where it is described as Type 384. Since no information is found about such a type, we assume that the type is 304.

No information is given for the grid. Since we have to choose between Zirc-4 and Incomel, we assume the latter.

Input Items

CLAD = 3 (SS - 304)

GRID = 2 (Incomel)

3.2.3 Moderator

The water density is set by the code according to the operating conditions (to be discussed later). The ferrules that wrap the rods are accounted for in the moderator; according to Table 4-8 of (3) the volume fraction is 0.7%.

Input Item

VFMOD (3) = .007 (SS - 304 fraction).

3.3 Reference Operation Conditions

The uranium equivalent atomic mass:

$$AU = \frac{1}{\sum \frac{WF_i}{A_i}} = \left(\frac{2.1\text{-}4}{234.041} + \frac{3.4\text{-}2}{235.044} + \frac{2.0\text{-}4}{236.044} + \frac{.96559}{238.051} \right)^{-1} = 237.95$$

$$AUO_2 = AU + 31.99 = 269.94$$

Therefore, the uranium cold density:

$$\rho_u = 10.96 * RHFUEL * \frac{AU}{AUO_2} = 8.9840 \quad (gr/cm^3)$$

For specific power of p = 29.854 (w/gr):

$$q' = \pi*(PELOR)^2 * (1-DISH) *\rho_u*p = \pi*.3734^2*.9856*8.9849*29.854 = 115.80 \text{ (w/cm)}$$

(Note: The (1-DISH) was erroneously omitted in the run itself.)

Input Items

POWR = 115.80	(w/cm)
TFUEL = 1219.0	(^oF)
TCLAD = 549.0	(^oF)
TMOD = 514.0	(^oF)
PRESS = 2000.0	(psia)

3.4 Miscellaneous Input

MESH = 1	(8 mesh point @ fuel)
OPTION (7) = 1	(Buckling search)
OPTION (22) = 1	(Temp. in ^oF)
OPTION (23) = 1	(Pressure in psia)
OPTION (24) = 1	(Time steps in hrs)

3.5 Buckling

As mentioned above, we use the buckling search option. The desired k_{eff} is 1.0. For initial guess of the buckling we calculate one for a cylindrical core with 6 cm reflector saving. From p. 5 of (2):

Core diameter = 75.1"

Core height = 91.9"

$$B^2 = \left(\frac{\pi}{H+12}\right)^2 + \left(\frac{2.405}{R+6}\right)^2 = \left(\frac{\pi}{231.39+12}\right)^2 + \left(\frac{2.405}{95.38+6.0}\right)^2 = 8.02\text{-}4 \ (cm^{-2})$$

Input Items

BUCKL = 8.02-4 (cm^{-2})

DSIRDK = 1.0 (Desired k_{eff})

EPSILN = .01 (k_{eff} convergence)

3.6 Time Dependent Information

Since EPRI-CELL is limited to 30 time steps, we ran Core I and II only. In retrospect, it seems that longer time steps could be used so as to enable the running of Core IV as well.

Core I life of 10836 hours is divided into 13 time steps. Core II life of 7993 hours is divided into 12 time steps and there is a zero power step in between 3096 hours long.

We assume constant operation conditions throughout each core life. No boron is present in these cores.

Input Items

NTS = 27 (No. of steps +1)

TIMSTP(1) = 100., 400., 500., 10*983.6, 3096., 100., 400., 10*749.3

(length of each step in hours)

RELPWR(1) = 13*1.0, 1.-7, 12*1.1097 (Relative power)

TRES(1) = 14*1149., 12*1188 (Resonance eff. temp.: ^{o}F)

3.7 Computer/Library Dependent Input

3.7.1 U^{235} fission spectrum is used. Yet the indicator for that spectrum differs for the different libraries and computers:

In Berkeley

SPECT = 1 (Essentially NAI library)

In ORNL

SPECT = -1 (NAI library)

SPECT = 1 (ENDF library)

3.7.2 The disadvantage factor is calculated in the ORNL version of EPRI-CELL and is applicable for ENDF libraries only. Thus, in ORNL only:

DISAD = -1. (NAI library)

DISAD = 0. (ENDF library)

References

1. R. J. Nodvik, "Supplementary Report on Evaluation of Mass Spectrometric and Radiochemical Analyses of Yankee Core I Spent Fuel, Including Isotopes of Elements Thorium Through Curium," WCAP-6086 (August 1969).

2. S. Jedruch and R. J. Nodvik, "Experimentally Determined Burnup and Spent Fuel Composition of Yankee Core I," WCAP-6071 (July 1965).

3. P. G. Lacey and R. E. Radcliffe, "Diffusion-Theory Depletion Analysis of the Yankee Core," WCAP-6077.

4. "Advanced Recycle Methodology Program System Documentation," EPRI Report CCM-3, Electric Power Research Institute (September 1977).

5. "PWR Core Modeling Procedures for Advanced Recycle Methodology Program," EPRI Draft (August 1979).

6. R. J. Nodvik, "Evaluation of Mass Spectrometric and Radiochemical Analyses of Yankee Core I Spent Fuel," WCAP-6068 (March 1966).

7. Part I of Ref. 4, Chapter 3, Section 2.

8. Part II of Ref. 4, Chapter 5.

9. J. M. Kallfelz and P. Levin, "Progress Report for ORNL Subcontract 7802, Period February 12 - March 4, 1980," Memorandum to C. R. Weisbin, J. H. Marable, and M. L. Williams, dated March 5, 1980, Section 2.1.

Attachment 2 to April 2, 1980 Ga. Tech Progress Report to ORNL

Modeling of Yankee Rowe Zircaloy-clad Fuel Elements for EPRI-CELL (P. Levin)
(ENGINEERING Input)

1. Introduction

We refer to two fuel assemblies that were irradiated in Yankee Rowe Core V. Unlike the rest of the assemblies, these included Zircaloy-4 cladded fuel elements (part of A-264-C and the entire A-263-C except for 3 rods). The complete description is given in Ref. 1.

It is assumed that the reader is familiar with the EPRI-CELL documentation[3] and its terminology. ARMP Modeling Procedures[4] are referred to as guidelines for several items.

2. Operation Conditions

Since measurements were done in assemblies that are different from their surroundings, we try to model the least effected sampling zones. We assume the innermost rods of A-263-C (Fig. 2.1 of (1)) which is least perturbed. The axial gamma scan of the rods (Fig. 12.1 of (1)) shows that sampling Zone 3 had an almost flat flux. Thus, assuming a pin cell calculation with an asymptotic spectrum, we refer to Zone 3 in the following modeling.

Operating conditions are taken from Table C-3 of (1), and are given in Table 1. For the sake of presentation, we adapt the asymptotic conditions as "reference". Practically, it does not make any difference since the time-dependent variables are input relatively.

The calculations extend over Core V life (9839 hrs) only. Once adequate information as of the cooling period is available, an additional zero power step should be added, since the plutonium isotopic content kept on changing (especially the decay of Pu-241).

The reference operation conditions:

Specific power : 45.212 (kw/kg)

Fuel avg. Temp. : 1515.50 ^{o}F

Clad avg. Temp. : 578.95 ^{o}F

Moderator avg. temp. : 530.00 ^{o}F

System pressure : 2000.0 (psia)*

Assumptions

2.1 Buckling

We follow procedure C2 (p. 7-3) of (4), by assuming critical buckling throughout the operation.

2.2 Boron

According to procedure C4 (p. 7-3) of (4) we follow the boron letdown curve until it reaches 400 ppm. Then keeping that concentration for the rest of the cycle.

3. Preparation of the ENGINEERING Input

3.1 Geometry (cold dimensions)

Pellet O.D. = .3145"

Clad O.D. = .362"

Clad thickness = .021"

Fuel Rod Pitch = .465"

No dishing information is given, so we assume it is zero.

---

*No information is given as for the pressure in Core V. We adapt the nominal pressure of Core I-IV.

Input Items

PELOR = .3994 (Pellet outer radius, cm)

CLADIR = .4064 (Clad inner radius, cm)

CLADOR = .4594 (Clad outer radius, cm)

PITCH = 1.1811 (cm)

(Dish is set to zero by default.)

3.2 Materials

3.2.1 Fuel

UO_2: 94% dense, 2.9% enriched (p. 2-1 of (1)). The isotopic composition of the uranium (weight fractions) are drawn from Table D-1 of (1).

Input Items

WF234 = 2.577-4

WF235 = 2.90495-2

WF236 = 1.339-4

RHFUEL = .94 (94% of 10.96 gr/cm^3)

3.2.2 Clad and Grid

Cladding material: Zircaloy-4. Spacer grid material not specified; we assume it is the same as the cladding material.

Input Items

CLAD = 2 (Zirc-4)

GRID = 1 (Zirc-4)

3.3 Reference Operation Conditions

The uranium equivalent atomic mass:

$$AU = \frac{1}{\sum \frac{WF_i}{A_i}} = \left(\frac{2.5774}{234.041} + \frac{2.905-2}{235.044} + \frac{1.339-4}{236.044} + \frac{.97056}{238.051}\right)^{-1} = 237.96$$

$AUO_2 = AU + 31.99 = 269.95$

Therefore, the uranium cold density:

$$\rho_u = 10.96 * RHFUEL * \frac{AU}{AUO_2} = 9.0815 \ (gr/cm^3)$$

For specific power of p = 45.212 (w/gr)

$$q' = \pi*(PELOR)^2 *\rho_u*p = \pi*.3994^2*9.0815*45.212 = 205.77 \ (w/cm)$$

Input Items

POWR = 205.77	(w/cm)
TFUEL = 1515.50	(^oF)
TCLAD = 578.95	(^oF)
TMOD = 530.00	(^oF)
PRESS = 2000.0	(psia)

3.4 Miscellaneous Input

MESH = 1	(8 mesh points @ fuel)
OPTION(7) = 1	(Buckling search)
OPTION(22) = 1	(Temp. in ^oF)
OPTION(23) = 1	(Pressure in psia)
OPTION(24) = 1	(Time steps in hrs)

Buckling

As mentioned above, we use the buckling search option. The desired k_{eff} is 1.0.

For initial guess of B^2, we use equivalent cylindrical core with 6 cm reflector saving.

The equivalent radius of 76 assemblies 16 x 16 rods is

$$R_{eq}^2 = 76*16*16*PITCH^2$$

$$R_{eq} = 92.95 \text{ cm}$$

Core Height = 91.68" = 232.87 cm

$$B^2 = \left(\frac{\pi}{H+12}\right)^2 + \left(\frac{2.405}{R+6}\right)^2 = 7.531 \ (cm^{-2})$$

Input Items

BUCKL = 7.531-4	(cm^{-2})
DSIRDK = 1.0	(Desired k_{eff})
EPSILN = .01	(k_{eff} convergence)

3.6 Time Dependent Information

(Refer to Table 1 at the end of this section)

The 9839 hours long cycle is divided into 19 time steps. The following parameters were taken from Table C-3 of (1):

a) TRES - Resonance effective temperature

b) RELPWR - Ratio of specific power at any time step to the referecen one

c) PPMB - Boron concentration follows letdown curve until it reaches 400 ppm, then it is kept constant.

Moderator Density

The FORTRAN routine VCL listed in Appendix 1 is used in EPRI-CELL to calculate water specific volume as a function of pressure and temperature. Using TMOD from Table 1 we calculate DRATIO which is the ratio of water density at any time step to the reference one.

Input Items

NTS = 20 (No. of steps +1)

TIMSTP(1) = 96., 100., 188., 24., 376., 500., 708., 660., 2*390.,

TIMSTP(11) = 72., 444., 816., 744., 636., 744., 823., 2*1064.

RELPWR(1) = .979, 2*.978, 3*1.165, 1.105, 1.031, 2*1.079

RELPWR(11) = 2*1.069, .987, .962, .994, .883, .775, 2*1.0

PPMB(1) = 1012, 994, 969, 950, 2*859, 719, 598, 2*470, 9*400

TRES(1) = 1273.42, 2*1370.84, 3*1453.91, 1425.70, 1395.55, 2*1417.33,

TRES(11) = 2*1411.12, 1375.79, 1363.53, 1378.70, 1319.51, 1245.23, 2*1377.6

DRATIO(1) = 1.0146, 2*.9962, 3*.9924, .9937, .9924, 2*.9899,

DRTIO(11) = 2*.9924, .9950, .9962, .9950, 1.0086, 1.0374, 2*1.

3.7 Computer/Library Dependent Input

3.7.1 Fission Spectrum: U^{235} fission spectrum is used. Yet the indicator for that spectrum differs for the different libraries and computers:

In Berkeley

SPECT = 1 (Essentially NAI library)

In ORNL

SPECT = -1 (NAI library)

SPECT = 1 (ENDF library)

3.7.2 Disadvantage Factor: Is calculated in ORNL version of EPRI-CELL, and is applicable for ENDF libraries only. Thus, in ORNL only:

DISAD = -1.0 (NAI library)

DISAD = 0. (ENDF libraries)

Table 1. Time Dependent Variables[a]

Time step #	Δt (hrs)	Accum. Time (hrs)	TMOD (°F)	Specific Power (kw/kg)	PPMB	RELPWR	DRATIO	TRES (°F)
1	96	96	518	35.970	1012	.796	1.0146	1273.42
2	100	196	533	44.214	994	.978	.9962	1370.84
3	188	384	533	44.212	969	.978	.9962	1370.84
4	24	408	536	52.669	950	1.165	.9924	1453.91
5	376	784	536	52.669	859	1.165	.9924	1453.91
6	500	1284	536	52.669	859	1.165	.9924	1453.91
7	708	1992	535	49.938	719	1.105	.9937	1425.70
8	660	2652	536	46.630	598	1.031	.9924	1395.55
9	390	3042	538	48.783	470	1.079	.9899	1417.33
10	390	3432	538	48.783	470	1.079	.9899	1417.33
11	72	3504	536	48.310	400[b]	1.069	.9924	1411.12
12	444	3948	536	48.310	400[b]	1.069	.9924	1411.12
13	816	4764	534	44.635	400[b]	.987	.9950	1375.79
14	744	5508	533	43.479	400[b]	.962	.9962	1363.53
15	636	6144	534	44.950	400[b]	.994	.9950	1378.70
16	744	6888	523	39.909	400[b]	.883	1.0086	1319.51
17	823	7711	498	35.025	400[b]	.775	1.0374	1245.23
18	1064	8775	530	45.212	400[b]	1.	1.	1377.60
19	1064	9839	530	45.212	400[b]	1.	1.	1377.60

(a) Table C-3 of Ref. 1

(b) Actual PPMB 400, but we use 400.

Reference

1. J. B. Melehan, "Yankee Core Evaluation Program, Final Report," WCAP-3017-6094 (January 1971).

2. "Advanced Recycle Methodology Program System Documentation," EPRI Report CCM-3, Electric Power Research Institute (September 1977).

3. Part II of (2), Chapter 5.

4. "PWR Core Modeling Procedures for Advanced Recycle Methodology Program," EPRI Draft (August 1979).

Appendix 1

EPRI-CELL Function VCL (P,T)

For given pressure P (psia) and temperature T (^{o}F) this function calculates specific volume of water VCL (ft^3/lb).

Water density (gr/cm^3) = 0.0160185/VCL.

LISTING

```
      FUNCTION VCL (P,T)                                                    00013840
      IMPLICIT REAL*8(A-H,O-Z)                                              00013850
      DIMENSION A(10)                                                       00013860
      DATA A/7.4690826900,-7.50675994D-3,-.462032290-8,-.12154701110-2,     00013870
     *0.0D0,7.7051704300,-5.29739118D-2,-2.96725673D-9,-.7663600550-2,       00013880
     *1.4398702060-11/                                                      00013890
      IF (T.LT.50.0.OR.T.GT.705.4) GO TO 10                                 00013900
      X=T-705.398                                                           00013910
      X3=X**3                                                               00013920
      I=0                                                                   00013930
      IF (T.GE.200.0) I=5                                                   00013940
      PSL=DEXP(X*(A(I+1)+A(I+2)*X+A(I+3)*X3+A(I+5)*X3*X)/((1.+A(I+4)*X)*    00013950
     1(T+459.688))+8.0728362)                                               00013960
      IF (P.LE.PSL) GO TO 10                                                00013970
      E1=DLOG(P-PSL)-2.68756849                                             00013980
      E3=E1*2.                                                              00013990
      E4=E1/2.                                                              00014000
      E2=-T*.55555555+391.88778                                             00014010
      E5=E2**(1.0/6.0)                                                      00014020
      E6=E5*E5                                                              00014030
      E7=E6*E5                                                              00014040
      E5=E7/(-8.21761572)*E5                                                00014050
      E5=DEXP((E7*1.05467592E-3-.0160537197)*E2+E5-3.7166732+E1+4.1340100014060
     191)+62.4278183                                                        00014070
      E8=DEXP(((E7*1.35599875E-3-.0297916028)*E7-.22389889)*E7-2.9762622 00014080
     14+E1)                                                                 00014090
      E8=DEXP(E2*(-6.85078156E-2)-11.4147912+E3)-E8                         00014100
      E8=DEXP(E7*(-.92085142)-.9504583+E4)+E8                               00014110
      E7=1.0+0.134248 9*E6-0.00394626 3*E2                                  00014120
      E4=E2*(E2**3/1.33527748E12-1.203374E-3)                               00014130
      VCL=((E6*(-.3151548)+E4+3.1975)/E7-E8)/E5                             00014140
      RETURN                                                                00014150
10    WRITE (6,20) P,T                                                      00014160
      STOP                                                                  00014170
C                                                                           00014180
20    FORMAT (4H1 P=,E15.7,4H, T=,E15.7,21H NOT SUBCOOLED. PUNT.)           00014190
C     DEBUG UNIT(06),SUBCHK                                                 00014200
      END                                                                   00014210
```

Attachment 3 to April 2, 1980 Ga. Tech Progress Report to ORNL

Modeling of H. B. Robinson Unit 2 (P. Levin)

1. Introduction

There is so much information available for this particular reactor. Since it was mentioned as one of the benchmarking cases of ARMP we decided to model it to the best of our knowledge. The main goal of this modeling is to link the "real" operating core with its representation, so that one may still benefit from such a study even if the "real" differs somewhat from the exact reality. Our main reference[1] summarizes part of the required data. Other pieces of information are scattered in the attachments to that reference. It is impossible to relate that information to a specific rod, so there is no point in trying to compensate for such extra regions as burnable poison and water gaps. We model a pin cell, assuming asymptotic spectrum.

It is assumed that the reader is familiar with the EPRI-CELL document[3] and its terminology. ARMP Modeling Procedures[4] are referred to as guidelines in several items.

2. Operation Conditions

Only one set of temperatures is specified for the entire calculation. The time dependent specific power is listed for both "peak" and "average" along the fuel rod. Since everything else is averaged, we adopted the "average" specific power*. Yet, it may be reasonable to try the "peak" historgram since it lends to higher burnups.

---

*Because of the limit (30) on depletion steps, we further averaged these values with time.

The fuel was irradiated for two cycles 487 days and 312 days long, respectively. 64 days of zero power in between and additional cooling period of 669 days (zero power).

The boron is claimed to vary linearily with time from 855 ppm to 45 ppm. According to procedure C4 (p. 7-3) of (4) we should follow the letdown curve until 400 ppm and thereafter keep it constant (400 ppm). Right now we preferred the average of 450 ppm constant over the entire calculation. We do not anticipate a large discrepancy due to it.

Assumption

We follow procedure C2 (p. 7-3) of (4) assuming critical buckling throughout the operation period.

3. Preparation of the ENGINEERING Input

3.1 Geometry (cold dimensions)

Pellet O.D. = .3659"

Clad I.D. = .3734"

Clad O.D. = .4220"

Fuel Rod Pitch = .5630"

Dish Volume = 1.18%

Input Items

PELOR = .4647	(Pellet outer radius, cm)
CLADIR = .4742	(Clad inner radius, cm)
CLADOR = .5359	(Clad outer radius, cm)
PITCH = 1.4300	(cm)
DISH = .0118	

3.2 Materials

3.2.1 Fuel

3.2.1.1. Weight Fraction: U^{234} - .023 w/o

U^{235} - 2.561 w/o

No information about U^{236}. We assume it is 0.2% (as in Yankee-SS).

3.2.1.2. Density: There is 443.7 kg U per assembly of 204 rods, i.e. 2175 gr U/rod.

Fuel stack length = 365.76 cm

Actual fuel volume: π *(PELOR)^2 *(1-DISH)*365.76 = 2.4520+2 cm^3/rod

Cold uranium density ρ_u = 8.8703 gr/cm^3

The uranium equivalent atomic mass:

$$AU = \frac{1}{\sum \frac{WF_i}{A_i}} = \left(\frac{2.3\text{-}4}{234.041} + \frac{2.561\text{-}2}{235.044} + \frac{2.\text{-}4}{236.044} + \frac{.97396}{238.051} \right)^{-1} = 237.97$$

AUO_2 = Au + 31.99 = 269.96

$$\rho_{UO_2} = \rho_u * \frac{269.96}{237.97} = 10.063 \text{ gr/cm}^3$$

i.e. 91.81% of 10.96 gr/cm^3 (theoretical)

Input Items

RHFUEL = .9181 (fraction of 10.96)

WF234 = 2.3-4
WF235 = 2.561-2
WF236 = 2.0-2

} (weight fractions)

3.2.2 Clad and Grid

Cladding material: Zircalloy-4. Spacer grid material: Incomel.

Input Items

CLAD = 2 (Zirc-4)

GRID = 2 (Incomel)

3.3 Reference Operation Conditions

Reference power = 6.984 kw/ft

Fuel average temp. = 1200^{o}F

Clad average temp. = 612^{o}F

Moderator average temp. = 572^{o}F

System Pressure = 2250 (psia)

Input Items

POWR = 229.13 (w/cm)

TFUEL = 1200.00 (^{o}F)

TCLAD = 612.0 (^{o}F)

TMOD = 572.0 (^{o}F)

PRESS = 2250.0 (psia)

(Note: EPRI-CELL regards the above power as "cold" and modifies it according to a built-in function of the fuel temperature. That means about 0.5% reduction in POWR. Knowing this internal function, one should use POWR = 229.13/.9948 = 230.32).

3.4 Miscellaneous Input

MESH = 1 (8 mesh points @ fuel)

OPTION(7) = 1 (Buckling search)

OPTION(22) = 1 (Temp. in ^{o}F)

OPTION(23) = 1 (Pressure in psia)

OPTION(24) = 1 (Time steps in hrs)

3.5 Buckling

As mention above the buckling search option is used, with desired k_{eff} of 1.0. For initial guess of B^2 we use equivalent cylindrical core with 6 cm reflector saving: Core Height : 365.76 cm, Core Radius : 152.02 cm

$$B^2 = \left(\frac{\pi}{H+12.}\right)^2 + \left(\frac{2.405}{R+6.}\right)^2 = 3.0081\text{-}4 \text{ cm}^{-2}$$

Input Items

BUCKL = 3.008-4

DSIRDK = 1.0 (desired k_{eff})

EPSILN = .01 (convergence criterion)

3.6 Time Dependent Information

(Refer to Table 1 at the end of this section.)

The calculations cover Cycle I (11692 hrs), 1530 hours of zero power, Cycle II (7482 hrs), and 16056 hours (669 days) of zero power (cooling).

Constant boron concentration of 450 ppm is assumed throughout the calculations.

The only parameter which is varied with time is the power.

We have no information about resonance effective temperature. Following EPRI-CELL documentation[3] we let the code use the defauld which is TFUEL.

Input Items

NTS = 30 (No. of steps + 1)

TIMSTP(1) = 100., 700., 1493.8, 585.7, 712.8, 660.4, 674.7,

TIMSTP(8) = 1436.9, 573.7, 555.9, 687., 667.1, 710.1, 600.5,

TIMSTP(15) = 882.1, 642.4, 1536., 610.3, 800.9, 690.9, 695.4,

TIMSTP(22) = 687.7, 502.7, 635.2, 684.7, 640.7, 726., 807.7,

TIMSTP(29) = 16056.

PPMB(1) = 30*450

RELPWR(1) = 3*1., .9977, 1.0170, 1.0368, 1.0444, .9994, .9808,

RELPWR(10) = .9890, .9422, .9294, .9370, .9062, .9103, .9198,

RELPWR(17) = 1.-7, .7455, .7984, .8046, .7801, .7536, .7620,

RELPWR(24) = .7669, .7709, .7682, 2*.7659, 1.-7

3.7 Computer/Library Dependent Input

3.7.1 Fission Spectrum: U^{235} fission spectrum is used. Yet, the indicator for that spectrum differs for the different libraries and computers.

In Berkeley

SPECT = 1 (Essentially NAI library)

In ORNL

SPECT = -1 (NAI library)

SPECT = 1 (ENDF libraries)

3.7.2 Disadvantage Factor: Is calculated in ORNL version of EPRI-CELL, and is applicable for ENDF libraries only. Thus, in ORNL only:

DISAD = -1. (NAI library)

DISAD = 0. (ENDF libraries)

Table 1. Power History

Step #		Period	Step length (hrs)	Cumulative Time (hrs)	Average Power (w/ft)	Relative Power
1		Till	100.0	100.0	6.984	1.
2		(incl.)	700.0	800.0	6.984	1.
3		Oct. 1971	1493.8	2293.8	6.984	1.
4		Nov. 1971	585.7	2879.5	6.968	.9977
5		Dec. 1971	712.8	3592.3	7.103	1.0170
6		Jan. 1972	660.4	4252.7	7.241	1.0368
7		Feb. 1972	674.7	4927.4	7.294	1.0444
8	Cycle I	Mar.-Apr. 1972	1436.9	6364.3	6.9795	.9994
9		May-June 1972	582.7	6947.0	6.850	.9808
10		July 1972	555.9	7502.9	6.907	.9890
11		Aug. 1972	687.0	8189.9	6.580	.9422
12		Sept. 1972	667.1	8857.0	6.490	.9294
13		Oct. 1972	710.1	9567.1	6.544	.9370
14		Nov. 1972	600.5	10167.6	6.329	.9062
15		Dec'72-Jan'73	882.1	11049.7	6.3575	.9103
16		Feb.-Mar. 1973	642.4	11692.1	6.4242	.9198
17		Shutdown	1536.0	13228.1	0	0
18		May-June 1973	610.3	13838.4	5.2063	.7455
19		July 1973	800.9	14639.3	5.576	.7984
20		Aug. 1973	690.9	15330.2	5.619	.8046
21		Sept. 1973	695.4	16025.6	5.448	.7801
22		Oct. 1973	687.7	16713.3	5.263	.7536
23	Cycle II	Nov. 1973	502.7	17216.0	5.322	.7620
24		Dec. 1973	635.2	17851.2	5.356	.7669
25		Jan. 1974	684.7	18535.9	5.384	.7709
26		Feb. 1974	640.7	19176.6	5.365	.7682
27		Mar. 1974	726.0	19902.6	5.349	.7659
28		Apr.-May 1974	807.7	20710.3	5.3473	.7657
29		Cooling	16056.0	36766.3	0	0

References

1. O. W. Hermann (ORNL), Letters to H. Lowenberg (NRC) dated April 20 and May 2, 1979. These were Attachment 2 to a letter from M. L. Williams (ORNL) to O. Ozer (EPRI) titled: "ORNL Thermal Reactor Studies During May," dated June 11, 1979.

2. Advanced Recycle Methodology Program System Documentation," EPRI Report CCM-3, Electric Power Research Institute (September 1977).

3. Part II of Ref. 2, Chapter 5.

4. "PWR Core Modeling Procedures for Advanced Recycle Methodology Program," EPRI Draft (August 1979).

DESIGN AND SENSITIVITY ANALYSIS OF A CDS-TYPE LMFBR HETEROGENEOUS CORE

J. M. Kallfelz
Georgia Institute of Technology
Atlanta, Georgia 30332

C. L. Cowan
General Electric Company
Sunnyvale, California 94086

J. H. Marable, M. L. Williams, C. R. Weisbin,
J. D. Drischler, and T. B. Fowler
Oak Ridge National Laboratory
Oak Ridge, Tennessee 37830

Submitted for presentation at the American Nuclear Society Topical Meeting, 1980 Advances in Reactor Physics and Shielding, to be held September 14-17, 1980, in Sun Valley, Idaho.

---

*Research sponsored by the U.S. Department of Energy under Contract No. W-7405-eng-26 with the Union Carbide Corporation.

I. INTRODUCTION

The Conceptual Design Study (CDS) concerns the development of an LMFBR in the 1000 MWe class. We have considered a heterogeneous LMFBR design characteristic of the models being studied for the CDS. We report various performance parameters and sensitivity-analysis results, with particular emphasis on studies related to the peak linear power. Reduction of uncertainties in this parameter have obvious importance both for licensing and economic considerations.

II. GENERAL REACTOR PARAMETERS

The reactor model considered is a parfait design, with three driver zones and three internal blanket zones. Table I gives some design and performance parameters of interest for this reactor.

III. SENSITIVITY STUDIES

Using the methods of generalized perturbation theory,[1-3] the nuclear data sensitivity $(\partial I/I)/(\partial\sigma_i / \sigma_i)$ of integral parameter I has been studied for the two parameters considered in an earlier work[3] for a homogeneous LMFBR, namely k_{eff} and the breeding ratio, as well as a ratio significant for determining the uncertainty in the calculated peak linear power. Considerable attention has been devoted in recent studies[4] to determining the maximum allowable value of this quantity.

Calculations were performed in 2D (R-Z) using VENTURE[5] to determine the sensitivity coefficients. Figure 1 shows results for the generalized importance function, Γ^*, for the ratio (point power density)/(total

Table I. General Design Parameters and Calculated Performance Parameters for a CDS-Type LMFBR Heterogeneous Core

Core Height (cm)	101.6
Core Effective Outer Radius (cm)	166.8
Total Power (MWth)	2540
Driver Clad IR/OR (cm)	0.312/0.349
Internal and Radial Blanket Clad IR/OR (cm)	0.523/0.608
Clad and Can Material	D-9 Alloy
Radial and Axial Blanket Thickness (cm)	35
Avg. MOEC Driver Enrichment (fissile atoms)/(heavy metal atoms)	16.8%
Breeding Ratio, MOEC	1.30
Doubling Time (years)	20
Driver, Internal Blanket Residence Time (years)	2
Avg. Discharge Driver Burnup (MWd/Metric Ton)	52,200

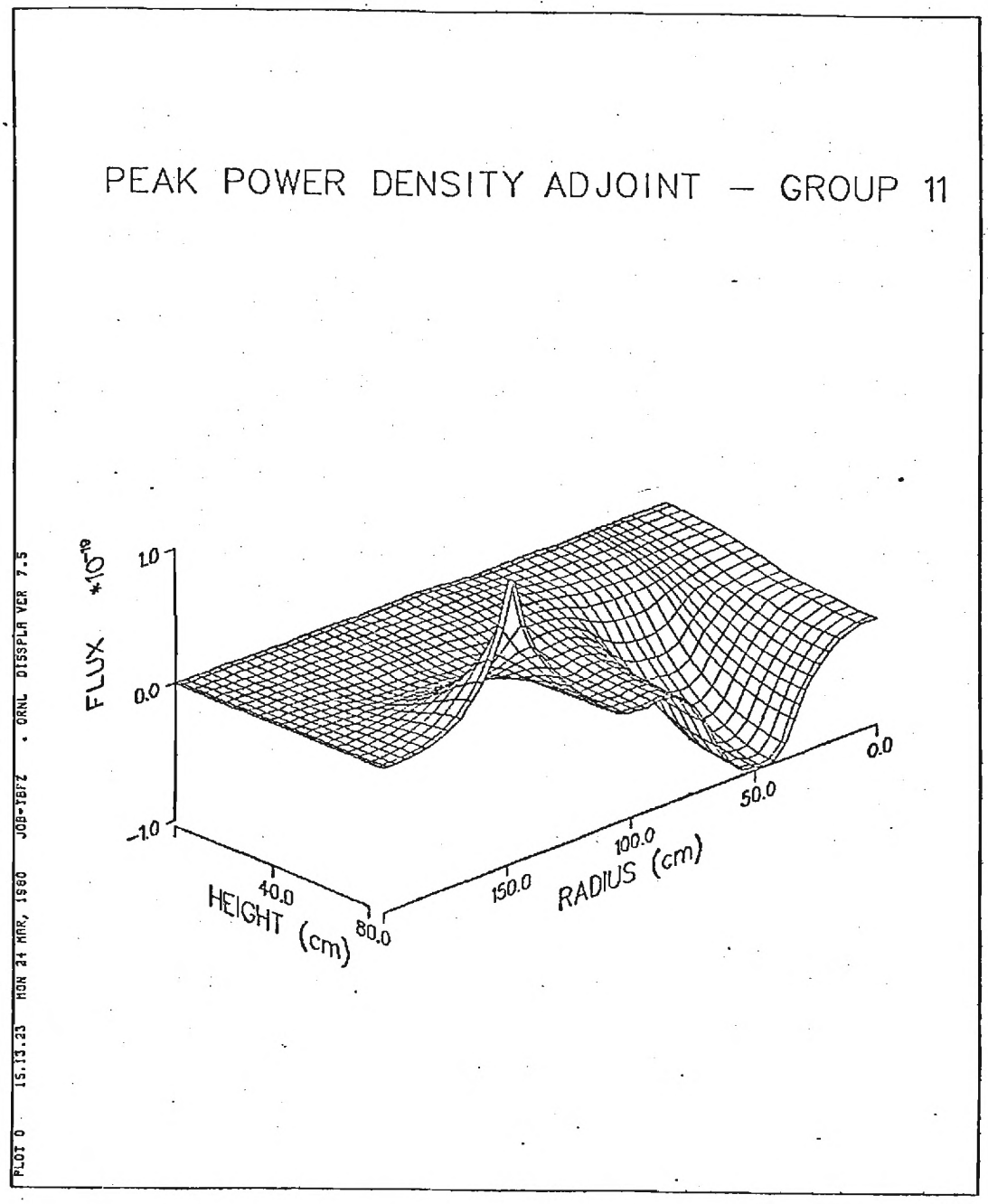

Fig. 1. Peak-power density generalized adjoint Γ^* for energies 67-111 keV in the lower half of the heterogeneous reactor model.

power), (PPD) for the base case point of peak power, a location which can change with sigma changes. The base case peak power occurs at a point in the outer driver zone, and Γ^* is strong positive near this point, decreasing and eventually becoming negative as the distance from this point increases. The strong negative region is the innermost driver zone, which strongly affects the denominator of PPD.

Sensitivity coefficients were calculated for the nuclear data as shown in Table II. The five largest total sensitivities for k and BR for this case and for a homogeneous reactor[3] are for the same reactions. Note the strong sensitivity of PPD to $^{238}U\ \sigma_c$, which influences the power distribution among zones.

Sensitivity coefficients can be folded with covariance files to determine the Variance (Var) of the integral parameter.[3] We have performed this folding for the data in Table II, and their contribution to Var is given. To obtain the standard deviation ($\sqrt{Var}$) all data which contribute appreciably to Var should be included, and further data are being investigated, particularly those which influence the neutron transport between zones; e.g., calculations indicate that the Na σ_{tr} sensitivity for PPD is about -0.05.

IV. NEUTRON-GAMMA TRANSPORT EFFECTS AND ENERGY DEPOSIT

To accurately relate the peak power density to the peak linear power, coupled (n-γ) transport calculations are necessary,[6] both on a reactor and pin cell level. It has long been recognized that such transport effects are particularly significant in a heterogeneous core.

Table II. Total Relative Sensitivities, Integrated Over All Energies and Regions

Nuclide	Reaction	k	BR[a]	PPD[b]
^{235}U	ν	0.00861	0.00559	-0.01165
	σ_f	0.00621	-0.01277	-0.01811
	σ_c	-0.00068	-0.00596	0.00097
^{238}U	ν	0.12226	0.02623	-0.05593
	σ_f	0.07520	0.01550	-0.06512
	σ_c	-0.19177	0.69384	0.22736
^{239}Pu	ν	0.66479	-0.01427	0.01567
	σ_f	0.48184	-0.66995	0.00467
	σ_c	-0.04372	-0.17261	0.01010
^{240}Pu	ν	0.08402	-0.00865	0.03083
	σ_f	0.05833	-0.00584	0.03555
	σ_c	-0.02310	0.07006	0.00080
^{241}Pu	ν	0.11543	-0.00831	0.01882
	σ_f	0.08454	-0.11304	0.02037
	σ_c	-0.00539	-0.01878	-0.00077
^{242}Pu	ν	0.00489	-0.00061	0.00227
	σ_f	0.00334	-0.00042	0.00260
	σ_c	-0.00180	0.00068	0.00005
Variance[c]		9.47×10^{-4}	$4.65 \times 10^{-}$	2.77×10^{-4}
Variance[c] (k-reset to 1 by enrichment)		--	9.66×10^{-4}	4.90×10^{-4}

[a] Convert BR to k-reset values (through changing Pu/U ratios in fuel) by adding 1.74068 × k sensitivities.

[b] Convert PPD to k-reset values by subtracting 0.385911 × k sensitivities.

[c] These variances are calculated from covariances and sensitivities of the above reactions only.

To determine the actual percentage of energy deposited in the fuel, Kerma factors, often used in fusion reactor studies,[8] have been employed.

Results of coupled (n-γ) calculations using the AMPX[9] system were folded with Kerma factors. We have compared the radial-dependent energy deposition rate from this calculation to results from a diffusion calculation which employed the common approximation that all recoverable energy stems from fission and is deposited at the point of fission.

The n-γ transport results for the percent of the total energy deposited in the driver regions and internal blanket regions are 2% lower and 10% higher, respectively, than for the diffusion calculation. At the point of maximum energy deposition, the energy deposited in the fuel pellet materials is 98.5% of the total.

References

1. A. Gandini, J. Nucl. Energy 21, 755 (1967).

2. G. P. Cecchini and M. Salvatores, Nucl. Sci. Eng. 46, 304 (1971).

3. J. H. Marable and C. R. Weisbin, "Uncertainties in the Breeding Ratio of a Large LMFBR," Proc. ANS Advances in Reactor Physics, Gatlinburg, Tennessee (April 10-12, 1978).

4. J. C. Chandler et al., "The Proliferation Resistant Preconceptual Core Design Study," TC-1082, Hanford Engineering Development Laboratory (March 1978).

5. D. R. Vondy, T. B. Fowler, and G. W. Cunningham, "VENTURE: A Code Block for Solving Multigroup Neutronics Problems Aplying the Finite-Difference Diffusion-Theory Approximation to Neutron Transport, Version II," ORNL-5062/R1, (November 1977).

6. "Determination of Thermal Energy Deposition Rates in Nuclear Reactors," ANS Standards, ANSI N676.

7. M. A. Abdou and C. W. Maynard, Nucl. Sci. Eng. 56, 360 (1975).

8. M. L. Williams et al., Nucl. Tech. 29, 384 (1976).

9. N. M. Greene et al., A Modular Code System to Generate Coupled Multigroup Neutron-Gamma Cross Sections from ENDF/B, ORNL/TM-3706, (March 1976).

SCHOOL OF NUCLEAR ENGINEERING E-26-B01

Atlanta, Georgia 30332 (404) 894-3720

May 19, 1980

MEMORANDUM

TO: C. R. Weisbin, J. H. Marable, and M. L. Williams (ORNL)

FROM: J. M. Kallfelz, P. Levin, and M. Becker

SUBJECT: Progress Report for ORNL Subcontract 7802, Period April 1 - May 9, 1980

Accomplishments

- Results of our calculations for the joint Georgia Tech/ORNL/GE sensitivity analysis of a CDS-type heterogeneous LMFBR were analyzed further, various related theoretical questions were further investigated, and a status summary for this work was prepared. This summary documents some of our benchmark testing of the new sensitivity capabilities employing VENTURE. It further documents the overall status of this work, and discusses topics for which further theoretical investigations and/or calculations are necessary. This summary can thus be used for planning further work on this topic, which should be completed by the end of July.

- Further benchmark calculations were performed with the Italian sensitivity codes, to test the new VENTURE capabilities.

- XSDRN was used to collapse 91 group cross sections for TRX-1 and TRX-2 to be used in CSEWG data testing.

- Debugging of the ANISN-B1 code was continued, and a test case without upscatter ran correctly. However, a test case with upscatter has still not run successfully.

- A memorandum[27] was prepared requesting several consultants to perform work on the topic of economic impact of uncertainties in cross sections for thermal reactors. A report on this topic by M. Becker is enclosed as Appendix 2.

Plans for Work for the Next Report Period

- Planning will be accomplished for work at ORNL and Georgia Tech during the summer in the general area of LMFBR design analysis, with emphasis on development and utilization of sensitivity analysis capabilities. A memorandum outlining proposed plans for this work will be prepared.

- EPRI-CELL calculations for various TMI-1 unit cells will be performed, for use by M. Williams in analysis of this reactor.

- Also for use in the TMI analysis, a code will be prepared to read EPRI-CELL/NUPUNCHER output cross sections, and punch them in CITATION format.

- A low priority item, which will be continued only if it does not interfere with the completion of the two previous tasks before the departure of P. Levin, is the continuation of the debugging work on ANISN-B1.

jhr

1. Sensitivity Analysis of A CDS-Type LMFBR Heterogeneous Core - (J. Kallfelz)

As reported in our last progress report[2] a summary covering this topic[1] was submitted for presentation at the ANS Reactor Physics Division Topical Meeting in Septembewr 1980. This summary has been accepted, and the activity on this topic has concentrated on documenting the present status of this work, and identifying topics for which further theoretical investigations and/or calculations are necessary.

The following status summary can be used for planning further work on this topic and assigning responsibilities for its completion. Any revisions to our summary,[1] which will be distributed to meeting participants, must be submitted by August 1. The significant portions of our work on this topic should thus be completed by that date. Obviously a logical distribution of responsibilities for the further work would be based on the topics of the tasks already accomplished by the various co-authors for the summary.

These responsibilities will be verified shortly, as part of the overall planning for work at ORNL and Georgia Tech on this and related topics for this summer by the co-authors and several other staff members including J. W. White and D. Biswas. I have agreed to initiate this process by preparing a memorandum outlining proposed plans after consulation with ORNL staff members.

1.1 Testing VENTURE Γ^* Capability for the Peak Power Density

The basic equations for Γ^* for the (point power density)/(total power) ratio (PPD) were discussed in previous reports.[11,12] The basic equations were given as follows, for a reaction rate ratio, R:

$$R = \frac{\int_{Vol_1} \sum_j \Sigma_{1j}(\vec{r})\,\phi_j(\vec{r})\,d\vec{r}}{\int_{Vol_2} \sum_j \Sigma_{2j}(\vec{r})\,\phi_j(\vec{r})\,d\vec{r}} = \frac{a_1}{a_2} \qquad (1)$$

The source in the equation for the generalized adjoint function, $\Gamma_j^*(\vec{r})$ was given as

$$S_j^*(\vec{r}) = \frac{\Sigma_{1j}(\vec{r})}{a_1} - \frac{\Sigma_{2j}(\vec{r})}{a_2} \qquad (2)$$

where Σ_1 and Σ_2 are zero outside Vol_1, and Vol_2, respectively.

For the case of power density ratios, both Σ_1 and Σ_2 have the same form

$$\Sigma_{ij}(\vec{r}) = \sum_k P^k \Sigma_{f,ij}^k(\vec{r}) \qquad (3)$$

where P^k is the total recoverable energy release for one fission in the k-th isotope. As noted after Eqn. (2) Σ_{1j} and Σ_{2j} differ in their space range.

Since one is often interested in the power density peak-to-average ratio, we proposed considering Vol_1 as a unit volume at the point of maximum power density, $\vec{r}_m$, and defining the numerator of Eqn. (1) as a point value,

$$a_1 = \sum_j \Sigma_{1j}(\vec{r}_m)\,\phi_j(\vec{r}_m) \qquad (4)$$

We initially proposed defining the denominator

$$a_2 = \int_{Vol_2} \sum_j \Sigma_{2j}(\vec{r})\,\phi_j(\vec{r})\,d\vec{r} \Big/ Vol_2 \qquad (5)$$

where Vol_2 is some appropriately defined volume. In Ref. 11 we discussed some potential problems associated with the definition of this average, and we subsequently decided to define a_2 as the total reactor power. Thus,

Vol_2 for our further studies is the total reactor volume, and it does not appear as a divisor in a_2.

To test the incorporation of this Γ^* capability into VENTURE[13] a series of test cases[14] were performed with the Italian perturbation codes.[5-7] Lack of agreement between results for Γ^* from VENTURE and CIAP[6] for the first test is indicative of the potential pitfalls in calculating Γ^* for PPD. The reasons for the discrepancy were trivial, but this and a following case indicate the obvious necessity for very careful benchmark testing of this new capability.

The source defined in Eqn. (2) is a point source, and when the generalized adjoint equation is solved, this source is multiplied by the volume (ΔVol_i) associated with the discrete mesh point, $\vec{r}_i$. To be consistent with equation (4), this volume should be 1.0 for the first term of the source. To avoid confusion, it is better to define Vol_1 in a_1 as the ΔVol associated with the point of peak power density, $\vec{r}_m$.

The source passed to the VENTURE module for the Γ^* calculation already includes the ΔVol_i, and based on Eqn. (4) Tom Fowler initially programmed the source as follows:

$$S_j^*(\vec{r}_m) = \Delta Vol(\vec{r}_m)\left[\frac{\Sigma_{1j}}{\sum_j \Sigma_{1j}\phi_j(\vec{r}_m)} - \frac{\Sigma_{2j}(\vec{r}_m)}{a_2}\right] \qquad (6)$$

Based on the above discussion, $\Delta Vol(\vec{r}_m)$ should also be in the denominator of the first term in the square brackets, i.e. $\Delta Vol(\vec{r}_m)$ cancels out of the first term. When Tom made the appropriate change to Eqn. (6), the agreement between the CIAP and VENTURE Γ^* results for the simple 1D case described in Tables 1 and 2 agreed closely. As noted in the comparison in

Table 1. Characteristics of Three-Group Two-Region Model Used for Benchmarking VENTURE [7*] for (Peak Power Density)/(Total Power) Ratio (PPD).

A. Composition, from Ref. 3.

Isotope	Concentration (10^{24} atom/cc)	
	Core	Blanket
U-238	.006	.012
Pu-239	.001	---
Na	.01	.007

B. Macroscopic Cross Sections, Using 3-Group Core Data Set from CITATION Test Case[4] in CIAP[6] Format.

Core	Blkt.
SIGA	
4.85110E-03	5.92087E-03
2.64211E-03	1.91158E-03
6.50273E-03	6.66121E-03
VUSIG	
1.31830E-02	1.43489E-02
4.52881E-03	5.07960E-05
6.21792E-03	0.
CHI	
6.17000E-01	6.17000E-01
3.73000E-01	3.73000E-01
1.00000E-02	1.00000E-02
DIF	
6.45619E+00	4.78309E+00
3.65657E+00	2.73718E+00
1.99481E+00	1.53102E+00

REG. 1 TRANS (CORE)

0.	0.
1.89620E-02	0.
3.93890E-04	2.54200E-03

REG. 2 TRANS (BLKT)

0.	0.
3.02580E-02	0.
6.58053E-04	3.04400E-03

Table 2. Comparison of Results for Γ^* for PPD, Using Compositions and Cross Sections of Table 1, for a 1D Slab Reactor.[a,b]

		x (cm)[c]		Γ^* (d)		
Grp	Point	CIAP	VEN	CIAP	CIAP/S_v	VEN
1	100	59.5	60.0	-.301	-.103	-.118
2	10	4.5	4.75	.439	.157	.155
3	1	0	.25	1.236	.425	.428

(a) Core and blanket mesh spacings are 0.5 and 1 cm, respectively. Core ½ thickness and blanket thickness are 39.5 and 30 cm, respectively.

(b) Peak power occurs at point 1 which is at 0. and 0.25 cm for CIAP and VENTURE, respectively.

(c) CIAP and VENTURE are mesh point and interval oriented, respectively. Thus the slight difference in distances.

(d) VENTURE and TAIM[5] ϕ normalized to a total source of 2.90772 (S_v) and 1.0, respectively.

Table 2, an exact comparison cannot be made since CIAP and VENTURE are mesh point and interval oriented, respectively.

Table 3 indicates that the VENTURE test case yielded $\delta\nu/\nu$ sensitivity results which satisfied necessary conditions for both k and PPD sensitivities. The conditions stated in this table are valuable for checking new calculation capabilities, and in fact Jim Marable detected a second error in our PPD Γ^* calculations when the first runs were made for the CDS reactor. The initial sensitivity results did not satisfy the conditions A and B of Table 3, and subsequent investigations indicated the considerable potential for confusion with a "half-core" model, such as we were using for the CDS calculations.

Codes differ in their flux normalization conventions for the "partial core" case, and this, of course, influences the Γ^* values because of the direct impact on a_1 and a_2 in S*. This constant normalization should, of course, cancel out in the calculation of the sensitivities, which involve products of $\phi\Gamma^*$.

Less obvious is the fact that for the VENTURE conventions, the shape of S* for PPD for the half and full core cases is apparently different, because we chose to define a_2 as the total power. Presumably with the VENTURE convention for the "half-reactor" case the peak power density, a_1, is the same as for the full reactor, while a_2, the total power, differs for the two cases. Hence, $S_j^*(\vec{r})$ in Eqn. (2) clearly differs for the two cases. When Jim and Tom made the appropriate changes to VENTURE, the CDS sensitivities did satisfy the expressions A and B of Table 3.

In summary, we have checked our VENTURE results against benchmarks and necessary conditions which they must satisfy, and believe that our

Table 3. Check that Results for VENTURE Case of Table 2 Yield Proper $\delta\nu/\nu$ Sensitivity Normalization. (For $\delta\nu/\nu = 1.0$, $\delta(\nu\Sigma_f) = \nu\Sigma_f$)[a]

Case A. For ϕ^*, $\sum' \frac{\delta k}{k} \Big/ \frac{\delta\nu}{\nu} \doteq 1.0$ [b]

Case B. For Γ^* (Peak/Total Power) $\sum' \frac{\delta R}{R} \Big/ \frac{\delta\nu}{\nu} \doteq 0$

Zone	Grp	Zone $\nu\Sigma_f$ $\cdot 10^2$	"NU*SIGF"[c] A	"NU*SIGF"[c] B	A·$\nu\Sigma_f$	B·$\nu\Sigma_f$ $\cdot 10^2$
1	1	1.318	19.94	.613	.263	.809
	2	.453	104.8	1.478	.474	.669
	3	.623	38.7	.304	.241	.189
2	1	1.435	1.5	-1.127	.021	-1.618
	2	.005	12.4	-9.73	.001	-.049
	3	0	5.1	-4.06	0	0
				Sum =	1.000	0.000

[a] More significant figures used in calculation!

[b] $\sum'$ indicates summation over regions, groups, and nuclides.

[c] Integrals of ϕ and ϕ^* or Γ^* provided by VENTURE for use in calculating $\nu\Sigma_f$ perturbation components.

results contained in our summary are correct. However, it would obviously be prudent to perform more testing before our results are published.

One test which should be performed is to repeat VENTURE calculations for a full reactor model to insure that the sensitivities are identical with the "half-reactor" model results. I have spent considerable time attempting such a calculation with the Italian codes[5-7] for the simple slab case described in Tables 1 and 2. Unfortunately, for reasons which I have still not been able to determine, the GLOBPERT[7] calculation of the sensitivities for the "full reactor" case will not run to completion.

However, a comparison of the CIAP[6] results for these two cases supports the above conclusion that for the normalization conventions of some codes, S* for the "half-reactor" and "full-reactor" cases are different. The ratio between a_1 and a_2 for the "half-reactor" case is twice that for the "full-reactor" run, causing an associated difference in S*. The "full-reactor" Γ^* calculation is apparently not completely converged, since it is slightly asymetric about the mid plane. However, $\Gamma^*(E,x)$ values for the two cases differ only by a constant, to within a few percent.

A further check which should, of course, be made on the PPD sensitivity coefficients is to perform direct perturbations in VENTURE runs. The next section discusses this topic further.

1.2 Comparison of Perturbation Theory Results with Direct Calculations

A first attempt at such comparison was singularly unsuccessful! However, the direct perturbations were performed hurriedly at GE, and it is possible that there is some confusion in the definition of the case considered. At any rate, U-238 σ_c was reduced by 25% separately in GE

groups 3, 4, and 5 as defined in Table 4. The resulting $\delta k/k$ and $\delta BR/BR$ (with enrichment reset) values were transmitted to us by Charley Cowan.[9]

Table 5 illustrates my attempt to reproduce the GE results for group 3, using VENTURE values. The resulting values for $\delta k/k$ and $(\delta BR/BR)_{reset}$ are in poor agreement with the GE values of 0.82% and + 4.05%, respectively. Jim Marable compared all the values and found the agreement was generally as poor as indicated by this example. This discrepancy obviously needs to be resolved in consultation with GE.

Furthermore, direct perturbations should be performed in VENTURE, particularly to confirm our sensitivities for PPD calculated with Γ^*.

1.3 Cross Section Set

The cross section set used for our initial calculations was generated for the homogeneous core considered in Ref. 10. A new set should be generated for our final calculations, presumably utilizing the ANISN runs already performed by Mark Williams and discussed in section 1.7 below.

1.4 Generation of Sensitivities and Covariance for Further Cross Sections

Table 6 indicates the sensitivities and covariances which we used to calculate the variances (VAR) of the integral parameters reported in our summary.[1] As we point out in our summary, to obtain the standard deviation ($\sqrt{VAR}$) of the integral parameters all data which contribute appreciably to VAR should be included.

For k and BR the reactions given in Table 6 may be adequate, but for the peak power density further data should be included, particularly those which influence the neutron transport between zones. Even k and BR are probably more sensitive to such data for a heterogeneous core than for a homogeneous design.

Table 4. Group Structures Used for GE Direct Calculation and ORNL Perturbation Calculations.

GE Group[9]	Lethargy[(a)]	E Range (keV)	ORNL Groups[10]
3	4.0-6.0	182-24.5	10-13
4	6.0-8.0	24.5-3.4	14-17
5	8.0-10.0	3.4-0.444	18-21

[(a)] 0 Lethargy : 10 MeV

Table 5. VENTURE Perturbation Calculation of Change in k and Breeding Ratio (with k-reset by enrichment) for 25% Reduction of U-238 σ_c in GE Group 3.[a]

A. Definitions[b]

$$\left(\frac{\sigma_i}{BR}\frac{\partial BR}{\partial \sigma_i}\right)_{reset} = \left(\frac{\sigma_i}{BR}\frac{\partial BR}{\partial \sigma_i}\right) + A\left(\frac{\sigma_i}{k}\frac{\partial k}{\partial \sigma_i}\right)$$

where

$$A = \left(\frac{\epsilon}{BR}\frac{\partial BR}{\partial \epsilon}\right) \Big/ \left(\frac{\epsilon}{k}\frac{\partial k}{\partial \epsilon}\right) \quad = 1.74 \text{ for this case.}$$

and ϵ = enrichment (Pu/total H.M.).

B. Calculations

ORNL Grp	$\frac{\sigma_i}{BR}\frac{\partial BR}{\partial \sigma_i}$	$\frac{\sigma_i}{k}\frac{\partial k}{\partial \sigma_i}$	$\left(\frac{\sigma_i}{BR}\frac{\partial BR}{\partial \sigma_i}\right)_{reset}$
10	4.135-2	-1.300-2	1.87-2
11	4.897-2	-1.456-2	2.37-2
12	6.448-2	-1.820-2	3.38-2
13	6.902-2	-1.879-2	3.63-2
Sum		-6.46-2	11.25-2

Using above sums, for $\delta\sigma/\sigma = -0.25$:

$\delta k/k = 1.615\%$

$\left(\frac{\delta BR}{BR}\right)_{reset} = -2.812\%$

(a) See Table 4 for GE Group Structure

(b) See Ref. 10.

	25f	25c	25ν	28f	28c	28ν	49f	49c	49ν	40c	41f	41c	41ν
25f	X	X		X	X		X	X			X		
25c	X	X		X	X		X	X					
25ν			X			X			X				X
28f	X	X		X	X		X	X			X		
28c	X	X		X	X		X	X					
28ν			X			X			X				X
49f	X	X		X	X		X	X			X		
49c	X	X		X	X		X	X					
49ν			X			X			X				X
40c										X			
41f	X			X			X				X		
41c												X	
41ν			X			X			X				X

TABLE 6

COVARIANCE MATRIX PARTITIONS FOR DETERMINING INTEGRAL PARAMETER VARIANCES

For example, calculations performed by Jim Marable for our CDS model indicate that the Na σ_{tr} sensitivity for PPD is about -0.05, which is greater than the sensitivity for most of the reactions given in Table 6. Table 7 indicates similar results for a simple slab homogeneous reactor used for our test cases. The "diffusion" component (σ_{tr} sensitivity) for Na is approximately as large as any of the U-238 and Pu-239 sensitivity components.

This task will involve generation of new cross section matrices for our cross section set. An obvious source for the additional data are the ENDF/B-V based covariance files processed using PUFF-2[15] to prepare the new ORACLE library.[16] We should, in fact, give consideration to using the new ENDF/B-V covariance information for all reactions for which it is available.

1.5 Dependent Variable for Sensitivity Coefficient Definitions

For the sensitivity coefficients reported in Ref. 10 and in our summary, σ_{total} was considered the dependent variable. This choice obviously influences the value of the sensitivity coefficient, and as discussed in reference 17, it seemed that for the cross section evaluations available in 1975, σ_{el} was often more appropriate as the dependent variable.

As discussed in reference 17, for sensitivities of the fissile and fertile capture and fission cross sections this choice does not have an appreciable influence. However, for the perturbation of cross sections or isotopes for which the elastic "scatter" and "diffusion" components are significant, the choice of σ_t or σ_{el} as the independent variable can clearly have an appreciable influence on the sensitivity coefficient.

Table 7. GLOBPERT Results for 100% Perturbation of All Cross Sections of Indicated Isotopes, Γ^* for PPD, Slab Reactor[a]

δ R/R Component[b]	U-238	Pu-239	Na
Fission[c]	-.0112	+.0139	0
Scatter	+.0355	+.0014	+.0104
Absorption	-.0191	+.0179	~0
Diffusion	-.0067	-.0114	-.0323
Direct	-.0330	+.0365	0

[a] Reactor Model same as for Table 2 except core mesh spacing and ½ thickness are 1.0 cm and 40. cm, respectively.

[b] As defined in Ref. 8.

[c] Note that the summation of this component is ~0, as it should be. See Table 3.

Of course, a choice of different independent variables by two investigators would be compensated in the determination of the variance of an integral parameter by using a different combination of covariance files for the two cases. However, we should attempt to determine if there is an obvious choice for the dependent variable with the present evaluated cross sections. If so, we should make our reported sensitivities consistent with this choice.

1.6 Inclusion of Shift of Peak Power Location in Sensitivities

As discussed in previous reports,[11,18] the shape of heterogeneous core power distributions are much more complex than those of a homogeneous core. In particular, for the former case the location of the peak power is more prone to shift with burnup and cross section changes.

For our summary[1] we reported the sensitivity of PPD for the base case point of peak power. The possible shift of the location of peak power with sigma changes should be investigated further, and this effect should be included in our sensitivity studies if possible. Recent work by Wagschal et al.[19] and Cacuci et al.[20] should be useful for such studies.

1.7 Coupled (n-γ) Transport Calculations

These complex calculations were performed in a short time by Mark Williams, to obtain some results to be included in our summary. The time available was not sufficient to analyze all the work of interest. An apparent inconsistency in the edits, which should not influence our reported results, was not resolved. Several approximations used in the calculations need further examination. Further calculations, such as that for a pin-cell, would be of interest. Finally, these calculations

suggested a series of further topics which might be investigated in the future, e.g. uncertainties in the peak linear power in addition to those deriving from diffusion theory and neutron cross section data, such as uncertainties in pin-cell transport calculations and kerma factors.

Following are items which I feel should definitely be investigated further before our final summary is submitted (Aug. 1).

1.7.1 Self-Shielding for Neutron Kerma Factors

The transport theory neutron fluxes and gamma sources were obtained from calculations which used properly self-shielded cross sections. I do not recall the details of the approximations made to obtain the gamma sources from various reactions, and possibly these approximations need further investigations. However, assuming the gamma sources and approximations made in the gamma transport problem are sufficiemtly accurate (see the discussion the B^2 below) I know of no further approximations influencing the gamma heating results which obviously need further investigations.

However, the neutron flux was folded with kerma factors[21] which were not self-shielded to obtain the neutron heating. (Kermas contain reaction cross sections.) This causes obvious errors in the neutron heating in the fission and capture resonance range. We believed this error was small, for several reasons:

(1) We checked the Pu-239 shielded fission cross sections for the driver and internal blanket regions, and found practically no difference down to low energies (about 500 eV, I believe). Since the internal blanket Pu-239 concentration was about 1/5 that in the drivers, we assumed this self-shielding effect was quite small.

(2) Radiative capture involves a neutron kerma contribution due to the kinetic energy of the recoil nucleus,[21] but as far as I know this is generally small compared to the energy of the gamma photon(s), whose energy deposit is accounted for by the gamma kerma. Note that in Okrent et al.[22] it is stated that in the capture process the recoil energy of the nucleus "is enough to create two to ten displaced atoms." Since the displacement energy is in the range of 25 eV[22] this recoil energy is quite small compared to the typical capture gamma energy of 6-7 MeV. Based on these considerations, we were not concerned about the fact that the U-238 neutron kermas were not self-shielded.

However, subsequently it occurred to me that we had overlooked a factor illustrated by Table 8, from Ref. 23. As pointed out in ref. 21, if radiative capture occurs after an (n,γ) reaction, the neutron heating is the sum of the recoil energy and that of the emitted particle (usually β^- or β^+). As we see from Table 8, the β^- decay of U-239 and Np-239 after capture in U-238 accounts for about 2 MeV of the approximately 7 MeV total for this reaction. Note also that in this table the recoil energy of the nucleus is neglected . It should be remembered that capture γ energy from capture in all materials contributes only 6-7% of the total energy in a typical LMFBR.

Based on the above discussion, while it is not apparent that neglect of self-shielding can cause a significant error in neutron heating, it is obvious that this point should be checked further both for fission and capture.

Table 8. Energy Release by Element (From Ref. 23)

Tableau des énergies (en MeV) dégagées par élément

Numéro Physique	élément	E^{f} non γ	$E^{f}\gamma$	E^{c} non γ	$E^{c}\gamma$
4	U^{233}	175,8	11,2		6,0
6	U^{235}	176,0	14,3		6,37
12	U^{238}	170,7	17,9	2,08	4,78
14	Pu^{239}	183,0	13,2		6,38
15	Pu^{240}	183,0	13,2		5,33
16	Pu^{241}	183,0	13,2		6,2
17	Pu^{242}	183,0	13,2		6,0
20	Fer				7,78
21	Cr				8,12
22	Ni				8,64
23	Mo				6,97
62	Mn			2,15	8,83
36	Na			1,40	11,08
30	Bore			2,31	0,48
31	Bore nat			2,31	0,48
29	Ta			0,52	7,28

— Pour tous les autres éléments la valeur de l'énergie gamma due aux captures est de 7 MeV.

— Energie de ralentissement E^{R} = 1,7 MeV par neutron.

1.7.2 Buckling Approximation in the Gamma Transport

To be consistent with the neutron flux calculations, the same B^2 value used therein was employed in the gamma transport calculation. However, we had no definitive information about the appropriateness of this approximation, and it should be checked further.

1.7.3 Inconsistency in Edits

At one point we attempted to calculate the difference between the diffusion and transport option results for the peak power. This difference appeared to be about 25%, but Mark found what appeared to be an inconsistency between two different output edits which might have been related to the normalization. Mark made some inquiries, but this matter was not resolved, and it should be pursued further.

1.7.4 Pin-Cell Calculations

Transport and nuclear heating calculations should also be performed for a pin-cell, to determine the influence of heterogeneity on our results for energy deposit in the driver pin materials.

2. CSEWG Thermal Data Testing (P. Levin)

91-group XSDRN calculations were done for the TRX-1 and TRX-2 critical assemblies. Four group averaged cross sections were generated and sent to M. L. Williams during the report period.

The main input parameters are given in the Appendix. The AMPX 91 groups were collapsed into 4 broad groups in two sets of boundaries:

a) EPRI-CELL[25] 4 group structure (.821 MeV, 5.53 keV, and .625 eV boundaries).

b) Hardy[26] 4 group structure (67.4 keV, 3.35 keV, and .625 eV boundaries).

For each combination of TRX/4 group, the cell averaged cross sections were calculated. For the EPRI-CELL structure zone averaged cross sections were calculated too - for both lattices. Following are the results of TRX-1 run for EPRI-CELL broad group structure. The comparison of the results with other works was performed at ORNL.

TRX 1 Calculations
(NITAWL with tape #X18228)

1. Four Group Cell Averaged Cross Sections (barns)

(Groups upper energies: 10 MeV, .821 MeV, 8.53 keV, .625 eV)

1.1 MAT = 1262 U-238:

grp#	σ^c	σ^g	$\nu\sigma^g$	$\sum_{g' \neq g} \sigma_{g \to g'}$
1	6.51767-2	4.00275-1	1.12420	1.44173
2	2.43618-1	3.99191-4	9.65639-4	1.21122-2
3	1.54198	5.48779-5	1.27307-4	2.03276-2
4	1.62462	0	0	1.59888-2

1.2 MAT = 1261 U-235:

grp#	σ^c	σ^f	$\nu\sigma^f$	$\sum_{g' \neq g} \sigma_{g \to g'}$
1	6.84165-2	1.33802	3.64802	8.08095-1
2	4.61990-1	1.67400	4.09479	1.08570-2
3	1.17837+1	2.45358+1	5.93477+1	3.09065-2
4	5.69623+1	3.30687+2	7.99866+2	2.19837-2

1.3 MAT = 1193 Al-27:

grp#	σ^a	$\sum_{g' \neq g} \sigma_{g \to g'}$
1	6.23602-3	2.23181-1
2	1.88027-3	2.10880-2
3	1.02811-2	2.55207-2
4	1.57558-1	5.02118-4

1.4 MAT = 1276 O-16:

1	1.03645-2	2.76028-1
2	1.00506-7	4.80693-2
3	7.40390-6	5.37286-2
4	1.38287-4	4.49101-3

1.5 MAT = 1301 H-1:

1	3.36397-5	1.55094
2	1.42951-4	2.08803
3	1.38073-2	1.97901
4	2.56464-1	1.17347-2

2. Cell Average Flux

grp#	Flux
1	2.72244
2	3.61984
3	2.93516
4	2.54225

3. Integral Parameters

3.1 Eigenvalues: k = 1.16918

3.2 Reaction Rates: (per 1 fission neutron)

U^{238} Capture: Epithermal: 2.00025-1 Total: 3.47989-1

Thermal: 1.47964-1

U^{235} Capture: Epithermal: 1.72882-2 Total: 8.60094-2

Thermal: 6.87212-2

U^{238} fission: 3.90961-2

U^{235} fission: Epithermal: 3.87672-2 Total: 4.37719-1

Thermal: 3.98952-1

3.3 Reaction Rate Ratios:

ρ_{28} = 1.35186

δ_{25} = 9.71728-2

δ_{28} = 8.93178-2

CR = 7.95005-1

References

1. J. M. Kallfelz, C. L. Cowan, J. H. Marable, M. L. Williams, C. R. Weisbin, J. D. Drischler, and T. B. Fowler, "Design and Sensitivity Analysis of a CDS-Type LMFBR Heterogeneous Core," Paper accepted for presentation at ANS Topical Meeting, 1980 Advances in Reactor Physics and Shielding, September 14-17, 1980.

2. J. M. Kallfelz and P. Levin, "Progress Report for ORNL Subcontract 7802, Period March 5 - 31, 1980," Memo to C. R. Weisbin, J. H. Marable, and M. L. Williams dated April 2, 1980.

3. J. M. Kallfelz et al., "Burnup Calculations with Time-Dependent Generalized Perturbation Theory," Nucl. Sci. Engr. 62, 304 (1977).

4. T. B. Fowler, D. R. Vondy, and G. W. Cunningham, "Nuclear Reactor Analysis Code: CITATION," ORNL-TM-2496, Rev. 2, Oak Ridge National Laboratory (1971).

5. I. Dal Bono, "TAIM: Multigroup One-Dimensional Diffusion Code," CNEN Doc. CEC.(66)-12, Comitato Nazionale per l'Energia Nucleare, Bologna (1966).

6. I. Dal Bono, V. Leproni, and M. Salvatores, "The CIAP-1D Code," CNEN RT/FI(68) 9, Comitato Nazionale per l'Energia Nucleare, Rome (1968).

7. I. Dal Bono, V. Leproni, and M. Salvatores, "The GLOBPERT-1D Code," CNEN RT/FI(68) 10, Comitato Nazionale per l'Energia Nucleare, Rome (1968).

8. G. P. Cecchini and M. Salvatores, Nucl. Sci. Engr. 46, 304 (1971).

9. C. L. Cowan (GE-Sunnyvale), private communication to J. H. Marable, March 19, 1980.

10. J. H. Marable and C. R. Weisbin, "Uncertainties in the Breeding Ratio of a Large LMFBR," in E. Silver, Ed., Advances in Reactor Physics, CONF-780401, 1978.

11. J. M. Kallfelz and P. Levin, "Progress Report on Work for ORNL Subcontract 7802, Period January 9 - February 11, 1980," Memorandum to C. R. Weisbin, J. H. Marable, and M. L. Williams, dated February 12, 1980.

12. J. M. Kallfelz, "VENTURE Γ^{*} Calculations, Peak/Ave Power Density," Memo to D. Vondy, ORNL, dated February 25, 1980.

13. D. R. Vondy, T. B. Fowler, and G. W. Cunningham, "VENTURE: A Code Block for Solving Multigroup Neutronics Problems Applying the Finite-Difference Diffusion-Theory Approximation to Neutron Transport, Version II," ORNL-5062/R1, Oak Ridge National Laboratory (November 1977).

14. J. M. Kallfelz, "Test Cases for Γ^*, Peak/Total Power," Memorandum to D. Vondy, dated March 12, 1980.

15. J. D. Smith and B. L. Broadhead, "Multigroup Covariance Matrices for Fast Reactor Studies," in preparation.

16. J. J. Wagschal, J. H. Marable, Y. Yeivin, and C. R. Weisbin, "ORACLE: An Adjusted Cross Section and Covariance Library for Fast Reactor Analysis."

17. J. M. Kallfelz, "Status Report for the Georgia Institute of Technology Project E-26-610," Memo to F. C. Maienschein dated March 19, 1975.

18. J. M. Kallfelz, J. H. Marable, and C. R. Weisbin, letter to C. L. Cowan (GE) dated January 25, 1980.

19. J. J. Wagschal et al., "Extrapolation of Surveillance Dosimetry Information to Predict Pressure Vessel Fluences," to be presented at ANS Las Vegas Meeting, June 1980.

20. D. G. Cacuci et al., "Development in Sensitivity Theory," to be presented at the ANS Sun Valley Meeting, September 1980.

21. M. A. Abdou and C. W. Maynard, Nucl. Sci. Engr. 56, 360 (1975).

22. D. Okrent, W. B. Loewenstein, A. D. Rossin, A. B. Smith, B. A. Zolotar, and J. M. Kallfelz, "Neutron-Energy Spectra for Fast Reactor Irradiation Effects," Nucl. Appl. and Tech. 9, 454 (1970).

23. "Option Puissance," private communication from CEA-Cadarache.

24. W. Rothenstein, "Thermal Reactor Lattice Analysis Using ENDF/B-IV Data with Monte Carlo Resonance Reaction Rates," Nucl. Sci. Eng. 59, 337 (1976).

25. "Advanced Recycle Methodology Program System Documentation," EPRI Report CCM-3, Electric Power Research Institute, Part II, Chapter 5 (September 1977).

26. John Hardy, Memorandum, Thermal Reactor Data Testing Subcommittee of CSEWG (1978).

27. J. M. Kallfelz, "Economic Impact of Uncertainties in Cross Sections for Thermal Reactors," Memorandum to M. Becker (RPI), R. W. Carlson (Nuclear Assurance) and W. R. Cobb (Southern Services) dated April 11, 1980.

May 19, ORNL Progress Report

APPENDIX 1

TRX-1 and TRX-2 XSDRN Calculations - Input Description

The description of TRX-1 and TRX-2 was taken from Ref. 24. Infinite lattices were assumed (white radial boundary condition). The fuel rods and clad for both lattices are the same (dimensions and materials). The only difference is the hexagonal pitch.

1.1 Number Densities: Fuel: U-238 = 4.7205-2

U-235 = 6.253-4

Clad: Al-27 = 6.025-2

H-1 = 6.676-2

Moderator: O-16 = 3.338-2

1.2 Geometry: Fuel outer radius = .4915 cm

Clad inner radius = .5042 cm

Clad outer radius = .5753 cm

(The void was represented by Al with zero density.)

For hexagonal arrays: Req = $\rho^* \sqrt{\frac{1.5}{\pi \operatorname{tg} 60}}$

Lattice	Pitch (cm)	Req (cm)	Vw/Vu
TRX-1	1.8060	.9482	2.352
TRX-2	2.1740	1.1414	4.023

All cases were run in cylindrical S8-P3 transport calculations.

May 19, 1980 ORNL Progress Report

Appendix 2

Department of Nuclear Engineering

Rensselaer Polytechnic Institute Troy, New York 12181

April 21, 1980

Dr. John Kallfelz
School of Nuclear Engineering
Georgia Institute of Technology
Atlanta Georgia 30332

Dear John,

Enclosed as per your request is a commentary on your memo of January 14. I have not made any specific proposals about participation in further research, though this is any area of continuing interest to me and to my colleagues.

Sincerely,

Martin Becker
Professor

MB/rl

Commentary by M. Becker

on

Memorandum of 1/14/80; J.M. Kallfelz to C.R. Weisbin and M.L. Williams

It is appropriate to go directly to the principal subject of the memo, Economic Impact of Uncertainties in Cross-Sections for Thermal Reactors. It may be helpful to look to the type of question that motivated the RPI study in the first place. EPRI had been receiving proposals and requests to improve data, and was interested in finding a basis on which to set priorities on improvements to data. Fuel cycle cost was selected as a significant measure of merit, although it was recognized that other measures exist. At this point in time, it may be fruitful to identify and analyze other measures, and to bring these to the point to which the fuel cycle cost measure already has been brought.

To assess economic impact, several questions may be asked.

(1) Why do we wish to know a particular piece of information, (e.g., a cross-section), i.e., what will we calculate with this piece of information?

(2) What is the value of improving the accuracy of the calculation?

(3) How would an improvement in the particular piece of information improve the accuracy of the calculation?

(4) How does uncertainty in the particular information relate to other uncertainties?

(5) What empirical information might compensate for the uncertanties?

(6) How do engineers now compensate for existing uncertainties?

The second question actually can be quite complicated, and may involve subtle considerations (e.g., if major design changes are implied). However, the question should be addressed.

It should be noted that if one cannot place at least an approximate "real world" value on improving nuclear data, then one would have a difficult time justifying additional measurement or evaluation to improve the data. In some sense, there should be a benefit to the improved data which, on a present-worth basis, exceeds the cost of bringing about the improvement. For a research organization having a limited budget, the net benefit not only should be positive but also should exceed the net benefits of other research options.

It should be observed that many of the comments received in the discussions cited in the memo were not germane to the question raised. The fact that a utility may place greater priority on plant availability than on fuel cycle cost does not mean that much money is not tied up in fuel cycle cost nor does it mean that much money is not tied up in fuel cycle cost nor, in turn, that data uncertainties do not impact fuel cycle cost. The response that an improved fission cross-section would probably just reduce extent of coastdown is itself an assertion of economic impact, since an increment of valuable energy is implied.

I would conclude by making three types of recommendations. These follow:

(1) An assessment should be made of how nuclear fule cycle design decision margins should be related to uncertainties in nuclear data, and thereby to refine assessment of impacts of improvements in data. For example, in order to assure to a specified level of probability, in view of the uncertainties, that the cycle will operate to a specified exposure, what does the initial enrichment have to be? How would this initial enrichment be affected by refining specific data?

(2) Assessments should be made of impacts (and associated costs) of uncertainties in data on plant design variables (e.g., rod worth) other than fuel cycle cost and of the economic impact of reducing uncertainty in these variables. Such assessments would complement those done first for fuel cycle cost. Effort in this area should begin with identification of the design information of interest.

(3) I believe that coupling of the subject problem to LEAP is premature. The highly refined nuclear data would have to be processed considerably prior to having any influence on a LEAP imput parameter.

In closing I suggest bearing in mind a simple concept. If data of a particular type are important, then uncertainties in these data also are improtant.

A comment on a specific point made in the subject memo is included an as Appendix.

Appendix A

A specific comment on point (1), page 8 would be in order. This point addresses the possibility that while RPI adjusted initial enrichment to maintain fixed energy output per cycle, utilities might actually prefer to compensate by refueling early or late within a "window" acceptable to that utility and/or to the power pool in which it operates. Two points should be recognized.

(1) Going to a modified cycle length is not much different from changing enrichment from a sensitivity analysis view point, in that the benefits and penalties in both options are determined by end of cycle conditions. Mathematically, we may say that with the reference initial enrichment, a cross-section $\delta\sigma$ change leads to a multiplication factor change $\delta k\ (t_{co})$ at the nominal end-of-cycle-time t_{co}.

$$\delta k\ (t_{co}) = \frac{\partial k(t_{co})}{\partial \sigma}\ \delta\sigma$$

This can lead either to a change in exposure to get to a point where k_{EOC} is unity, i.e.,

$$\delta E = \frac{\partial E}{\partial k(t_{co})}\ \delta k(t_{co}) = \frac{\partial E}{\partial k(t_{co})}\ \frac{\partial k(t_{co})}{\partial \sigma}\ \delta\sigma$$

or to change in initial enrichment e_{BOC} to preserve cycle length

$$\delta e_{BOC} = \frac{\partial e_{BOC}}{\partial k(t_{co})}\ \delta k(t_{co}) = \frac{\partial e_{BOC}}{\partial k(t_{co})}\ \frac{\partial k(t_{co})}{\partial \sigma}\ \delta\sigma$$

The relative rank-ordering of uncertainties should still turn out to be the same. There can be, however, an absolute difference in economic value of additional exposure and reduced enrichment, depending of how the additional energy is valued.

(2) A principal argument for preferring fixed cycle length is that fuel contracts frequently involve a warranty of energy extractable from the fuel. Thus, the bids provided to utility for fuel supply and fabrication involve whatever margin is appropriate to assure a specified cycle exposure in the face of the uncertainties that may exist.

GEORGIA INSTITUTE OF TECHNOLOGY

SCHOOL OF NUCLEAR ENGINEERING E-26-B01

Atlanta, Georgia 30332 (404) 894-3720

June 11, 1980

MEMORANDUM

TO: C. R. Weisbin, J. H. Marable, and M. L. Williams (ORNL)

FROM: J. M. Kallfelz and P. Levin

SUBJECT: Progress Report for ORNL Subcontract 7802, Period May 10 - June 10, 1980

Accomplishments

- In cooperation with several ORNL staff members, plans have been made for work at ORNL and Georgia Tech during the summer in the general area of LMFBR design analysis. These plans are discussed in section 1 of this report.
- We participated in a meeting with GE and WARD at Oak Ridge concerning application of sensitivity and uncertainty analysis to design. Following this meeting a memorandum (1) concerning cooperation with vendors on this topic was prepared.
- Work was initiated to acquire the capability to use VENTURE at Georgia Tech.
- EPRI-CELL runs for various TMI-1 unit cells have been performed, for use by M. Williams in analysis of this reactor.
- Two programs were written which interface between the cross section output of EPRI-CELL and VENTURE. Output cross section decks for the TMI-1 cases have been punched at ORNL, where they are being tested.

Plans for Work for the Next Report Period

- Work will continue on the CDS sensitivity analysis.
- VENTURE test runs and study will be continued to acquire the capability to use this code at Georgia Tech.
- Documentation will be prepared and transmitted to M. Williams which describes the EPRI-CELL TMI cases, the use of the EPRI-CELL cross section interface codes, and the status of the ANISN-B1 debugging effort.

jhr

cc: J. R. White, ORNL

1. Planning LMFBR Calculations for Summer (J. Kallfelz)

In cooperation with several ORNL staff members, plans have been made for work at ORNL and Georgia Tech during the summer in the general area of LMFBR design analysis, with emphasis on development and utilization of sensitivity analysis capabilities. The general topics and individuals responsible for taking the lead in each of these areas are indicated below:

A. CDS Analysis with GE - J. M. Kallfelz

B. LCCEWG Testing - J. Marable

C. PHENIX Analysis - E. Tomlinson

D. Time-Dependent Sensitivity - J. White

Plans for work on topic A are described below. Jim Marable and Ed Tomlinson agreed to prepare plans for topics B and C, respectively. A general plan for topic D, prepared with John White, is given below; I suggest that John prepare a more detailed plan.

1.1 Comments on Personnel and Code Capabilities

As Chuck Weisbin has pointed out, the above topics are clearly related, and often involve the same codes, particularly VENTURE.[2] John White is familiar with VENTURE, and it was suggested that he might help us on task A, besides his primary involvement in D. Under this option, D. Biswas, who will arrive at Tech about July 1, might have helped with task B.

However, it was decided that while John White might provide some help on calculations for Task A, his secondary commitment should be mainly to provide assistance with Task B, the LCCEWG testing. There are several reasons for this decision:

- It was felt that John's time-dependent sensitivity development should not be included in the main "driving force" for Task A, the paper for the Sun Valley Meeting.[3]
- The administrative and communications difficulties of having staff members at different sites from the lead person for a particular task are obvious and should be avoided where practical.
- Because VENTURE is becoming the primary code for general reactor analysis at ORNL, and because of its expanding sensitivity capability, it was deemed highly desirable to develop capability for its use at Georgia Tech. It was felt that this learning process would proceed much more rapidly if Biswas and I work together on Task A at Georgia Tech.

Thus, one of our primary goals is to develop capability to use VENTURE at Georgia Tech as soon as possible. I have already initiated this process, and with my experience with CITATION and Biswas' experience with similar French codes, I anticipate that acquiring this capability will not be difficult.

1.2 Further Work on CDS Analysis

As discussed in our previous monthly progress report,[4] there are many topics which should be investigated before August 1, when any changes to our published summary of the Sun Valley paper[3] must be finalized. All pertinent calculations and analysis must be completed by the middle of August, to allow time for writing the full paper.

In our conference at ORNL we agreed on the following responsibilities for accomplishing the necessary investigations and/or calculations.

a) J. Marable - Comparison of Sensitivity Results for "Full-reactor" and "Half-reactor" Models

This topic is described in section 1.1, p. 8, of Ref. 4.

b) J. Marable - Comparison of Peak Power Sensitivity Coefficients with Direct VENTURE Perturbations.

See section 1.2 of Ref. 4.

c) J. Kallfelz - Comparison of VENTURE Results with Direct Perturbations at GE.

See section 1.2 of Ref. 4.

d) M. Williams - Generation of New Cross Section Set

See section 1.3 of Ref. 4.

e) J. Marable - Generation of Sensitivities and Covariances for Further Cross Sections

See section 1.4 of Ref. 4.

f) J. Kallfelz - Appropriate Dependent Variable for Sensitivity Coefficient Definitions

See section 1.5 of Ref. 4.

If it proves not possible to resolve this question in time for the meeting, at least pertinent information should be included in the discussion in the paper.

g) M. Williams - Inclusion of Shift of Peak Power Location in Sensitivities

See section 1.6 of Ref. 4

The same comment applies here as for topic (f). Possible methods of treating this shift might be discussed and present methods could be used to obtain some related results, e.g. by analyzing

the sensitivity and covariance of the power density at several points.

h) M. Williams - Coupled (n-γ) Transport Calculations

Several topics related to these calculations which need further investigation are described in section 1.7 of Ref. 4.

1.3 Development and Application of Time-Dependent Sensitivity Theory

I have discussed this topic with John White, and the following comments are drawn from these discussions and a draft memo on this topic he prepared May 5. The proposed work will involve development and application of the capability to calculate time-dependent nuclear data sensitivity coefficients. This capability would be incorporated in the existing Depletion Perturbation Theory (DEPTH) module[5] for use with VENTURE.

This work will be completed by the end of September and will involve two phases, development of capability (Phase I) and application to a specific LMFBR problem or problems (Phase II). John estimates that Phase I will be finished by about the end of July, while Phase II will be accomplished primarily in August and September. Of course, there will be considerable overlap of the phases.

Concerning the model to be used, it appears that the CDS model we are presently studying with GE would be most appropriate, for the following reasons:

- o It promotes cooperation with GE, from which both installations could benefit.
- o The CDS is a funded project for which there is presently considerable interest.

- The CDS is a realistic design with long burn-up periods, good for testing our methods.

Use of the CDS model for burn-up studies will require some modifications from the model we are presently using, which is representative of MOEC. Charley Cowan says that he will probably be able to provide us with an appropriate BOEC model. If unexpected problems are encountered in obtaining such a model because of proprietary reasons, the LCCEWG Model[6] which has a simple burn-up problem, would be the obvious alternative.

Two problems which are obviously appropriate for the application phase will be studied:

a) Breeding Ratio - As mentioned in one of our joint papers with GE,[7] COROPT[8] uses a breeding ration defined from the cycle breeding and burn-up.[9] For calculating the doubling time this definition is, of course, more accurate than a static breeding ratio.

Thus, one goal of the applications phase is to compare sensitivity curves and standard deviations of the "cycle-averaged" and static breeding ratios, to determine if there are significant differences.

It may be that the differences will not be significant, considering the accuracy of our covariance matrices. This negative result would be useful information, indicating that static analysis of this parameter is adequate. I have suggested that John initially try to obtain an estimate of the possible differences using simple models, perhaps using some expressions and results from our NIRA work on time-dependent sensitivity.[10]

b) Cycle Δk due to breeding and burn-up - This topic is, of course, related to the breeding and burn-up processes of (a), but has a different emphasis. In fact, Adkins[11] has attempted to define breeding ratio correlations to the cycle reactivity variation. An ANS standard draft by Karl Ott[12] is also related. For these studies the emphasis is on the space-dependent buildup and worth of individual isotopes. As mentioned below, inclusion of fission products would be desirable, but difficult.

In closing, we should consider two more topics which present more formidable problems. They might be studied if time allows, in light of interest therein expressed in our recent discussions with WARD and GE.

c) Time-dependence of the peak power location.

d) Uncertainty of the fission product worth at EOC.

2. LWR Calculations (P. Levin)

2.1 TMI-1 Cell Calculations

EPRI-CELL was used to generate broad group cross sections for further use in VENTURE. The calculations refer to three types of cells in TMI-1 fuel assemblies:

a) Fuel pin cells, for several enrichment values.

b) Water holes where instrument and control rods are removed.

c) Lumped burnable poison cells.

The output of these runs has been transmitted to Mark Williams. As an indication of the influence of enrichment on the microscopic cell-averaged cross sections, σ_{a4}^{25} is 5% lower for the high enriched case than for the low enrichment.

The description of the cases and input preparation will be transmitted to Mark Williams before I leave Georgia Tech.

2.2 Cross Section Interface Codes

Two programs were written to extract EPRI-CELL calculated cross sections from their interfaces with NUPUNCHER and PDQ. The format of the former code can be obtained only for "engineering input" to EPRI-CELL, while PDQ format can be obtained for either of the EPRI-CELL input format options.

The punched card output in CITATION format has been routed to ORNL, where it is being tested as input for VENTURE. A description of the codes and instructions for their usage will be provided to Mark Williams before my departure.

References

1. J. M. Kallfelz, "Cooperation with Vendors-Sensitivity and Uncertainty Analysis," Memorandum to J. Marable dated June 9, 1980.

2. D. R. Vondy, T. B. Fowler, and G. W. Cunningham, "VENTURE: A Code Block for Solving Multigroup Neutronics Problems Applying the Finite-Difference Diffusion-Theory Approximation to Neutron Transport, Version II," ORNL-5062/R1, Oak Ridge National Laboratory (November 1977).

3. J. M. Kallfelz, C. L. Cowan, J. H. Marable, M. L. Williams, C. R. Weisbin, J. D. Drischler, and T. B. Fowler, "Design and Sensitivity Analysis of a CDS-Type LMFBR Heterogeneous Core," Paper accepted for presentation at ANS Topical Meeting, 1980 Advances in Reactor Physics and Shielding, September 14-17, 1980.

4. J. M. Kallfelz, P. Levin, and M. Becker, "Progress Report for ORNL Subcontract 7802, Period April-May 9, 1980," Memo to C. R. Weisbin, J. H. Marable, and M. L. Williams dated May 19, 1980.

5. J. White, "The Depletion Perturbation Theory Formulation," private communication, 1980.

6. N. C. Horning, M. B. Parker, and R. P. Omberg, "Second Revision, Proposed Third Benchmark Problem for the Large Core Code Evaluation Working Group," HEDL, May 1980.

7. D. Rinaldis, J. M. Kallfelz, E. Kujawski, and J. H. Marable, "Evaluation of Integral Parameter Correlations and Reactor Performance Using Nuclear Data Covariances," Trans. ANS 33, 859 (1979).

8. G. V. Neill and D. P. Johnson, "COROPT: A Computer Program for Finding Optimum LMFBR Mixed-Oxide Fuel Cores," GEFR-00006, UC-798, General Electric, Sunnyvale, CA (January 1977).

9. H. L. Wyckoff and P. Greebler, Nucl. Tech., March 1974.

10. J. M. Kallfelz et al., "Burnup Calculations with Time-Dependent Generalized Perturbation Theory," Nucl. Sci. Engr. 62, 304 (1977).

11. C. R. Adkins, Nucl. Tech. 13, 114 (1972).

12. K. O. Ott, "First Draft - Breeding Terms" for ANS Standards Committee 19.2. (Copy available from F. Maienschein.)

GEORGIA INSTITUTE OF TECHNOLOGY

SCHOOL OF NUCLEAR ENGINEERING E-26-801

Atlanta, Georgia 30332 (404) 894-3720

July 3, 1980

MEMORANDUM

TO: C. R. Weisbin, J. H. Marable, and M. L. Williams (ORNL)

FROM: J. M. Kallfelz, P. Levin, and D. Biswas ✓

SUBJECT: Progress Report for ORNL Subcontract 7802, Period June 11 - June 30, 1980

Effort on the project during this report period was much lower than usual. J. Kallfelz was on vacation for most of the period, P. Levin returned to Israel at the middle of the month, and our new staff member, D. Biswas, arrived near the end of the month.

Accomplishments

- Documentation was prepared and transmitted to M. Williams which describes the EPRI-CELL TMI cases, the use of the EPRI-CELL cross section interface codes, and the status of the ANISN-B1 debugging effort.
- Work was continued to acquire the capability to use VENTURE at Georgia Tech.

Plans for Work for the Next Report Period

- Work will continue on the CDS sensitivity analysis.
- VENTURE test runs and study will be continued to acquire the capability to use this code at Georgia Tech.

lm

GEORGIA INSTITUTE OF TECHNOLOGY

SCHOOL OF NUCLEAR ENGINEERING

Atlanta, Georgia 30332 (404) 894-3720

E-26-B01

8 August 1980

MEMORANDUM

TO: C. R. Weisbin, J. H. Marable and M. L. Williams (ORNL)

FROM: J. M. Kallfelz, D. Biswas and A. Gandini

SUBJECT: Progress Report for ORNL Subcontract 7802, Period July 1 - August 6, 1980

Accomplishments

- We have acquired the capability to use VENTURE at Georgia Tech.
- Work has continued on the CDS sensitivity analysis being performed jointly with ORNL and GE, and progress on this topic is described in section 1 of this report.
- On a visit to ORNL, D. Biswas presented a seminar on the nuclear analysis of Super Phenix, and the planning of LMFBR calculations discussed in our previous report[6] was further coordinated by J. Kallfelz with ORNL staff members.
- A. Gandini performed project consulting work on sensitivity analysis at Georgia Tech, and a method he developed for including the spatial uncertainty in the peak power density variance is described in section 2 of this report.

Plans for Work for the Next Report Period

- Top priority will be given to completing the remaining tasks[6] to be completed for our Sun Valley paper,[1] and to preparing this paper. The first draft of this paper will be provided to the co-authors by 25 August 1980 for their comments, with the final draft to be provided by 2 September 1980.
- Related to the previous topic, D. Biswas will visit ORNL to learn how to use the DEPTH code module developed by J. R. White for sensitivity analysis with VENTURE.

JMK:jg

1. Sensitivity Analysis of a CDS-Type LMFBR Heterogeneous Core

As stated in our progress report[6] which discussed the planning of LMFBR calculations for the summer, one of our primary goals was to develop capability to use VENTURE at Georgia Tech, in order to perform further analysis necessary for the Sun Valley paper.[1] We have accomplished this goal this month, and have utilized VENTURE to investigate various questions concerning the CDS analysis, to be discussed below. These questions are described in our May 19 progress report,[4] while our following report[6] states our agreement concerning responsibilities for accomplishing the necessary analysis.

These tasks have either been completed or should be accomplished in time for inclusion in the final paper, through the efforts of ORNL and Georgia Tech staff members. At our 14 July meeting we agreed that D. Biswas should work on topics related to tasks (a), (b) and (g) of Ref. 6, and it is this work as well that of J. Kallfelz on topics (f) and (g) which we report below. Task (c) completion has been delayed pending further calculations at GE.

1.1. Sensitivity Results for "Full-Reactor" and "Half-Reactor" Models, and Comparison with Direct Perturbations

These are tasks (a) and (b) of Ref. 6, and the investigations at Georgia Tech have been performed with the simple 3-group slab reactor model described in Table 1 of Ref. 4.

The reason for the comparison of the "half" and "full" reactor models is discussed at length in Ref. 4. We are investigating the ratio

$$R = \frac{a_1}{a_2} \tag{1.1}$$

where a_1 is defined at the power density at the point of maximum value, $\vec{r}_m$,

$$a_1 = \sum_j \Sigma_{1j}(\vec{r}_m)\,\phi_j(\vec{r}_m) \tag{1.2}$$

and a_2 is the total power,

$$a_2 = \int_{\substack{\text{reactor}\\ \text{model vol.}}} \sum_j \Sigma_{2j}(\vec{r})\,\phi_j(\vec{r})\,d\vec{r} \tag{1.3}$$

where the Σ_{ij} are the "energy-production cross sections".[4] The adjoint source for the $\Gamma_j^*(\vec{r})$ equation is

$$S_j^*(\vec{r}) = \frac{\Sigma_{1j}(\vec{r})}{a_1} - \frac{\Sigma_{2j}(\vec{r})}{a_2} \tag{1.4}$$

Σ_{1j} and Σ_{2j} have the same form, except that Σ_{1j} is zero for $\vec{r} \neq \vec{r}_m$.

VENTURE has various options for input which can keep either the peak flux or the total power the same for the half and full slab case, but not both; this has an obvious influence on the S_j^* and Γ_j^* values. To check for possible inconsistencies in the Γ^* or perturbation integrals, e.g.

$$SIGA_j = \int_{Vol} \phi_j \Gamma_j^* \tag{1.5}$$

four cases were compared:

Base Case: Full reactor model, with power (RXX4 in DVENTR) = 1.0 and RXX6 = 1.0 indicating a full reactor. (RXX6 = fraction of reactor considered and applied to the power level.)

Case 2: Same as case 1, except power level = 2.0.

Case 3: Half slab case, with a power level of 1.0, but with RXX6 = 1.0 so that it is considered a full reactor for the power calculation.

Case 4: Identical with case 3, except that RXX6 = 0.5, indicating that it is actually a half reactor.

As indicated in Tables 1-3, the above cases can result in differing ϕ, S^*, and Γ^* values. However the significant result is that for all four cases the perturbation integrals, e.g. SIGA (eqn. 1.5), NU*SIGF, etc. of VENTURE were identical. Thus apparently the VENTURE programming is consistent.

A further check on the above question is obviously provided by a comparison of VENTURE results with direct perturbations. Thus three more cases were considered:

Case 5: Full slab, identical to base case, except Σ_{a_2} in the core perturbed +10%.

Case 6: Half-slab, identical with case 3 except Σ_{a_2} in the core perturbed +10%.

Case 7: Half-slab, identical with case 3 except D_2 in the core perturbed+7.226%.

As indicated in Tables 4-6, the agreement between the direct and perturbation theory results for the percent peak power density change was excellent for all cases. Such comparisons made at ORNL by Jim Marable for 10% perturbations of $\sigma_{f_{10}}^{49}$ and $\sigma_{c_{10}}^{49}$ in the CDS model also yielded excellent agreement.

1.2. Dependent Variable for Sensitivity Coefficient Definitions

This is topic (f) of Ref. 6, and concerns the possible choice of σ_t or σ_{el} as the dependent variable. As discussed in Ref. 7 (attached as Appendix A; see section IV thereof), this choice influences the resulting components of the sensitivity coefficient. For example, for

Case a: σ_t assumed dependent, then an introduced $\delta\sigma_c$ gives

$$\delta\sigma_{tr} = \delta\sigma_c \tag{1.6}$$

while for

Case b: σ_{el} dependent, then for an introduced $\delta\sigma_c$,

$$\delta\sigma_{tr} = \bar{\mu}_{el} \cdot \delta\sigma_c \tag{1.7}$$

and furthermore a scattering component is introduced, as discussed in Appendix A.

Our reported sensitivity coefficients assume case a, while for the early cross section evaluations σ_{el} was often more appropriate as the dependent variable, as discussed in Appendix A. This choice was not obvious in 1975, and for the k and BR sensitivities

for the fissile and fertile σ_c and σ_f this choice does not have an appreciable influence. Furthermore, a choice of different independent variables by two investigators would be compensated in the determination of the variance of an integral parameter by using a different combination of covariance files for the two cases. However, since the PPD sensitivities to σ_{tr} changes in heavy and light nuclides (e.g., Na) can be significant, we have attempted to determine if there is an obvious choice for the dependent variable with the present evaluated cross sections.

Based on discussions with Bob Peele and Larry Weston, it appears that there is no obvious general choice, with the answer depending on the nuclide and energy range, and no clear choice for many cases. Bob said that it has been recently determined that many σ_t values are not nearly as accurate as was assumed. Larry said that σ_t values for U235, U238 and Pu239 are accurate, but that for most other isotopes, the σ_t data is "pretty lousy," even though σ_t can be measured in the high energy range, while σ_{el} can not be "directly" measured. He said that for many isotopes, σ_{el} is estimated using theoretical calculations, and added to σ_{nonel} to get σ_t .

Furtherfore, I have noted a recent evaluation of nickel non-elastic scattering cross sections[8] which were derived from measured σ_t and differential σ_{el} values. This report also mentions "questions as to the general accuracies of neutron total cross sections in the fluctuating energy region of interest."[8]

The above facts indicate that our choice of σ_t as dependent appears more appropriate for present cross section data than it did

for early cross section evaluations. At any rate we should indicate our choice when reporting sensitivities.

Francis Perey said that he thinks that the view of the problem is wrong, and that the whole question of dependent and independent variables is not meaningful. He said that to determine the desired sensitivities, one would use the chain rule, and the results should not depend on which cross section is defined as a function of the others. It appears to me however that our sensitivities <u>are</u> a function of this choice because there is redundancy, which must be eliminated, in the potential variable set (cross sections). Further discussions with Francis should be valuable to clear up this point.

Finally, the question arises as to how much our PPD sensitivity values are influenced by our choice of σ_t as dependent. We considered this question for the case of the U238 σ_c sensitivity, which is one of the largest. Using the CDS model on which our initial Sun Valley summary results were based, we examined the relative importance of the "SIGA" (A) and "DIFF. COEF." (L) components for this perturbation. Making several approximations,

$$\frac{\text{Absorption Component}}{N_F^{28} \cdot \delta\sigma_c^{28}} = A_F + \frac{N_{AB2}}{N_F} A_{AB2} + \frac{N_{IB}}{N_F}\left(A_{IB} + A_{RB} + A_{AB1}\right) \tag{1.8}$$

and where all N values signify N^{28}, and the subscripts F, IB, RB, AB1 and AB2 refer to driver, internal blanket, radial blanket, axial blanket above IB, and AB above F, respectively.

Also,

$$\frac{\text{Diffusion Component}}{N_F^{28}\,\delta\sigma_c^{28}} = 3D_F^2 \cdot L_F + \tag{1.9}$$

$$+\frac{N_{AB2}}{N_F}\,3D_{AB2}^2\,L_{AB2} + \frac{N_{IB}}{N_F}\,3D_{IB}^2\left(L_{IB} + L_{RB} + L_{AB1}\right)$$

As indicated in Table 7, the diffusion component for this perturbation is generally much less than the absorption component, except in the high energy range where σ_c^{28} is at any rate small. This result was verified by a calculation by John White for the inner driver region PPD in which the $^{total}\gamma$ sensitivity for U238 σ_c without an associated σ_{tr} perturbation was within about 1% of the result when the related $\delta\sigma_{tr}$ was included. Thus for this particular case the choice of independent variable appears to have a small influence on the calculated sensitivity value. However, based on John's results this is probably not true for some other cases, e.g. the U238 σ_s sensitivity.

1.3. Space-Dependent Aspects of Peak Power Density Sensitivities

This includes the items of topic (g), Ref. 6, as well as new considerations. Since the initiation of this research, we have drawn attention to the fact that the peak power density sensitivity investigations will be much more complex for a heterogeneous core than for a homogeneous model, due to the fact that for the former the location of peak power is more prone to shift with burnup and cross section changes.[2,4,9]

We have considered various methods of treating the spatial uncertainty, including possible new methods and use of present methods to obtain related results, e.g. by analyzing the sensitivity and covariance of the power density at several points.[4,6]

A possible method of treating the spatial uncertainty, proposed by A. Gandini, is discussed in section 2 of this report. This approach might prove useful for restricted space ranges, e.g. within one driver zone, when the number of terms in the Taylor series can be small. It appears that for the Sun Valley paper we will have to rely on present methods. At any rate the calculation of the variance of the power density (PD) at several points, and correlations between them, $COR(PD_1, PD_2)$ are desirable because of the following considerations.

For our first CDS calculations the PD was strongly peaked in the outer driver zone, so we concentrated on the sensitivities for that point. However, in recently analyzing that run and later information sent us by GE,[10] I found various errors in the model. When they were corrected the PD distribution became quite "flat," i.e. the distributions in the three driver zones were approximately the same. Thus an analysis of VAR(PD) for all driver rings appeared even more necessary.

Consideration of this case led to the conclusion that the PD sensitivities were probably a strong function of the driver zone for which they were calculated, as has since been verified. A cross section change which causes a flux decrease in the outer driver ring will probably cause an associated increase in the inner driver ring flux, since the total power is constant. Thus the PD sensitivity for this cross section could be expected to have opposite signs for these two driver zones.

We performed VENTURE calculations of the PD Γ^* for the middle of the three driver rings, which confirmed the above conclusion. As would be expected, the Γ^* curve for the inner driver case was roughly the mirror image of that for the outer driver, Fig. 1 of our Sun Valley summary.[1] Thus the phenomena discussed above of sensitivity sign change could be expected.

Tables 8 and 9 give some results for these cases. Using eqn. (1.8), we have calculated the relative absorption component given in the right hand column. As can be seen, these values are of roughly the same absolute value for the inner and outer ring, but of opposite sign, while the absolute values for the middle ring are smaller. These results are consistent with subsequent calculations by John White, who calculated total relative sensitivities as reported in our summary.[1] The U238 σ_c PD sensitivities were - 0.33 and + 0.24 for the inner and outer driver rings, respectively.

Thus it is obvious that when reporting PPD sensitivities for a particular heterogeneous core design, we should consider the PD for each driver zone to be a separate response function. For a similar model a designer can pick the response(s) of most interest to him, depending on the shape of his calculated PD curve. In this context, it is of interest to consider the two ν_{CDS} models we used, i.e. the initial and corrected

models, with different driver and internal blanket zone widths and other less significant changes. For these two models the PD density distributions were quite different, but the total PPD sensitivities for the same driver ring were roughly the same.

The PD variance at different points is of particular interests. Based on the previous considerations it seems likely that they will be roughly the same for the inner and outer ring, since a simple sign switch on all sensitivity coefficients would of course cancel in the variance calculation. The middle driver ring PPD variance will probably be somewhat smaller than those of the other rings.

For a relatively "flat" power distribution the driver region with the maximum PPD variance may be of particular interest. The inner driver ring seems a likely candidate for this category, since it has the smaller volume to compensate for power changes in the other rings. However, such changes can be influenced by control rod motion strategies, and the PPD variance should be investigated for all driver rings.

2. Variance of Peak Power Density including Spatial Uncertainty

The following theory was developed by A. Gandini as part of his consultant activities for the project. Editing and insertion of additions to his manuscript was performed by J. Kallfelz. Some of the basic expressions for this theory are contained in footnote 26b of an article by Gandini[5] (to be published). His discussions with E. M. Oblow, M. L. Williams and D. G. Cacuci about the draft of this article induced the inclusion of this footnote.

Let us consider expressions of the form

$$Q_1 = \int_{Vol_1} F_1[\vec{\phi}(\sigma_j)] \equiv \langle F_1 \vec{\phi}(\sigma_j) \rangle_1 \tag{2.1}$$

Where $\vec{\phi}$ satisfies the equation: $\mathcal{M}\vec{\phi} = 0$, (2.2)

$\sigma_j \hat{=}$ all nuclear data, group dependent,

and $$Q_2 = \langle h_2 \vec{\phi} \rangle_2 \quad . \tag{2.3}$$

Then consider the ratio

$$R = \frac{Q_1}{Q_2} \tag{2.3a}$$

and differentiate to obtain

$$\frac{\delta R}{R} = \frac{\delta Q_1}{Q_1} - \frac{\delta Q_2}{Q_2} \quad . \tag{2.4}$$

Consider the case for

$$F_1 [\vec{\phi}(\sigma_j)] = \vec{g}(\sigma_j)\vec{\phi} \tag{2.5}$$

and $\vec{g}$ an n-component vector of scalar quantities.

E.g., for the case of power density, $\vec{g}(\vec{r})$ is as defined in eqn. (3) of ref. 4, i.e.

$$g_j(\vec{r}) = \sum_k P^k \Sigma^k_{f,j}(\vec{r}) \tag{2.6}$$

where P^k is the total recoverable energy release for one fission in the k-th isotope.

Now consider the case for

$$F_1 [\vec{\phi}(\sigma_j)] = \mathcal{L}\vec{\phi} \tag{2.6a}$$

with $\mathcal{L}$ an n-row matrix containing derivative operations.

Let us extend the field so that

$$\hat{\vec{f}} = \begin{pmatrix} \vec{\phi} \\ \vec{g} \end{pmatrix} \tag{2.7}$$

Governed by the equation

$$\begin{bmatrix} \mathcal{U} & 0 \\ -\mathcal{L} & \mathcal{U} \end{bmatrix} \begin{pmatrix} \vec{\phi} \\ \vec{g} \end{pmatrix} = \hat{\mathcal{M}}\hat{\vec{f}} = 0 \tag{2.8}$$

where $\mathcal{U}$ is a unit matrix, and

$$\vec{g} = \mathcal{L}\vec{\phi} \tag{2.9}$$

We can write

$$\hat{Q}_1 = \langle \vec{g}\,\vec{y} \rangle \equiv \langle \hat{\vec{h}}_1^{+}\,\hat{\vec{f}} \rangle \tag{2.10}$$

$$Q_2 = \langle \vec{h}_2\,\vec{\phi} \rangle \equiv \langle \hat{\vec{h}}_2^{+}\,\hat{\vec{f}} \rangle \tag{2.11}$$

which define the following vectors:

$$\hat{\vec{h}}_1^{+} = \begin{pmatrix} 0 \\ \vec{g} \\ 0 \end{pmatrix} \quad \text{and} \quad \hat{\vec{h}}_2^{+} = \begin{pmatrix} \vec{h}_2 \\ 0 \end{pmatrix} \tag{2.12}$$

and then proceed normally with generalized perturbation theory (GPT).

The source for the integrated importance $\hat{\vec{\Gamma}}^*$ will be:

$$\hat{\vec{S}}^* = \frac{\hat{\vec{h}}_1^{+}}{\hat{Q}_1} - \frac{\hat{\vec{h}}_2^{+}}{Q_2} \tag{2.13}$$

$\hat{\vec{\Gamma}}^*$ will obey the eqn.

$$\begin{bmatrix} \mathcal{M}^* & -\mathcal{L} \\ 0 & \mathcal{U}^* \end{bmatrix} \begin{pmatrix} \vec{\Gamma}^* \\ \vec{y}^* \end{pmatrix} + \hat{\vec{S}}^* = \hat{\mathcal{M}}^* \hat{\vec{\Gamma}}^* + \hat{\vec{S}}^* = 0 \tag{2.14}$$

We can then calculate the perturbation of

$$\hat{R} = \frac{\hat{Q}_1}{Q_2} \tag{2.15}$$

with the following expression:

$$\frac{\delta \hat{R}}{\hat{R}} = \langle \delta \hat{\vec{S}}^* \hat{\vec{f}} \rangle + \langle \hat{\vec{\Gamma}}^* \delta \hat{\eta} \hat{\vec{f}} \rangle \qquad (2.16)$$

(for a $\delta\eta$ which maintains criticality.)

Equation (2.16) is the normal GPT expression with a "direct" and "indirect" effect component on the right side.

Now let us consider the Taylor's series expansion for the case of one space variable, x:

$$Q_1(x) = Q_1(x_0) + Q_1^{(1)}(x - x_0) + \frac{1}{2!} Q_1^{(2)}(x-x_0)^2 + \frac{1}{3!} Q_1^{(3)}(x-x_0)^3 + \cdots \qquad (2.17)$$

where

$$Q_1^{(i)}(x) = \langle F_1^{(i)}[\vec{\phi}(\sigma_j)] \rangle_{x_0} = \left\langle \frac{\partial^i F_1[\vec{\phi}(\sigma_j)]}{\partial x^i} \right\rangle_{x_0} \qquad (2.18)$$

At x_0, $Q_1^{(1)} = 0$ if x_0 is the point of maximum Q_1.

Let us perturb σ_j, and obtain the perturbed value of Q_1:

$$Q_1'(x) = Q_1'(x_0) + Q_1^{(1)'}(x_0)(x-x_0) + \frac{1}{2!} Q_1^{(2)'}(x_0)(x-x_0)^2 + \frac{1}{3!} Q_1^{(3)'}(x_0)(x-x_0)^3 + \cdots \qquad (2.19)$$

Divide by Q_2' and obtain

$$\frac{Q_1'(x)}{Q_2'} = R'(x) = R'(x_0) + R^{(1)'}(x_0)(x-x_0) \tag{2.20}$$

$$+ \frac{1}{2!} R^{(2)'}(x_0)(x-x_0)^2 + \frac{1}{3!} R^{(3)'}(x_0)(x-x_0)^3 + \cdots$$

The quantities

$$R^{(i)}(x) = \frac{Q_1^{(i)}}{Q_2} \tag{2.21}$$

fall in the category of the functionals $\hat{R}$ considered above (see eqn. 2.15). Then, neglecting the direct effect, as in eqn. (2.16)

$$\frac{\delta R^{(i)}}{R^{(i)}} = \left\langle \hat{\vec{\Pi}}^{*(i)} \, \delta \hat{m} \, \hat{\vec{F}}^{(i)} \right\rangle \tag{2.22}$$

$$\equiv \left\langle \vec{\Pi}^{*(i)} \, \delta m \, \vec{\Phi} \right\rangle$$

where

$$\delta \hat{m} = \begin{bmatrix} \delta m & 0 \\ 0 & 0 \end{bmatrix} \tag{2.23}$$

and

$$\hat{\vec{\Pi}}^{*(i)} = \begin{pmatrix} \vec{\Gamma}^{*(i)} \\ \vec{y}^{\,*} \end{pmatrix}, \tag{2.24}$$

which obeys the following equation, analagous to egns. (2.12)-(2.14):

$$\begin{bmatrix} m^* & -\frac{\partial^i}{\partial x^i} \\ 0 & u^* \end{bmatrix} \begin{pmatrix} \vec{\Gamma}^{*(i)} \\ \vec{y}^{\,*} \end{pmatrix} + \frac{1}{Q_1^{(i)}} \begin{pmatrix} 0 \\ \vec{g} \end{pmatrix} - \frac{1}{Q_2} \begin{pmatrix} \vec{h}_2 \\ 0 \end{pmatrix} = 0 \qquad (2.25)$$

This equation must be solved for $\vec{\Gamma}^{*(i)}$ and $\vec{y}^{\,*}$.

Setting $\frac{\partial Q_1'}{\partial x} = 0$ determines the location x_0' of the maximum value $Q_1'(x_0')$. To third order, we have

$$R^{(1)'} + R^{(2)'}(x-x_0) + \frac{1}{2!} R^{(3)'}(x-x_0)^2 = 0 \qquad (2.26)$$

and from this, recalling eqn. (2.22), an expression for x_0' :

$$x_0' = X(\delta m) \qquad (2.27)$$

Inserting this expression in eqn. (2.20), we have

$$R'(x_0') = R'(x_0) + R^{(1)'}(x_0)(x_0' - x_0) + \cdots \qquad (2.28)$$

with x_0' given by eqn. (2.27), i.e. we can obtain

$$\delta R = R'(x_0') - R(x_0) \qquad (2.29)$$

at the maximum point x_o' in terms of the perturbation, i.e.

$$\delta R_{max} = F(\delta M) \tag{2.30}$$

Since we can also write, introducing the system parameters σ_j,

$$\delta R_{max} = \sum_j \frac{\partial R_{max}}{\partial \sigma_j} \delta \sigma_j , \tag{2.31}$$

where the sensitivities are derived with eqn. (2.30), we can evaluate the variance of R_{max}:

$$VAR(R_{max}) = \sum_{i,j} \frac{\partial R_{max}}{\partial \sigma_i} \frac{\partial R_{max}}{\partial \sigma_j} COV(\sigma_i, \sigma_j) . \tag{2.32}$$

This is the variance of R_{max} including its spatial uncertainty.

References

[1] J. M. Kallfelz, C. L. Cowan, J. H. Marable, M. L. Williams, C. R. Weisbin, J. D. Drischler, T. B. Fowler and J. R. White, "Design and Sensitivity Analysis of a CDS-Type LMFBR Heterogeneous Core," Paper accepted for presentation at ANS Topical Meeting, 1980 Advances in Reactor Physics and Shielding, September 14-17, 1980.

[2] J. M. Kallfelz and P. Levin, "Progress Report on Work for ORNL Subcontract 7802, Period January 9 - February 11, 1980," Memorandum to C. R. Weisbin, J. H. Marable and M. L. Williams dated February 12, 1980.

[3] J. M. Kallfelz and P. Levin, "Progress Report on Work for ORNL Subcontract 7802, Period February 12 - March 4, 1980," Memorandum to C. R. Weisbin, J. H. Marable and M. L. Williams dated March 5, 1980.

[4] J. M. Kallfelz, P. Levin and M. Becker, "Progress Report on Work for ORNL Subcontract 7802, Period April-May 9, 1980," Memorandum to C. R. Weisbin, J. H. Marable and M. L. Williams dated May 19, 1980.

[5] A. Gandini, "Generalized Perturbation Theory for Non-linear Systems from the Importance Conservation Principle," to be published in Nucl. Sci. Engr.

[6] J. M. Kallfelz and P. Levin, "Progress Report on Work for ORNL Subcontract 7802, Period May 10 - June 10, 1980," Memorandum to C. R. Weisbin, J. H. Marable and M. L. Williams dated June 11, 1980.

[7] J. M. Kallfelz, "Status Report for the Georgia Institute of Technology Project E-26-610," Memorandum to F. C. Maienschein dated March 19, 1975.

[8] A. B. Smith, P. T. Guenther and J. F. Whalen, "The Nonelastic-scattering Cross Sections of Elemental Nickel," ANL/NDM-54, Argonne National Laboratory, June 1980.

[9] J. M. Kallfelz, J. H. Marable and C. R. Weisbin, Letter to C. L. Cowan (GE) dated January 25, 1980.

[10] S. L. Beaman (GE-ARSD), Memorandum to J. M. Kallfelz dated June 18, 1980.

Table 1.

PPD Γ^* Calculation for a Full and a Half Slab Case with the same peak flux (see Text, Page 3)

Items	Base Case (Full slab)	Case 4 (Half-slab)
Group flux, centre		
Φ_1	0.86	0.86
Φ_2	4.35	4.35
Φ_3	1.58	1.58
Power Density, centre (W/c.c)	1.40	1.40
Fixed source		
Total	-0.38	-0.38
Max	0.32	0.32
Min	-0.005	-0.010
Group Γ^*, centre		
Γ_1^*	0.30	0.61
Γ_2^*	0.22	0.44
Γ_3^*	0.42	0.86

Table 2.

PPD Γ^* Calculation for a Full Slab with different peak flux (see Text ; Page 3).

Items	Base Case (Full slab)	Case 2 (Full slab)
Group flux, centre		
ϕ_1	0.86	1.72
ϕ_2	4.35	8.70
ϕ_3	1.58	3.16
Power density, centre (W/c.c)	1.40	2.80
Fixed Source		
Total	-0.38	-0.19
Max	0.32	0.16
Min	-0.0052	-0.0026
Group Γ^*, centre		
Γ_1^*	.30	0.15
Γ_2^*	.22	0.11
Γ_3^*	.42	0.21

Table 3.

PPD Γ^* Calculation for a Full and a Half Slab Case with the same total power (a2). (see Text, Page 3).

Items	Base Case (Full slab)	Case 3 (Half slab)
Group flux, centre		
ϕ_1	0.86	1.72
ϕ_2	4.35	8.70
ϕ_3	1.58	3.16
Power density, centre (W/c.c)	1.40	2.80
Fixed source		
Total	-0.38	-0.19
Max	0.32	0.16
Min	-0.005	-.005
Group Γ^*, centre		
Γ_1^*	0.30	0.30
Γ_2^*	0.22	0.22
Γ_3^*	0.42	0.43

Table 4.

Comparison of $\delta\Sigma_a$ effect on PPD by direct and perturbation calculations for a full slab model.

Items	Base case	Case 5
Σ_a (Group 2, driver region)	2.642 E-3	2.906 E-3
$\delta\Sigma_a$ (+ 10%)	-	0.264 E-3
PPD	1.4011E-2	1.3988E-2
Direct $\frac{\delta PPD}{PPD}$	-	0.161 %
$\frac{\delta PPD}{PPD}$ (= $\delta\Sigma_a$ *"SIGA")	0.163 %	-

Table 5.

Comparison of $\delta\Sigma_a$ effect on PPD by direct and perturbation calculations for a half slab model.

Items	Case-3	Case- 6
Σ_a (Group 2, driver region)	2.642 E-3	2.906 E-3
$\delta\Sigma_a$ (* 10%)	-	0.264 E-3
PPD	2.8022E-2	2.7976E-2
Direct $\frac{\delta PPD}{PPD}$	-	0.161 %
$\frac{\delta PPD}{PPD}$ (= $\delta\Sigma_a$ *"SIGA")	0.163 %	-

Table 6.

Comparison of δD effect on PPD by direct and perturbation calculations for a half slab model.

Items	Case-3	Case-7
D (Group 2, driver region)	3.6565	3.9207
δD (7.226%)	-	0.2642
PPD	2.8022E-2	2.7901E-2
Direct $\frac{\delta PPD}{PPD}$	-	-0.43%
$\frac{\delta PPD}{PPD}$ (= δD *"DIFF.COEF.")	-0.45%	-

TABLE 7. Comparison of Relative Absorption and Diffusion Components (Eqns. 1.8 and 1.9) for PPD Sensitivity of U-238 σ_c Perturbation. (Outer driver zone, initial CDS model)

Group	E-range	$\frac{\text{Abs. Comp.}}{N_F^{28}\,\delta\sigma_c^{28}}$	$\frac{\text{Diff. Comp.}}{N_F^{28}\,\delta\sigma_c^{28}}$
1	10-17.3 MeV	+3.28-2	-9.25-3
5	1.35-2.23	+2.95+0	-4.23-1
9	0.18-0.30	+7.11+0	-1.90-1
13	24.8-40.9 keV	+7.01+0	-3.12-2
17	3.36-5.53	+2.34+0	-4.67-3
21	0.45-0.75	+1.47+0	-3.18-3
25	E_{upper}: 100 eV	+1.48-1	-8.78-3

Table 8.

Sensitivity Calculation at different space point.
- CDS Model.

Item		Inner Ring (Driver)	Middle Ring (Driver)	Outer Ring (Driver)
Space point location; (Column; Row)		14;19	23;19	35,19
Power Density, W/c.c.		552.5	577.2	569.1
Max Power Density, W/c.c		558.0 (13;19)	577.2	569.1
Fixed source,	Total	4.96E-14	-5.41E-14	-5.26E-14
	Max.	7.18E-14	6.87E-14	6.94E-14
	Min.	-5.67E-16	-5.67E-16	-5.67E-16
Γ^*, Group 11				
Col 14; Row 19		5·67 E-19	4·92 E-20	-1·10 E-19
Col 23;	"	5·16 E-20	2·36 E-19	-5·04 E-20
Col 35;	"	-1·24 E-19	-5·73 E-20	1·72 E-19

Table - 9

Results for the Absorption Components of the PD sensitivity for the three driver rings.

- CDS MODEL (Ref: eq. 1.8)

Group	Region	$A_{AB1} * \frac{N_{1B}}{N_F}$	$A_{AB2} * \frac{N_{AB2}}{N_F}$	$A_{RB} * \frac{N_{1B}}{N_F}$	$A_{1B} * \frac{N_{1B}}{N_F}$	A_{F1}^*	A_{F2}^*	$\frac{\text{Abs. Component}}{N_F^{2B}\ \delta\sigma_c^{2B}}$ (eq. 1.8)
11	Outer Ring	0.78	1.00	-4.07	15.95	25.05	-29.41	9.30
	Middle Ring	0.04	1.00	6.43	-15.40	-19.53	21.44	-6.02
	Inner Ring	-0.32	1.04	11.35	-28.19	-56.56	61.06	-11.62
16	Outer Ring	0.21	0.27	-0.79	4.43	6.81	-6.85	4.08
	Middle Ring	0.04	0.27	1.67	-3.34	-5.58	4.92	-2.02
	Inner Ring	-0.05	0.28	2.84	-6.94	-15.36	14.67	-4.56

* For these calculations the driver was divided into two zones, F1 corresponding to the inner driver ring and inner part of the middle ring, F2 being the remainder of the driver regions.

GEORGIA INSTITUTE OF TECHNOLOGY
ATLANTA, GEORGIA 30332

SCHOOL OF
NUCLEAR ENGINEERING

March 19, 1975

TO: Dr. F. C. Maienschein, Director
Neutron Physics Division
Oak Ridge National Laboratory
Oak Ridge, Tennessee 37830

FROM: John M. Kallfelz

SUBJECT: Status Report for the Georgia Institute of Technology Project E-26-610 (Subcontract No. 3986 of the Union Carbide Corporation, Nuclear Division)

I. Introduction

This status report is occasioned by the departure for Europe of one of the principal investigators for this project. As stated in the proposal for the second renewal of the subcontract, J. M. Kallfelz is the principal investigator through December 1974, and from January to June 1975 M. Salvatores will direct the project.

The main results of this work are described in the attached paper by Kallfelz, Lal, Williams and Flanagan,[1] which will be published in the proceedings of the Atlanta ANS Topical Meeting. The final calculations for the sensitivity curves reported in Section 3 of the attached paper were calculated this fall after the conference, since errors were discovered in the ENDF/B-III cross section sets used in the initial calculations. The project monitor at ORNL, G. F. Flanagan, has requested that we document certain details and data not contained in the attached paper; this memo contains this information.

II. 1D vs. 2D Comparison -- Sensitivity Coefficient Calculations

Direct comparisons were made between 1D and 2D region-wise results for various components of the sensitivity coefficients, to check the accuracy of a 1D spherical model which we used for calculating these coefficients. Some results and the conclusions from these comparisons are given in par. 2.3 of the attached reference 1. Tables 1-5 give all the numerical results of this comparison, for the components given by Eqs. (4)-(8) of ref. 1.

III. "k-Reset"

The influence of a cross section change on an integral parameter depends on the method used for "k-reset", i.e. the change in the reactor configuration made to retain criticality by compensating for the change in k caused by the initial cross section change. The influence of "k-reset" is discussed in par. 3.1 of the attached reference 1. It is pointed out that the reset method used in our calculations (control rod adjustment) had only a small influence on the sensitivity coefficient values. This fact is illustrated in Tables 6 and 7, which give numerical results for the sensitivity coefficients and k-reset components for U-238 σ_c and Pu-239 σ_f.

IV. Dependent and Independent Variables

When calculating the sensitivity coefficients, one must make a decision as to which cross sections are to be considered the independent variables in the diffusion equation. For instance, if σ_f and σ_c are considered as independent variables, as they were in this work, then a $\delta\sigma_f$ causes a contribution to the sensitivity curve both from the fission and absorption components, Eqs. (5) and (6) of reference 1.

In principle, a choice of different independent variables by two investigators would be compensated in the determination of the variance

of a calculated integral parameter (see sec. 3.3 of reference 1) by using a different combination of covariance files for the two cases; these files express the actual correlation between cross sections. Of course in the evaluation of the variance the coefficients and covariances used must be consistent and non-redundant; e.g. one should not use sensitivity coefficients for σ_c, σ_f and σ_a. Further, as a practical matter one should not pick as an independent variable a cross section, ratio, or sum for which it is unlikely that covariance files will be determined.

A choice must be made between σ_t or one of the partial cross sections as a dependent variable. The most usual choice for the dependent variable has been σ_{el}, since it is generally determined, particularly in older evaluations, as the difference between σ_t and σ_{nonel}. However, as discussed below, increased independent information about σ_{el} in more recent evaluations makes the more appropriate choice less clear, for some isotopes. Furthermore, the most appropriate choice often depends on the energy range. For instance, Pendlebury et al. (ref. 2, p. 4) state that at high energies σ_{el} is the most appropriate dependent variable, whereas when at low energies the nonelastic cross section is relatively large, it is preferable to consider σ_t as dependent; their perturbation code DUNDEE[2] has an option to treat either σ_{el} or σ_t as dependent. As also discussed below, for diffusion theory calculations of sensitivity coefficients, more detailed cross section information is needed in the sigma library if σ_t instead of σ_{el} is considered to be independent.

In our study, σ_t was considered dependent; it should be emphasized that for the results reported in our attached paper[1] (sensitivity of the breeding ratio to fertile and fissile capture and fission cross sections) this choice does not have an appreciable influence. This choice influences

only the "scatter" and "diffusion" components, Eqs. (7) and (8) of ref. 1; the diffusion component was much smaller than the other components for the reported cases, and the scatter component is influenced through the elastic scatter out of the group [see Eq. (8) below] which is quite small for the heavy elements. However, for the perturbation of cross sections or isotopes for which the elastic scatter and diffusion components are significant, the choice of σ_t or σ_{el} as the independent variable can clearly have an appreciable influence on the sensitivity coefficient. Following are some comments about this choice.

For the ENDF/B-III evaluation,[3] it is not clear for all isotopes which is the most appropriate dependent variable. For U-238 (see p. 92-238-13 of ref. 3) σ_{el} is clearly determined as the difference between the evaluated total and nonelastic cross sections. However, for Pu-239, which has a σ_{nonel} generally larger than for U-238, the situation is not as clear (see p. 94-239-1 of ref. 3). For Pu-239, shape and compound elastic sigma calculations as well as calculations for other reactions were carried out, results were combined in a "consistent manner", and various competitive reactions were adjusted to obtain values for σ_f and σ_c as recommended in another evaluation.

If σ_{el} is considered dependent, more independent cross section data are required for the perturbation calculation than are commonly supplied in processed cross section sets. For instance, if:

A. σ_t is dependent, then

$$\sigma_{tr} = \sigma_c + \sigma_f + \sigma_{inel} + \sigma_{el}(1-\bar{\mu}_{el}) \qquad (1)$$

and for example an introduced $\delta\sigma_c$ gives (assuming σ_c and σ_f are independent)

$$\delta\sigma_{tr} = \delta\sigma_c \tag{2}$$

However, if:

B. σ_{el} is dependent, then,

$$\sigma_{el} = \sigma_t - \sigma_{nonel} \tag{3}$$

and

$$\sigma_{tr} = \sigma_{in} + \sigma_c + \sigma_f + (\sigma_t - \sigma_{nonel})(1-\bar{\mu}_{el}) \tag{4}$$

or

$$\sigma_{tr} = (\sigma_c + \sigma_f + \sigma_{in})\bar{\mu}_{el} + \sigma_t(1-\bar{\mu}_{el}) \tag{5}$$

so that for an introduced $\delta\sigma_c$,

$$\delta\sigma_{tr} = \bar{\mu}_{el} \cdot \delta\sigma_c \tag{6}$$

Furthermore, for this case:

$$\sigma_{el}(j\to k) = (\sigma_{t_j} - \sigma_{nonel_j})\, f_{el}(j\to k) \tag{7}$$

so that an introduced $\delta\sigma_c$ also causes a scattering component contribution (Eq. (7) of ref. 1) since

$$\delta\sigma(j\to k) = -\,\delta\sigma_{c_j}\, f_{el}(j\to k) \tag{8}$$

This component is not present for an introduced $\delta\sigma_c$ in case A. Thus in summary, for case B, one needs $\bar{\mu}_{el}$ and $f_{el}(j\to k)$ separate from the other group data.

For the heavy elements, $\bar{\mu}_{el}$ varies from about 0.5 to 0.8 between about 1 and 10 MeV (e.g., see ref. 4, p. 73). Thus from Eqs. (1) and (5) it can be seen that for these elements for a perturbated partial cross section the

$\delta\sigma_{tr}$ values obtained in cases A and B approach each other at high energies.

V. 2D Sensitivity Study Codes

Our studies to the present, reported in reference 1, have utilized the new Italian two dimensional sensitivity code package only for four group calculations. These codes have been initiated on both the Georgia Tech U-1108 and the ORNL IBM-360, and have a capacity of up to 26 groups. However, to make such calculations practical, interface codes are needed to read the ORNL ANINSN cross section data format and prepare the input for the Italian codes. For DDV, SORCI and CIAP-2D, these interface programs for the case of real flux functionals have been written and tested at Georgia Tech.

APPENDIX A
REFERENCES

1. J. M. Kallfelz, M. L. Williams, D. Lal and G. F. Flanagan, "Sensitivity Studies of the Breeding Ratio for the Clinch River Breeder Reactor," in Advanced Reactors; Physics, Design and Economics, Ed., J. M. Kallfelz and R. A. Karam, Pergamon Press, 1975 (in print).

2. P. C. E. Hemment, E. D. Pendlebury, et al., "The Multigroup Neutron Transport Perturbation Program DUNDEE," AWRE 0-40/66, UKAEA Aldermaston, October 1966.

3. O. Ozer and D. Garber, Ed., "ENDF/B Summary Documentation," BNL-17541, Brookhaven National Laboratory, May 1973.

4. S. Yiftah, D. Okrent and P. A. Moldauer, Fast Reactor Cross Sections, Pergamon Press, New York, 1960.

5. DDV, SORCI, CIAP-2D, GLOBPERT-2D, a two dimensional Italian sensitivity code package developed by G. P. Cecchini and co-workers at NIRA. Private communication.

SCHOOL OF NUCLEAR ENGINEERING E-26-B01

Atlanta, Georgia 30332 (404) 894-3720

August 29, 1980

MEMORANDUM

TO: C. R. Weisbin, J. H. Marable, and M. L. Williams (ORNL)

FROM: J. M. Kallfelz and D. Biswas

SUBJECT: Progress Report for ORNL Subcontract 7802, Period August 7-31, 1980

Accomplishments

- Top priority was given to completing the remaining tasks to be completed for our Sun Valley paper,[1] and to preparing this paper. The first draft of this paper was provided to the co-authors on August 25, 1980 for their comments, and the final draft is attached as the body of this report.

- Related to the previous topic, D. Biswas visited ORNL to learn how to use the DEPTH code module developed by J. R. White for sensitivity analysis with VENTURE.

Plans for Work for the Next Report Period

- The final version of the Sun Valley paper[1] will be completed and the paper will be presented at the ANS topical meeting on September 16. As stated in Ref. 2, we need all your comments based on the attached 2nd draft, plus all significant numbers which might change text, by September 4. All reduced camera-ready tables and figures as requested in Ref. 2 are needed by September 8; if possible, please provide me also with the negatives thereof, in case we have to reduce them even further to conserve space.

- Work will continue on the CDS sensitivity analysis being performed jointly with ORNL and GE, which is described in the attached paper.

- D. Biswas will present a seminar at ORNL on the nuclear analysis of Super Phenix as part of a presentation to CRBR project office staff members.

jhr

cc: J. R. White, D. Cacuci (ORNL)
C. L. Cowan (GE-Sunnyvale)

References

1. J. M. Kallfelz, D. Biswas, C. L. Cowan, J. H. Marable, M. L. Williams, C. R. Weisbin, J. D. Drischler, T. B. Fowler, and J. R. White, "Design and Sensitivity Analysis of a CDS-Type LMFBR Heterogeneous Core," Paper accepted for presentation at ANS Topical Meeting 1980 Advances in Reactor Physics and Shielding, September 14-17, 1980.

2. J. M. Kallfelz, "1st Draft Plus Your Input for Sun Valley Paper," Memo to co-authors of Ref. 1, dated August 24, 1980.

2d DRAFT

DESIGN AND SENSITIVITY ANALYSIS OF A CDS-TYPE HETEROGENEOUS CORE

J. M. Kallfelz and D. Biswas
Georgia Institute of Technology
Atlanta, Georgia 30332

C. L. Cowan
General Electric Company
Sunnyvale, California 94086

J. H. Marable, M. L. Williams, C. R. Weisbin
J. D. Drischler, T. B. Fowler, and J. R. White
Oak Ridge National Laboratory
Oak Ridge, Tennessee 37830

ABSTRACT

The design of a heterogeneous LMFBR of the type being considered for the Conceptual Design Study (CDS) is analyzed, using sensitivity study methods. Nuclear data sensitivities for k_{eff}, the breeding ratio, and parameters related to the peak linear power (space-dependent power densities) are determined with generalized perturbation theory. These sensitivities are folded with extensive nuclear data covariance information to determine the associated integral parameter uncertainties and correlations. The effects of non-localized energy deposition we investigated by folding the results of coupled (n-γ) calculations with kerma factors.

INTRODUCTION

The development of the Conceptual Design Study (CDS) reactor plant[1] was intended to provide direction and focus to the LMFBR technology programs, and the research and development needs for these

programs will be outlined in the final report to Congress by DOE after April, 1981. The joint work reported in this paper involved a cooperative effort by university, vendor, and national laboratory staff, with the principle goal of investigating the uncertainties of some significant reactor performance parameters.

To accomplish this aim we utilized both direct perturbations and the methods of generalized perturbation theory,[2-6] together with nuclear data covariance information[4-8] which has become available in the last few years. Several of the performance parameters considered, namely k_{eff} and the breeding ratio, have been the object of a similar study,[4,5] for a homogeneous LMFBR, thus allowing comparison of the importance of various nuclear data to these parameters for the two reactor types.

We have placed particular emphasis on studies related to the peak linear power. Reduction of uncertainty in this parameter has obvious importance both for licensing and economic consideration, and considerable attention has been devoted in recent studies[9] to determining the maximum allowable value of this quantity. For sensitivity calculations we considered the power density with diffusion theory, but we have investigated the effects of non-localized energy deposition performing coupled (n-γ) calculations and folding the results with kerma factors.[10] In the following sections we discuss the design and typical configuration of the CDS reactor, and the methods and results of our sensitivity analysis.

GENERAL REACTOR DESCRIPTION

The key design parameters for a large heterogeneous LMFBR of the 1000 MWe class were specified as part of the DOE sponsored CDS project. The design objectives and criteria for the CDS project emphasized the following:

1. High reliability,
2. Near term design features (components that can be developed within five years),
3. Sufficiently low sodium void worth to preclude hypothetical core disruptive accidents from consideration as design basis accidents,
4. Breeding of fissile fuel at a rate equivalent to a compound system doubling time of twenty years or less, and
5. Allowances for the future accomodation of advanced fuels.

On the basis of the above objectives, the CDS Reference Design was chosen to be a 2540 MW_{th}, mixed plutonium uranium oxide, heterogeneous reactor with three driver fuel zones and three inner blanket zones. The core layout for the Reference Design is shown in Fig. 1, and a summary of the principal core design and performance parameters is given in Table I. All design calculations discussed in this section were carried out in linked r-z and x-y triangular mesh geometry using the two-dimensional diffusion theory code SN2D[11] and the fuel management and burnup code FUMBLE,[12] and cross sections based on ENDF/B-IV data.

The fuel pin diameter for the CDS Reference Design was selected on the basis of earlier sensitivity studies to give near-optimum breeding and economic performance for the heterogeneous core. The fuel pins are

clad with the austenitic stainless steel alloy, D9, with material properties which closely resemble those of 20% CW316 SS. However, on the basis of available data the irradiation induced creep and swelling are expected to be significantly lower for the D9 alloy.

The core layout as shown in Fig. 1 was specified to minimize the peak radial power throughout the operating cycle based upon a single fissile enrichment for the supplied fuel in all driver fuel regions. The twelve burnup control rods in the outer driver fuel zone are also utilized to shape the radial power profile during reactor operations.

Reactor shutdown of the CDS Design is accomplished by each of two independent control systems. The primary control system consists of 21-24 natural boron carbide rods, including 12 rods in the outer control ring for burnup reactivity adjustments. The secondary control system consists of 6-9 enriched boron carbide rods which are distributed in the inner and middle control rings. The final requirements for the two independent systems will be determined in follow-up studies and will include an assessment of control reliability requirements.

SENSITIVITY STUDIES MODEL AND DATA

For the sensitivity studies we considered an MOEC design characteristic of those being considered for the CDS. the r-z model used for these studies is shown in Fig. 2, while Table II describes the composition of the principle regions. The shield was not included in our calculations, and control in the outer control ring was inserted to achieve criticality for the model.

The further reported results were calculated with the ENDF/B-IV cross section set of 32 groups used in Refs. 4 and 5, unless noted

otherwise. We also generated ENDF/B-IV cross sections for the CDS-type reactor from the 171 group Vitamin-C library.[13] Resonance shielding for both the blanket and driver zones was done with the BONAMI module of the AMPX system,[14] and the 171 group cross sections were collapsed to 32 groups using fluxes obtained from a 1-D, cylindrical XSDRW-PM[14] transport calculations (S4P1) of the reactor. Sensitivity results for the two cross section sets were practically the same.

UNCERTAINTY ANALYSIS THEORY AND METHODS

Using the methods of generalized perturbation theory,[2-6] the group-dependent nuclear data sensitivity $(\partial I/I)/(\partial\sigma_i/\sigma_i)$ of integral parameter I has been studied for two parameters considered in an earlier works,[4,5] namely k_{eff} and the breeding ratio, as well as ratios significant for determining the uncertainty in the calculated peak linear power. For sensitivity values involving the criticality constraint, "k-reset"[4-6] has been performed by altering the driver zone "plutonium enrichment", i.e., (total Pu)/(total heavy metal), as in previous studies.[4,5] Perturbation theory results were checked by direct perturbation calculations performed at General Electric, ORNL and Georgia Tech.

Generalized perturbation theory[2-6] provides a method of calculating a generalized adjoint function, $\Gamma^*(\vec{r})$, where $\Gamma_j^*(\vec{r})$ is the importance of a neutron in energy group j at space point $\vec{r}$ to the ratio being considered. We have incorporated in VENTURE[15] the capability to generate $\vec{\Gamma}^*$ for the ratio of point power density to total power (PD):

$$PD(\vec{r}_p) = \frac{a_1}{a_2} = \frac{\sum_j \Sigma_{1j}(\vec{r}_p)\,\phi_j(\vec{r}_p)}{\int_{\text{reactor}} \sum_j \Sigma_{2j}(\vec{r})\,\phi_j(\vec{r})\,d\vec{r}} \qquad (1)$$

where Σ_{ij}, the "energy-production cross sections", have the same form:

$$\Sigma_{ij}(\vec{r}) = \sum_k p^k \Sigma^k_{f,j}(\vec{r}) \qquad (2)$$

and p^k is the total energy release per fission in the k-th isotope.

Thus, the fixed source in the equation for $\vec{\Gamma}^*$ for PD ($\vec{r}_p$) has the form:

$$S^*_j(\vec{r}) = \frac{\Sigma_{1j}(\vec{r})}{a_1} - \frac{\Sigma_{2j}(\vec{r})}{a_2} \qquad (3)$$

where Σ_{1j} is zero for $\vec{r} \neq \vec{r}_p$.

To determine the uncertainty of an integral parameter, I, one can calculate its variance (VAR):

$$VAR(I) = \sum_{i,j} \frac{\partial I}{\partial \sigma_i} \frac{\partial I}{\partial \sigma_j} cov(\sigma_i, \sigma_j) \qquad (4)$$

The nuclear data covariance files (COV) contain information on both the standard deviation, SD, and correlation of various cross sections.[4-6] To obtain a reliable estimate of SD(I) = $\sqrt{VAR(I)}$, equation (4) should include all data which have a significant impact on I.

Due to the space-dependent nature of the PD sensitivities which we will discuss in the following section, a parameter of particular interest is the covariance of two integral parameters:

$$cov(I_1, I_2) = \sum_{i,j} \frac{\partial I_1}{\partial \sigma_i} \frac{\partial I_2}{\partial \sigma_j} cov(\sigma_i, \sigma_j) \qquad (5)$$

The correlation (COR) between I_1 and I_2 is expressed more explicitly by:

$$COR(I_1, I_2) = \frac{COV(I_1, I_2)}{SD(I_1)\ SD(I_2)} \qquad (6)$$

S* of equation (3) can be calculated by VENTURE or DEPTH.[16] The later code was used to process the $\vec{\Gamma}^*$ and ϕ files from VENTURE to determine the sensitivities. For all reported sensitivities, σ_t was treated as dependent, i.e. a perturbation in one of the partial cross sections had an associated $\delta\sigma_{tr}$. This convention will not influence the VAR values if consistent COV(σ_i, σ_j) data are used in equation (5).

SENSITIVITY STUDY RESULTS AND DISCUSSION

k_{eff} AND BREEDING RATIO

For these parameters, selected total (energy integrated) sensitivities are given in Table III. The largest sensitivities are for heavy metals, and the five largest total sensitivity for k_{eff} and breeding ratio (BR) for this case and for a homogeneous reactor[4], are for the same reactions and have roughly the same values for the two reactors.

To obtain the standard deviation and correlation values from equations (4) and (6), we have included nuclear data sensitivities and covariances for the reactions indicated in Fig. 3. The heavy metal covariance data from an earlier study[4] includes most of the large sensitivities indicated in Table III and this data was supplemented with new covariance information[8] for other reactions.

The resulting standard deviations with and without k-reset are indicated in Table III. These values are slightly larger than those

reported for a homogeneous reactor,[4] for unadjusted cross section and COV data. It should be noted that if adjusted cross section and COV data presently being developed[18] were employed, the SD values would probably be reduced. This adjusted data incorporates integral experiment information, and a reduction of performance parameter uncertainties by using adjusted data has been demonstrated for a homogeneous LMFBR.[4]

POWER DENSITY SENSITIVITIES

Figure 4 shows results for the generalized importance function, Γ^*, for the ratio (point power density)/(total power), (PD), for the base case point of peak power, a location which can change with sigma changes, burn-up, etc. The base-case peak power occurs at a point in the outer driver zone, and Γ^* is strong positive near this point, decreasing and eventually becoming negative as the distance from this point increases. The strong negative region is the innermost driver zone, which strongly affects the denominator of PD.

Due to the complicated spatial and time-dependent nature of the peak value of the power density for a heterogeneous reactor, PD sensitivities are of interest at more than the point of maximum value for the base case. Considering the nature of the PD ($\vec{r}_p$) sensitivity, it is obvious that the volume integral of these sensitivities for all points in the reactor must be zero. Physically, it is clear that what causes an increased power density at one point will cause a decrease elsewhere, since the total power is constant. Thus, it is not surprising that for an isotope distributed fairly evenly throughout the reactor, i.e. U-235

and U-238, the PD σ_c and σ_s sensitivities for the inner and outer driver zone have opposite signs, as indicated in Table IV.

Since the PD sensitivities are space dependent, we have considered "near-range" (near the maximum PD in a particular driver zone) and "far-range" (between various driver zones) effects. Clearly the latter effects are strong, negating the possibility of determining a unique set of "peak power density sensitivities" for a particular design. For a power density which is fairly "flat" in the sense that the peak power in each driver zone is about the same, minor changes in the reactor design, control positioning, or nuclear data could shift the peak power from one driver zone to another. Thus it is clear that we should consider the sensitivities for at least three response functions, namely the PD at the point of peak power for each of the driver zones. Table IV gives these values at $\vec{r}_I$, $\vec{r}_M$ and $\vec{r}_O$ respectively.

The "near-range" spatial effects raise the question of whether a single set of sensitivities can be determined for each driver zone which are significant for the peak power density. The answer to this question is yes, with certain restrictions. The primary values given in Table IV are for the peak zonal PD mesh point, near the center of the associated driver zone and several centimeters to the right of the control channel. For the outer driver zone we also calculated sensitivities for the next radial mesh point, $\vec{r}_{O2}$, about 5 centimeters further toward the zone outer boundary. These calculations were performed both for the identical (base) reactor model and for a second model which had altered middle driver and internal blanket zone dimensions, such that the PD distribution was significantly different from that of the base model. The base

model results are given in Table IV, and the principal sensitivities were close to those for $\vec{r}_0$, indicating that the "near-range" effects are generally small near the extrema of the PD, and that these sensitivity values are fairly independent of the actual power distribution.

Obviously, PD($\vec{r}_p$) sensitivities for strongly localized nuclides, e.g. B^{10} (and to a lesser extent Na near a control channel) will be a strong function of the position of $\vec{r}_p$, even in the "near-range" sense. Furthermore, as the distance from the point of maximum PD is increased and the driver zone edge is approached, one would expect some of the sensitivities to change appreciably due to the proximity of the internal blanket. However, it is obvious that a point next to the edge of a driver zone is not significant for peak power investigations.

A more rigorous treatment of the peak power sensitivity would utilize a more detailed theory, which considers explicitly the spatial shift in the peak power due to "near-range" effects. Cacuci[19,20] has developed a sensitivity theory which treats extrema of functions, and he shows[20] that spatial shift effects in the extremum sensitivity are "second-order" in $\delta\sigma$. While these "second-order" effects may be significant for some special cases, it appears from the above results that the sensitivities of the PD at the base point of peak power are generally adequate to describe the peak PD uncertainty in each driver zone.

As would be expected, the PD sensitivities are particularly large for those reactions which influence the neutron transport between zones, e.g. U-238 σ_c. Also the PD sensitivities for other such data, e.g. Fe and O σ_s, can be equally or more important than many of the heavy metal reactions.

The VAR and SD values of the PD for the three driver zones were determined using the same nuclear data covariance information as those used for the k and BR values. Changes only of sensitivity signs from one zone to another will, of course, cancel out in the associated variances. As can be seen in Table IV, without k-reset the SD of the peak zone power density is calculated as 2.0%*, 1.1%*, and 1.8%* for the inner, middle, and outer drive zones respectively, reflecting the smaller sensitivities for the middle zone. With k-reset the corresponding values are __*, __*, and __* respectively.

To illustrate the previously discussed "short-range" and "long-range" PD correlation, we have applied equations (5) and (6) for the PD at the two points in the outer driver discussed previously, $\vec{r}_0$ and $\vec{r}_{02}$ and these in the inner and middle drivers, $\vec{r}_I$ and $\vec{r}_M$, yielding the following results* (without k-reset).

$$COR[PD(\vec{r}_I), PD(\vec{r}_0)] \equiv COR(\vec{r}_I, \vec{r}_0) = -0.98$$
$$COR(\vec{r}_0, \vec{r}_{02}) \approx +0.99$$
$$COR(\vec{r}_I, \vec{r}_M) = +0.99$$
$$COR(\vec{r}_0, \vec{r}_M) \approx -0.94$$

These results verify the previously discussed behavior of this response. Correlation values of +1 and -1 are limiting values for positive and negative correlation of uncertainties.

NEUTRON-GAMMA TRANSPORT EFFECTS AND ENERGY DEPOSIT

To study the effects of non-localized energy deposition, coupled (n, γ) transport calculations are necessary.[21] It has long been recognized that such transport effects are particularly significant in a heterogeneous core.

*(Preliminary or incomplete data; only H.M. COV included)

All calculations for this study were done for a 1-D cylindrical reactor model, using the discrete ordinates code XSDRN-PM.[14] Two sets of calculations were done in this study. The first was a diffusion theory calculation which made the common approximation that all liberated energy stems from fission and is deposited at the point of fission. The second calculation was a coupled (n,γ) run (S8-P3) which explicitly accounted for the transport of fission neutrons and gammas, as well as for that of secondary gammas generated by neutron capture and inelastic scatter. The spatial energy deposition of the neutrons and gammas was obtained by folding the fluxes with KERMA factors[10] from MACKLIB IV.[21]

Results* of these calculations indicate that for our CDS-type MOEC model, diffusion theory with the approximation of localized energy deposition underpredicts the power production in the internal blankets by 10% and overpredicts it in the driver zones by 2%, when compared to the more rigorous coupled (n,γ) calculation. At the point of peak power production, the diffusion theory power density results are 2% higher than those for coupled transport theory. At this point, the (n,γ) results for the energy deposited in the fuel-pellet materials is 98.5% of the total. Figure 5 shows the space dependent ratio of the energy deposition for the two calculations.

SUMMARY AND CONCLUSIONS

(a) For the heterogeneous LMFBR considered herein and a typical commercial-sized homogeneous reactor, the largest total sensitivities for k_{eff} and the breeding ratio are for the same reactions and have roughly the same values for the two reactors.

* Preliminary results; final results will be for corrected reactor model.

(b) For power density sensitivities, reactions which influence neutron transport between zones are proportionally more important than for the sensitivities of (a).

(c) "Near-range" changes to power density sensitivities near the zonal peak power location are small, while "~~long~~ far-range" changes between driver zones can be quite large. Thus, near-range correlation between point power densities is strongly positive, while for different zones the power densities can be strongly anti-correlated.

(d) Since in a heterogeneous core the peak power density can shift from one driver zone to another, a power density sensitivity must be considered for each driver zone. These "zone-peak" sensitivity values are fairly independent of the actual power distribution and of which zone contains the reactor peak power density.

(e) Coupled (n,γ) calculations and kerma factors can be effectively used to study the effects of non-localized energy deposition and to relate power density to linear power.

ACKNOWLEDGMENTS

The authors thank Dan Cacuci and Augusto Gandini for informative discussions on topics related to this ~~paper.~~ research. Julia Rankin did an excellent job of typing the paper. This research was sponsored by the U.S. Department of Energy under Contract No. W-7405-eng-26 with the Union Carbide Corporation.

REFERENCES

1. S. M. DAVIES, R. E. MURATA, and B. TALWAR, Trans. Am. Nucl. Soc., 34, (1980).

2. A. GANDINI, J. Nucl. Energy, 21, 755 (1967).

3. G. P. CECCHINI AND M. SALVATORES, Nucl. Sci. Eng., 46, 304 (1971).

4. J. H. MARABLE and C. R. WEISBIN, "Uncertainties in the Breeding Ratio of a Large LMFBR," in E. G. Silver, Ed., Advances in Reactor Physics, CONF-780401, U. S. Dept. of Energy, p. 231 (1978).

5. J. H. MARABLE, C. R. WEISBIN, and G. DE SAUSSURE, Nucl. Sci. Eng., 75, 30 (1980).

6. C. R. WEISBIN et al., Sensitivity and Uncertainty Analysis of Reactor Performance Parameters, Advances in Nuclear Science and Technology, Plenum Press, Vol. 14 (1980).

7. J. D. DRISCHLER and C. R. WEISBIN, "Compilation of Multigroup Cross Section Covariance Matrices for Several Important Reactor Materials," ORNL-5318 (ENDF-235), Oak Ridge National Laboratory (1977).

8. PUFF-II Reference.

9. J. C. CHANDLER et al., "The Proliferation Resistant Preconceptual Core Design Study," TC-1082, Hanford Engineering Development Laboratory (1978).

10. M. A. ABDOU and C. W. MAYNARD, Nucl. Sci. Eng., 56, 360 (1975).

11. R. PROTSIK, General Electric-Sunnyvale, Private Communication (1971).

12. C. L. COWAN and C. S. RUSSELL, "FUMBLE-II: A Fast Reactor Fuel Management and Burnup Code with an Influence Function Option for Predicting the Three-Dimensional Effects of Control Rod Movements," GEAP-14138, General Electric-Sunnyvale (1976).

13. Vitamin-C reference.

14. N. M. GREENE et al., AMPX: A Modular Code System to Generate Coupled Multigroup Neutron-Gamma Cross Sections from ENDF/B, ORNL/TM-3706, (1976).

15. D. R. VONDY, T. B. FOWLER, and G. W. CUNNINGHAM, "VENTURE," ORNL-5062/R1, Oak Ridge National Laboratory (1977).

16. J. R. WHITE, "The Development, Implementation, and Verification of Multicycle Depletion Perturbation Theory for Reactor Burnup Analysis, ORNL/TM-7305, Oak Ridge National Laboratory (1980).

17. J. LUCIUS et al., "A User's Manual for the FORSS Sensitivity and Uncertainty Analysis Code System," ORNL-5316, Oak Ridge National Laboratory (1980).

18. J. J. WAGSCHAL et al., "ORACLE: An Adjusted Cross Section and Covariance Library for Fast Reactor Analysis," these procedings.

19. D. G. CACUCI et al., "Developments in Sensitivity Theory," these proceedings.

20. D. G. CACUCI, "Sensitivity Theory of Nonlinear Systems, II. Extensions to Additional Classes of Responses," ORNL/TM-7511, Oak Ridge National Laboratory (to be published).

21. "American National Standard for the Determination of Thermal Energy Deposition Rates in Nuclear Reactors," ANS-19.3.4, ANSI N676-1976, American Nuclear Society, 1976.

22. Y. GOHAR and M. A. ABDOU, "MACK-IV," ANL/FPP/TM-106, Argonne National Laboratory," (1978).

GENERAL ELECTRIC

(CLC) TABLE I

General Design Parameters & Calculated
Performance Parameters for a CDS-Type
LMFBR Heterogeneous Core

Design Parameters

Core Height (cm)	101.6
Core Effective Outer Radius (cm)	166.8
Axial Blanket Thickness (cm)	35.6
Radial Blanket Thickness (cm)	34.2
Number of Assemblies	
Driver Fuel	300
Inner Blanket	115
Radial Blanket	204
Control	30
Assembly Pitch (cm)	15.06
Pin Diameter (cm) - Driver Fuel/Blankets	0.6985/1.118
Clad Thickness (cm) - Driver Fuel/Blankets	0.03683/0.03556
Smeared Fuel Density (%TD) - Driver Fuel/Blankets	86.5/93.3
Refueling Interval (Days)	365
Fuel and Internal Blanket Residence Time (Days)	730
Capacity Factor (%)	80

Performance Parameters

Total Power (MW_{th})	2540
Loaded Fissile Enrichment (%)	17.7
Average Breeding Ratio	1.35
Doubling Time, CSDT (years)	17
Average Discharge Driver Burnup (MWD/MT)	58,600

(JMK) Table II. Approximate Nuclide Densities, Principal Constituents of CDS-Type Reactor Model, Fig. 2. [10^{21} atoms/cc] [a]

NUCLIDE	CF	IB	AB over CF	AB over IB	RB	Prim. CTL Out	Second CTL Out	Prim. CTL In	Second CTL In
U238	6.75	12.4	9.58	12.6	12.6				
PU239	1.33	2.4-1	5.1-2	7.5-2	1.0-2				
PU240	4.4-1	7.8-3	4.1-4	7.2-4	2.0-4				
PU241	1.8-1	1.9-4							
PU242	5.4-2								
U235	1.2-2	2.1-2	1.8-2	2.4-2	2.3-2				
FP PAIRS	2.6-1	5.4-2	5.1-3	6.3-3	1.3-2				
O	18.1	25.4	↑	↑	↑				
NA	8.2	6.1	As CF	As IB	As IB	20.8	19.6	8.5	8.9
FE	11.9	9.6				3.7	6.7	17.8	18.4
CR	2.4	2.0				7.5-1	1.4	3.6	3.7
NI	2.8	2.2	↓	↓	↓	8.7-1	1.6	4.2	4.3

NUCLIDES FOR	CTL IN	CTL IN ONLY
B10	13.3	11.7
B11	2.3	2.0
C	7.2	6.4

a) CF, IB, AB, RB and CTL signify driver, internal blanket, axial blanket, radial blanket and control zones, respectively.

(JMIC) Table III. Standard Deviations (SD) and Selected Total Relative Sensitivities for k_{eff} and Breeding Ratio (BR). All values in %.

Nuclide, Reaction		k_{eff}	BR[a]
U235	ν	+0.9	+0.4
	σ_f	+0.7	−1.3
	σ_c	b	−0.6
U238	ν	+12.4	+1.8
	σ_f	+7.7	+1.1
	σ_c	−21.9	+75.6
	σ_s	−3.1	−0.4
Pu239	ν	+69.1	−1.3
	σ_f	+50.1	−66.8
	σ_c	−4.9	−17.4
	σ_s	−2.5	−0.3
Pu240,	ν	+5.1	−0.3
	σ_f	+3.5	−0.2
	σ_c	−1.5	+4.7
Pu241,	ν	+12.0	−0.6
	σ_f	+8.8	−11.2
	σ_c	+0.6	−1.9
Pu242	ν	+0.5	b
	σ_f	+0.3	b
	σ_c	−0.2	b
Na	σ_c	−0.2	b
	σ_s	−0.6	−3.3
O	σ_s	−3.7	−0.2
Fe	σ_c	−1.2	−0.5
	σ_s	−0.7	−2.5
Cr	σ_c	−0.5	−0.3
	σ_s	b	−1.0
Ni	σ_c	−0.5	−0.3
	σ_s	b	−1.4
SDC		3.2%	7.1% *
SD(k reset by enrichment)			3.3% *

a) Convert BR to k-reset values by adding 1.73 x k sensitivity.
b) Values $\leq 10^{-3}$
c) SD values calculated from COV and sensitivities of Fig. 3.

* preliminary values (only w/ H.M. COV)

Table IV. Standard Deviations (SD) and Selected Total Relative Sensitivities for Mid-plane Power Density, $PD(\vec{r}_p)$, at points of zone Peak Power (r_I, r_M, r_O for inner, middle, and outer driver zone, respectively). All values in %.

Nuclide, Reaction		$PD(r_I)$[a]	$PD(r_M)$ *[a]	$PD(r_O)$[a]	$PD(r_{O2})$[c]
U235	ν	+ 1.6	+ 0.3	− 1.1	+ 1.2
	σ_f	− 0.6	− 0.7	− 1.7	+ 1.8
U238	ν	+5.7	+ 2.3	− 5.9	− 6.5
	σ_f	− 1.4	− 4.3	− 6.6	− 6.4
	σ_c	− 26.2	− 14.4	+ 24.0	+ 26.8
	σ_s	− 22.7	− 6.1	+ 21.1	+ 23.6
Pu239	ν	b	b	+ 2.0	+ 2.1
	σ_c	− 3.4	− 1.3	+ 1.2	+ 1.4
	σ_s	b	b	+ 1.5	+ 1.6
Pu240	ν	− 4.0	− 1.4	+ 2.7	+ 3.0
	σ_c	− 2.0	b	+ 2.7	+ 3.1
Pu241	ν	− 2.4	− 1.0	+ 2.0	+ 2.2
	σ_f	b	+ 1.5	+ 2.7	+ 2.2
N/a	σ_s	b	b	+ 6.7	+ 6.7
O	σ_s	− 24.4	− 7.1	+ 18.7	+ 21.3
Fe	σ_c	− 1.0	b	+ 1.0	+ 1.0
	σ_s	− 7.5	− 1.8	+ 10.4	+ 11.2
SD[d]		2.0 *	1.1 *	1.8 *	
SD (k-reset by enrichment)					

* = Prelim. values!

a) Convert *PD to k-reset values by subtracting 0.392x ___, ___, and .392x ___ k sensitivities. for r_I, r_M, and r_O, respectively.

b) Value < 1% c) Point 5 cm to right of r_O — see text.

d) SD calculated from COV and sensitivities of Figure 3

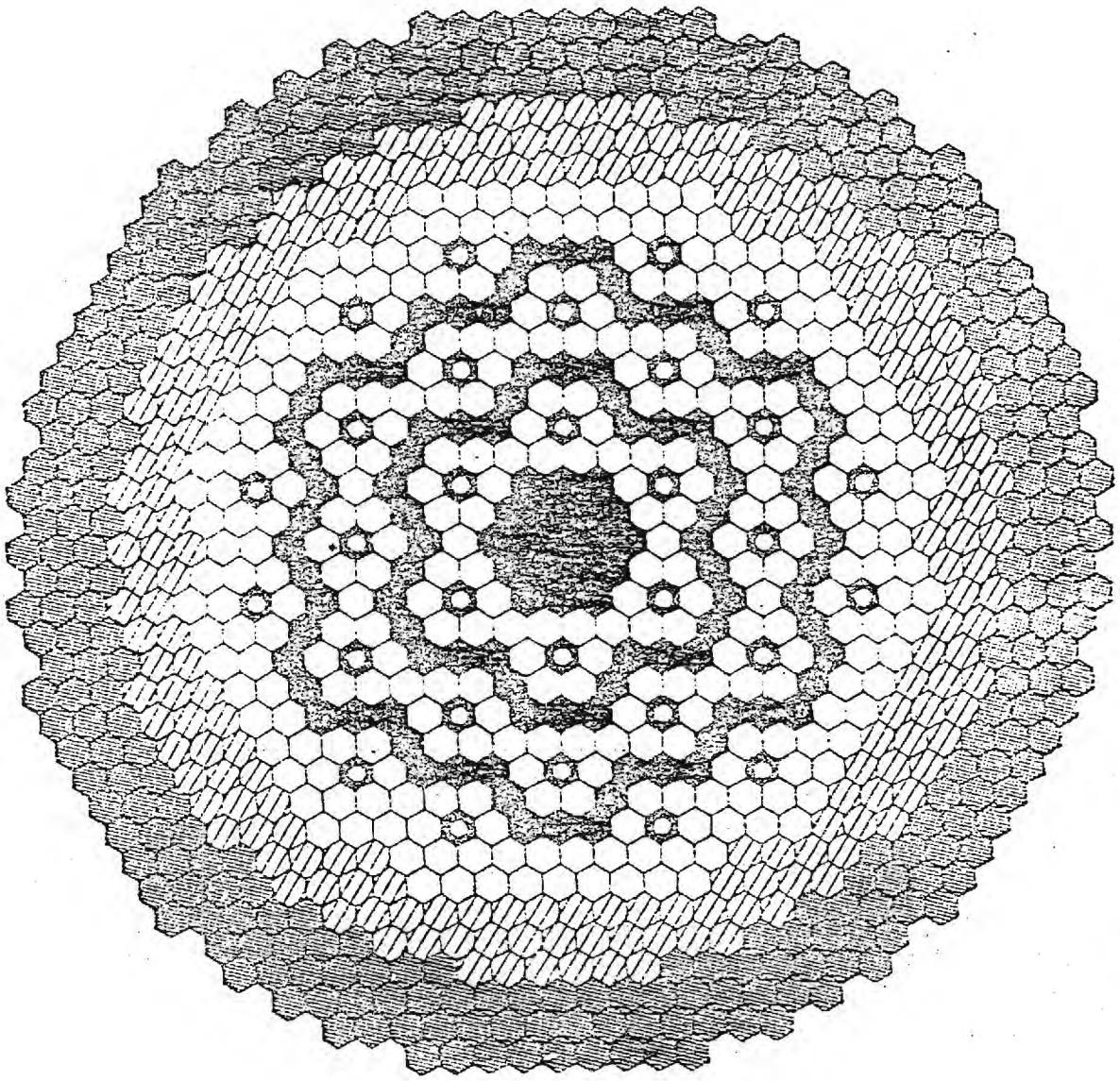

(CLC)

Figure 1

Core and Blanket Layout for a ~~Typical~~ Heterogeneous Core

CDS - Type

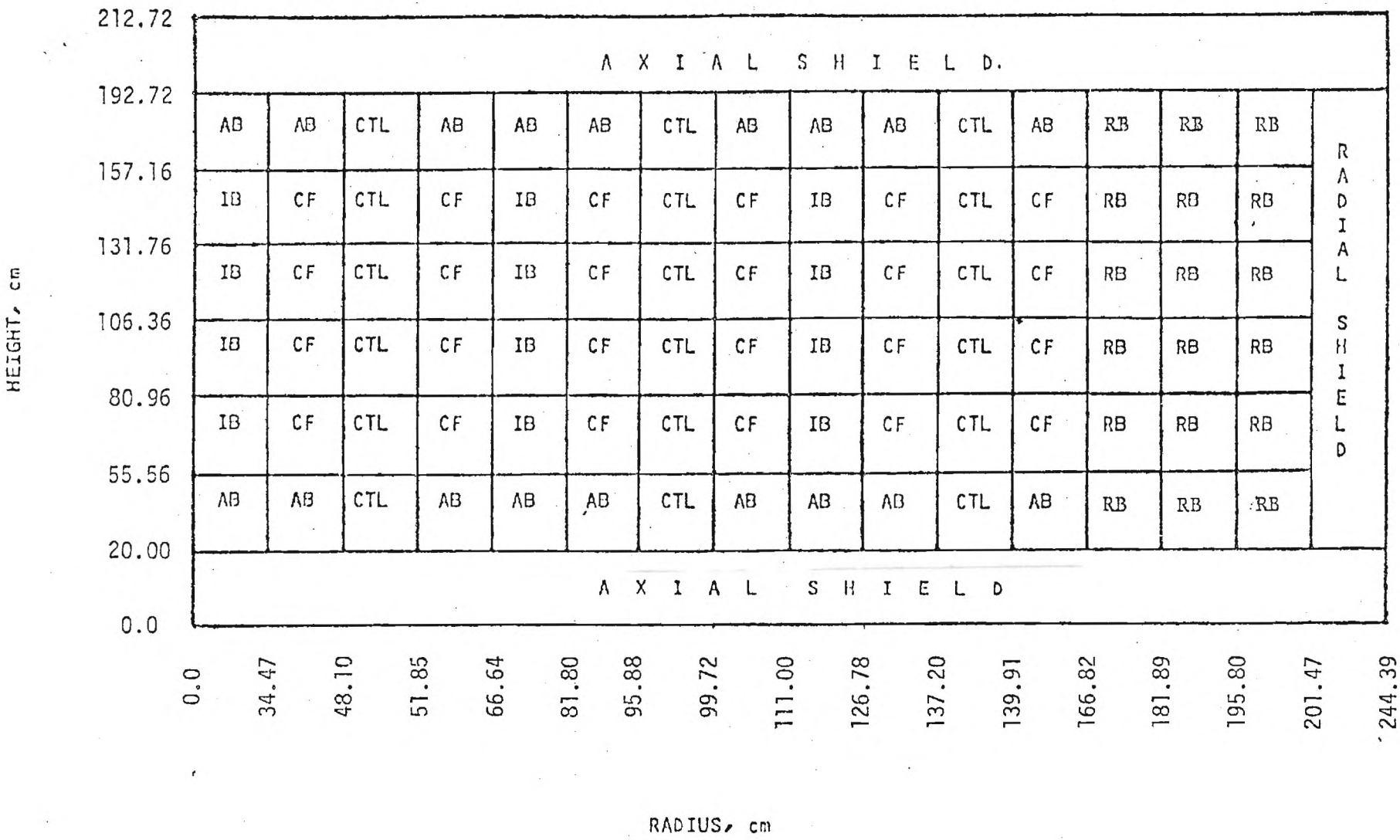

Fig 2- Region Map of a ~~Typical~~ COS-Type Heterogeneous Core

(CLC) Basis for Fig. 2. Please simplify, e.g. eliminate subzones; also possibly eliminate shield & 1/2 reactor!

	25f	25c	25ν	28f	28c	28ν	49f	49c	49ν	40c	41f	41c	41ν
25f	X	X		X	X		X	X			X		
25c	X	X		X	X		X	X					
25ν			X			X			X				X
28f	X	X		X	X		X	X			X		
28c	X	X		X	X		X	X					
28ν			X			X			X				X
49f	X	X		X	X		X	X			X		
49c	X	X		X	X		X	X					
49ν			X			X			X				X
40c										X			
41f	X			X			X				X		
41c												X	
41ν			X			X			X				X

Figure 3.

~~TABLE 6~~

COVARIANCE MATRIX PARTITIONS FOR DETERMINING INTEGRAL PARAMETER VARIANCES

(JHM) Basis for Fig. 3 - to be extended

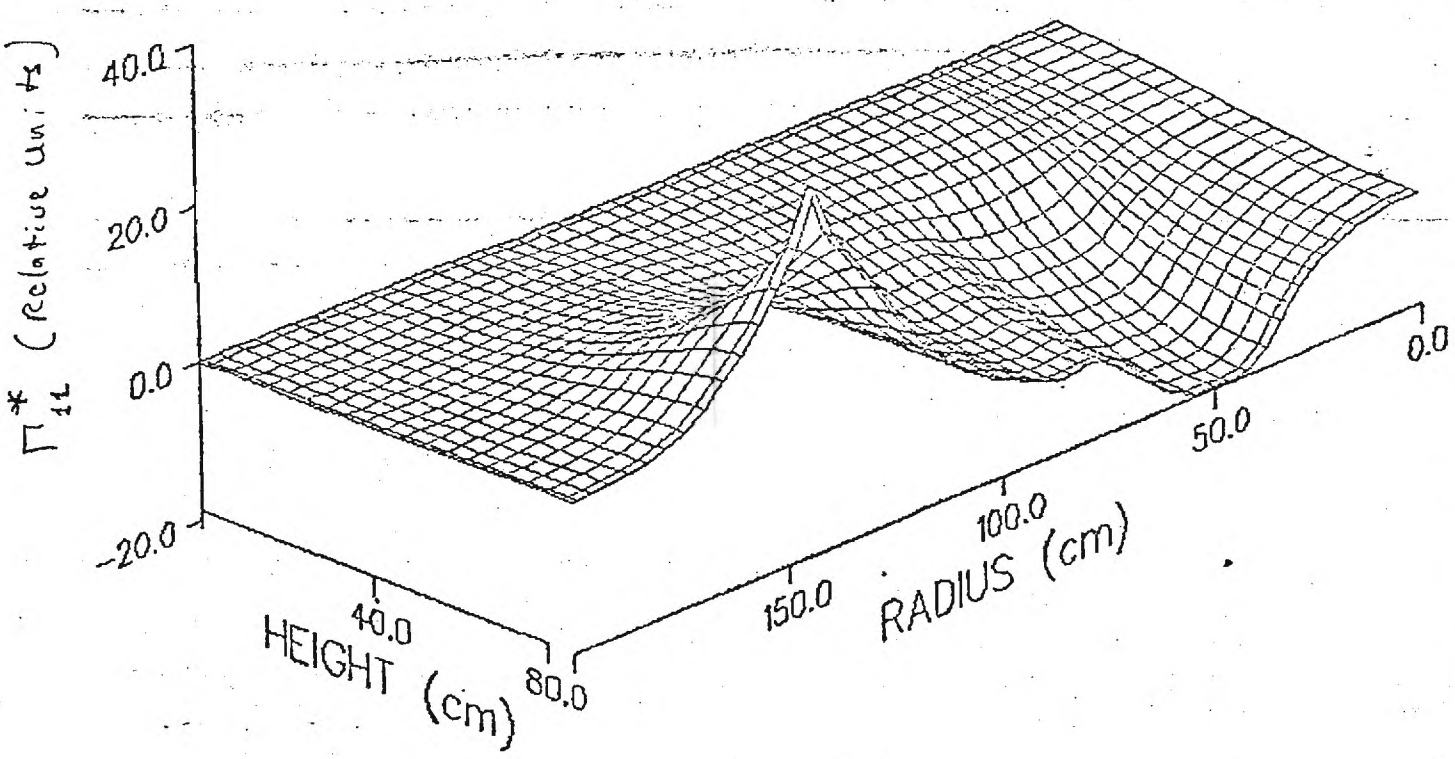

(JHM)

Fig. 4 Peak-power density generalized adjoint Γ* for energies 67-111 keV in the lower half of the heterogeneous reactor model.

(MLW) Fig 5. Comparison of diffusion theory and (n,γ) calculation results for r-dependent energy deposit.

SCHOOL OF NUCLEAR ENGINEERING E-26-B01

Atlanta, Georgia 30332 (404) 894-3720

September 30, 1980

MEMORANDUM

TO: C. R. Weisbin, J. H. Marable, and M. L. Williams (ORNL)

FROM: J. M. Kallfelz and D. Biswas

SUBJECT: Progress Report for ORNL Subcontract 7802, Period September 1-30, 1980

Accomplishments and Highlights

- Top priority was given to completing the paper[1] describing our joint analysis of the CDS reactor. This paper was presented at the Sun Valley ANS Topical Meeting, and is attached as the body of this report.

- J. Kallfelz attended a meeting organized by C. R. Weisbin at Sun Valley concerning uncertainty analysis applications.[2] A significant result was Hemmig's agreement to promote the formation of a "sensitivity users group".

- Planning has been initiated for further analysis of the Phenix reactor, using ENDF/B-V cross sections. In particular, we have discussed with Chuck Wilson of Westinghouse the use of this analysis to substantiate the value of the uncertainty for the calculated CRBR breeding ratio.

Plans for Work for Next Month

- We will visit ORNL to make plans for further work on the CDS analysis.[1] In particular, we will consider a similar analysis which utilizes the ENDF/B-V-based adjusted cross section and covariance data of ORACLE.[3] After consultation with GE this work will be initiated.

- We will attend an October 9 meeting with Westinghouse staff members at Oak Ridge to discuss the applicabiity of the Phenix analysis and ORNL uncertainty analysis methods to CRBR problems. Tentatively, J. Kallfelz has responsibility for the overall presentation, and J. Marable will provide the necessary information on the potential application of time-dependent sensitivity studies and adjusted cross sections to these problems. The outcome of this meeting will determine the direction and effort to be devoted to Phenix analysis next month.

References

1. J. M. Kallfelz, D. Biswas, C. L. Cowan, J. H. Marable, M. L. Williams, C. R. Weisbin, J. D. Drischler, T. B. Fowler, and J. R. White, "Design and Sensitivity Analysis of a CDS-Type LMFBR Heterogeneous Core," Paper presented at ANS Topical Meeting 1980, Advances in Reactor Physics and Shielding, September 14-17, 1980.

2. C. R. Weisbin, "Trip Report for ANS Topical Meeting on Reactor Physics and Shielding," Sun Valley, Idaho, September 14-18, 1980.

3. J. J. Wagschal et al., "ORACLE: An Adjusted Cross Section and Covariance Library for Fast Reactor Analysis," Paper presented at ANS Topical Meeting 1980, Advances in Reactor Physics and Shielding, September 14-17, 1980.

DESIGN AND SENSITIVITY ANALYSIS OF A CDS-TYPE HETEROGENEOUS CORE

J. M. Kallfelz and D. Biswas
Georgia Institute of Technology
Atlanta, Georgia 30332

C. L. Cowan
General Electric Company
Sunnyvale, California 94086

J. H. Marable, M. L. Williams, C. R. Weisbin
J. D. Drischler, T. B. Fowler, and J. R. White
Oak Ridge National Laboratory
Oak Ridge, Tennessee 37830

ABSTRACT

The design of a heterogeneous LMFBR of the type being considered for the Conceptual Design Study (CDS) is analyzed, using sensitivity analysis methods. Nuclear data sensitivities for k_{eff}, the breeding ratio, and parameters related to the peak linear power (space-dependent power densities) are determined with generalized perturbation theory. These sensitivities are folded with extensive nuclear data covariance information to determine the associated integral parameter uncertainties and correlations. The effects of non-localized energy deposition were investigated by folding the results of coupled $(n-\gamma)$ calculations with kerma factors.

INTRODUCTION

The development of the Conceptual Design Study (CDS) reactor plant[1] was intended to provide direction and focus to the LMFBR technology programs, and the research and development needs for these programs will be outlined in the final report to Congress by DOE after April, 1981. The joint work reported in this paper involved a cooperative effort by university, vendor, and national laboratory staff, with the principal goal of investigating the uncertainties of some significant reactor performance parameters.

To accomplish this aim we utilized both direct perturbations and the methods of generalized perturbation theory,[2-6] together with nuclear data covariance information[4-8] which has become available in the last few years. Several of the performance parameters considered, namely k_{eff} and the breeding ratio, have been the object of a similar study[4,5] for a homogeneous LMFBR, thus allowing comparison of the importance of various nuclear data to these parameters for the two reactor types.

We have placed particular emphasis on studies related to the peak linear power. Reduction of uncertainty in this parameter has obvious importance both for licensing and economic considerations, and considerable attention has been devoted in recent studies[9] to determining the maximum allowable value of this quantity. For sensitivity calculations we considered the power density with diffusion theory, but we have investigated the effects of non-localized energy

deposition by performing coupled (n-γ) calculations and folding the results with kerma factors.[10] In the following sections we discuss the design and typical configuration of the CDS reactor, and the methods and results of our sensitivity analysis.

GENERAL REACTOR DESCRIPTION

The key design parameters for a large heterogeneous LMFBR of the 1000 MWe class were specified as part of the DOE sponsored CDS project. The design objectives and criteria for the CDS project emphasized the following:

1. High reliability,
2. Near term design features (components that can be developed within five years),
3. Sufficiently low sodium void worth to preclude hypothetical core disruptive accidents from consideration as design basis accidents,
4. Breeding of fissile fuel at a rate equivalent to a compound system doubling time of twenty years or less, and
5. Allowances for the future accomodation of advanced fuels.

On the basis of the above objectives, the CDS Reference Design was chosen to be a 2540 MW_{th}, mixed plutonium uranium oxide, heterogeneous reactor with three driver fuel zones and three inner blanket zones. The core layout for the Reference Design is shown in Fig. 1, and a summary of the principal core design and performance parameters is given in Table I. All design calculations discussed in this section were carried out in linked r-z and x-y triangular mesh geometry using the two-dimensional diffusion theory code SN2D[11] and the fuel management and burnup code FUMBLE,[12] and cross sections based on ENDF/B-V data.

The fuel pin diameter for the CDS Reference Design was selected on the basis of earlier sensitivity studies to give near-optimum breeding and economic performance for the heterogeneous core. The fuel pins are clad with the austenitic stainless steel alloy, D9, with material properties which closely resemble those of 20% CW316 SS. However, on the basis of available data the irradiation induced creep and swelling are expected to be significantly lower for the D9 alloy.

The core layout as shown in Fig. 1 was specified to minimize the peak radial power throughout the operating cycle based upon a single fissile enrichment for the supplied fuel in all driver fuel regions. The twelve burnup control rods in the outer driver fuel zone are also utilized to shape the radial power profile during reactor operations.

Reactor shutdown of the CDS Design is accomplished by each of two independent control systems. The primary control system consists of 21-24 natural boron carbide rods, including 12 rods in the outer control ring for burnup reactivity adjustments. The secondary control system consists of 6-9 enriched boron carbide rods which are distributed in the inner and middle control rings. The final requirements for the two independent systems will be determined in follow-up studies and will include an assessment of control reliability requirements.

SENSITIVITY STUDIES MODEL AND DATA

For the sensitivity studies we used an MOEC design characteristic of those being considered for the CDS, henceforth referred to as the basic model. This r-z model is shown in Fig. 2, while Table II describes the composition of the principal regions. The shield was not included in our calculations, and

control in the outer control ring was inserted to achieve criticality for the model.

The further reported results were calculated with the ENDF/B-IV cross section set of 32 groups used in Refs. 4 and 5, unless noted otherwise. We also generated ENDF/B-IV cross sections for the CDS-type reactor from the 171 neutron group Vitamin-C library.[13] Resonance shielding for both the blanket and driver zones was done with the BONAMI module of the AMPX system.[14] For further sensitivity calculations, the 171 group cross sections were collapsed to 32 groups using fluxes obtained from a 1-D, cylindrical XSDRN-PM[14] transport calculation (S4P1) of the reactor. Sensitivity results for the two 32 group cross section sets were practically the same.

UNCERTAINTY ANALYSIS THEORY AND METHODS

Using the methods of generalized perturbation theory,[2-6] the group-dependent nuclear data sensitivity $(\partial I/I)/(\partial \sigma_i / \sigma_i)$ of integral parameter I has been studied for two parameters considered in earlier works,[4,5] namely k_{eff} and the breeding ratio, as well as ratios significant for determining the uncertainty in the calculated peak linear power. For sensitivity values involving the criticality constraint, "k-reset"[4-6] has been performed by altering the driver zone "plutonium enrichment", i.e., (total Pu)/(total heavy metal), as in previous studies.[4,5] Perturbation theory results were checked by direct perturbation calculations performed at General Electric, ORNL, and Georgia Tech.

Generalized perturbation theory[2-6] provides a method of calculating a generalized adjoint function, $\vec{\Gamma}^*(\vec{r})$, where $\Gamma_j^*(\vec{r})$ is the importance of a neutron in energy group j at space point $\vec{r}$ to the ratio being considered. We have incorporated in VENTURE[15] the capability to generate $\vec{\Gamma}^*$ for the ratio of point power density to total power (PD):

$$PD\ (\vec{r}_p) = \frac{a_1}{a_2} = \frac{\sum_j \Sigma_{1j}\ (\vec{r}_p)\ \phi_j\ (\vec{r}_p)}{\int_{reactor} \sum_j \Sigma_{2j}\ (\vec{r})\ \phi_j\ (\vec{r})\ d\vec{r}} \qquad (1)$$

Considering only fission energy and assuming localized energy deposit, the Σ_{ij} have the form:

$$\Sigma_{ij}\ (\vec{r}) = \sum_k p^k\ \Sigma^k_{f,j}(\vec{r}) \qquad (2)$$

and p^k is the total energy release per fission in the k-th isotope.

Thus, the fixed source in the equation for $\vec{\Gamma}^*$ for PD $(\vec{r}_p)$ has the form:

$$S^*_j\ (\vec{r}) = \Sigma_{1j}(\vec{r})/a_1 - \Sigma_{2j}(\vec{r})/a_2 \qquad (3)$$

where Σ_{1j} is zero for $\vec{r} \neq \vec{r}_p$.

To determine the uncertainty of an integral parameter, I, one can calculate its variance (VAR):

$$VAR\ (I) = \sum_{i,j} \frac{\partial I}{\partial \sigma_i} \frac{\partial I}{\partial \sigma_j}\ COV\ (\sigma_i, \sigma_j) \qquad (4)$$

The nuclear data covariance files (COV) contain information on both the standard deviation, (SD), and correlation of various cross sections.[4-6] To obtain a reliable estimate of $SD(I) = \sqrt{VAR(I)}$, equation (4) should include all data which have a significant impact on I.

Due to the space-dependent nature of the PD sensitivities, which we will discuss in the following section, a parameter of particular interest is the covariance of two integral parameters:

$$COV\ (I_1,\ I_2) = \sum_{i,j} \frac{\partial I_1}{\partial \sigma_i} \frac{\partial I_2}{\partial \sigma_j}\ COV\ (\sigma_i,\ \sigma_j) \qquad (5)$$

The correlation (COR) between I_1 and I_2 is expressed more explicitly by:

$$COR(I_1,I_2) = COV(I_1,I_2)/[SD(I_1)\ SD(I_2)] \qquad (6)$$

S* of equation (3) can be calculated by VENTURE and DEPTH.[16] The latter code was used to process the $\vec{\Gamma}^*$ and $\vec{\phi}$ files from VENTURE to determine the sensitivities. For all reported sensitivities, σ_t was treated as dependent, i.e. a perturbation in one of the partial cross sections had an associated $\delta\sigma_{tr}$. This convention will not influence the VAR values if consistent $COV(\sigma_i,\sigma_j)$ data are used in equation (5).

SENSITIVITY STUDY RESULTS AND DISCUSSION

k_{eff} AND BREEDING RATIO

For these parameters, selected total (energy integrated) sensitivities are given in Table III. The largest sensitivities are for heavy metals, and the five largest total sensitivities for k_{eff} and breeding ratio (BR) for this case and for a homogeneous reactor[4], are for the same reactions and have roughly the same values for the two reactors.

To obtain the standard deviation and correlation values from equations (4) and (6), we have included nuclear data sensitivities and covariances for the reactions indicated in Fig. 3. The primary source of covariance data was the ORNL evaluation,[7] based for the most part on ENDF/B-IV, which was used and discussed in earlier studies.[4,5] For reactions not included in this source, new covariance information[8] was employed. The quality of covariance information is being scrutinized in another study.[18]

The resulting standard deviations for the indicated parameters are:

k_{eff}: 3.2% BR: 7.1% BR(with k-reset): 3.3%

These results can be compared to corresponding values (in the same order) of 2.0%, 6.1%, and 3.1% reported for a homogeneous reactor,[4] for unadjusted cross section and COV data. It should be noted that if adjusted cross section and COV data presently being developed[18] were employed, the SD values would probably be reduced. This adjusted data incorporates integral experiment information, and a reduction of performance parameter uncertainties by using adjusted data has been demonstrated for a homogeneous LMFBR.[4]

POWER DENSITY SENSITIVITIES

General Nature of PD Sensitivities

We refer to the use of the basic reactor model and unperturbed cross sections as the "base case". Figure 4 shows results for the generalized importance function $\vec{\Gamma}^*$ for PD, for the base case point of peak power, a location which can change with sigma changes, burn-up, etc. The base-case peak power occurs at a point in the outer driver zone, and $\vec{\Gamma}^*$ is strong positive near this point, decreasing and eventually becoming negative as the distance from this point increases. The strong negative region is the innermost driver zone, which strongly affects the denominator of PD.

Due to the complicated spatial and time-dependent nature of the peak value of the power density for a heterogeneous reactor, PD sensitivities are of interest at more than the point of maximum value for the base case. Considering the nature of the PD ($\vec{r}_p$) sensitivity, it is obvious that the volume integral of these sensitivities for all points in the reactor must be zero. Physically, it is clear that what causes an increased power density at one point will cause a decrease elsewhere, since the total power is constant. Thus, it is not surprising that for an isotope distributed fairly evenly throughout the reactor, i.e. U-238, the PD σ_c and σ_s sensitivities for the inner and outer driver zone have opposite signs.

Space Dependent PD Sensitivities: Results and Discussion

Since the PD sensitivities are space dependent, we have considered "near-range" (near the maximum PD in a particular driver zone) and "far-range" (between various driver zones) effects. Clearly the latter effects are strong, negating the possibility of determining a unique set of "peak power density sensitivities" for a particular design. For a power density which is fairly "flat" in the sense that the peak power in each driver zone is about the same, minor changes in the reactor design, control positioning, or nuclear data could shift the peak power from one driver zone to another. Thus it is clear that we should consider the sensitivities for at least three response functions, namely the PD at the point of peak power for each of the driver zones. Table IV gives these values at radii of r_I, r_M and r_O in the core mid-plane.

The "near-range" spatial effects raise the question of whether a single set of sensitivities can be determined for each driver zone which are significant for the peak power density. The answer to this question is yes, with certain restrictions. The primary values given in Table IV are for the peak zonal PD mesh point, near the center of the associated driver zone and several centimeters to the right of the control channel. For the outer driver zone we also calculated sensitivities for the next radial mesh point, r_{02}, about 5 centimeters further toward the zone outer boundary. These calculations were performed both for the basic reactor model and for a second model which had altered middle driver and internal blanket zone dimensions, such that the PD distribution was significantly different from that of the basic model. The results for the basic model are given in Table IV, and for both models the principal sensitivities at r_{02} were close to those for the basic model at r_O. This indicates that the "near-range" effects are generally small near the extrema of the PD, and that these sensitivity values are fairly independent of the actual power distribution.

Obviously, PD($\vec{r}_p$) sensitivities for strongly localized nuclides, e.g. B^{10}, will be a strong function of the position of $\vec{r}_p$, even in the "near-range"

sense. Furthermore, as the distance from the point of maximum PD is increased and the driver zone edge is approached, one would expect some of the sensitivities to change appreciably due to the proximity of the internal blanket. However, it is obvious that a point next to the edge of a driver zone is not significant for peak power investigations.

A more rigorous treatment of the peak power sensitivity would utilize a more detailed theory, which considers explicitly the spatial shift in the peak power due to "near-range" effects. Cacuci[19,20] has developed a sensitivity theory which treats extrema of functions, and he shows[20] that spatial shift effects in the extremum sensitivity are "second-order" in $\delta\sigma$. While these "second-order" effects may be significant for some special cases, it appears from the above results that the sensitivities of the PD at the base case point of peak power are generally adequate to describe the peak PD uncertainty in each driver zone.

As would be expected, the PD sensitivities are particularly large for those reactions which influence the neutron transport between zones, e.g. U-238 σ_c. Also the PD sensitivities for other such data, e.g. Fe and O σ_s, can be larger than for many of the heavy metal reactions.

PD Standard Deviations and Correlations

For the points of peak zone PD at mid-plane radii of r_I, r_M, and r_O for the inner, middle, and outer driver zones respectively, as well as the previously discussed second point in the outer driver at r_{O2} near r_O, VAR and SD values of the PD were determined using the same nuclear data covariance information as that used for the k_{eff} and BR values. Changes only of sensitivity signs from one zone to another will, of course, cancel out in the associated variances. Without k-reset, the resulting SD values for PD at the indicated points are:

r_I: 2.2% r_M: 1.0% r_O: 2.1% r_{O2}: 2.3%

These values reflect the smaller sensitivities for the middle zone. With k-reset the values for the outer and inner zones were increased somewhat. E.g., for the location of peak reactor power density, r_O, the corresponding SD value with k-reset is 2.6%.

To illustrate the previously discussed "near-range" and "far-range" PD correlation, we have applied equations (5) and (6) for the PD at the points discussed above, yielding the following values (without k-reset) of COR [PD(r_1), PD(r_2)] for the indicated points:

r_I, r_O: − 0.97 r_I, r_M: + 0.99

r_O, r_{O2}: + 1.00 r_O, r_M: − 0.94

These results verify the previously discussed behavior of this response. Correlation values of +1 and −1 are limiting values for positive and negative correlation of uncertainties.

NEUTRON-GAMMA TRANSPORT EFFECTS AND ENERGY DEPOSIT

To study the effects of non-localized energy deposition, coupled (n, γ) transport calculations are necessary.[21] It has long been recognized that such transport effects are particularly significant in a heterogeneous core.

All calculations for this study were done for a 1-D cylindrical version of the basic reactor model with critical axial buckling, using the discrete ordinates code XSDRN-PM,[14] and coupled data created by merging 36 group VITAMIN-C gamma cross sections with the 171 group neutron data discussed earlier. Two

sets of calculations were done in this study. The first was a diffusion theory calculation which made the common approximation that all liberated energy stems from fission and is deposited at the point of fission. The second calculation was a coupled (n, γ) run (S8-P3) which explicitly accounted for the transport of fission neutrons and gammas, as well as for that of secondary gammas generated by neutron capture and inelastic scatter. The spatial energy deposition of the neutrons and gammas was obtained by folding the fluxes with kerma factors[10] from MACKLIB IV.[22]

Results of these calculations indicate that for our CDS-type MOEC model, diffusion theory with the approximation of localized energy deposition underpredicts the fraction of the reactor power produced in the internal blankets by 8 % and overpredicts this fraction for the driver zones by 2 %, when compared to the more rigorous coupled (n, γ) calculation. The diffusion theory result for the peak to total power ratio is 1 % higher than that for coupled transport theory. At the point of peak power, the (n, γ) results for the energy deposited in the fuel-pellet materials is 98.5 % of the total energy deposition at that point.

SUMMARY AND CONCLUSIONS

(a) For the heterogeneous LMFBR considered herein and a typical commercial-sized homogeneous reactor, the five largest total sensitivities for k_{eff} and the breeding ratio are for the same reactions and have roughly the same values for the two reactors.

(b) For power density sensitivities, reactions which influence neutron transport between zones are proportionally more important than for the sensitivities of (a).

(c) "Near-range" changes to power density sensitivities near the zonal peak power location are small, while "far-range" changes between driver zones can be quite large. Thus, near-range correlation between point power densities is strongly positive, while for different zones the power densities can be strongly anti-correlated.

(d) In a heterogeneous core the calculated peak power density can shift from one driver zone to another due to input data and operational changes. Thus a power density sensitivity must be considered for each driver zone of the design being studied. These "zone-peak" sensitivity values vary considerably for different zones, but are fairly invariant for different realistic power density spatial distributions.

(e) Coupled (n, γ) calculations and kerma factors can be effectively used to study the effects of non-localized energy deposition and to relate power density to linear power.

ACKNOWLEDGMENTS

The authors thank Dan Cacuci and Augusto Gandini for informative discussions on topics related to this research. Julia Rankin did an excellent job of typing this paper. This research was sponsored by the U.S. Department of Energy under Contract No. W-7405-eng-26 with the Union Carbide Corporation.

REFERENCES

1. S. DAVIES, R. MURATA, and B. TALWAR, Trans. Am. Nucl. Soc, 34, (1980).

2. A. GANDINI, J. Nucl. Energy, 21, 755 (1967).

3. G. P. CECCHINI AND M. SALVATORES, Nucl. Sci. Eng., 46, 304 (1971).

4. J. H. MARABLE and C. R. WEISBIN, "Uncertainties in the Breeding Ratio of a Large LMFBR," in E. G. Silver, Ed., Advances in Reactor Physics, CONF-780401, U. S. Dept. of Energy, p. 231 (1978).

5. J. H. MARABLE, C. R. WEISBIN, and G. DE SAUSSURE, Nucl. Sci. Eng., 75, 30 (1980).

6. C. R. WEISBIN et al., Sensitivity and Uncertainty Analysis of Reactor Performance Parameters, Advances in Nuclear Science and Technology, Plenum Press, Vol. 14 (1980).

7. J. D. DRISCHLER and C. R. WEISBIN, "Compilation of Multigroup Cross Section Covariance Matrices for Several Important Reactor Materials," ORNL-5318/R, Oak Ridge National Laboratory, to be published.

8. J. D. SMITH and B. L. BROADHEAD, "Multigroup Covariance Matrices for Fast Reactor Studies," ORNL report to be published.

9. J. C. CHANDLER et al., "The Proliferation Resistant Preconceptual Core Design Study," TC-1082, Hanford Engineering Development Laboratory (1978).

10. M. A. ABDOU and C. W. MAYNARD, Nucl. Sci. Eng., 56, 360 (1975).

11. R. PROTSIK, General Electric-Sunnyvale, Private Communication (1971).

12. C. L. COWAN and C. S. RUSSELL, "FUMBLE-II," GEAP-14138, General Electric-Sunnyvale (1976).

13. "VITAMIN-C," RSIC Report DLC-41/VITAMIN C, Oak Ridge National Laboratory (1978).

14. N. M. GREENE et al., "AMPX," ORNL/TM-3706, Oak Ridge National Laboratory(1976).

15. D. R. VONDY, T. B. FOWLER, and G. W. CUNNINGHAM, "VENTURE," ORNL-5062/R1, Oak Ridge National Laboratory (1977).

16. J. R. WHITE, "The Development, Implementation, and Verification of Multicycle Depletion Perturbation Theory for Reactor Burnup Analysis, ORNL/TM-7305, Oak Ridge National Laboratory (1980).

17. J. LUCIUS et al., "A User's Manual for the FORSS Sensitivity and Uncertainty Analysis Code System," ORNL-5316, Oak Ridge National Laboratory (1980).

18. J. J. WAGSCHAL et al., "ORACLE: An Adjusted Cross Section and Covariance Library for Fast Reactor Analysis," these procedings.

19. D. G. CACUCI et al., "Developments in Sensitivity Theory," these proceedings.

20. D. G. CACUCI, "Sensitivity Theory of Nonlinear Systems, II. Extensions to Additional Classes of Responses," ORNL/TM-7511, Oak Ridge National Laboratory (to be published).

21. American National Standard ANS-19.3.4, (ANSI N676-1976), American Nuclear Society (1976).

22. Y. GOHAR and M. A. ABDOU, "MACKLIB-IV," ANL/FPP/TM-106, Argonne National Laboratory," (1978).

TABLE I

General Design Parameters & Calculated Performance Parameters for a CDS-Type LMFBR Heterogeneous Core

Design Parameters	
Core Height (cm)	101.6
Core Effective Outer Radius (cm)	166.8
Axial Blanket Thickness (cm)	35.6
Radial Blanket Thickness (cm)	34.2
Number of Assemblies	
Driver Fuel	300
Inner Blanket	115
Radial Blanket	204
Control	30
Assembly Pitch (cm)	15.06
Pin Diameter (cm) - Driver Fuel/Blankets	0.6985/1.118
Clad Thickness (cm) - Driver Fuel/Blankets	0.03683/0.03556
Smeared Fuel Density (%TD) - Driver Fuel/Blankets	86.5/95.3
Refueling Interval (Days)	365
Fuel and Internal Blanket Residence Time (Days)	730
Capacity Factor (%)	80
Performance Parameters	
Total Power (MW_{th})	2540
Loaded Fissile Enrichment (% - Atoms of U-235 + Pu239 + Pu241/Total Atoms of Fuel)	17.7
Average Breeding Ratio	1.35
Doubling Time, CSDT (years)	17
Average Discharge Driver Burnup (MWD/MT)	58,600

Table II. Approximate Nuclide Densities, Principal Constituents of CDS-type Reactor Model, Fig. 2 [10^{21} atoms/cc][a]

Nuclide	CF	IB	AB over CF	AB over IB	RB	Prim. CTL Out	Second. CTL Out	Prim. CTL In	Second. CTL In
U^{238}	6.75	12.4	9.58	12.6	12.6				
Pu^{239}	1.33	2.4-1	5.1-2	7.5-2	1.0-1			Nuclides for CTL In only	
Pu^{240}	4.4-1	7.8-3	4.1-4	7.2-4	2.0-3				
Pu^{241}	1.8-1	1.9-4						B10:13.3	11.7
Pu^{242}	5.4-2							B11: 2.3	2.0
U^{235}	1.2-2	2.1-2	1.8-2	2.4-2	2.3-2			C: 7.2	6.4
FP PAIRS	2.6-1	5.4-2	5.4-3	6.3-3	1.3-2				
O	18.1	25.4	As CF	As IB	As IB				
Na	8.2	6.1	"	"	"	20.8	19.6	8.3	8.9
Fe	11.9	9.6	"	"	"	3.7	6.7	17.8	18.4
Cr	2.4	2.0	"	"	"	7.5-1	1.4	3.6	3.7
Ni	2.8	2.2	"	"	"	8.7-1	1.6	4.2	4.3

[a] CF, IB, AB, RB and CTL signify driver, internal blanket, axial blanket, radial blanket, and control zones, respectively.

Table III. Selected Total Relative Sensitivities (x 100) for k_{eff} and Breeding Ratio (BR).

Nuclide, Reaction	k_{eff}	BR[a]	Nuclide, Reaction	k_{eff}	BR[a]
U^{235} ν	+0.9	+0.4	Pu^{241} ν	+12.0	-0.6
σ_f	+0.7	-1.3	σ_f	+8.8	-11.2
σ_c	b	-0.6	σ_c	-0.6	-1.9
U^{238} ν	+12.4	+1.8	Pu^{242} ν	+0.5	b
σ_f	+7.7	+1.1	σ_f	+0.3	b
σ_c	-21.9	+75.6	σ_c	-0.2	b
σ_s	-3.1	-0.4	Na σ_c	-0.2	b
Pu^{239} ν	+69.1	-1.3	σ_s	-0.6	-3.3
σ_f	+50.1	-66.8	O σ_s	-3.7	-0.2
σ_c	-4.9	-17.4	Fe σ_c	-1.2	-0.5
σ_s	-0.2	-0.3	σ_s	-0.7	-2.5
Pu^{240} ν	+5.1	-0.3	Cr σ_c	-0.5	-0.3
σ_f	+3.5	-0.2	σ_s	b	-1.0
σ_c	-1.5	+4.7	Ni σ_c	-0.5	-0.3
			σ_s	b	-1.4

[a] Convert BR sensitivities to k-reset values by adding 1.76 x k_{eff} sensitivity.

[b] Table entry has absolute value < 0.1

Table IV. Selected Total Relative Sensitivities (x 100) for Mid-plane Power Density, PD (r_p), at Points of Zone Peak Power (r_I, r_M, r_O for inner, middle, and outer driver zone, respectively).[a]

Nuclide, Reaction	PD (r_I)	PD (r_M)	PD (r_O)	PD (r_{O2})[c]
U^{235} ν	+ 1.0	b	- 1.1	- 1.2
σ_f	b	b	- 1.7	- 1.8
U^{238} ν	+ 5.7	+ 2.0	- 5.9	- 6.5
σ_f	- 1.4	- 3.6	- 6.6	- 6.6
σ_c	-26.2	-11.5	+24.0	+26.8
σ_s	-22.7	- 8.7	+21.1	+23.6
Pu^{239} ν	b	b	+ 2.0	+ 2.1
σ_c	- 3.4	- 2.0	+ 1.2	+ 1.4
σ_s	b	b	+ 1.5	+ 1.6
Pu^{240} ν	- 4.0	- 1.8	+ 2.7	+ 3.0
σ_f	- 2.0	b	+ 2.7	+ 3.1
Pu^{241} ν	- 2.4	b	+ 2.0	+ 2.2
σ_f	b	+ 1.0	+ 2.3	+ 2.2
Na σ_s	b	+ 1.4	+ 6.7	+ 6.7
O σ_s	-24.4	-10.9	+18.7	+21.3
Fe σ_c	- 1.0	b	+ 1.0	+ 1.0
σ_s	- 7.5	- 1.8	+10.4	+11.2

[a] Convert PD sensitivities to k-reset values by adding 0.22, -0.01, -0.41, and -0.42 x k_{eff} sensitivities for r_I, r_M, r_O, and r_{O2}, respectively.

[b] Table entry has absolute value < 1.0

[c] Point 5 cm to right of r_O; see text.

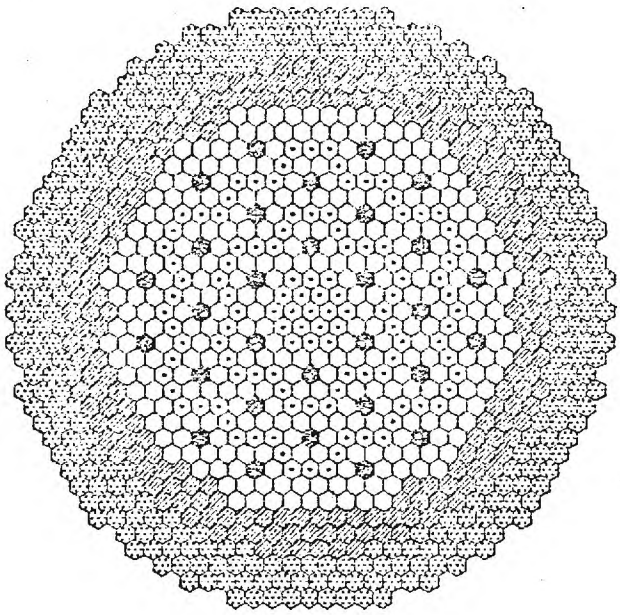

FIGURE 1 - CDS OXIDE REFERENCE CORE LAYOUT

CF - CORE FUEL (DRIVER FUEL) ASSEMBLIES
IB - INTERNAL BLANKET ASSEMBLIES
AB - AXIAL BLANKET EXTENSIONS
RB - RADIAL BLANKET ASSEMBLIES
CTL - CONTROL ASSEMBLIES

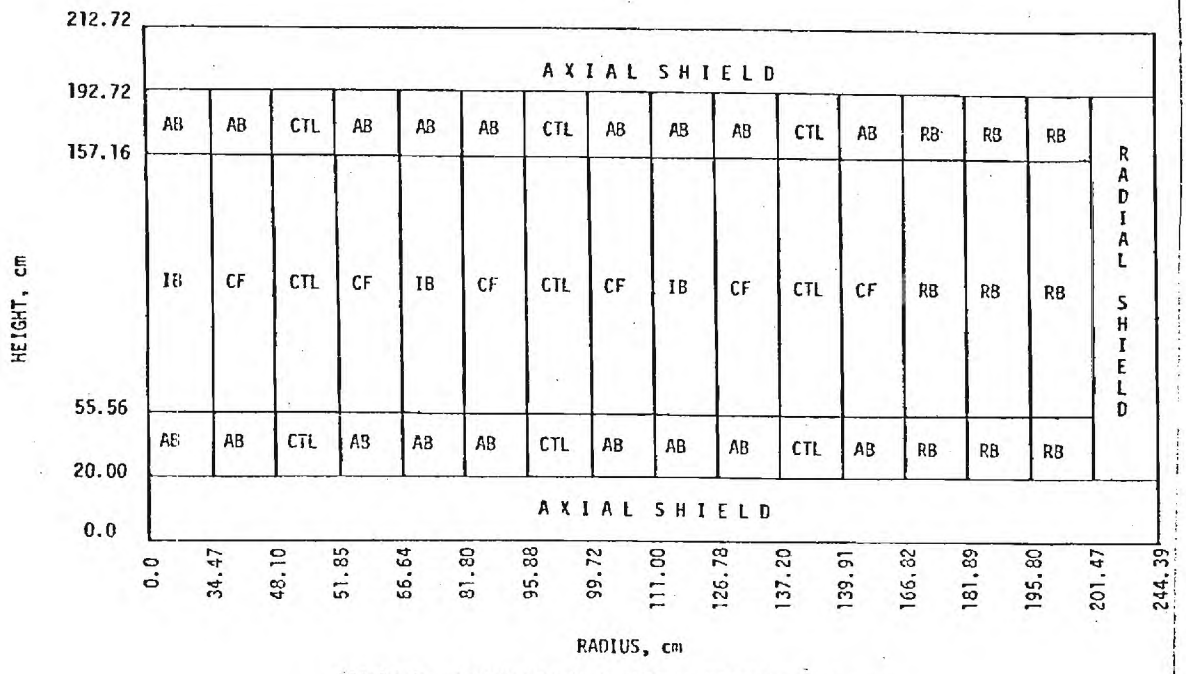

FIGURE 2. REGION MAP OF A TYPICAL HETEROGENEOUS CORE
(Not to Scale)

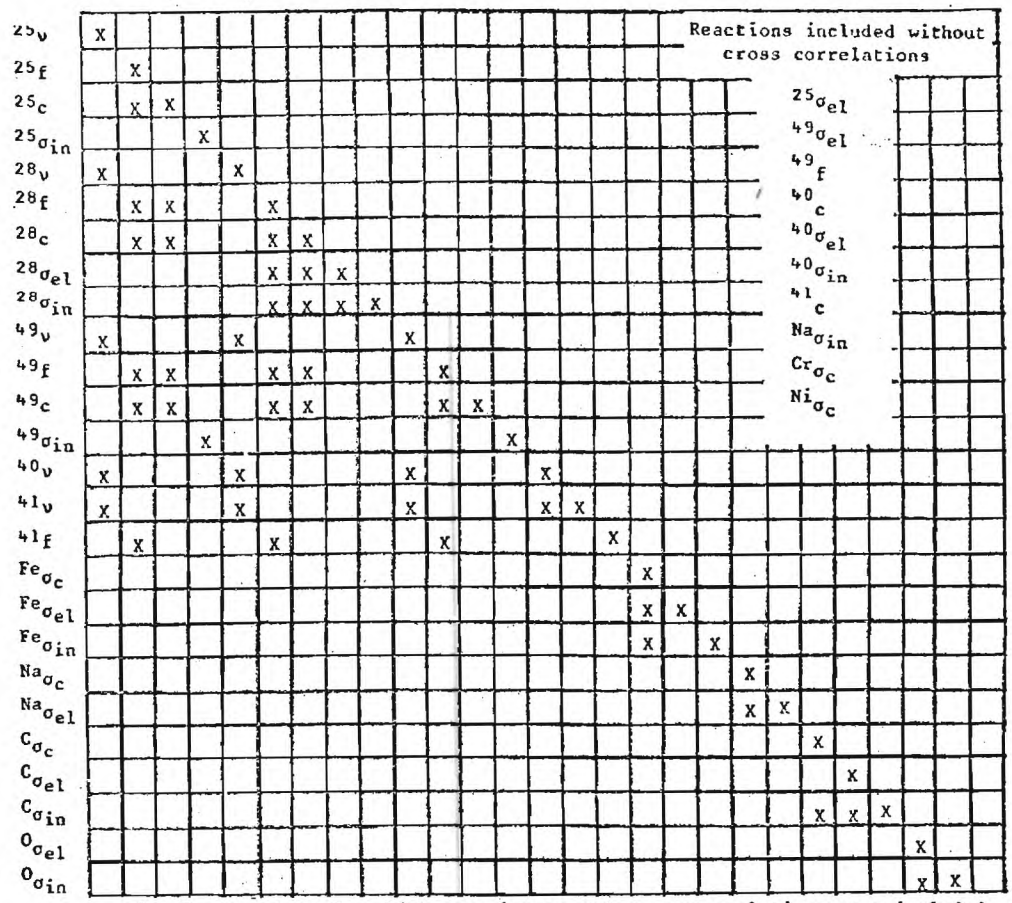

Fig. 3 Reactions for which covariances and cross-correlations were included in the calculations of performance parameter uncertainties are indicated by X. Above and to the right of the principal diagonal, X's should be inferred from symmetry. Column labels are the same as row labels. Reactions for which covariances without cross correlations were included are given in the inset.

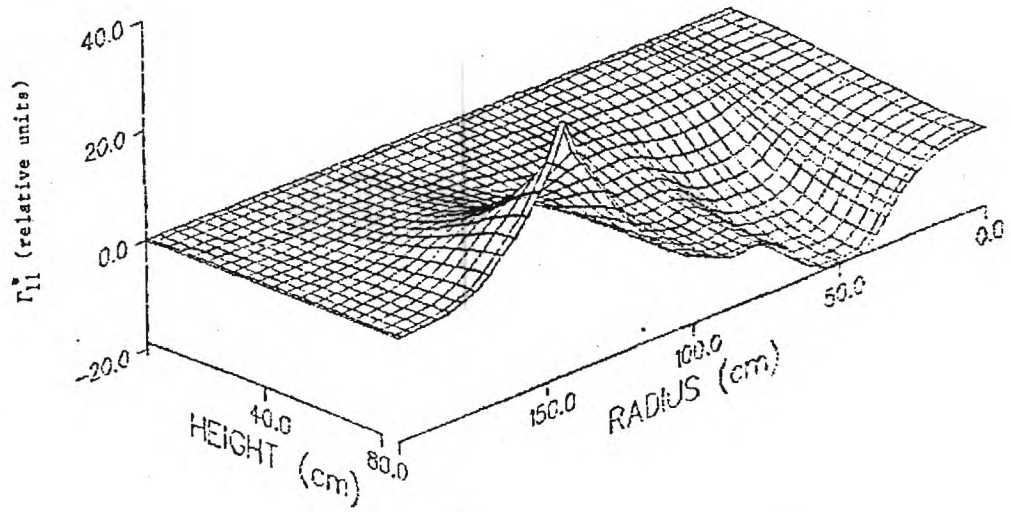

Fig. 4. Peak-power density generalized adjoint Γ_{11}^{*} for energies 67-111 keV in the lower half of the heterogeneous reactor model.

GITNE-80/1

THERMAL REACTOR DATA FOR THE ARMP SYSTEM

AND

FAST REACTOR SENSITIVITY THEORY DEVELOPMENT AND APPLICATION

by J. M. Kallfelz, P. Levin, and D. Biswas

Annual Progress Report for ORNL Subcontract 7802-X01

October 1980

ABSTRACT

This annual progress report covers the activity of the Georgia Institute of Technology during the period October 1, 1979 - September 30, 1980 under Oak Ridge National Laboratory Subcontract 7802-X01. One primary area of this activity was the testing of new thermal reactor nuclear data generated for the Advanced Recycle Methodology Program (ARMP) System of EPRI. The second primary research area was the further development of generalized perturbation theory capabilities and the application thereof to the design and sensitivity analysis of a heterogeneous LMFBR characteristic of the type being considered for the Conceptual Design Study (CDS).

This and other work has been reported in detail in our monthly progress reports[1-13] and activity in the two main areas is summarized in the present document.

TABLE OF CONTENTS

1. Thermal Reactor Data for the ARMP System

During this project year we participated in the ORNL activity involving testing of methods and ENDF/B-IV and -V data developed for the Advanced Recycle Methodology Program (ARMP) system[14] of the Electric Power Research Institute (EPRI). Both ENDF/B-IV[1,15] and ENDF/B-V[2] data, as well as the "NAI data"[16] originally supplied with the ARMP package were utilized in this testing.

Most of the ARMP investigations were performed with the EPRI-CELL module,[17] and all the studies discussed in this section were with this code. Both critical assemblies[18] and power reactors[19] were used in these investigations.

1.1 Critical Assembly Calculations

For the initial studies, six mixed oxide criticals[20,21] and BAPL-1 through -3[22] were calculated and analyzed using ENDF/B-IV data.[1] Various corrections in EPRI-CELL, the cross section set, and the models used were incorporated and assessed.[1] These calculations were repeated with ENDF/B-V data[2] and the results were compared with our previous calculations[1] and those of others.[21]

1.2 Power Reactor Calculations

Various power reactor results used in the original EPRI-CELL benchmarking[19] were employed in our investigations. The first calculations[3] were for the Yankee Rowe Core V,[23] performed on the Berkeley computer to insure that our results for isotopic ratios as a function of burn-up were the same as those previously reported.[19] For the same case, ENDF/B-IV calculations were performed for the beginning of life,[4] but due to various program and data errors,[4,5] we were not successful in

performing burn-up calculations with ENDF/B data during the period of this activity.

Subsequent efforts on this activity concentrated on performing PWR calculations on both the Berkeley and ORNL computers, using the "NAI" cross sections.[16,24] EPRI-CELL isotopics calculations were performed for both the Zr and SS clad elements in the Yankee Rowe reactor,[23,25-27] as well as for the H. B. Robinson reactor.[19] The results of these calculations were reported and analyzed in our progress reports.[6,7] For example, Fig. 1.A shows a comparison between experimental isotopic ratio values and results calculated with the Berkeley and ORNL computers.[6] The poor agreement for the ORNL case was attributed to an error discovered in the treatment of the Pu-240 1 eV resonance.[28]

One goal of this work was to check for consistency between the Berkeley and ORNL versions of the ARMP components used. A second major goal was to determine the appropriate techniques and data sources necessary to model the power reactors in question. A detailed summary[7] was prepared describing these techniques and sources, to serve as a guide for future power reactor calculations.

EPRI-CELL runs for various TMI-1 unit cells were also performed for use in further analysis of that reactor.[9] Documentation was prepared describing these cases and the use of several EPRI-CELL cross section interface codes developed at Georgia Tech.[10]

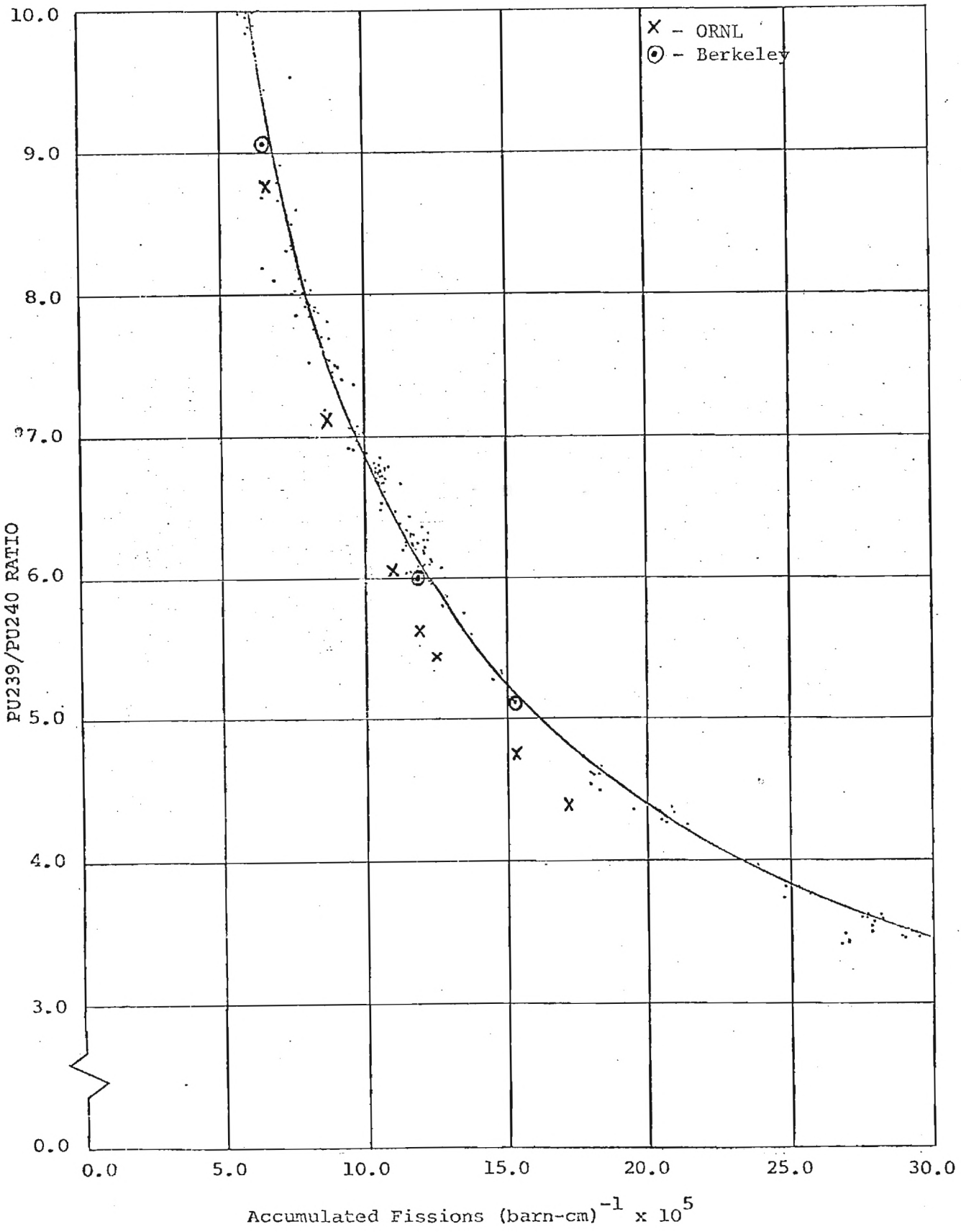

FIGURE 1.A COMPARISON BETWEEN ANALYSIS AND YANKEE STAINLESS ISOTOPIC RATIOS (From: Ref. 6)

2. Fast Reactor Sensitivity Theory Development and Application

2.1 Development Activities

Continuing previous joint work with General Electric in the area of sensitivity analysis and the economic impact of data uncertainties[29,30] related topics were further investigated.[2] A meeting was held with General Electric[3] and recommendations and information concerning addition of several important integral parameters to the capability of the ORNL sensitivity codes were reported.[3]

A joint program was planned with General Electric,[32] and a study of the feasibility of performing sensitivity analysis of the maximum linear power using VENTURE was made.[5] Based on this study and the above planning, it was proposed to perform jointly with General Electric a sensitivity and uncertainty analysis of a heterogeneous LMFBR, including parameters related to the peak linear power.[6]

A goal was set to prepare a joint paper for the Sun Valley ANS Topical Meeting, describing the design and sensitivity analysis of a CDS-type LMFBR.[7] Georgia Tech was assigned the lead responsibility for this task,[7] and the major effort of this project year in the fast reactor area involved performing the necessary investigations and coordinating the work of co-authors at ORNL and General Electric to accomplish this goal.

Various technical problems involved in implementing new capabilities were investigated and reported.[6-13] Particular attention was paid to the implementation and application of the new capability to investigate the peak power density,[8,11] including the necessity for sensitivity and covariance data for more reactions than were considered for previous studies of other integral parameters. Coupled (n,γ) calculations and utilization of kerma[33] factors to investigate the effects of

non-localized energy deposition were proposed, and the associated problems thereof discussed and analyzed.[8]

In conference with ORNL staff members, responsibilities for the various areas of investigation were established.[9] The associated tasks were accomplished during the summer of 1980, with considerable coordination and iteration among the co-authors.[9-13]

The result of this effort was a paper[34] which described the design and sensitivity analysis of a CDS-type heterogeneous core. k_{eff}, the breeding ratio, and the peak linear power were studied, and integral parameter uncertainties and correlations were determined. A detailed description of this work and the associated results is discussed in the aforementioned paper,[34] which is incorporated in this report in the following section.

2.2 DESIGN AND SENSITIVITY ANALYSIS OF A CDS-TYPE HETEROGENEOUS CORE

J. M. Kallfelz and D. Biswas
Georgia Institute of Technology
Atlanta, Georgia 30332

C. L. Cowan
General Electric Company
Sunnyvale, California 94086

J. H. Marable, M. L. Williams, C. R. Weisbin
J. D. Drischler, T. B. Fowler, and J. R. White
Oak Ridge National Laboratory
Oak Ridge, Tennessee 37830

ABSTRACT

The design of a heterogeneous LMFBR of the type being considered for the Conceptual Design Study (CDS) is analyzed, using sensitivity analysis methods. Nuclear data sensitivities for k_{eff}, the breeding ratio, and parameters related to the peak linear power (space-dependent power densities) are determined with generalized perturbation theory. These sensitivities are folded with extensive nuclear data covariance information to determine the associated integral parameter uncertainties and correlations. The effects of non-localized energy deposition were investigated by folding the results of coupled (n-γ) calculations with kerma factors.

INTRODUCTION

The development of the Conceptual Design Study (CDS) reactor plant[1]* was intended to provide direction and focus to the LMFBR technology programs, and the research and development needs for these programs will be outlined in the final report to Congress by DOE after April, 1981. The joint work reported in this paper involved a cooperative effort by university, vendor, and national laboratory staff, with the principal goal of investigating the uncertainties of some significant reactor performance parameters.

To accomplish this aim we utilized both direct perturbations and the methods of generalized perturbation theory,[2-6] together with nuclear data covariance information[4-8] which has become available in the last few years. Several of the performance parameters considered, namely k_{eff} and the breeding ratio, have been the object of a similar study[4,5] for a homogeneous LMFBR, thus allowing comparison of the importance of various nuclear data to these parameters for the two reactor types.

We have placed particular emphasis on studies related to the peak linear power. Reduction of uncertainty in this parameter has obvious importance both for licensing and economic considerations, and considerable attention has been devoted in recent studies[9] to determining the maximum allowable value of this quantity. For sensitivity calculations we considered the power density with diffusion theory, but we have investigated the effects of non-localized energy

---

*Reference for section 2.2 are listed separately, on pages 12 and 13.

deposition by performing coupled (n-γ) calculations and folding the results with kerma factors.[10] In the following sections we discuss the design and typical configuration of the CDS reactor, and the methods and results of our sensitivity analysis.

GENERAL REACTOR DESCRIPTION

The key design parameters for a large heterogeneous LMFBR of the 1000 MWe class were specified as part of the DOE sponsored CDS project. The design objectives and criteria for the CDS project emphasized the following:

1. High reliability,
2. Near term design features (components that can be developed within five years),
3. Sufficiently low sodium void worth to preclude hypothetical core disruptive accidents from consideration as design basis accidents,
4. Breeding of fissile fuel at a rate equivalent to a compound system doubling time of twenty years or less, and
5. Allowances for the future accomodation of advanced fuels.

On the basis of the above objectives, the CDS Reference Design was chosen to be a 2540 MW_{th}, mixed plutonium uranium oxide, heterogeneous reactor with three driver fuel zones and three inner blanket zones. The core layout for the Reference Design is shown in Fig. 1, and a summary of the principal core design and performance parameters is given in Table I. All design calculations discussed in this section were carried out in linked r-z and x-y triangular mesh geometry using the two-dimensional diffusion theory code SN2D[11] and the fuel management and burnup code FUMBLE,[12] and cross sections based on ENDF/B-V data.

The fuel pin diameter for the CDS Reference Design was selected on the basis of earlier sensitivity studies to give near-optimum breeding and economic performance for the heterogeneous core. The fuel pins are clad with the austenitic stainless steel alloy, D9, with material properties which closely resemble those of 20% CW316 SS. However, on the basis of available data the irradiation induced creep and swelling are expected to be significantly lower for the D9 alloy.

The core layout as shown in Fig. 1 was specified to minimize the peak radial power throughout the operating cycle based upon a single fissile enrichment for the supplied fuel in all driver fuel regions. The twelve burnup control rods in the outer driver fuel zone are also utilized to shape the radial power profile during reactor operations.

Reactor shutdown of the CDS Design is accomplished by each of two independent control systems. The primary control system consists of 21-24 natural boron carbide rods, including 12 rods in the outer control ring for burnup reactivity adjustments. The secondary control system consists of 6-9 enriched boron carbide rods which are distributed in the inner and middle control rings. The final requirements for the two independent systems will be determined in follow-up studies and will include an assessment of control reliability requirements.

SENSITIVITY STUDIES MODEL AND DATA

For the sensitivity studies we used an MOEC design characteristic of those being considered for the CDS, henceforth referred to as the basic model. This r-z model is shown in Fig. 2, while Table II describes the composition of the principal regions. The shield was not included in our calculations, and

control in the outer control ring was inserted to achieve criticality for the model.

The further reported results were calculated with the ENDF/B-IV cross section set of 32 groups used in Refs. 4 and 5, unless noted otherwise. We also generated ENDF/B-IV cross sections for the CDS-type reactor from the 171 neutron group Vitamin-C library.[13] Resonance shielding for both the blanket and driver zones was done with the BONAMI module of the AMPX system.[14] For further sensitivity calculations, the 171 group cross sections were collapsed to 32 groups using fluxes obtained from a 1-D, cylindrical XSDRN-PM[14] transport calculation (S4P1) of the reactor. Sensitivity results for the two 32 group cross section sets were practically the same.

UNCERTAINTY ANALYSIS THEORY AND METHODS

Using the methods of generalized perturbation theory,[2-6] the group-dependent nuclear data sensitivity $(\partial I/I)/(\partial \sigma_i / \sigma_i)$ of integral parameter I has been studied for two parameters considered in earlier works,[4,5] namely k_{eff} and the breeding ratio, as well as ratios significant for determining the uncertainty in the calculated peak linear power. For sensitivity values involving the criticality constraint, "k-reset"[4-6] has been performed by altering the driver zone "plutonium enrichment", i.e., (total Pu)/(total heavy metal), as in previous studies.[4,5] Perturbation theory results were checked by direct perturbation calculations performed at General Electric, ORNL, and Georgia Tech.

Generalized perturbation theory[2-6] provides a method of calculating a generalized adjoint function, $\vec{\Gamma}^*(\vec{r})$, where $\Gamma_j^*(\vec{r})$ is the importance of a neutron in energy group j at space point $\vec{r}$ to the ratio being considered. We have incorporated in VENTURE[15] the capability to generate $\vec{\Gamma}^*$ for the ratio of point power density to total power (PD):

$$PD\ (\vec{r}_p) = \frac{a_1}{a_2} = \frac{\sum_j \Sigma_{1j}\ (\vec{r}_p)\ \phi_j\ (\vec{r}_p)}{\int_{reactor} \sum_j \Sigma_{2j}\ (\vec{r})\ \phi_j\ (\vec{r})\ d\vec{r}} \qquad (1)$$

Considering only fission energy and assuming localized energy deposit, the Σ_{ij} have the form:

$$\Sigma_{ij}\ (\vec{r}) = \sum_k p^k\ \Sigma^k_{f,j}(\vec{r}) \qquad (2)$$

and P^k is the total energy release per fission in the k-th isotope.

Thus, the fixed source in the equation for $\vec{\Gamma}^*$ for PD $(\vec{r}_p)$ has the form:

$$S^*_j\ (\vec{r}) = \Sigma_{1j}(\vec{r})/a_1 - \Sigma_{2j}(\vec{r})/a_2 \qquad (3)$$

where Σ_{1j} is zero for $\vec{r} \neq \vec{r}_p$.

To determine the uncertainty of an integral parameter, I, one can calculate its variance (VAR):

$$VAR\ (I) = \sum_{i,j} \frac{\partial I}{\partial \sigma_i} \frac{\partial I}{\partial \sigma_j}\ COV\ (\sigma_i, \sigma_j) \qquad (4)$$

The nuclear data covariance files (COV) contain information on both the standard deviation, (SD), and correlation of various cross sections.[4-6] To obtain a reliable estimate of $SD(I) = \sqrt{VAR(I)}$, equation (4) should include all data which have a significant impact on I.

Due to the space-dependent nature of the PD sensitivities, which we will discuss in the following section, a parameter of particular interest is the covariance of two integral parameters:

$$COV\ (I_1,\ I_2) = \sum_{i,j} \frac{\partial I_1}{\partial \sigma_i} \frac{\partial I_2}{\partial \sigma_j}\ COV\ (\sigma_i,\ \sigma_j) \qquad (5)$$

The correlation (COR) between I_1 and I_2 is expressed more explicitly by:

$$COR(I_1,I_2) = COV(I_1,I_2)/[SD(I_1)\ SD(I_2)] \qquad (6)$$

S* of equation (3) can be calculated by VENTURE and DEPTH.[16] The latter code was used to process the $\vec{\Gamma}^*$ and $\vec{\phi}$ files from VENTURE to determine the sensitivities. For all reported sensitivities, σ_t was treated as dependent, i.e. a perturbation in one of the partial cross sections had an associated $\delta\sigma_{tr}$. This convention will not influence the VAR values if consistent $COV(\sigma_i,\sigma_j)$ data are used in equation (5).

SENSITIVITY STUDY RESULTS AND DISCUSSION

k_{eff} AND BREEDING RATIO

For these parameters, selected total (energy integrated) sensitivities are given in Table III. The largest sensitivities are for heavy metals, and the five largest total sensitivities for k_{eff} and breeding ratio (BR) for this case and for a homogeneous reactor[4], are for the same reactions and have roughly the same values for the two reactors.

To obtain the standard deviation and correlation values from equations (4) and (6), we have included nuclear data sensitivities and covariances for the reactions indicated in Fig. 3. The primary source of covariance data was the ORNL evaluation,[7] based for the most part on ENDF/B-IV, which was used and discussed in earlier studies.[4,5] For reactions not included in this source, new covariance information[8] was employed. The quality of covariance information is being scrutinized in another study.[18]

The resulting standard deviations for the indicated parameters are:

k_{eff}: 3.2% BR: 7.1% BR(with k-reset): 3.3%

These results can be compared to corresponding values (in the same order) of 2.0%, 6.1%, and 3.1% reported for a homogeneous reactor,[4] for unadjusted cross section and COV data. It should be noted that if adjusted cross section and COV data presently being developed[18] were employed, the SD values would probably be reduced. This adjusted data incorporates integral experiment information, and a reduction of performance parameter uncertainties by using adjusted data has been demonstrated for a homogeneous LMFBR.[4]

POWER DENSITY SENSITIVITIES

General Nature of PD Sensitivities

We refer to the use of the basic reactor model and unperturbed cross sections as the "base case". Figure 4 shows results for the generalized importance function $\vec{\Gamma}^*$ for PD, for the base case point of peak power, a location which can change with sigma changes, burn-up, etc. The base-case peak power occurs at a point in the outer driver zone, and $\vec{\Gamma}^*$ is strong positive near this point, decreasing and eventually becoming negative as the distance from this point increases. The strong negative region is the innermost driver zone, which strongly affects the denominator of PD.

Due to the complicated spatial and time-dependent nature of the peak value of the power density for a heterogeneous reactor, PD sensitivities are of interest at more than the point of maximum value for the base case. Considering the nature of the PD $(\vec{r}_p)$ sensitivity, it is obvious that the volume integral of these sensitivities for all points in the reactor must be zero. Physically, it is clear that what causes an increased power density at one point will cause a decrease elsewhere, since the total power is constant. Thus, it is not surprising that for an isotope distributed fairly evenly throughout the reactor, i.e. U-238, the PD σ_c and σ_s sensitivities for the inner and outer driver zone have opposite signs.

Space Dependent PD Sensitivities: Results and Discussion

Since the PD sensitivities are space dependent, we have considered "near-range" (near the maximum PD in a particular driver zone) and "far-range" (between various driver zones) effects. Clearly the latter effects are strong, negating the possibility of determining a unique set of "peak power density sensitivities" for a particular design. For a power density which is fairly "flat" in the sense that the peak power in each driver zone is about the same, minor changes in the reactor design, control positioning, or nuclear data could shift the peak power from one driver zone to another. Thus it is clear that we should consider the sensitivities for at least three response functions, namely the PD at the point of peak power for each of the driver zones. Table IV gives these values at radii of r_I, r_M and r_O in the core mid-plane.

The "near-range" spatial effects raise the question of whether a single set of sensitivities can be determined for each driver zone which are significant for the peak power density. The answer to this question is yes, with certain restrictions. The primary values given in Table IV are for the peak zonal PD mesh point, near the center of the associated driver zone and several centimeters to the right of the control channel. For the outer driver zone we also calculated sensitivities for the next radial mesh point, r_{02}, about 5 centimeters further toward the zone outer boundary. These calculations were performed both for the basic reactor model and for a second model which had altered middle driver and internal blanket zone dimensions, such that the PD distribution was significantly different from that of the basic model. The results for the basic model are given in Table IV, and for both models the principal sensitivities at r_{02} were close to those for the basic model at r_O. This indicates that the "near-range" effects are generally small near the extrema of the PD, and that these sensitivity values are fairly independent of the actual power distribution.

Obviously, $PD(\vec{r}_p)$ sensitivities for strongly localized nuclides, e.g. B^{10}, will be a strong function of the position of $\vec{r}_p$, even in the "near-range"

sense. Furthermore, as the distance from the point of maximum PD is increased and the driver zone edge is approached, one would expect some of the sensitivities to change appreciably due to the proximity of the internal blanket. However, it is obvious that a point next to the edge of a driver zone is not significant for peak power investigations.

A more rigorous treatment of the peak power sensitivity would utilize a more detailed theory, which considers explicitly the spatial shift in the peak power due to "near-range" effects. Cacuci[19,20] has developed a sensitivity theory which treats extrema of functions, and he shows[20] that spatial shift effects in the extremum sensitivity are "second-order" in $\delta\sigma$. While these "second-order" effects may be significant for some special cases, it appears from the above results that the sensitivities of the PD at the base case point of peak power are generally adequate to describe the peak PD uncertainty in each driver zone.

As would be expected, the PD sensitivities are particularly large for those reactions which influence the neutron transport between zones, e.g. U-238 σ_c. Also the PD sensitivities for other such data, e.g. Fe and O σ_s, can be larger than for many of the heavy metal reactions.

PD Standard Deviations and Correlations

For the points of peak zone PD at mid-plane radii of r_I, r_M, and r_O for the inner, middle, and outer driver zones respectively, as well as the previously discussed second point in the outer driver at r_{O2} near r_O, VAR and SD values of the PD were determined using the same nuclear data covariance information as that used for the k_{eff} and BR values. Changes only of sensitivity signs from one zone to another will, of course, cancel out in the associated variances. Without k-reset, the resulting SD values for PD at the indicated points are:

r_I: 2.2% r_M: 1.0% r_O: 2.1% r_{O2}: 2.3%

These values reflect the smaller sensitivities for the middle zone. With k-reset the values for the outer and inner zones were increased somewhat. E.g., for the location of peak reactor power density, r_O, the corresponding SD value with k-reset is 2.6%.

To illustrate the previously discussed "near-range" and "far-range" PD correlation, we have applied equations (5) and (6) for the PD at the points discussed above, yielding the following values (without k-reset) of COR [PD(r_1), PD(r_2)] for the indicated points:

r_I, r_O: - 0.97 r_I, r_M: + 0.99

r_O, r_{O2}: + 1.00 r_O, r_M: - 0.94

These results verify the previously discussed behavior of this response. Correlation values of +1 and -1 are limiting values for positive and negative correlation of uncertainties.

NEUTRON-GAMMA TRANSPORT EFFECTS AND ENERGY DEPOSIT

To study the effects of non-localized energy deposition, coupled (n, γ) transport calculations are necessary.[21] It has long been recognized that such transport effects are particularly significant in a heterogeneous core.

All calculations for this study were done for a 1-D cylindrical version of the basic reactor model with critical axial buckling, using the discrete ordinates code XSDRN-PM,[14] and coupled data created by merging 36 group VITAMIN-C gamma cross sections with the 171 group neutron data discussed earlier. Two

sets of calculations were done in this study. The first was a diffusion theory calculation which made the common approximation that all liberated energy stems from fission and is deposited at the point of fission. The second calculation was a coupled (n,γ) run (S8-P3) which explicitly accounted for the transport of fission neutrons and prompt gammas, as well as for that of secondary gammas generated by neutron capture and inelastic scatter. The spatial energy deposition of the neutrons and gammas was obtained by folding the fluxes with kerma factors[10] from MACKLIB IV.[22]

Results of these calculations indicate that for our CDS-type MOEC model, diffusion theory with the approximation of localized energy deposition underpredicts the fraction of the reactor power produced in the internal blankets by about 10 % and overpredicts this fraction for the driver zones by 2 %, when compared to the coupled (n,γ) calculation. The diffusion theory result for the peak to total power ratio is 1 % higher than that for coupled transport theory. At the point of peak power, the (n,γ) results for the energy deposited in the fuel-pellet materials is 98.5 % of the total energy deposition at that point.

SUMMARY AND CONCLUSIONS

(a) For the heterogeneous LMFBR considered herein and a typical commercial-sized homogeneous reactor, the five largest total sensitivities for k_{eff} and the breeding ratio are for the same reactions and have roughly the same values for the two reactors.

(b) For power density sensitivities, reactions which influence neutron transport between zones are proportionally more important than for the sensitivities of (a).

(c) "Near-range" changes to power density sensitivities near the zonal peak power location are small, while "far-range" changes between driver zones can be quite large. Thus, near-range correlation between point power densities is strongly positive, while for different zones the power densities can be strongly anti-correlated.

(d) In a heterogeneous core the calculated peak power density can shift from one driver zone to another due to input data and operational changes. Thus a power density sensitivity must be considered for each driver zone of the design being studied. These "zone-peak" sensitivity values vary considerably for different zones, but are fairly invariant for different realistic power density spatial distributions.

(e) Coupled (n, γ) calculations and kerma factors can be effectively used to study the effects of non-localized energy deposition and to relate power density to linear power.

ACKNOWLEDGMENTS

The authors thank Dan Cacuci and Augusto Gandini for informative discussions on topics related to this research. Julia Rankin did an excellent job of typing this paper. This research was sponsored by the U.S. Department of Energy under Contract No. W-7405-eng-26 with the Union Carbide Corporation.

REFERENCES*

* 1. S. DAVIES, R. MURATA, and B. TALWAR, Trans. Am. Nucl. Soc, 34, (1980).

* 2. A. GANDINI, J. Nucl. Energy, 21, 755 (1967).

*References for section 2.2 only

* 3. G. P. CECCHINI AND M. SALVATORES, Nucl. Sci. Eng., 46, 304 (1971).

* 4. J. H. MARABLE and C. R. WEISBIN, "Uncertainties in the Breeding Ratio of a Large LMFBR," in E. G. Silver, Ed., Advances in Reactor Physics, CONF-780401, U. S. Dept. of Energy, p. 231 (1978).

* 5. J. H. MARABLE, C. R. WEISBIN, and G. DE SAUSSURE, Nucl. Sci. Eng., 75, 30 (1980).

* 6. C. R. WEISBIN et al., Sensitivity and Uncertainty Analysis of Reactor Performance Parameters, Advances in Nuclear Science and Technology, Plenum Press, Vol. 14 (1980).

* 7. J. D. DRISCHLER and C. R. WEISBIN, "Compilation of Multigroup Cross Section Covariance Matrices for Several Important Reactor Materials," ORNL-5318/R, Oak Ridge National Laboratory, to be published.

* 8. J. D. SMITH and B. L. BROADHEAD, "Multigroup Covariance Matrices for Fast Reactor Studies," ORNL report to be published.

* 9. J. C. CHANDLER et al., "The Proliferation Resistant Preconceptual Core Design Study," TC-1082, Hanford Engineering Development Laboratory (1978).

* 10. M. A. ABDOU and C. W. MAYNARD, Nucl. Sci. Eng., 56, 360 (1975).

* 11. R. PROTSIK, General Electric-Sunnyvale, Private Communication (1971).

* 12. C. L. COWAN and C. S. RUSSELL, "FUMBLE-II," GEAP-14138, General Electric-Sunnyvale (1976).

* 13. "VITAMIN-C," RSIC Report DLC-41/VITAMIN C, Oak Ridge National Laboratory (1978).

* 14. N. M. GREENE et al., "AMPX," ORNL/TM-3706, Oak Ridge National Laboratory(1976).

* 15. D. R. VONDY, T. B. FOWLER, and G. W. CUNNINGHAM, "VENTURE," ORNL-5062/R1, Oak Ridge National Laboratory (1977).

* 16. J. R. WHITE, "The Development, Implementation, and Verification of Multicycle Depletion Perturbation Theory for Reactor Burnup Analysis," ORNL/TM-7305, Oak Ridge National Laboratory (1980).

* 17. J. LUCIUS et al., "A User's Manual for the FORSS Sensitivity and Uncertainty Analysis Code System," ORNL-5316, Oak Ridge National Laboratory (1980).

* 18. J. J. WAGSCHAL et al., "ORACLE: An Adjusted Cross Section and Covariance Library for Fast Reactor Analysis," these procedings.

* 19. D. G. CACUCI et al., "Developments in Sensitivity Theory," these proceedings.

* 20. D. G. CACUCI, "Sensitivity Theory of Nonlinear Systems, II. Extensions to Additional Classes of Responses," ORNL/TM-7511, Oak Ridge National Laboratory (to be published).

* 21. American National Standard ANS-19.3.4, (ANSI N676-1976), American Nuclear Society (1976).

* 22. Y. GOHAR and M. A. ABDOU, "MACKLIB-IV," ANL/FPP/TM-106, Argonne National Laboratory," (1978).

*References for section 2.2 only

TABLE I

General Design Parameters & Calculated Performance Parameters for a CDS-Type LMFBR heterogeneous Core

Design Parameters	
Core Height (cm)	101.6
Core Effective Outer Radius (cm)	166.8
Axial Blanket Thickness (cm)	35.6
Radial Blanket Thickness (cm)	34.2
Number of Assemblies	
Driver Fuel	309
Inner Blanket	115
Radial Blanket	204
Control	30
Assembly Pitch (cm)	15.05
Pin Diameter (cm) - Driver Fuel/Blankets	0.6985/1.118
Clad Thickness (cm) - Driver Fuel/Blankets	0.03683/0.03555
Smeared Fuel Density (%TD) - Driver Fuel/Blankets	85.5/95.3
Refueling Interval (Days)	365
Fuel and Internal Blanket Residence Time (Days)	730
Capacity Factor (%)	80
Performance Parameters	
Total Power (MW_{th})	2540
Loaded Fissile Enrichment (% - Atoms of U-235 + Pu239 + Pu241/Total Atoms of Fuel)	17.7
Average Breeding Ratio	1.35
Doubling Time, CSDT (years)	17
Average Discharge Driver Burnup (MWD/MT)	58,600

Table II. Approximate Nuclide Densities, Principal Constituents of CDS-type Reactor Model, Fig. 2 [10^{21} atoms/cc][a]

Nuclide	CF	IB	AB over CF	AB over IB	RB	Prim. CTL Out	Second. CTL Out	Prim. CTL In	Second. CTL In
U^{238}	6.75	12.4	9.58	12.6	12.6				
Pu^{239}	1.33	2.4-1	5.1-2	7.5-2	1.0-1			Nuclides for CTL In only	
Pu^{240}	4.4-1	7.8-3	4.1-4	7.2-4	2.0-3			B10:13.3	11.7
Pu^{241}	1.8-1	1.9-4						B11: 2.3	2.0
Pu^{242}	5.4-2							C: 7.2	6.4
U^{235}	1.2-2	2.1-2	1.8-2	2.4-2	2.3-2				
FP PAIRS	2.6-1	5.4-2	5.4-3	6.3-3	1.3-2				
O	18.1	25.4	As CF	As IB	As IB				
Na	8.2	6.1	"	"	"	20.8	19.6	8.3	8.9
Fe	11.9	9.6	"	"	"	3.7	6.7	17.8	18.4
Cr	2.4	2.0	"	"	"	7.5-1	1.4	3.6	3.7
Ni	2.8	2.2	"	"	"	8.7-1	1.6	4.2	4.3

[a] CF, IB, AB, RB and CTL signify driver, internal blanket, axial blanket, radial blanket, and control zones, respectively.

Table III. Selected Total Relative Sensitivities (x 100) for k_{eff} and Breeding Ratio (BR).

Nuclide, Reaction	k_{eff}	BR[a]	Nuclide, Reaction	k_{eff}	BR[a]
U^{235} ν	+0.9	+0.4	Pu^{241} ν	+12.0	-0.6
σ_f	+0.7	-1.3	σ_f	+8.8	-11.2
σ_c	b	-0.6	σ_c	-0.6	-1.9
U^{238} ν	+12.4	+1.8	Pu^{242} ν	+0.5	b
σ_f	+7.7	+1.1	σ_f	+0.3	b
σ_c	-21.9	+75.6	σ_c	-0.2	b
σ_s	-3.1	-0.4	Na σ_c	-0.2	b
Pu^{239} ν	+69.1	-1.3	σ_s	-0.6	-3.3
σ_f	+50.1	-66.8	O σ_s	-3.7	-0.2
σ_c	-4.9	-17.4	Fe σ_c	-1.2	-0.5
σ_s	-0.2	-0.3	σ_s	-0.7	-2.5
Pu^{240} ν	+5.1	-0.3	Cr σ_c	-0.5	-0.3
σ_f	+3.5	-0.2	σ_s	b	-1.0
σ_c	-1.5	+4.7	Ni σ_c	-0.5	-0.3
			σ_s	b	-1.4

[a] Convert BR sensitivities to k-reset values by adding 1.76 x k_{eff} sensitivity.

[b] Table entry has absolute value < 0.1

Table IV. Selected Total Relative Sensitivities (x 100) for Mid-plane Power Density, PD (r_p), at Points of Zone Peak Power (r_I, r_M, r_O for inner, middle, and outer driver zone, respectively).[a]

Nuclide, Reaction	PD (r_I)	PD (r_M)	PD (r_O)	PD (r_{O2})[c]
U^{235} ν	+ 1.0	b	- 1.1	- 1.2
σ_f	b	b	- 1.7	- 1.8
U^{238} ν	+ 5.7	+ 2.0	- 5.9	- 6.5
σ_f	- 1.4	- 3.6	- 6.6	- 6.6
σ_c	-26.2	-11.5	+24.0	+26.8
σ_s	-22.7	- 8.7	+21.1	+23.6
Pu^{239} ν	b	b	+ 2.0	+ 2.1
σ_c	- 3.4	- 2.0	+ 1.2	+ 1.4
σ_s	b	b	+ 1.5	+ 1.6
Pu^{240} ν	- 4.0	- 1.8	+ 2.7	+ 3.0
σ_f	- 2.0	b	+ 2.7	+ 3.1
Pu^{241} ν	- 2.4	b	+ 2.0	+ 2.2
σ_f	b	+ 1.0	+ 2.3	+ 2.2
Na σ_s	b	+ 1.4	+ 6.7	+ 6.7
O σ_s	-24.4	-10.9	+18.7	+21.3
Fe σ_c	- 1.0	b	+ 1.0	+ 1.0
σ_s	- 7.5	- 1.8	+10.4	+11.2

a) Convert PD sensitivities to k-reset values by adding 0.22, -0.01, -0.41, and -0.42 x k_{eff} sensitivities for r_I, r_M, r_O, and r_{O2}, respectively.

b) Table entry has absolute value < 1.0

c) Point 5 cm to right of r_O; see text.

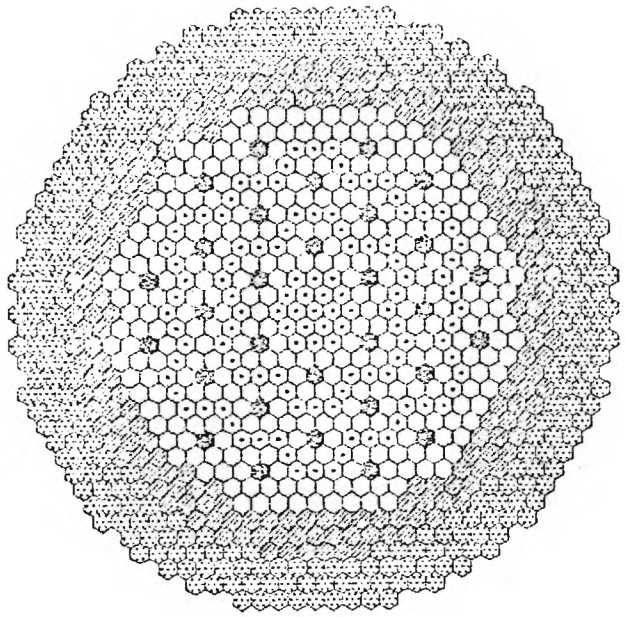

FIGURE 1 - CDS OXIDE REFERENCE CORE LAYOUT

CF - CORE FUEL (DRIVER FUEL) ASSEMBLIES
IB - INTERNAL BLANKET ASSEMBLIES
AB - AXIAL BLANKET EXTENSIONS
RB - RADIAL BLANKET ASSEMBLIES
CTL - CONTROL ASSEMBLIES

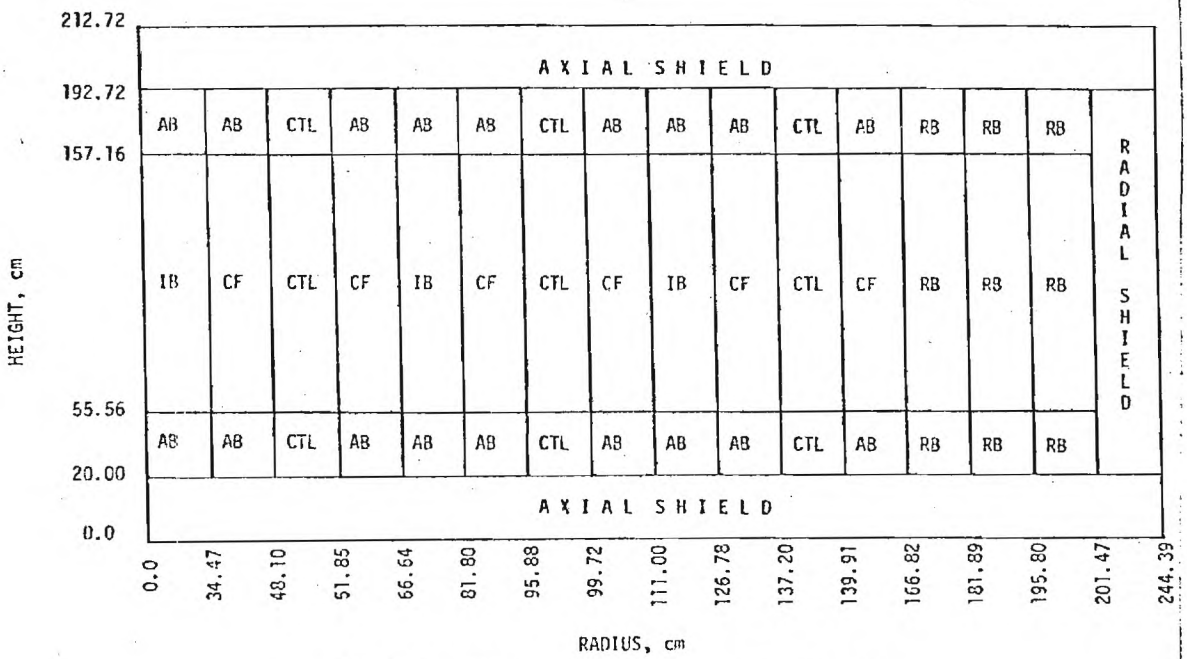

FIGURE 2. REGION MAP OF A TYPICAL HETEROGENEOUS CORE
(Not to Scale)

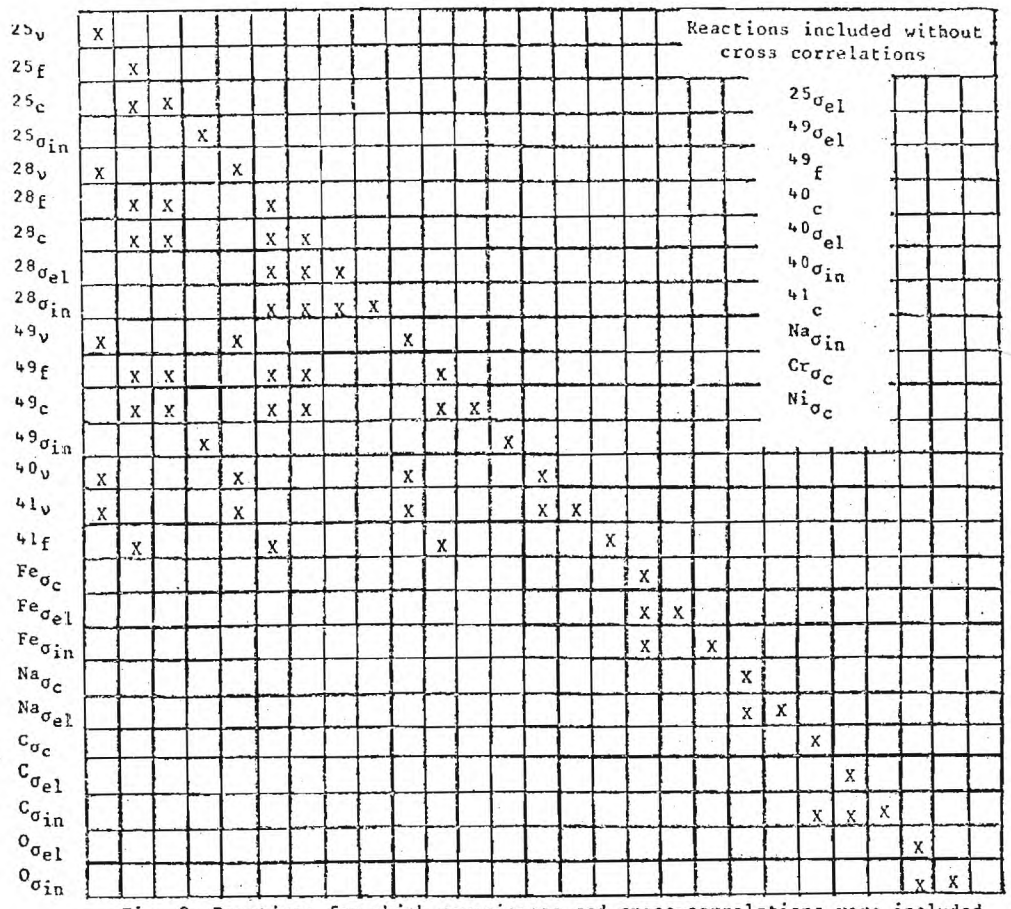

Fig. 3 Reactions for which covariances and cross-correlations were included in the calculations of performance parameter uncertainties are indicated by X. Above and to the right of the principal diagonal, X's should be inferred from symmetry. Column labels are the same as row labels. Reactions for which covariances without cross correlations were included are given in the inset.

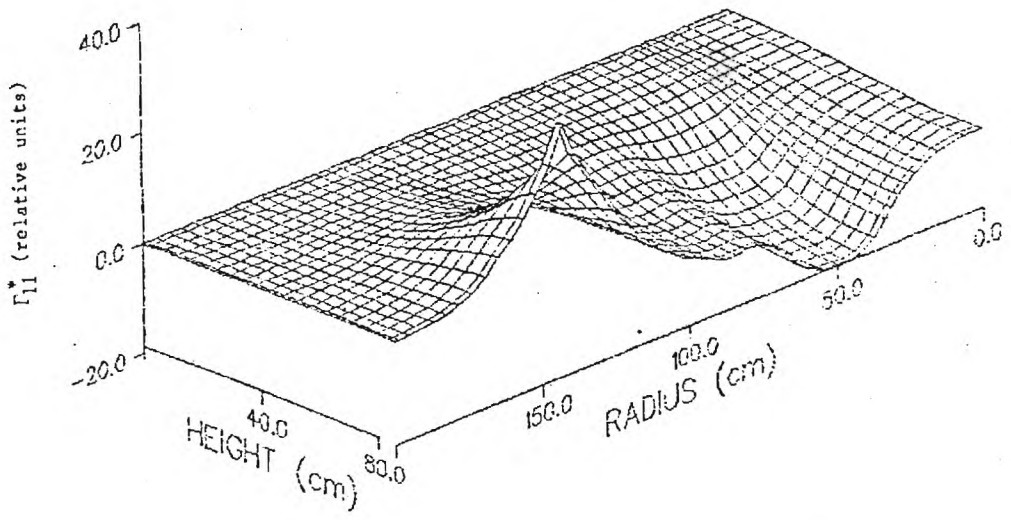

Fig. 4. Peak-power density generalized adjoint Γ_{11}^{*} for energies 67-111 keV in the lower half of the heterogeneous reactor model.

REFERENCES*

1. J. M. Kallfelz and P. Levin, "Progress Report on Work for ORNL Subcontract 3986, Period September 11 - October 12, 1979," Memorandum to C. R. Weisbin, J. H. Marable, and M. L. Williams (ORNL), School of Nuclear Engineering, Georgia Institute of Technology, October 15, 1979.

2. J. M. Kallfelz and P. Levin, "Progress Report for ORNL Subcontract 7802, Period October 13 - November 6, 1979," Memorandum to C. R. Weisbin, J. H. Marable, and M. L. Williams (ORNL), School of Nuclear Engineering, Georgia Institute of Technology, November 7, 1979.

3. J. M. Kallfelz and P. Levin, "Progress Report on Work for ORNL Subcontract 7802, Period November 7 - December 6, 1979," Memorandum to C. R. Weisbin, J. H. Marable, and M. L. Williams (ORNL), School of Nuclear Engineering, Georgia Institute of Technology, December 7, 1979.

4. J. M. Kallfelz and P. Levin, "Progress Report for ORNL Subcontract 7802, Period December 7, 1979 - January 8, 1980," Memorandum to C. R. Weisbin, J. H. Marable, and M. L. Williams (ORNL), School of Nuclear Engineering, Georgia Institute of Technology, January 9, 1980.

5. J. M. Kallfelz and P. Levin, "Progress Report for ORNL Subcontract 7802, Period January 9 - February 11, 1980," Memorandum to C. R. Weisbin, J. H. Marable, and M. L. Williams (ORNL), School of Nuclear Engineering, Georgia Institute of Technology, February 12, 1980.

6. J. M. Kallfelz and P. Levin, "Progress Report for ORNL Subcontract 7802, Period February 12 - March 4, 1980," Memorandum to C. R. Weisbin, J. H. Marable, and M. L. Williams (ORNL), School of Nuclear Engineering, Georgia Institute of Technology, March 5, 1980.

7. J. M. Kallfelz and P. Levin, "Progress Report for ORNL Subcontract 7802, Period March 5 - March 31, 1980," Memorandum to C. R. Weisbin, J. H. Marable, and M. L. Williams (ORNL), School of Nuclear Engineering, Georgia Institute of Technology, April 2, 1980.

8. J. M. Kallfelz, P. Levin, and M. Becker, "Progress Report for ORNL Subcontract 7802, Period April 1 - May 9, 1980," Memorandum to C. R. Weisbin, J. H. Marable, and M. L. Williams (ORNL), School of Nuclear Engineering, Georgia Institute of Technology, May 19, 1980.

9. J. M. Kallfelz and P. Levin, "Progress Report for ORNL Subcontract 7802, Period May 10 - June 10, 1980," Memorandum to C. R. Weisbin, J. H. Marable, and M. L. Williams (ORNL), School of Nuclear Engineering, Georgia Institute of Technology, June 11, 1980.

10. J. M. Kallfelz, P. Levin, and D. Biswas, "Progress Report for ORNL Subcontract 7802, Period June 11 - June 30, 1980," Memorandum to C. R. Weisbin, J. H. Marable, and M. L. Williams (ORNL), School of Nuclear Engineering, Georgia Institute of Technology, July 3, 1980.

*References for section 2.2 are listed separately, on pages 12 and 13.

References (continued)

11. J. M. Kallfelz, D. Biswas, and A. Gandini, "Progress Report for ORNL Subcontract 7802, Period July 1 - August 6, 1980," Memorandum to C. R. Weisbin, J. H. Marable, and M. L. Williams (ORNL), School of Nuclear Engineering, Georgia Institute of Technology, August 8, 1980.

12. J. M. Kallfelz and D. Biswas, "Progress Report for ORNL Subcontract 7802, Period August 7-31, 1980," Memorandum to C. R. Weisbin, J. H. Marable, and M. L. Williams (ORNL), School of Nuclear Engineering, Georgia Institute of Technology, August 29, 1980.

13. J. M. Kallfelz and D. Biswas, "Progress Report for ORNL Subcontract 7802, Period September 1-30, 1980," Memorandum to C. R. Weisbin, J. H. Marable, and M. L. Williams (ORNL), School of Nuclear Engineering, Georgia Institute of Technology, September 30, 1980.

14. "Advanced Recycle Methodology Program System Documentation," EPRI Report, CCM-3 Electric Power Research Institute, September 1977.

15. ENDF/B-IV - Based transport corrected EPRI-CELL libraries existing at ORNL were used: GAM library (FTO3) - Tape #X05013, file 2.
DSN = RQW. EPCELL.ENDFB4.GAMTAP.MOD1
THERMOS library (FTO4) - Tape #X20252, file 1.
DSN = RQW.EPCELL.ENDFB4.LIBRAR

16. "Advanced Recycle Methodology Program System Documentation," EPRI Report, CCM-3 Electric Power Research Institute, September 1977, Chapter 2, part II.

17. "Advanced Recycle Methodology Program System Documentation," EPRI Report,
CCM-3 Electric Power Research Institute, September 1977, Chapter 5, part II.

18. "Advanced Recycle Methodology Program System Documentation," EPRI Report, CCM-3 Electric Power Research Institute, September 1977, Chapter 2, part I.

19. "Advanced Recycle Methodology Program System Documentation," EPRI Report, CCM-3 Electric Power Research Institute, September 1977, Chapter 3, part I.

20. R. I. Smith and G. J. Konzek, "Clean Critical Experiment Benchmarks for Plutonium Recycle in LWRs," EPRI NP-196, Electric Power Research Institute, April 1976.

21. R. Sher and S. Fiarman, "Analysis of Some Uranium Oxide and Mixed-Oxide Lattice Measurements," EPRI NP-691, Electric Power Research Institute, February 1978.

References (continued)

22. H. Alter et al., "Cross Section Evaluation Working Group Benchmark Specification," BNL-19302 (ENDF-202), Brookhaven National Laboratory, Revised September, 1978. Pages T(18-20)-1-3.

23. J. B. Melehan, "Yankee Core Evaluation Program, Final Report," WACP-3017-6094 (January 1971).

24. "Advanced Recycle Methodology Program System Documentation," EPRI Report, CCM-3 Electric Power Research Institute, September 1977, Chapter 3, part II.

25. R. J. Nodvik, "Supplementary Report on Evaluation of Mass Spectroscopic and Radiochemical Analyses of Yankee Core I Spent Fuel, Including Isotopes of Elements Thorium through Curium," WCAP-6086 (August 1969).

26. S. Jedruch and R. J. Nodvik, "Experimentally Determined Burnup and Spent Fuel Composition of Yankee Core I," WACP-6071 (July 1965).

27. P. G. Lacey and R. E. Radcliffe, "Diffusion-Theory Depletion Analysis of the Yankee Core," WACP-6077.

28. P. Levin, "The Effect of the 1 eV Resonance of Pu-240 on Isotopic Calculations in EPRI-CELL," Memorandum to M. L. Williams, dated January 22, 1980.

29. J. M. Kallfelz, D. Rinaldis, M. Segev, and P. Levin, "Progress Report on Work for ORNL Subcontract 3986, Period June 1-30, 1979," Memorandum to C. R. Weisbin, J. H. Marable, and M. R. Williams, dated July 8, 1979.

30. D. Rinaldis, J. M. Kallfelz, E. Kujawski, and J. H. Marable, "Evaluation of Integral Parameter Correlations and Reactor Performance Using Nuclear Data Covariances," Trans. ANS 33, 859 (1979).

31. J. M. Kallfelz, "Cost Effectiveness of Sensitivity and Uncertainty Analysis for Reactor Design," Memorandum to C. R. Weisbin, dated October 7, 1979.

32. J. M. Kallfelz, J. H. Marable, and C. R. Weisbin, letter to C. L. Cowan (GE-ARSD), dated January 25, 1980.

33. M. A. Abdou and C. W. Maynard, Nucl. Sci. Eng. 56, 360 (1975).

34. J. M. Kallfelz, D. Biswas, C. L. Cowan, J. H. Marable, M. L. Williams, C. R. Weisbin, J. D. Drischler, T. B. Fowler, and J. R. White, "Design and Sensitivity Analysis of a CDS-type LMFBR Heterogeneous Core," Paper presented at ANS Topical Meeting 1980, Advances in Reactor Physics and Shielding, September 14-17, 1980.